UM-HSRI-PF-72-5

FINAL REPORT
AGREEMENT NH-69-0961
MAY 12, 1972

INVESTIGATION OF THE DYNAMIC IMPACT CHARACTERISTICS OF ROADSIDE STRUCTURES

DUANE F. DUNLAP
PHILIP GROTE
DAVID M. FRAM
WILLIAM MASHINTER

HIGHWAY SAFETY RESEARCH INSTITUTE
THE UNIVERSITY OF MICHIGAN
ANN ARBOR, MICHIGAN

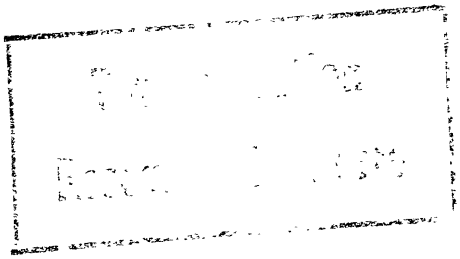

PREPARED FOR
WAYNE STATE UNIVERSITY

THE UNIVERSITY OF MICHIGAN
HIGHWAY SAFETY RESEARCH INSTITUTE

BIBLIOGRAPHIC DATA SHEET	1. Report No. UM-HSRI-PF-72-5	PB 230 468	3. Recipient's Acc...

UMTR

4. Title and Subtitle

INVESTIGATION OF THE DYNAMIC IMPACT CHARACTERISTICS OF ROADSIDE STRUCTURES.

5. Report Date: May 12, 1972

6.

19789

7. Authors: Duane F. Dunlap, Philip Grote, David M. Fram, William Mashinter

8. Performing Organization Rept. No. UM-HSRI-PF-72-5

9. Performing Organization Name and Address
Highway Safety Research Institute
University of Michigan
Huron Parkway and Baxter Road
Ann Arbor, Michigan 48105

10. Project/Task/Work Unit No.

11. Contract/Grant No.
Agreement
NH-69-0961

12. Sponsoring Organization Name and Address
Wayne State University
Detroit, Michigan 48202

13. Type of Report & Period Covered
Final report

14.

15. Supplementary Notes

Under primary sponsorship of the Michigan Department of State Highways, Lansing.

16. Abstracts

Impact performance assessments of four types of roadside structures are presented. An earthen mound guardrail end treatment is found to be unsatisfactory, while an absorber, break-away treatment is found to be more promising although requiring design modifications. Five MDSH standard curb configurations were subjected to simulated impacts and are found to affect vehicle motions as a function of height, face profile and surface texture. Eight common curb/guardrail combinations are evaluated in terms of vaulting potential; all are found to be safe, provided specific guardrail height and set back guidelines are adhered to. The MDSH standard median dike profile is found to be unsafe and in need of flatter side slopes. Appendices are presented which contain detailed discussions of simulation modeling methods, test acceleration measurements and roadside structure development procedures.

17. Key Words and Document Analysis. 17a. Descriptors

17b. Identifiers, Open-Ended Terms

17c. COSATI Field/Group

18. Availability Statement

UNLIMITED

19. Security Class (This Report) UNCLASSIFIED	21. No. of Pages 346
20. Security Class (This Page) UNCLASSIFIED	22. Price

PREFACE

This document is a final report which is being submitted in compliance with Item 11a. of Agreement NH-69-0961 between The University of Michigan and Wayne State University.

ABSTRACT

Impact performance assessments of four types of roadside structures are presented. An earthen mound guardrail end treatment is found to be unsatisfactory, while an absorber, break-away treatment is found to be more promising although requiring design modifications. Five MDSH standard curb configurations were subjected to simulated impacts and are found to affect vehicle motions as a function of height, fact profile and surface texture. Eight common curb/guardrail combinations are evaluated in terms of vaulting potential; all are found to be safe, provided specific guardrail height and set back guidelines are adhered to. The MDSH standard median dike profile is found to be unsafe and in need of flatter side slopes. Appendices are presented which contain detailed discussions of simulation modeling methods, test acceleration measurements and roadside structure development procedures.

CONTENTS

1. INTRODUCTION

The research described in this report constitutes the findings from a roadside structure impact evaluation program which has covered two and one-half years. The work was initiated by the Michigan Department of State Highways (MDSH) in the late 1960's when it became evident that little was known of the impact characteristics of most structures in place along Michigan freeways. In recognition of this deficiency, the Department contracted with Wayne State University (WSU) and the Highway Safety Research Institute (HSRI) of the University of Michigan (under subcontract to WSU) to undertake an impact evaluation program involving several varieties of roadside structures. The content of this report covers those activities carried on at HSRI.

A synopsis of results and their applicability to operational practice is given in Section 2. Sections 3, 4, 5, and 6 contain detailed evaluative findings relating to guardrail end treatments, curbs, curb/guardrail combinations, and median dikes, respectively.

Five appendices follow the main report body. The first contains a description of the computer simulation model used in evaluating the curbs, curb/guardrail combinations, and dikes. The second consists of a delineation of the vehicle parameters needed as simulation inputs while the third involves a description of the mathematical idealization for one of the guardrail end treatments. Test accelerometer measurements and barrier development procedures constitute the fourth and fifth appendices, respectively.

2. SYNOPSIS OF RESULTS AND APPLICABILITY TO OPERATIONAL PRACTICE

2.1 GUARDRAIL END TREATMENTS

Two guardrail end treatment configurations were analyzed through simulation analysis:

1. an earthen mound end treatment designed by the Michigan Department of State Highways [52]; and
2. a barrel-angle breakaway absorber end treatment

2.1.1 SYNOPSIS OF RESULTS. The earthen mound end treatment was subjected to two tests, both of which were considered to be unsatisfactory in terms of end treatment performance. The objective in the simulation exercises was to mathematically duplicate the vehicle trajectory in one of the tests and then use the validated simulation model as a tool in designing a more satisfactory mounded end treatment. The duplication objective was accomplished. Attempts to develop a new end treatment met with only qualified success, however. The main difficulty lies with creating a transition from road shoulder level to guardrail height without creating a ramp. Two alternatives are presented as a starting point toward an acceptable design. Neither is considered a workable solution, however, and for this reason were not subjected to simulation analysis.

Simulation results for the barrel angle end treatment were found to match test results very closely. There was a one-to-one correspondence between end treatment elements failing in the test and those which failed in the simulation. Photogrammetrically determined

velocity and acceleration histories from the test matched similar data obtained from the simulation within 10 percent. Onboard accelerometer data matched in a general sense but less precisely. This was due to the vastly greater frequency content of the accelerometer traces.

Extended simulation exercises using the validated model showed the barrel angle end treatment to perform reasonably well under most impact conditions. While redirection performance indicated no occupant injury at 60 mph and 10°, increasing the impact angle to 25° would have required the passenger to be restrained by a lap belt to arrive at the same no injury verdict. The breakaway absorbing action of the barrier was confirmed in an end on simulated impact although decelerations were high. To escape without probable injury, an occupant would have had to be restrained by both a lap belt and shoulder harness.

2.1.1 APPLICABILITY TO OPERATIONAL PRACTICE. Although representing a marked improvement over both the bare guardrail end and the ramped and twisted end in current use, the barrel angle end, as presently constituted, is not yet ready for field installation. Modifications to improve both the redirective (side impact) and breakaway (end on impact) performance are necessary so as to reduce expected impact loads. Suggestions along these lines are presented in Section 3 and are recommended for evaluation using simulation analysis.

The earthen end configuration is not recommended for field installation. Neither are the two modified earthen ends presented

in this report. Further, it is recommended that research on reflective type end treatments be postponed until the more promising types involving breakaway and absorbing features are evaluated.

2.2 CURBS

Curb impact test results from test programs conducted by other organizations were reviewed and synthesized. Five curb configurations were subjected to simulated impacts and the results where possible were compared with test results. The curbs correspond to MDSH standard curbs A, B, C, D, and K. Impact conditions for most cases were 40 mph, 25°; 60 mph, 10°; 60 mph, 25°; and 80 mph, 10°. For Curb C, impact conditions were 30 mph, 25°; 50 mph, 10°; and 50 mph, 25°.

2.2.1 SYNOPSIS OF RESULTS. Analysis of the test data indicates that a backward curb face slope of about 2:9 is best in terms of redirective performance. Slopes steeper than 2:9 allow the wheel rim to bite into the curb face, while flatter slopes cause the curb to act like a mountable ramp. A sharp upper corner was also found to enhance mounting and thus a corner of at least one inch radius was recommended.

Undercut curbs were found to trap the tire bulge and thereby discourage mounting. Smooth, low friction curb face material was also found to reduce the mounting tendency through a reduction in the induced tire side wall/curb face friction force. (This latter force is primarily responsible for the tire climbing the curb face.)

Redirective performance was found to increase in direct relation with curb height. A height of ten to twelve inches appeared to be near optimum in terms of the trade-off between redirection performance and vehicle damage.

Curb redirective performance was found to be predictable according to the equation:

$$V \sin \alpha = K \qquad (2\text{-}1)$$

where

V is vehicle velocity

α is the impact angle, and

K is a constant which depends on curb characteristics.

Using this equation, test data, and angle and velocity data characteristic of urban traffic conditions, it was found that a German designed curb would redirect 70% of the vehicles accidentally running off the road.

Of the five MDSH curbs evaluated, only the higher curbs (i.e., A, K, and to a lesser extent C) had a significant influence on vehicle path. As predicted by Equation (2-1), the most effect was noted for low speed, low angle cases. At 40 mph and 25°, both curbs A and K caused the vehicle to be redirected after mounting had occurred. At 60 mph and 10°, curb K eventually redirected the vehicle whereas a spinout occurred with Curb A. Neither curb influence the vehicle at 60 mph and 25°. Curb K caused a spinout at 80 mph and 10° while little influence was noted from Curb A.

Comparisons between simulation results and test results, when available, proved to be good.

2.2.2 APPLICABILITY TO OPERATIONAL PRACTICE. Carefully designed barrier curbs have been found to be effective redirection devices. None of the current MDSH standard configurations falls into this category. All could be improved through the application of specific design guidelines presented here. In particular, careful thought should be given to the use of the Elsholz curb developed in West Germany and modified from an earlier California Division of Highways design.

2.3 CURB/GUARDRAIL COMBINATIONS

Curb/guardrail test results from other organizations were reviewed. Eight standard MDSH curb/guardrail configurations were evaluated. These involved combinations of Curbs A, B, C, D, and K with type B and C guardrail, type B median barrier, and the concrete safety parapet. Most combinations were evaluated with a combined analysis and simulation method, while Curb B and the safety parapet was evaluated by simulation alone.

2.3.1 SYNOPSIS OF RESULTS. Vaulting of a guardrail as the result of first running into a curb has <u>not</u> been identified as a serious problem in any known test program. After reviewing nearly fifty tests, only one questionable case of vaulting was found. This case involved a 17,500 lb. bus running into a concrete bridge railing. The railing very probably contributed to the vaulting through structural failure.

Using very conservative analysis methods, no assessments of vaulting potential were found for any of the curb/guardrail combinations which were subjected to evaluation. Although intuition would suggest vaulting is a potential problem, this has not proven to be the case.

2.3.2 APPLICABILITY TO OPERATIONAL PRACTICE. The current trend is toward not using curbs in front of guardrail. It would seem worthwhile to examine this policy, however, in light of the current findings. As indicated earlier, a carefully designed barrier curb can be expected to redirect 70% of those vehicles striking it in urban traffic conditions. Vehicle damage in these encounters can be expected to be far less than if the vehicle struck a guardrail. For those vehicles climbing the curb, a secondary retainer is obviously required. Thus, the utility of the curb/guardrail combination is evident.

Based on the current findings, all of the curb/guardrail combinations examined are safe for operational installation. This finding specifically applies to only those combinations examined, however. Care should be taken to insure that the height and setback of guardrails installed behind curbs satisfy prescribed minimums. These are delineated as a part of design guidelines and are recommended for operational use.

2.4 MEDIAN DIKES

A preliminary parameter sensitivity analysis was carried out on the standard drainage dike configuration used in the median of

interstate freeways. The analysis consisted of determining the effect that impact velocity approach angle, vehicle type, dike slope, impact position, and soil have on vehicle impact dynamics.

2.4.1 SYNOPSIS OF RESULTS. Using a sophisticated vehicle simulation program, it was found that the current standard dike shape, with 1:6 side slope is unsafe. Possible injury to an unrestrained passenger can be expected when a vehicle strikes a standard dike at all speeds above 40 mph. At a speed of 80 mph, the potential for injury is at least twice as high.

When the dike slope is flattened to 1:10, passenger loading is reduced by a factor of two. Injury is still indicated for high speed impacts, however. Soft, moist soil was found to have a similar effect in reducing expected occupant loads.

2.4.2 APPLICABILITY TO OPERATIONAL PRACTICE. On the basis of these incomplete findings, a dike slope of 1:12 is recommended as an operational design guideline. In addition, it is recommended that the dike height be kept as low as possible consistent with local drainage conditions. Further, dike material should be chosen to promote wheel sinkage. This will enhance the possibility of vehicle containment within the median and reduce the probability of median crossover.

3. GUARDRAIL END TREATMENT INVESTIGATIONS

The guardrail end treatment investigations described here cover the simulation evaluation activities carried on at HSRI. The work complements the testing program activities.

The section is initiated with an historical review of guardrail end development. This review is followed by a discussion of the simulation evaluations of the earthen mound and barrel angle end treatments. Next a set of end treatment design guidelines are presented and these are followed by conclusions and recommendations.

3.1 HISTORICAL REVIEW

Metal beam guardrail ends represent a formidable hazard to highway traffic. The seriousness of spearing in guardrail end collisions was first reported by Stonex [1], at General Motors in 1960. Following a brief testing series at that organization, three modified end treatments were suggested as alternatives to the conventional unprotected rail end:

1. a ramp treatment
2. a flare treatment
3. an earthen mound treatment

The ramp and earthen mound treatments are designed to allow a vehicle to ride up the rail end without spearing. The purpose of the flare is to prevent end-on collisions altogether by presenting a surface which insures higher angle impacts.

In the General Motors test series, the ramp treatment was found to be satisfactory in preventing spearing. As planned, a vehicle in an end-on collision would ride up the ramp, bump along the top of the guardrail and gradually come to rest [1, 2].

As a result of these tests, several state highway departments adopted the ramp as a way of preventing spearing. The Texas Highway Department developed a modified version of the ramp wherein the end is rotated and anchored flat to the ground [3]. In this form, it has come to be known as the "Texas Twist;" a version of it being currently used by the Michigan Department of State Highways [4].

With the widespread use of the ramped end, the incidence of rail end spearing became less frequent, and a major problem appeared to have been solved. A different pattern began to emerge in guardrail end accidents, however, which indicated that a complete solution was still not at hand. Rather than spearing, the ramped end causes a vehicle to fly into the air and roll over under certain kinds of impact conditions. This behavior was not discovered in the General Motors tests because

the impact conditions were at low speed (50 mph, or less) and at 0° (end-on) incidence angle. While the roll over behavior is not as undesirable as spearing, passenger injury and vehicle damage are somewhat greater than that considered satisfactory. Therefore, three separate organizations independently decided to test the ramped end under conditions which would prove, or disprove, its roll-over producing tendencies.

The California Division of Highways conducted a test on the ramped portion of a Texas Twist rail in 1967 [5]. Test conditions involved an impact speed of 63 mph at an angle of 24°. The vehicle vaulted the rail and rolled over as had been suspected. A similar test on a ramped, but untwisted rail end, was carried out by the Ontario Department of Highways at about the same time [6]. In this case, the impact velocity and angle were 50 mph and 28°, respectively. The test vehicle did not roll over, but was vaulted into the air and remained airborne for 54 feet.

Final confirmation of the unsafe character of the ramped end came in 1969 when the Southwest Research Institute conducted a series of six tests on several varieties of end treatments [7]. Five of the six tests involved ramped ends and in all five cases the test vehicle vaulted into the air

and rolled over in a combined rolling and tumbling motion. The test vehicle in each case was considered to be a total loss. Three of the tests were with ramped W-beam rail, while the remaining two involved a ramped box beam. Test conditions varied from speeds of 51 through 61 mph at angles of 0°, 15° and 25°. These tests, coupled with the earlier tests in California and Ontario, provide convincing evidence of the roll-over producing nature of the ramped end.

The remaining test in the Southwest Research series involved a box beam flare. In this case, the test structure broke away without causing the vehicle to ramp, or roll over. Test conditions were at a velocity of 65.5 mph and an angle of 25° (about 40° with respect to the rail). Of the six tests in the series, this was the only one which was considered satisfactory.

Two other box-beam flare end tests were conducted by the New York State Department of Public Works [8]. The impact angle in each case was 25° with respect to the roadway and about 35° to 40° with respect to the rail. Redirection occurred in a 40 mph impact, while at 53 mph the vehicle broke through. Highest decelerations in the latter case were on the order of 4 g's, however, indicating relatively mild passenger loading.

On the basis of these and the Southwest Research tests, the flare end was considered to be more satisfactory than the ramp. Use of a flare end results in larger impact angles,

however, and repair costs for the break-away section are somewhat greater. The rail end must also be extended further upstream so that the vehicle, as it breaks through, does not penetrate to the area protected by the guardrail. Neither the ramp nor the flare were therefore considered to be final solutions to the end treatment problem.

In late 1969, the Southwest Research Institute began a second series of tests on end treatments, this time involving novel configurations [9]. Two similar designs were examined, each involving a rounded nose with an approximate 11 in. radius. In one case the nose was filled with vermiculite concrete and flared back from the roadway. In the other design, a 22 ga. steel diaphragm was tack welded into the nose with the end section being unflared. Both designs incorporated a special breakaway end anchorage.

Two tests were conducted on the flare configuration; one on the unflared design. All test speeds were in the vicinity of 60 mph. In two end-on tests, vehicle decelerations were listed as 10.8 and 8.6 g's for the flared and unflared designs, respectively. Vehicle damage was excessive in each case, although no roll over, spearing, or passenger compartment penetration occurred. A 15° impact on the flared terminal near the end produced a redirection.

On the basis of these tests, it was recommended that the flared terminal be installed in the field for operational evaluation. Test evaluation of the structure is not considered to be complete, however. It seems likely that more stringent test conditions would have produced less satisfactory results (e.g., an impact angle of 25° just downstream of the flared terminal may very well have produced pocketing).

A parallel evaluation program was conducted in 1971 by Wayne State University and the Highway Safety Research Institute of The University of Michigan. This program involved tests and simulation exercises on five different end treatments. These included an earthen mound end treatment [52], a break-away flare treatment, and three absorber, break-away configurations The portion of the program dealing with the simulation activities carried on at HSRI is discussed in the next subsection.

3.2 SIMULATION EVALUATION EXERCISES

Guardrail end simulation exercises were divided into two parts. Those exercises dealing with the MDSH earthen mound end treatment were carried out with the Cornell Aeronautical Laboratories Single Vehicle Accident (CALSVA) program [36, 45]. Exercises involving the other structures were conducted with the BARRIER Program [53]. Originally it had been planned to simulate vehicle impacts into each of the tested end treatments and to evaluate design modifications and new end treatments with the two programs. One of the end treatments was obviously

not a satisfactory design, however (the barrel sweep design evaluated in test 23), while two others were designed and tested so late in the contract year as to make any practical simulation program impossible. As a result, only the earthen mound treatment and one of the absorber, break-away treatments were evaluated.

3.3 EARTHEN MOUND END TREATMENT

A plan view and cross sections of the earthen mound guardrail end treatment are shown on Figure 3-1. The structure was tested twice at an impact speed of approximately 60 mph. In one case (test 20) the impact angle was 25° with respect to the road edge, while in the second case, the angle was 10° (test 21).

In test 20, the vehicle struck the end treatment such that the inside wheels ran over the concrete anchor while those on the outside impacted the guardrail between the first and second posts downstream from the anchor. Forces imparted to the vehicle by the anchor and guardrail caused it to vault into the air and roll over. As the vehicle landed, it struck on its left side (having rolled to this position), executed a ground loop about its yaw axis (now essentially horizontal), and came to rest facing approximately opposite to its original direction of travel.

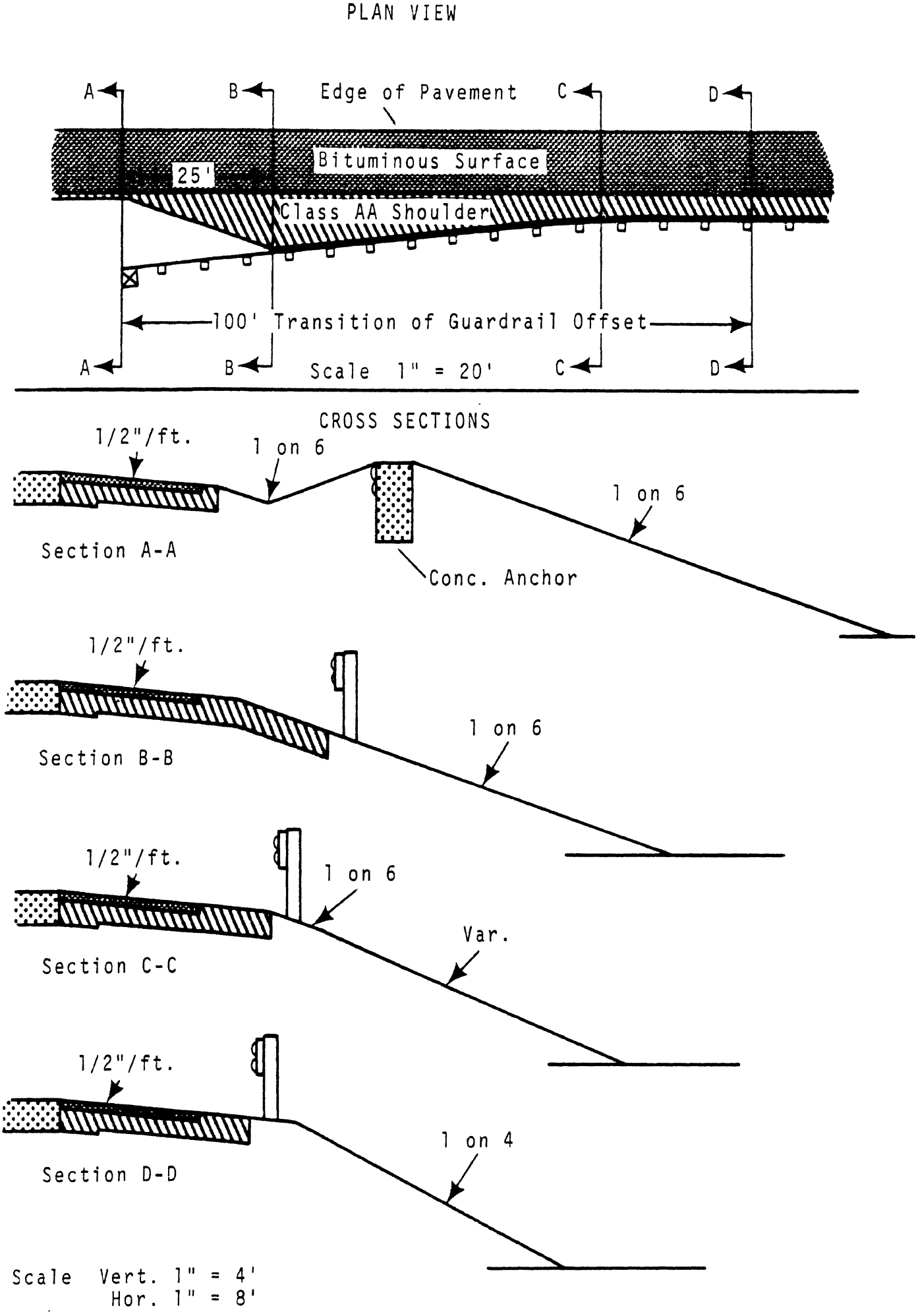

FIGURE 3-1. EARTHEN MOUND GUARDRAIL END TREATMENT

In test 21, the vehicle struck the end treatment with a shallower 10° angle at about the same position from the end anchor. Impulses imparted to the vehicle caused it to mount the rail and bump along on the rail top. The vehicle rode the guardrail in this manner for almost its entire length (about 100 ft.) before coming to rest, upright, on the traffic side of the rail.

Both tests were considered to be unsatisfactory in terms of end treatment performance. The objectives in the simulation exercises were to mathematically duplicate the vehicle impact motions for test 20, and then use the validated simulation as a tool to develop a modified earthen end treatment. As the following discussions will show, the first objective was accomplished within the limits of available photogrammetric test data. Efforts to develop a modified end treatment have met with only qualified success, however. While many improvements can be suggested, the problem of creating a transition from road shoulder level to guardrail height without creating a ramp has not been completely solved.

The CALSVA program which was used in simulating impacts into the earthen mound end is described in Appendix A. The vehicle modeled in the simulation is a 1966 Ford Custom, six cylinder, two-door sedan—the same impact vehicle which was used in the two tests. Vehicle parameters and mechanical

properties which were measured for use as inputs to the simulation program are described in Appendix B.

Comparisons of vehicle roll and pitch angle histories for both test and simulated inpact data are shown on Figure 3-2. Although the interval of test data is rather short (narrow camera field of view), these comparisons are obviously rather good. Attempts to correlate other impact variables, such as velocity, acceleration, C.G. height, etc., were not possible. This was due to the fact that the photogrammetrically reduced test data was either unavailable, or of doubtful accuracy. Roll and pitch angle correlation is indicative of well modeled suspension, tire, and inertia characteristics, however, and these are the primary vehicle properties which determine ramping dynamics. It can be concluded, therefore, that the vehicle model is validated with respect to simulatin vehicle motions in reflector type end treatments.

Although test and simulation results agree satisfactorily, the performance of the earthen mound guardrail end is obviously unsatisfactory. Properties which would produce a better design would include some or all of the following:

1. A mounded transition from shoulder level to guardrail level which is as short as practical and does not produce a ramp.
2. A mounded shape that acts as a reflector and prevents contact with the guardrail end.
3. An approach mound that would act to decelerate the vehicle before it reaches the guardrail end.

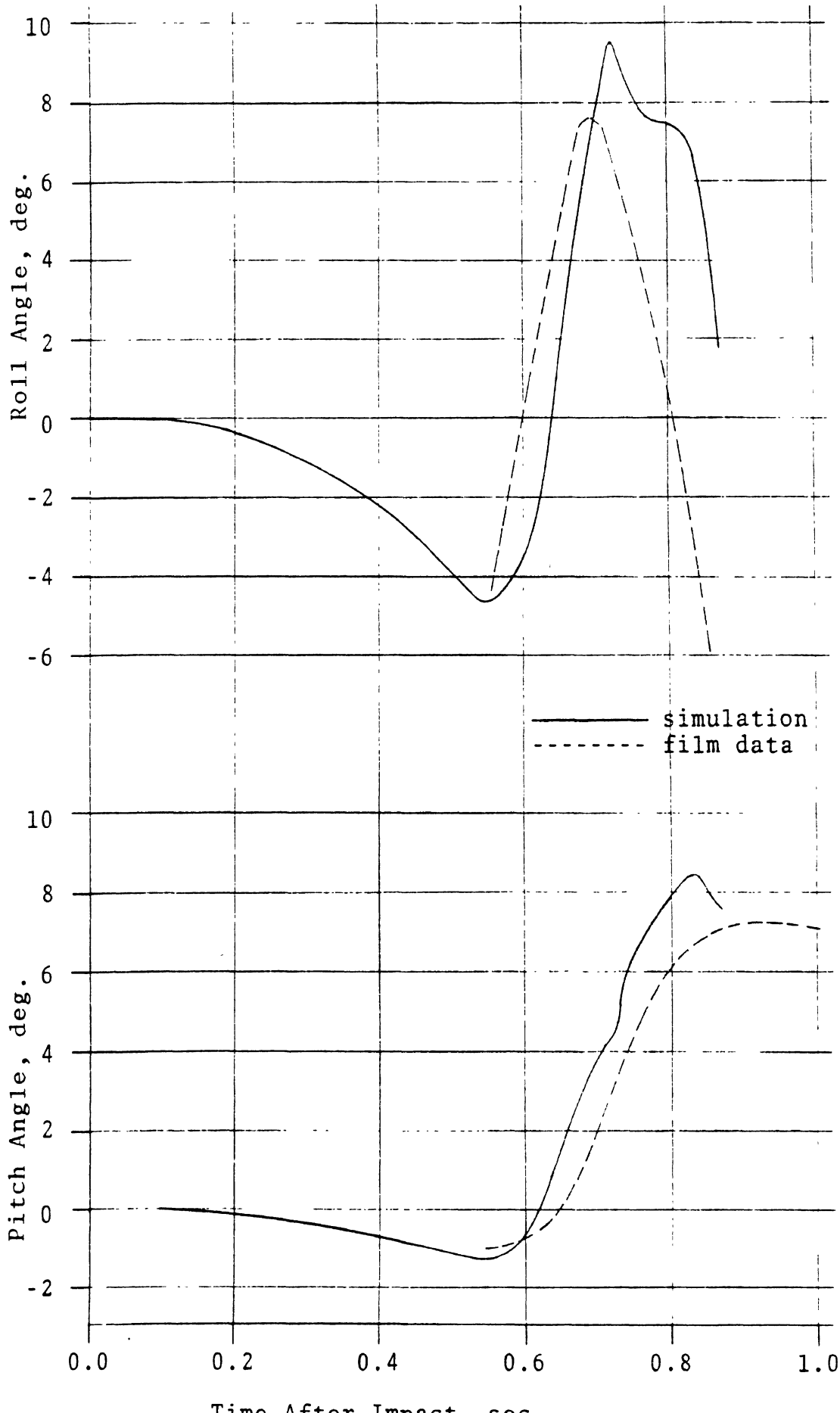

FIGURE 3-2 EARTHEN MOUND END TREATMENT TEST AND SIMULATION COMPARISONS (TEST 20-60 MPH, 10°)

A design incorporating some of these ideas is shown on Figure 3-3. A main feature of this design is a long low earth berm that extends for about two hundred feet upstream of the guardrail end. The purpose of the berm is to decelerate possible impacting vehicles before striking the rail end. The berm, in cross section, is four feet wide and one foot high. Standard passenger vehicles have a tread dimension of about five feet and a running ground clearance ranging from four to eight inches. Thus, in approaching the rail end head on, a vehicle will scrape its undercarriage on the berm and experience a deceleration. Assuming a coefficient of friction of 0.6 as the result of bulldozing, a vehicle traveling at 60 mph will require about 200 feet of stopping distance. The berm is low enough so that a vehicle approaching the berm at an angle will not be vaulted into the air to any appreciable extent.

The troublesome area is, as mentioned earlier, the transition region. The transition shown in considered to be a good one, but deficiencies are evident if an impact occurs in this area. Rollover is probable if one wheel strikes the 12 inch berm while the other strikes the parapet section. Although the transition region is short, a precise impact could be dangerous. (A rollover is considered to be preferable to spearing, but neither can be considered satisfactory.)

A suggested alternative consists of eliminating the transition region, leaving the bare end of the guardrail as is, and curving the berm near the guardrail end such that a vehicle is directed out in front of the rail. Vehicles approaching the end at an angle

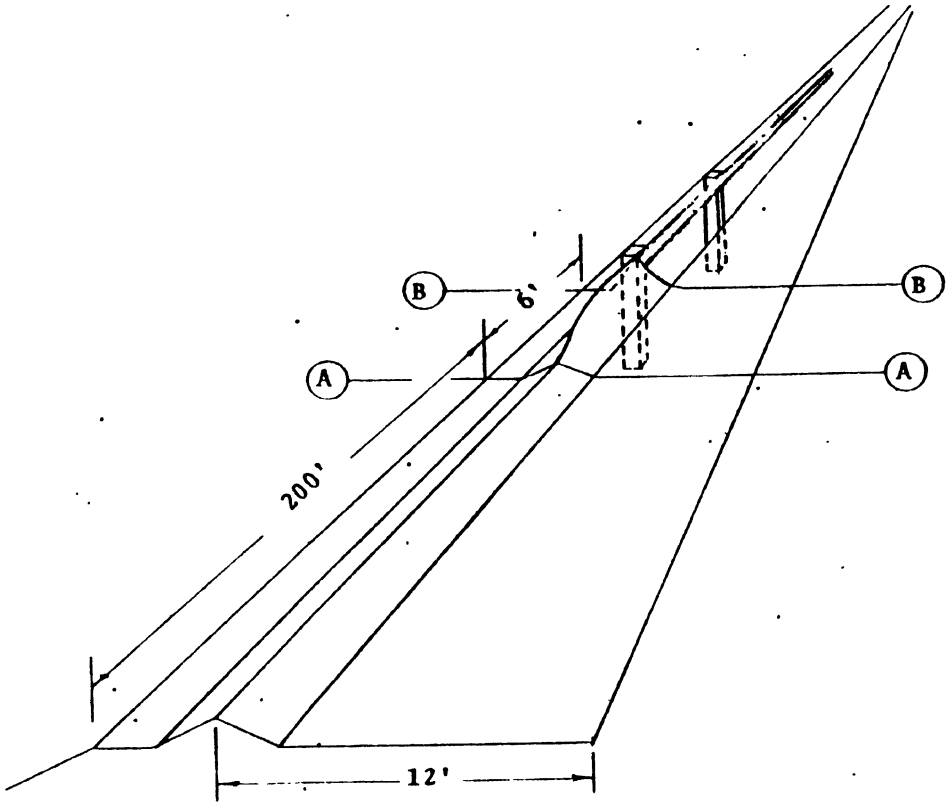

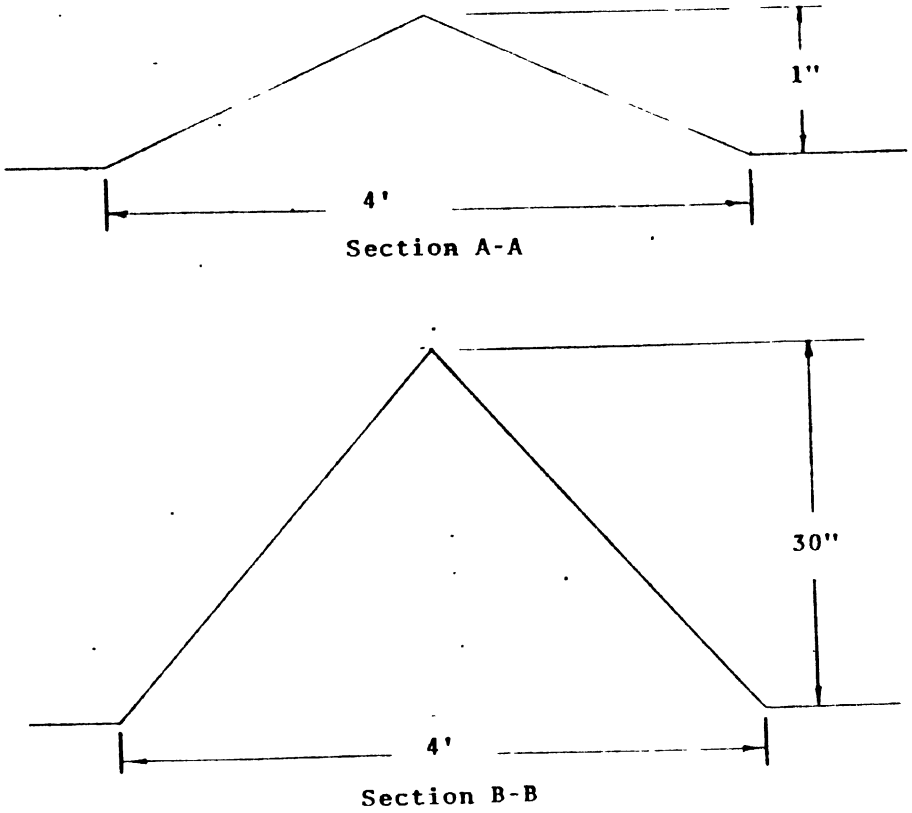

FIGURE 3-3. MODIFIED EARTHEN END TREATMENT

would break through via a suitable brak-away design and those approaching from the end would hopefully be redirected. Redirection is not clear cut, however, due to the uncontrolled nature of the turf interacting with the vehicle undercarriage.

A second alternative is shown on Figure 3-4. In this design, the earth berm is gradually merged into a concrete structure. The berm end of the structure is a curb. The curb merges into a low undercut barrier and this in turn merges into the GM safety parapet cross-section (Section C-C). The guardrail is attached to the parapet.

The purpose of this design as well as the one shown in Figure 3-3 is to raise the approach berm to guardrail height in a minimum distance without creating a ramp. An extensive test and simulation exercise program would be necessary to determine whether this has been accomplished. The priorities which were established in the current program made these exercises impractical.

3.4 BARREL-ANGLE BREAK-AWAY, ABSORBER END TREATMENT

A plan view drawing of the barrel angle guardrail end treatment is shown on Figure 3-5. In the test that was conducted on the structure (Test 24) the vehicle impacted midway between the fourth and fifth barrels from the end. The impact speed and angle (with respect to the road edge) were approximately 59 mph and 10°, respectively. Damage and deflection of the various post and barrel elements in the end treatment, following the test, is summarized

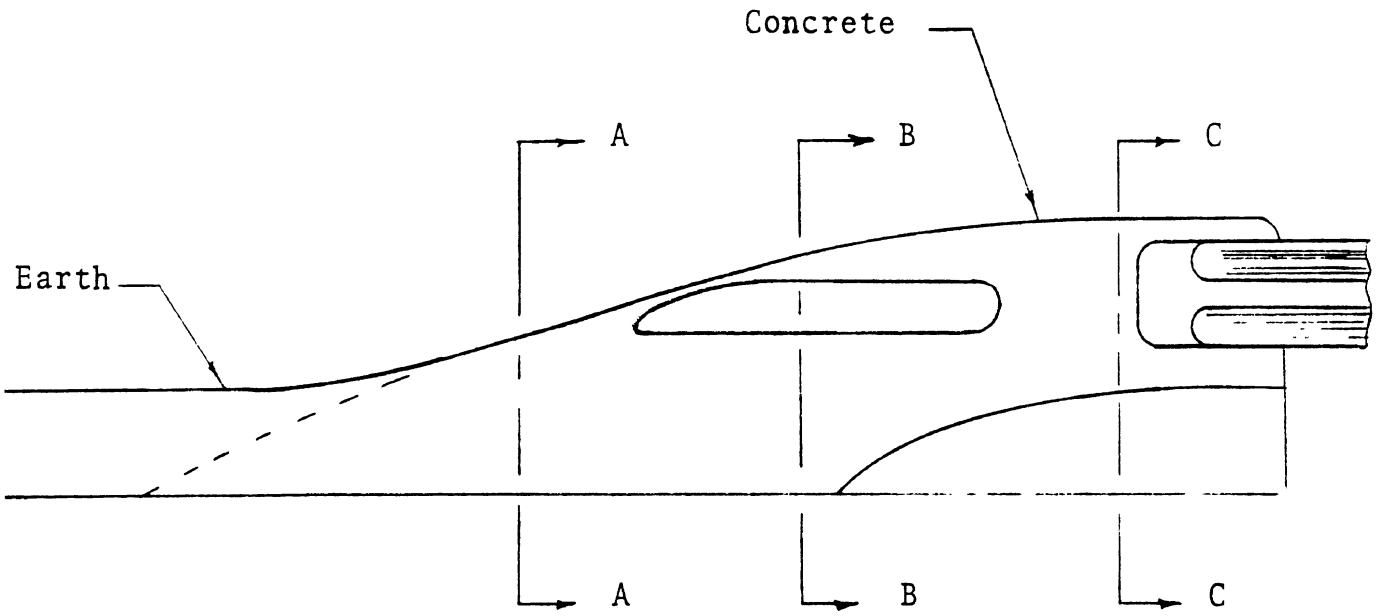

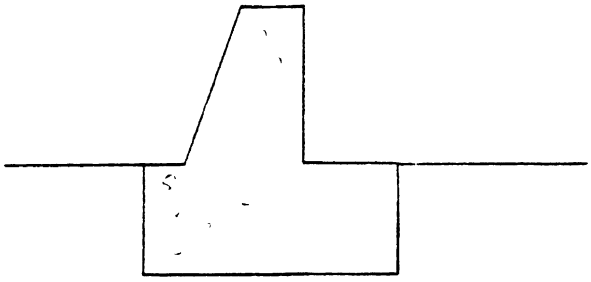

Section A-A

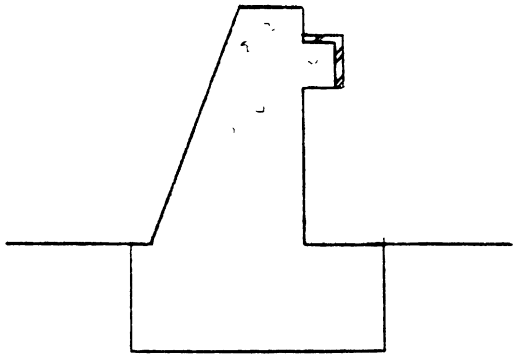

Section B-B

FIGURE 3-4 ALTERNATE TRANSITION

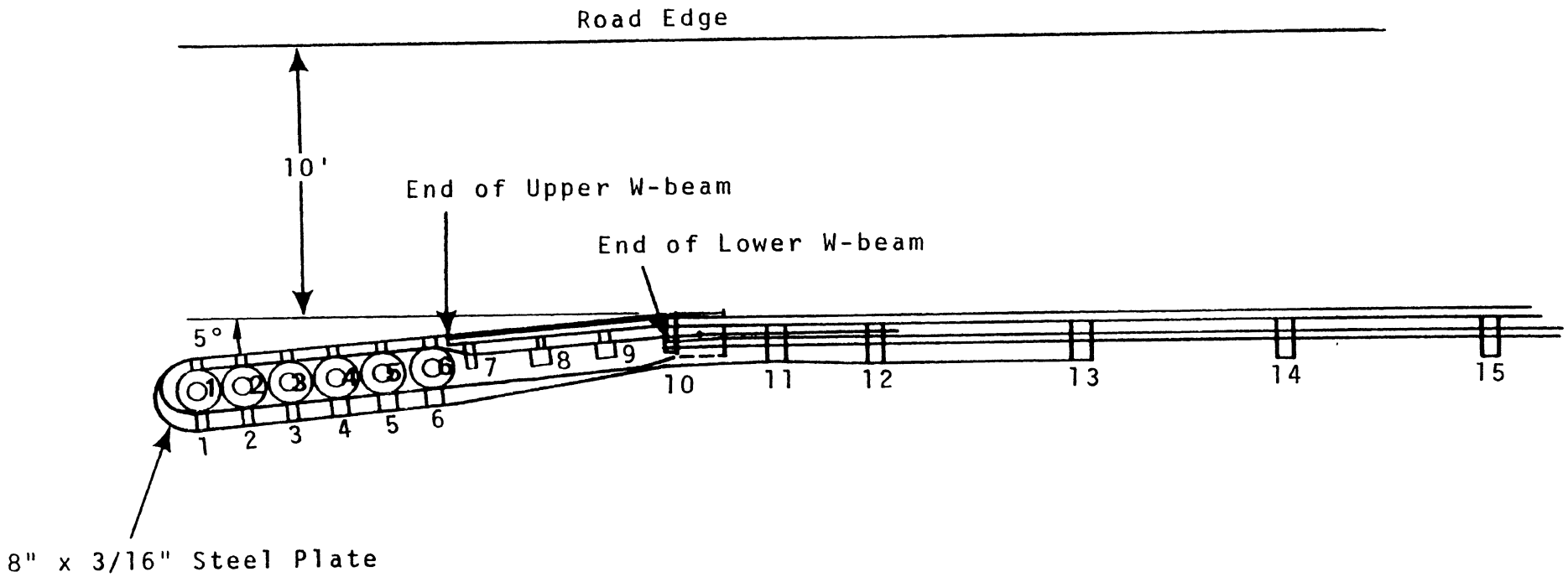

FIGURE 3-5 BARREL-ANGLE BREAK-AWAY ABSORBER END TREATMENT PLAN VIEW

in Table 3-1. In addition to this, the 8" X 3/16" steel strap between barrel 6 and post 7 was severely buckled. The strapping is attached to the W-beam at this point and was bent inward. This action allowed a part of the test vehicle to snag on the end of the W-beam with the result that a small piece of vehicle sheet metal was ripped away. This did not seem to impair the performance of the end treatment, however, in that the vheicle was eventually redirected.

In simulating impacts into the structure, the first goal was to match test results with what could be obtained from the BARRIER V digital computer program [53]. Prior to the test, a run was made with the program wherein the redirective performance was fully predicted. Failure of the strapping between barrel 6 and post 7 was also predicted, but the crushing of barrel 6 and the failure of posts 8 and 9 was not.

For the pretest simulation, barrel strength information was obtained from the static test data shown on Figure 3-6. Post strength data was obtained from several sources [55, 56, 57]. Ultimately this latter data proved to be the most difficult to apply in the simulation.

The difficulty in determining appropriate strength data for the posts lies in the fact that the post and soil act in concert to resist applied lateral forces. While post strength characteristics are predictable within ±20%, soil strength values can vary by an order of magnitude. Since no information was known about soil

TABLE 3-1

BARREL ANGLE END TREATMENT POST AND BARREL ELEMENT TEST DAMAGE AND DEFLECTION SUMMARY

Element	Description	Deflection*	Visible Damage
Posts 1,2,3	4X6 Wood Posts with 3" X 1" Cut-Out at Base Parallel to Rail	None	None
Post 4	6X6 Wood Post with 3" X 1" Cut-Out at Base Parallel to Rail	1/2"	None
Post 5	6X6 Wood Post with 3" X 1" Cut-Out at Base Parallel to Rail	1"	Split
Post 6	6X6 Wood Post with 3" X 1" Cut-Out at Base Parallel to Rail	1 1/2"	Split
Post 7	4X6 Wood Post with 2" X 1" Cut-Out at Base Parallel to Rail	5"	None
Post 8	6X6 Wood Post with 3" X 1" But-Out at Base Parallel to Rail	2"	Failed in Bending at Ground Level
Post 9	6X6 Wood Post with 3" X 1" Cut-Out at Base Parallel to Rail	6"	Failed in Bending at Ground Level
Post 10	4X6 Wood Post	6"	None
Post 11	6X6 Wood Post	5"	Cracked Below Ground Level
Post 12	6X8 Wood Post	3"	None
Post 13	6X8 Wood Post	1"	None
Post 14	6X8 Wood Post	1 1/2"	None
Post 15, on	6X8 Wood Post	None	None

*Permanent set in earthen foundation at base

TABLE 3-1 (cont.)

BARREL ANGLE END TREATMENT POST AND BARREL ELEMENT TEST DAMAGE AND DEFLECTION SUMMARY

Element	Description	Deflection	Visible Damage
Barrel 1,2,3,4	18" d., 20 ga., 30 gallon barrel with 6" end holes	N/A	None
Barrel 5	18" d., 20 ga., 30 gallon barrel with 6" end holes	N/A	Failure at Front Rail Connection
Barrel 6	18" d., 20 ga., 30 gallon barrel with 6" end holes	N/A	Front Quarter Crushed

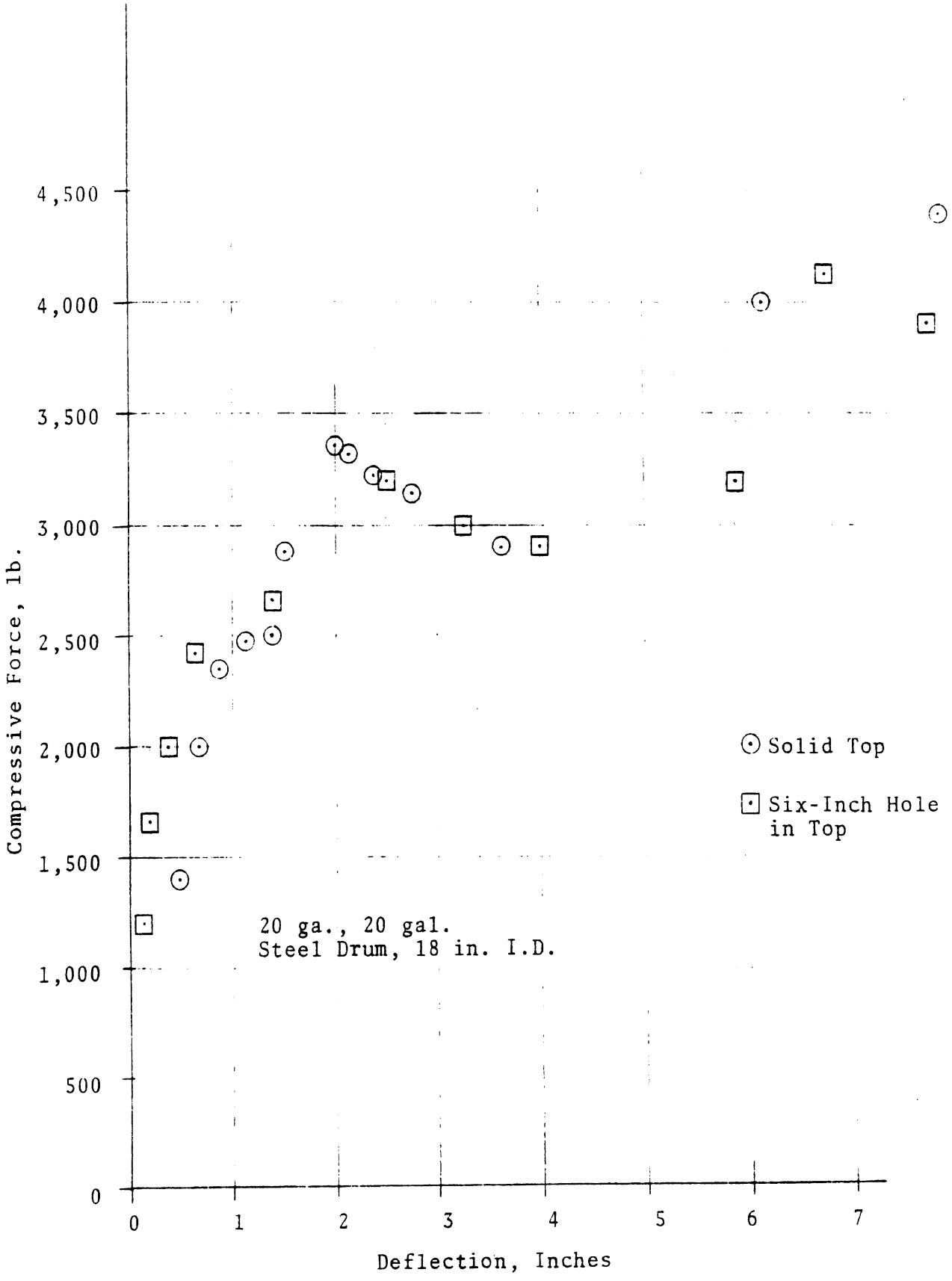

FIGURE 3-6 END TREATMENT BARREL COMPRESSIVE STRENGTH

strength values at the test site, a trial and error procedure was necessary so as to arrive at the actual post/soil strength characteristics which prevailed in the test. The final mathematical idealization of the barrier that resulted is described in Appendix C. In the remaining discussions in this section, this idealization was used to produce the simulated impact runs.

Three simulated runs were made on the barrel angle end treatment. These are summarized in Table 3-2.

TABLE 3-2

BARREL ANGLE END TREATMENT SIMULATION RUNS

Case	Velocity	Angle	Position on Barrier
1	60 mph	10°	Between 4th and 5th barrels
2	60 mph	25°	Between 4th and 5th barrels
3	60 mph	0°	Head on into the end

3.4.1 CASE 1 - 60 mph, 10°. Sequential plan view schmatics for case #1 are shown on Figures 3-7a through 3-7e. As indicated, the vehicle is redirected, posts 8 and 9 fail, and the front end of barrel 6 is crushed about one-fourth. Damage to these elements compares favorably to the damage observed in the test as noted on Table 3-1. As mentioned earlier, element strength characteristics were adjusted slightly so as to insure these comparisons.

Velocity, acceleration (with respect to vehicle coordinates), and heading angle data for the run are shown on Figure 3-8. A relatively smooth redirection is indicated. Peak acceleration

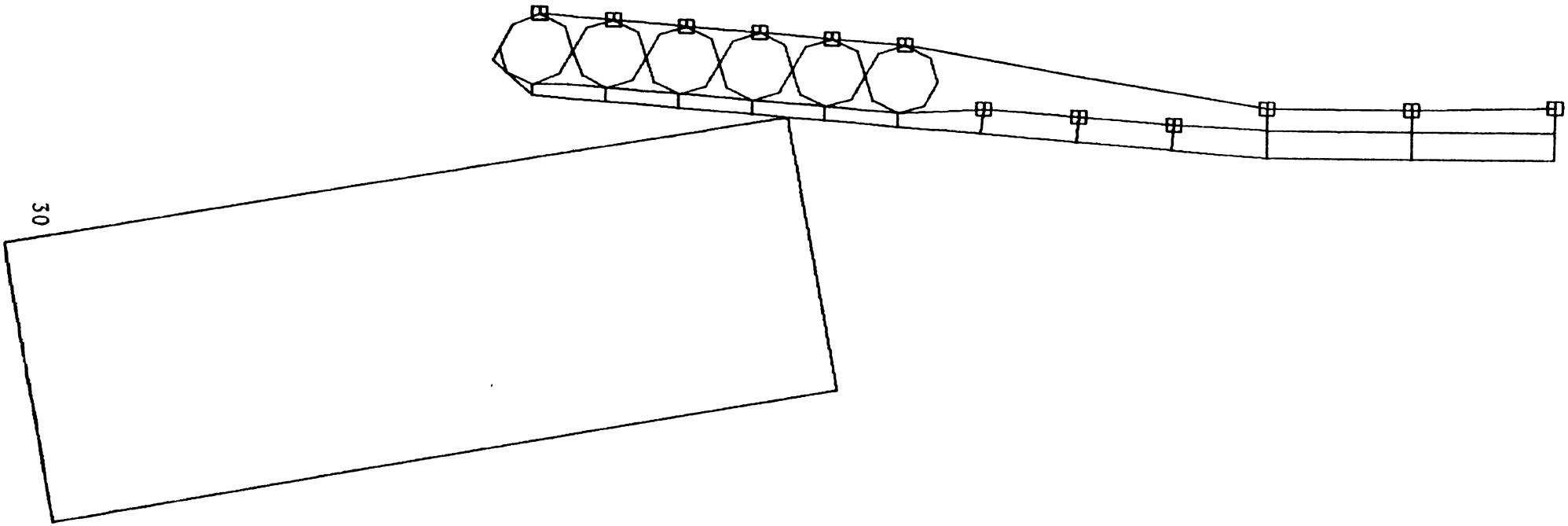

BARREL ANGLE END MØD#2--TEN DEGREES AT 60 MPH

TIME = 0.0000 SEC

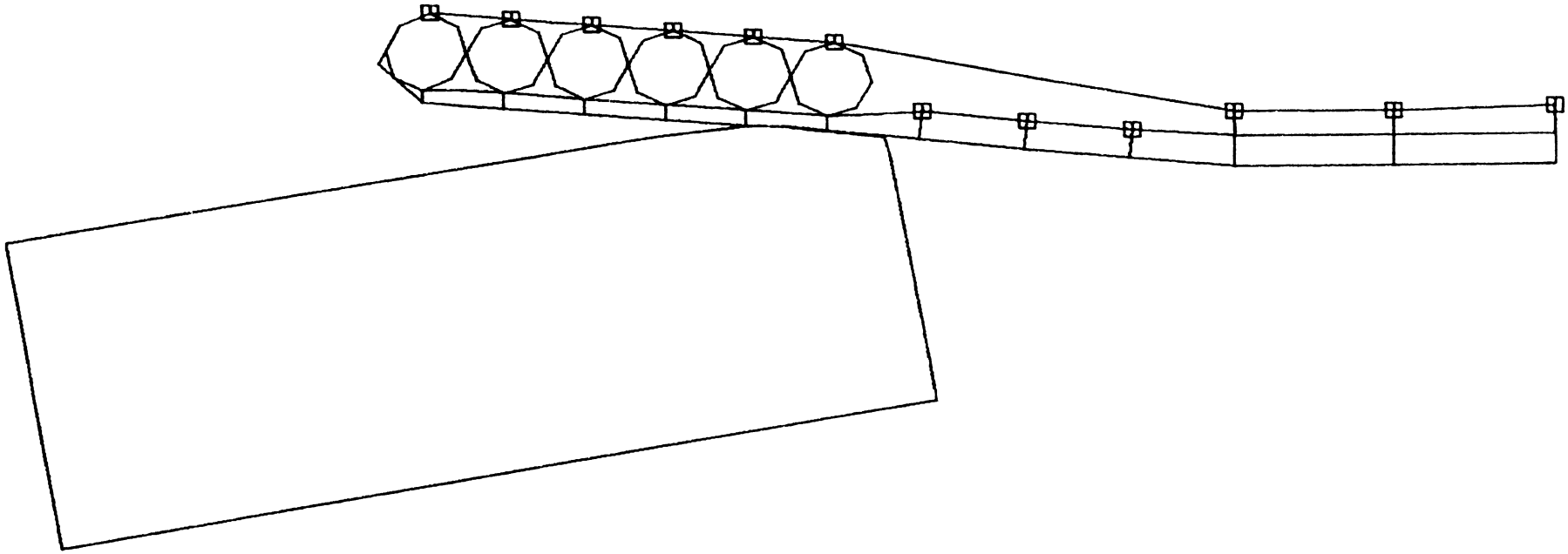

BARREL ANGLE END MOD#2--TEN DEGREES AT 60 MPH

TIME = 0.0400 SEC

FIGURE 3-7B

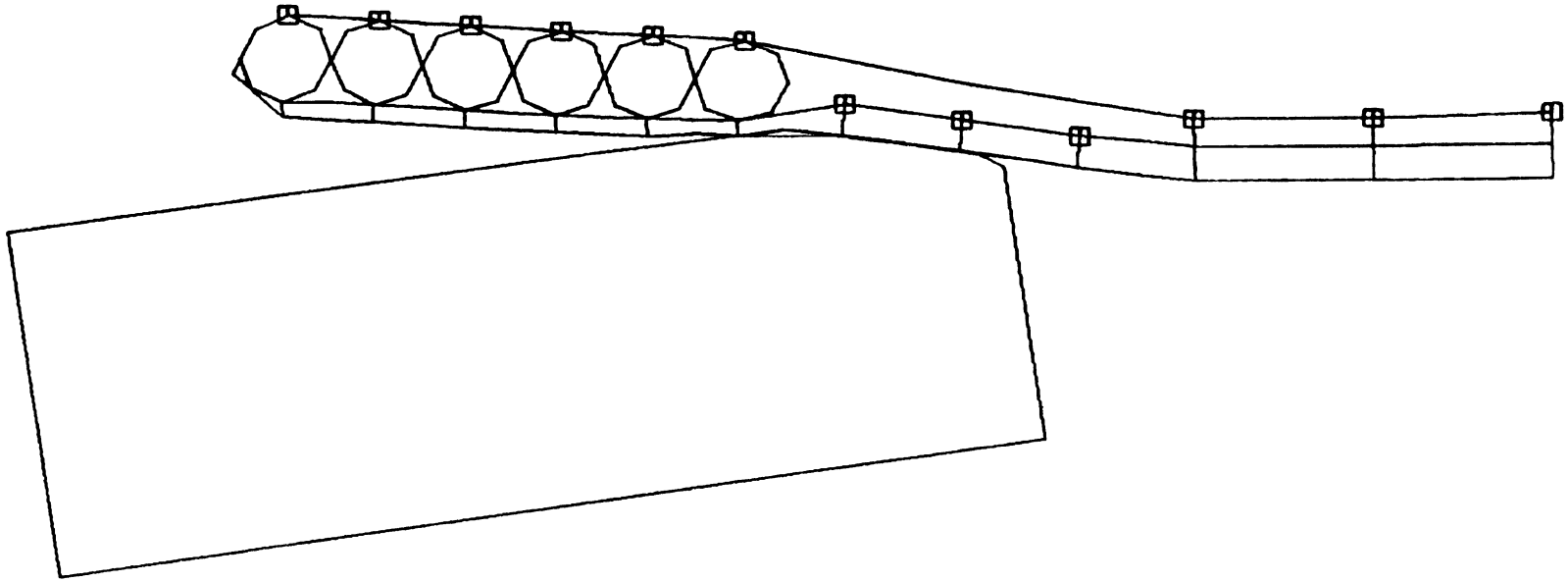

BARREL ANGLE END MOD#2--TEN DEGREES AT 60 MPH

TIME = 0.0800 SEC

FIGURE 3-7c

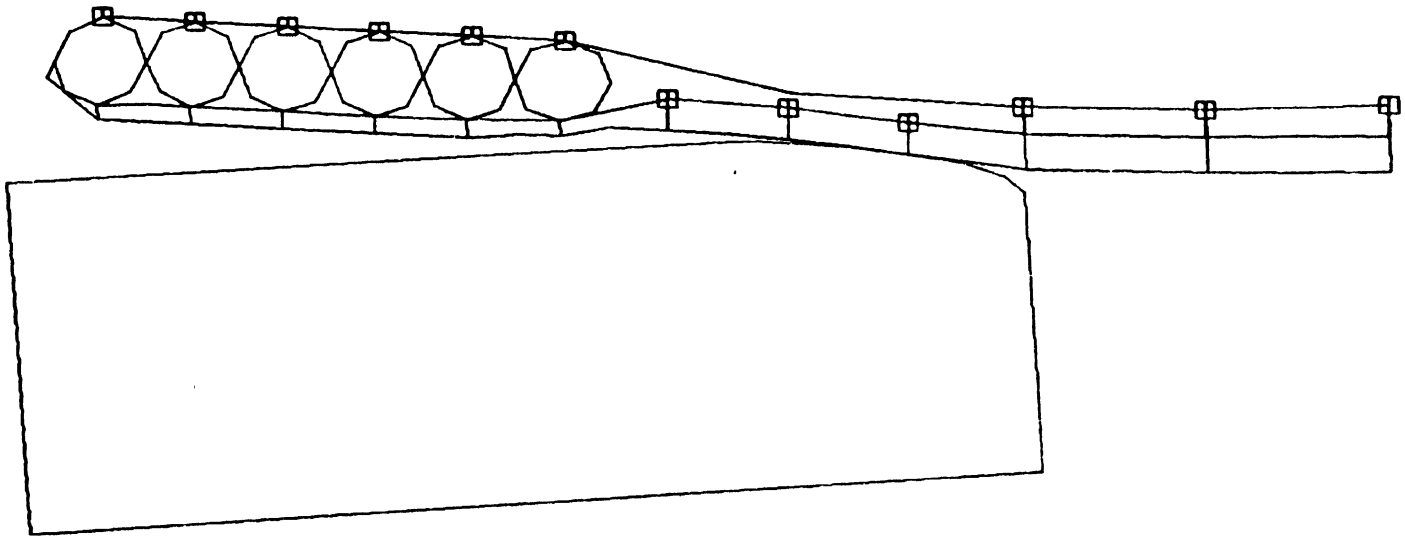

BARREL ANGLE END MOD#2--TEN DEGREES AT 60 MPH

TIME = 0.1200 SEC

FIGURE 3-7D

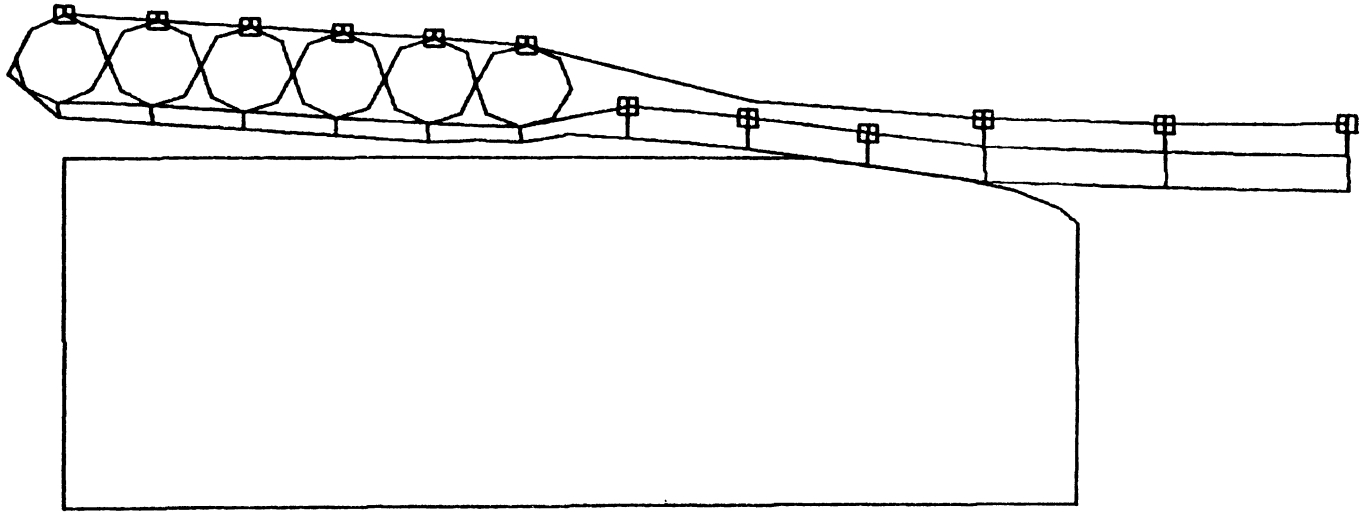

BARREL ANGLE END MOD*2--TEN DEGREES AT 60 MPH

TIME = 0.1400 SEC

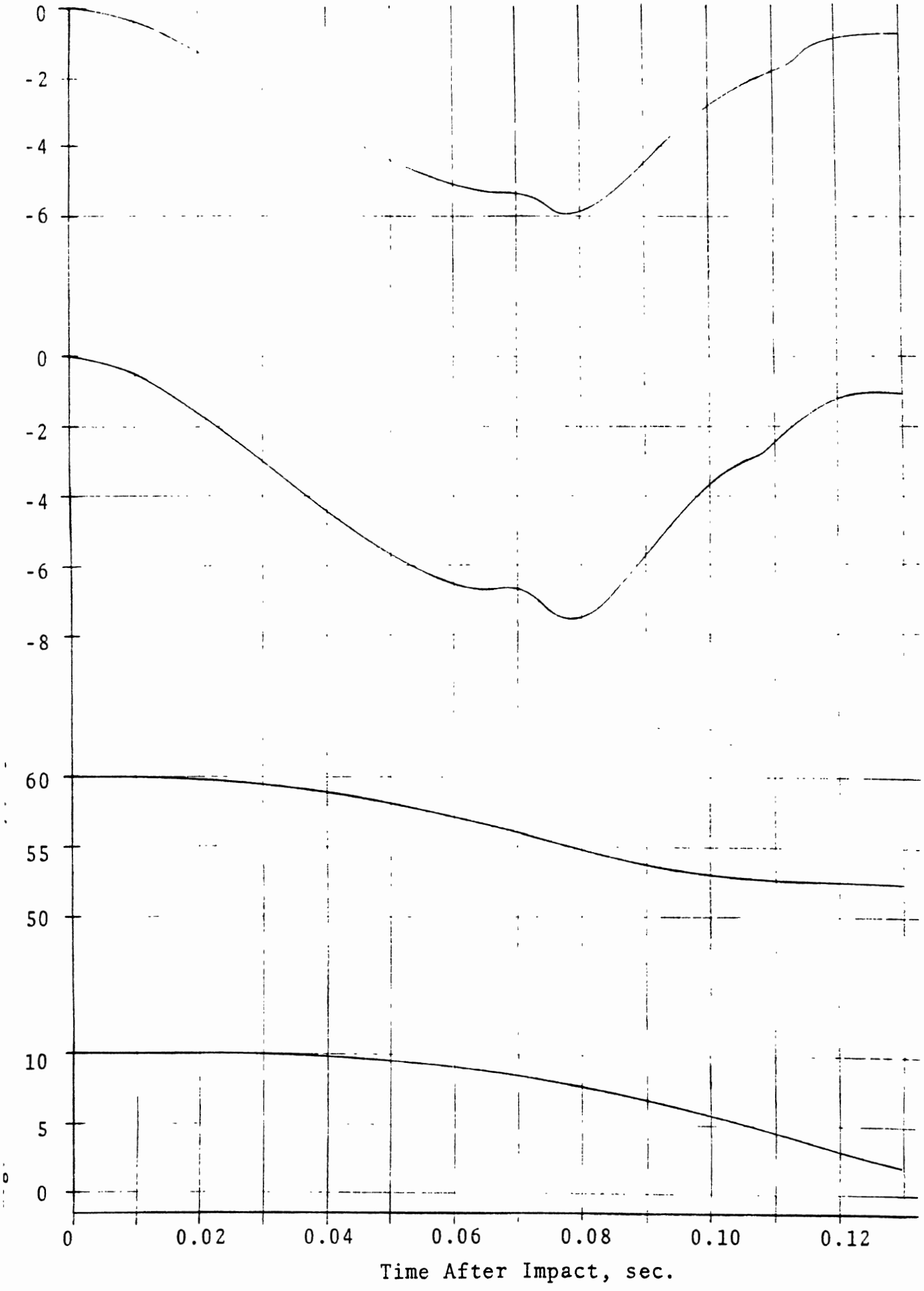

FIGURE 3-8 BARREL ANGLE END TREATMENT KINEMATIC DATA - 60 MPH, 10 DEG. IMPACT

in the longitudinal direction is about 5.9 g's with the maximum over a 100 msec interval being about 3.9 g's. Similar values for lateral acceleration are 7.5 g's maximum and 5.0 g's average, respectively. The longitudinal average value is below the threshold level listed in Table E-4 while corresponding lateral value is not.

It is likely, therefore, that an unrestrained passenger would have sustained some injury in the collision. A lap belt restrained occupant would probably go unharmed, however.

Additional comparative data between test and simulation results is shown on Figures 3-9 and 3-10. On Figure 3-9, longitudinal velocity and acceleration data for the simulation run are compared with similar data which were obtained from photogrammetrically reducing test data. (The acceleration data, in this case, is with respect to an earth fixed coordinate system.) Comparisons are remarkably good. Figure 3-10 shows a comparison of acceleration data in vehicle coordinates with similar data obtained from onboard accelerometers (see Appendix D). Although the accelerometer data is obviously from a much higher bandwidth signal, a general comparison in the two curves is again apparent. Comparisons, therefore, range from good to very good and indicate that a high degree of confidence can be placed in the barrier mathematical idealization.

3.4.2 CASE 2 - 60 mph, 25°. Case 2 is similar in all respects to case 1, except the impact angle was increased to 25°. Sequential plan view schematics for the run are shown on Figures 3-11a through 3-11f. Posts in the end treatment structure begin to fail at about 20 msec after impact. By 130 msec, all posts have failed, and the

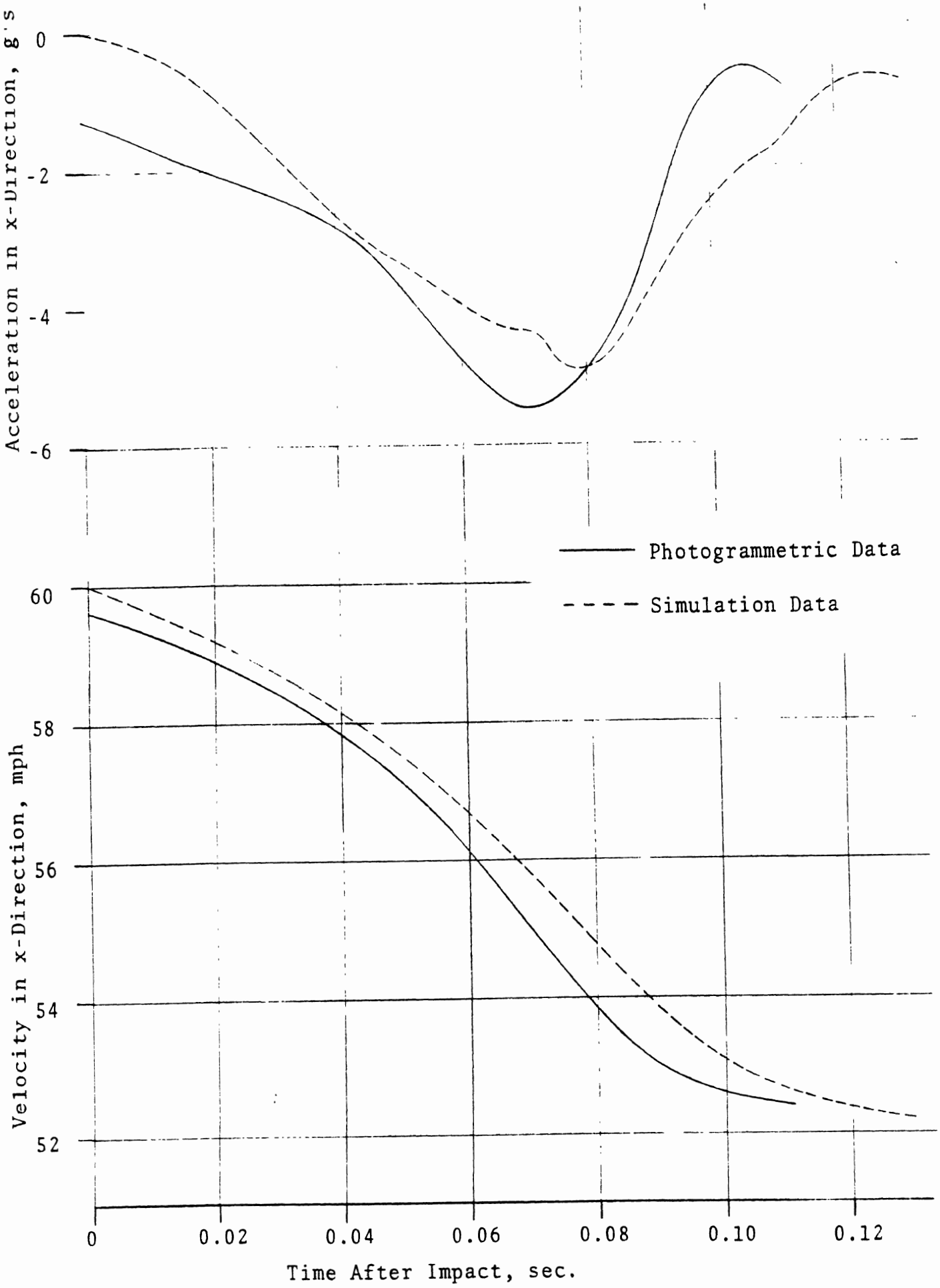

GURE 3-9 BARREL ANGLE END TREATMENT - 60 MPH, 10 DEG. - PHOTOGRAMMETRIC TEST AND SIMULATION DATA COMPARISON (TEST 24)

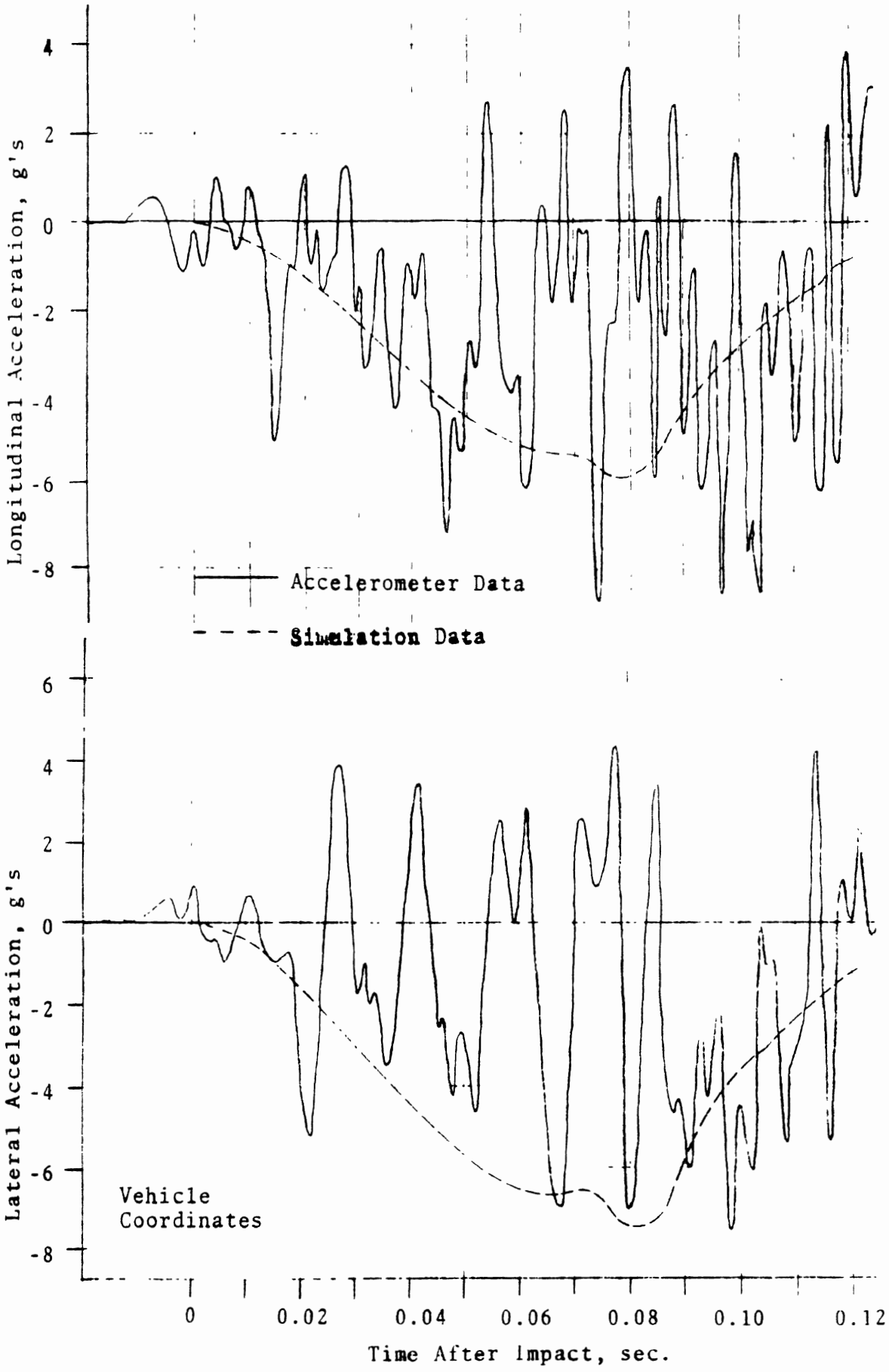

FIGURE 3-10 BARREL ANGLE END TREATMENT - 60 MPH, 10 DEG. - ACCELEROMETE
TEST AND SIMULATION DATA COMPARISON (TEST 24)

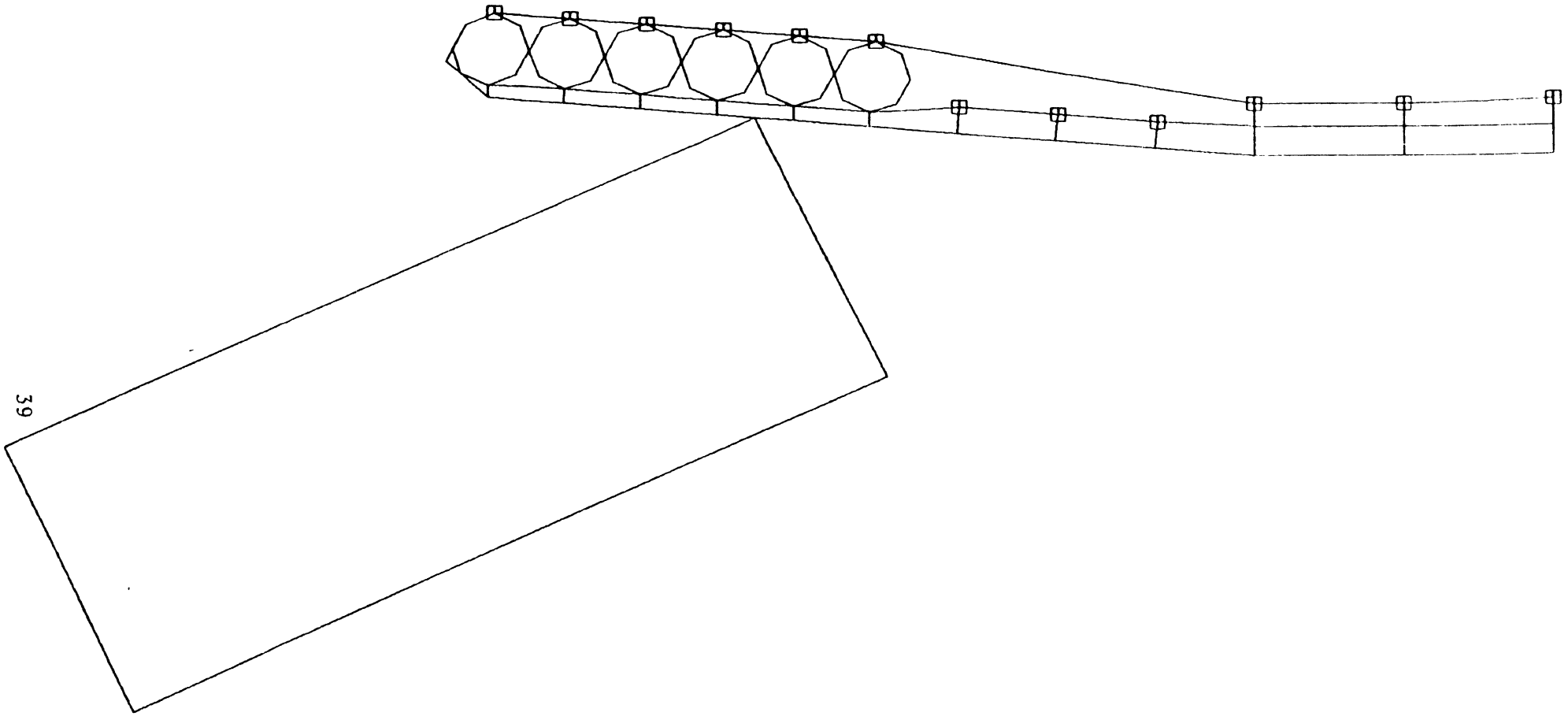

BARREL ANGLE END MOD#2 - 25 DEG AT 60 MPH

TIME = 0.0000 SEC

FIGURE 3-11A

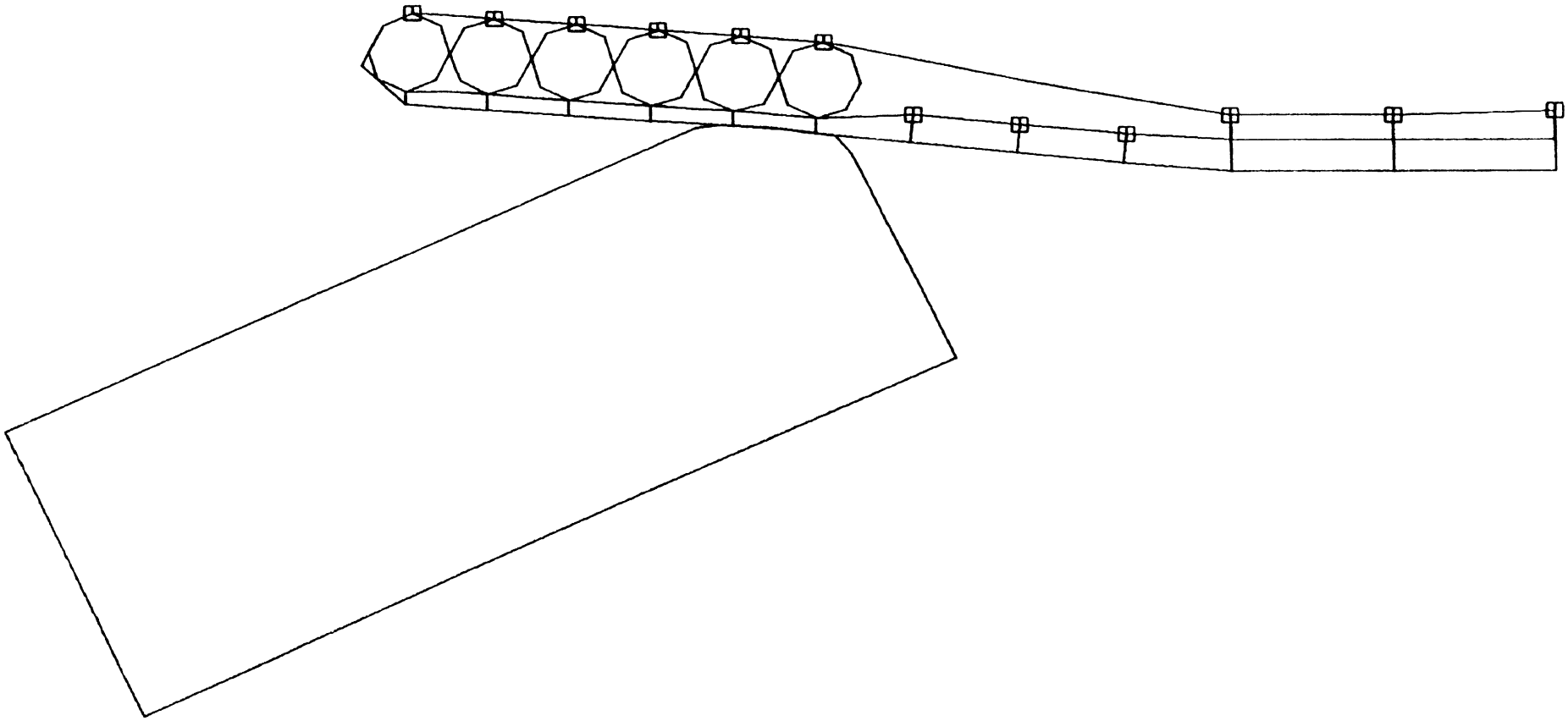

BARREL ANGLE END MOD#2 - 25 DEG AT 60 MPH

TIME = 0.0300 SEC

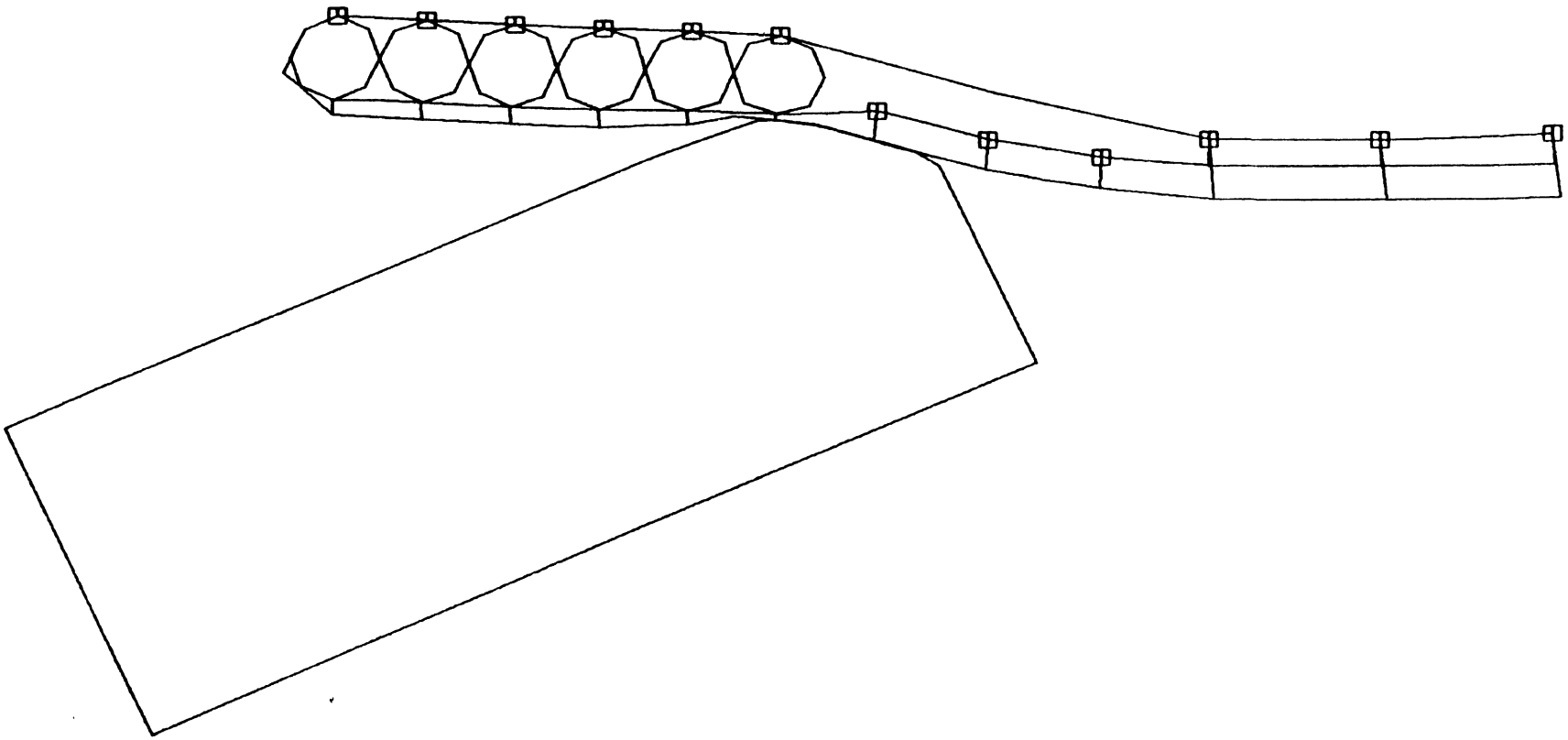

BARREL ANGLE END MOD#2 - 25 DEG AT 60 MPH

TIME = 0.0600 SEC

FIGURE 3-11c

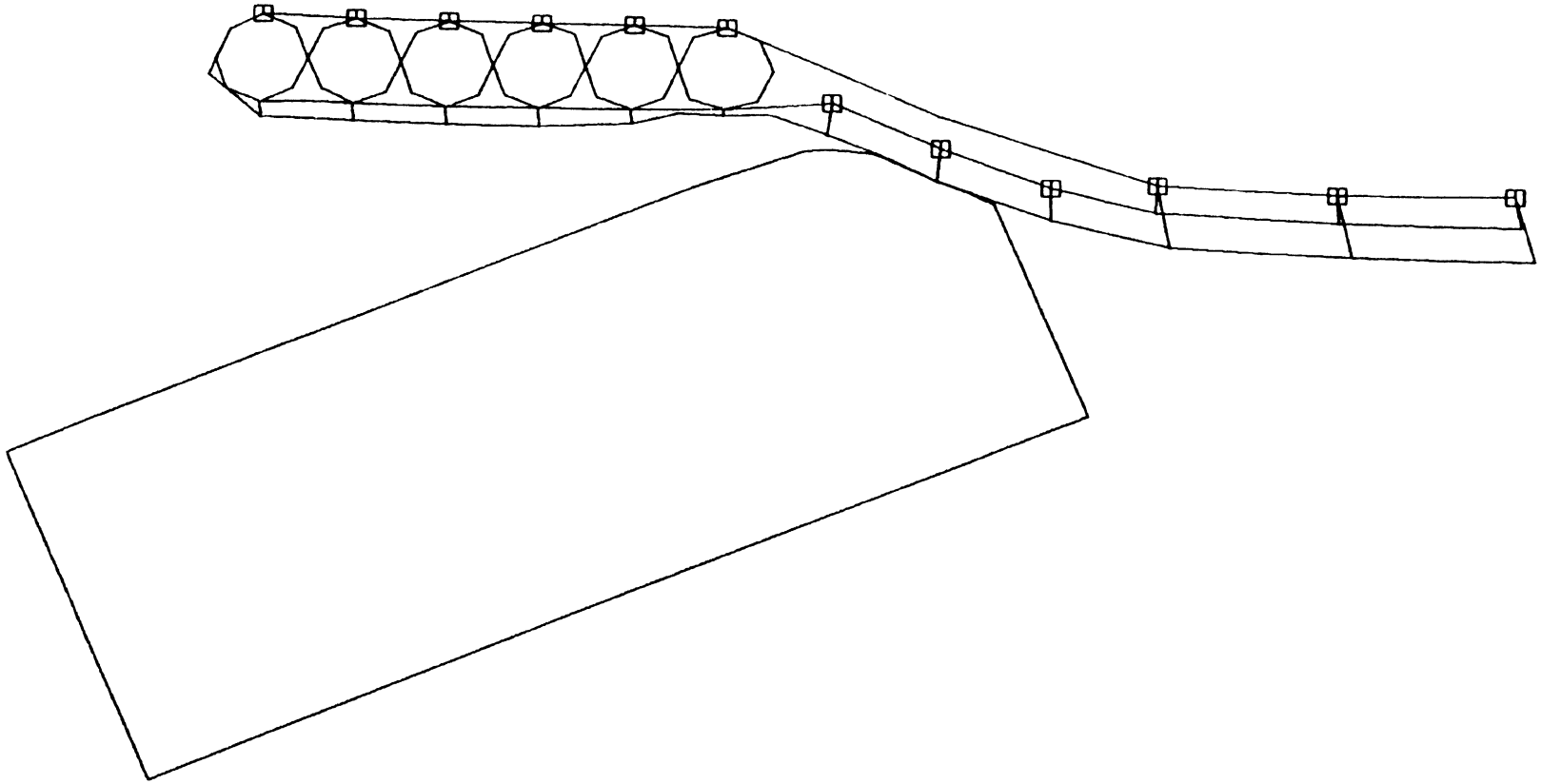

BARREL ANGLE END MOD#2 - 25 DEG AT 60 MPH

TIME - 0.0900 SEC

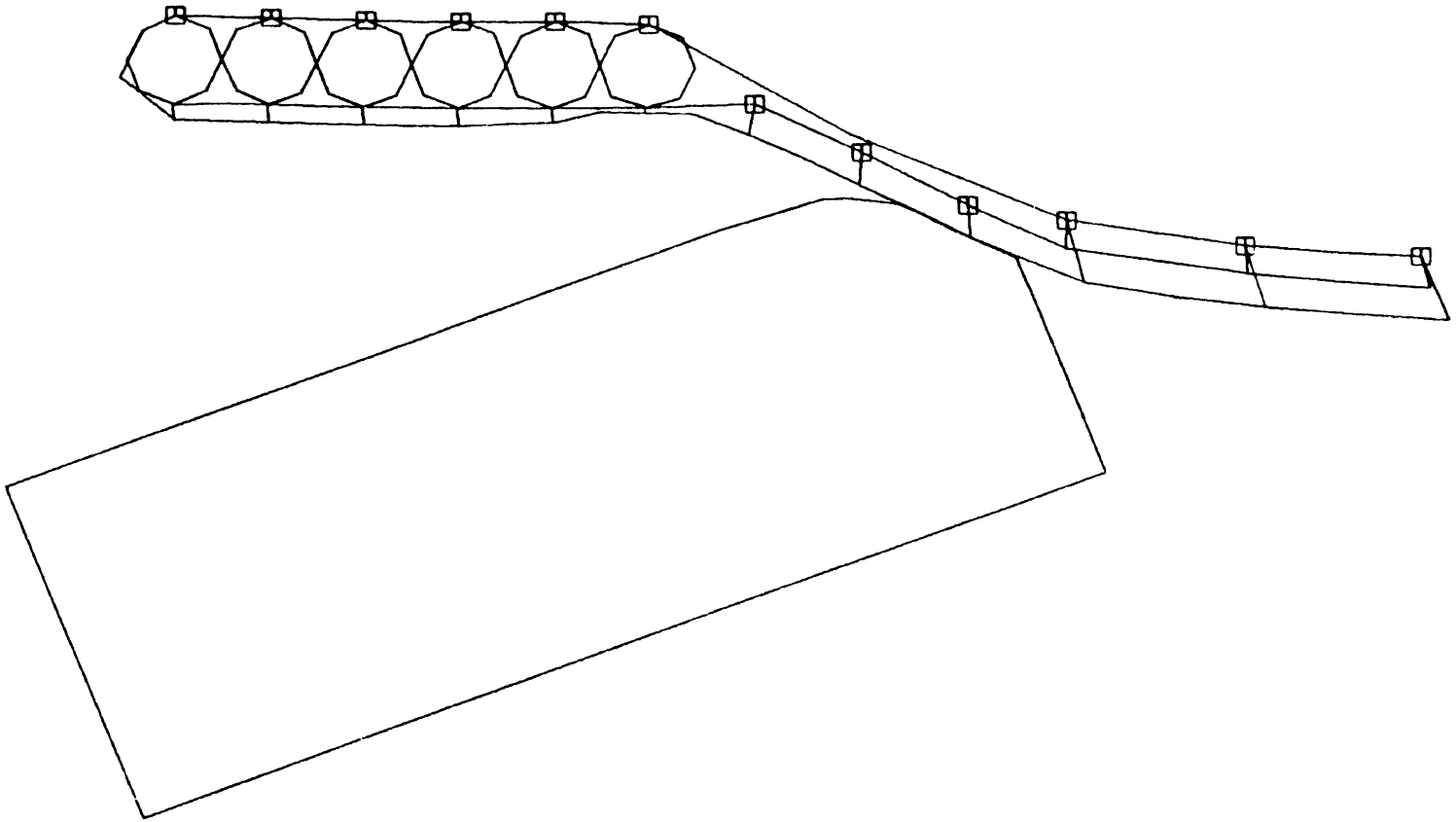

BARREL ANGLE END MOD#2 - 25 DEG AT 60 MPH

TIME = 0.1200 SEC

FIGURE 3-11E

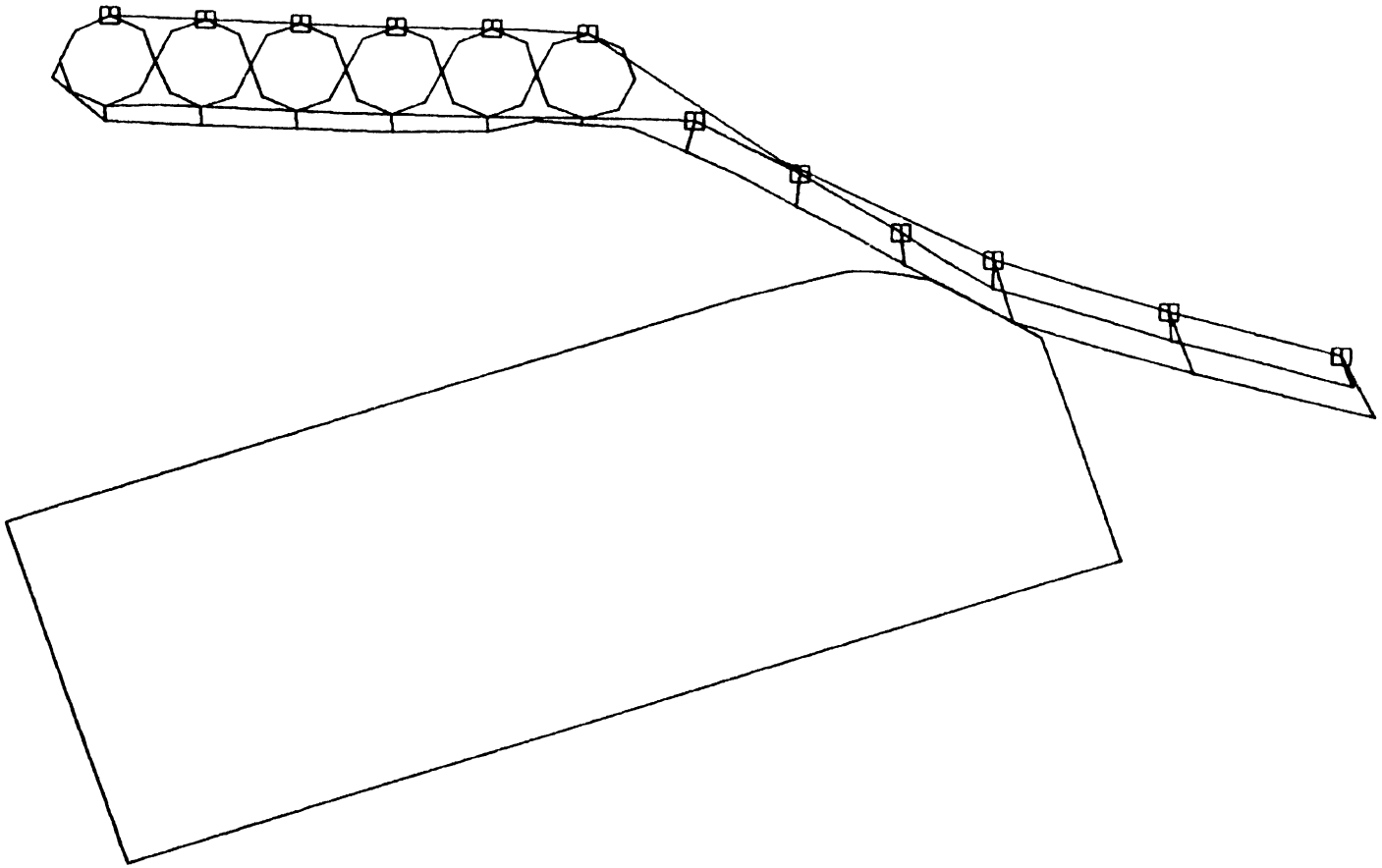

BARREL ANGLE END MØD#2 - 25 DEG AT 60 MPH

TIME = 0.1500 SEC

structure is essentially rotating intact about the rigid right end anchor post.

The right end anchor post is a simulation added feature which is necessary to produce a stable solution and does not represent a real barrier element. Therefore, after 130 msec, the simulation results are probably unreliable.

At the 120 msec point, the vehicle is traveling at 41 mph and has been redirected approximately 5° from its initial direction. The leading end of the barrier has deflected almost 40 inches, and the vehicle is sliding along the barrier near post 10. It seems probable but not entirely clear that the vehicle will eventually be redirected.

Acceleration (vehicle coordinates), velocity, and heading angle histories are shown on Figure 3-12. Maximum accelerations in the longitudinal and lateral directions are 13.4 g's and 8.8 g's, respectively. Average accelerations over 100 msec were 8.9 g's longitudinally and 4.4 g's laterally. Each of these represents probable injury to an unrestrained passenger, but not to one using a lap belt.

3.4.3 CASE 3 - 60 mph, 0°. This case differs from the others in that the vehicle was centered to impact directly on the barrier end. A great deal of difficulty was experienced on trying to make this run because of problems with the simulation program.

One problem involved an excessive number of divisions of the

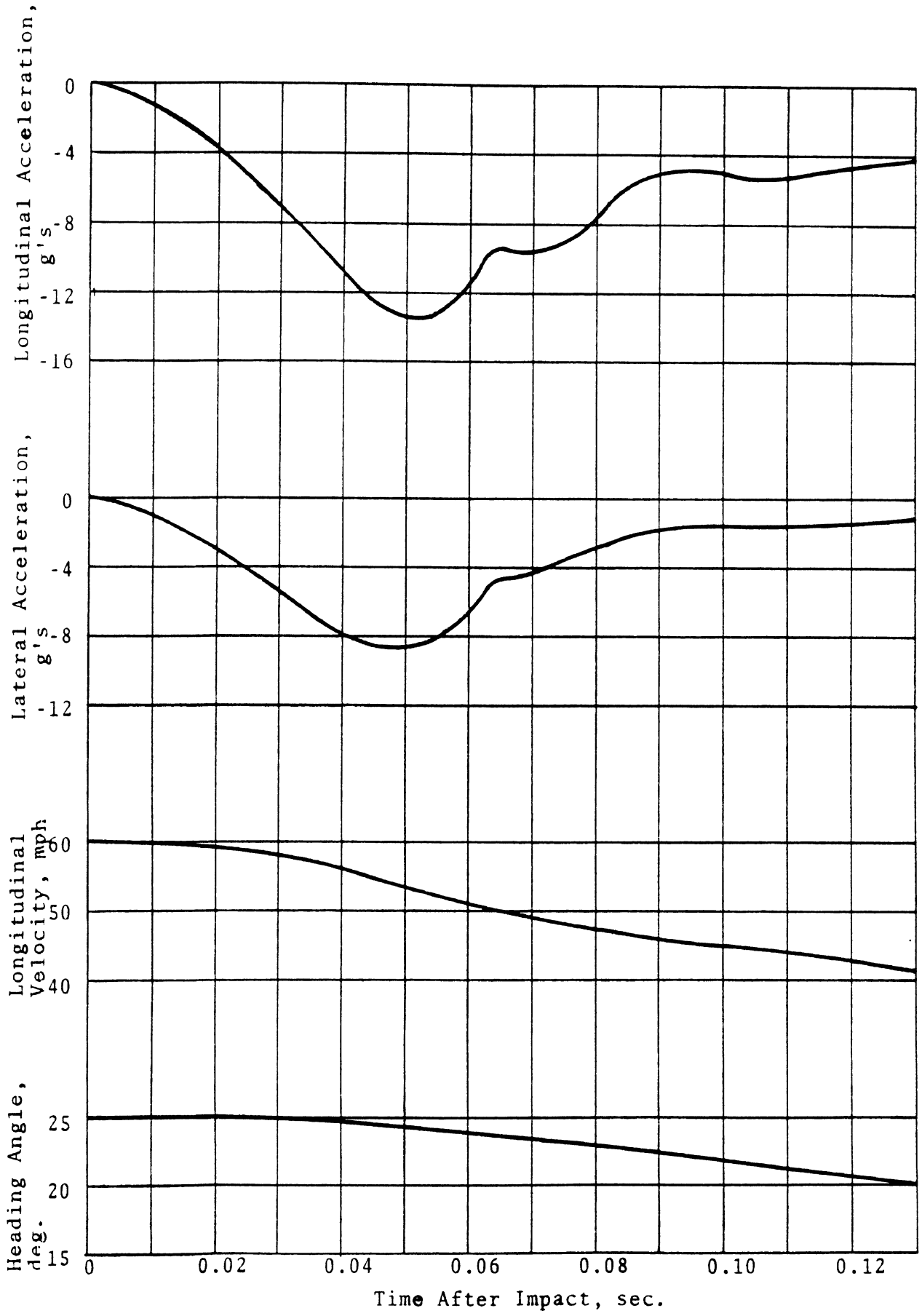

FIGURE 3-12 BARREL ANGLE END TREATMENT KINEMATIC DATA - 60 MPH, 25° IMPACT

integration interval. In the program, a typical structural member is assumed to fail according to the load-deflection curve shown on Figure 3-13. At the end of one integration interval (Point A), an element may be below the failure load, whereas at the end of the next interval, the load may be substantially above failure (Point B). (This is typical of digital simulations of dynamic events, since integration must be done in discrete steps.) If nothing were done to change the situation, the load would remain constant at the value B as the element undergoes plastic deformation. This is unsatisfactory, however, as the element would be stronger than is actually the case. In order to rectify the situation, the integration interval is shortened so that the element load at the new end point just equals the failure load. Actually, this operation is done such that the actual load is within some specified tolerance of the failure load.

If more than one element fails within a given integration interval, the situation gets more complicated. Several successive divisions of the integration interval may be necessary. If more than twenty divisions are required, however, an excessive amount of computer time is necessary and an automatic logic statement terminates the run.

A second problem was associated with the representation of vehicle crush characteristics. Vehicle crush is represented by nonlinear springs which can be arbitrarily arrayed around the vehicle boundary. For the end on impact case almost all of the

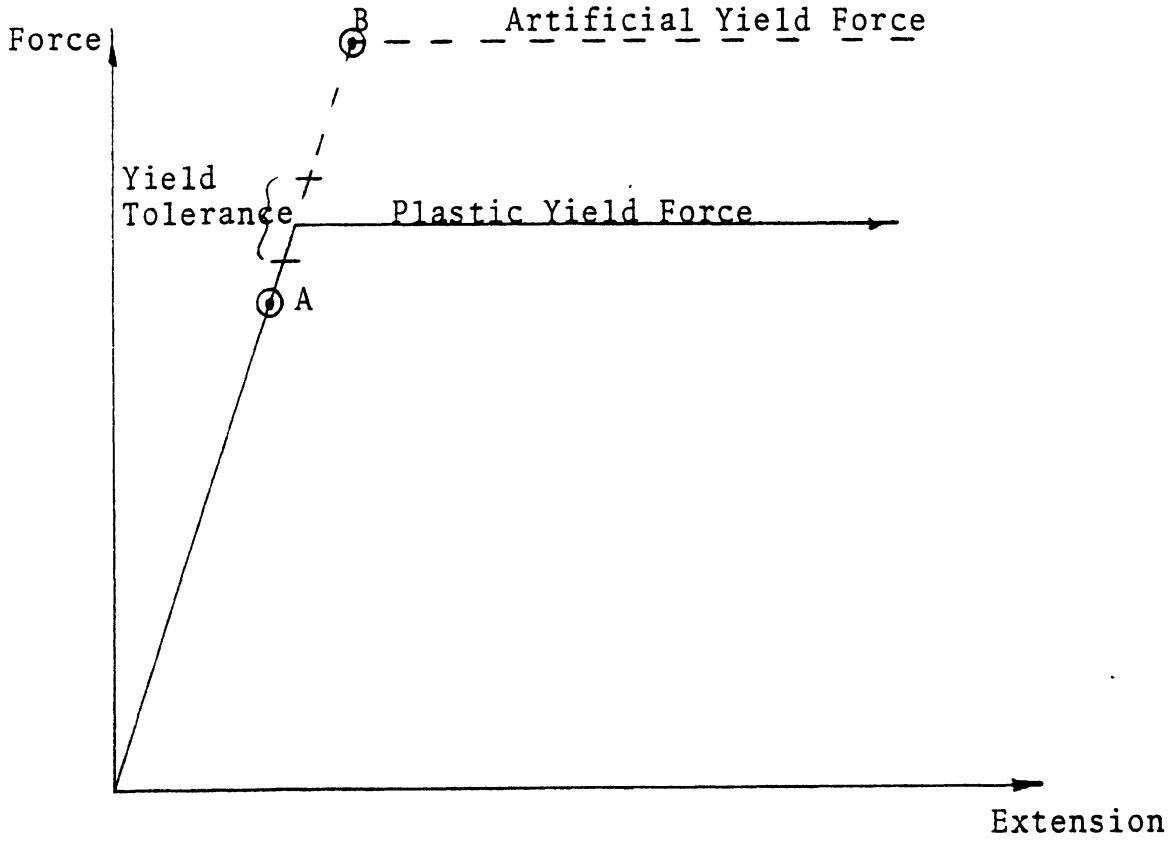

FIGURE 3-13 INTEGRATION INTERVAL YIELD ACCURACY PROBLEM

twenty available springs were located on the vehicle front end. As the front end deflects, the springs directly in contact with the barrier deflect far more than those just slightly to either side (see Figure 3-16). The result is that a sideward gap is created between the deflected and undeflected springs. After a certain stage, the barrier is able to slip sideways through this gap with the result that vehicle/barrier forces are greatly reduced.

Both problems have required realism compromises to achieve a representative end on performance assessment. This has been done by (1) making the vehicle about ten times stiffer in crush than is actually the case, and (2) suppressing the yield overshoot correction subroutine as described earlier. This latter compromise means that some structural elements will yield in the plastic range at load values which are higher than is actually the case.

A set of sequential plan view illustrations showing the end on impact behavior of the vehicle and structure with these two modifications are shown in Figures 3-14a through 3-14f. A comparative set with both the overshoot correction and proper vehicle stiffness are included on Figures 3-15a through 3-15c. The latter figures represent a good approximation to the actual collision mechanics until penetration occurs. A plan view illustrating the penetration problem is shown on Figure 3-16. It should be made clear that this figure in no way represents a case of predicted spearing as might be implied.

An examination of Figures 3-14a through 3-14f shows that the

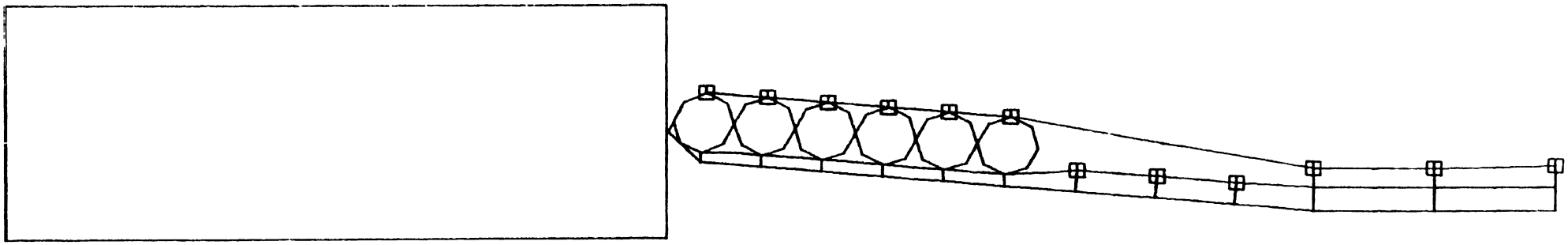

BARREL ANGLE END MOD#2 - END-ON IMPACT - ZERO DEGREES AT 60 MPH

TIME = 0.0000 SEC

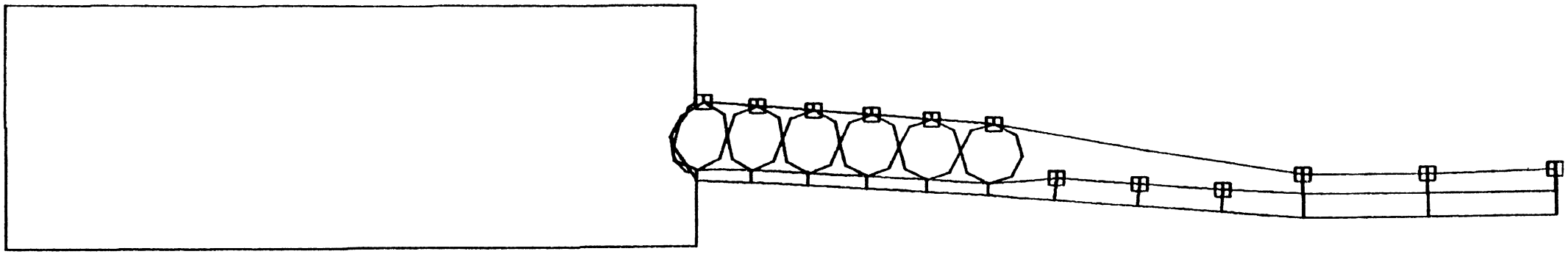

BARREL ANGLE END MOD#2 - END-ON IMPACT - ZERO DEGREES AT 60 MPH

TIME = 0.0200 SEC

FIGURE 3-14B (STIFFENED VEHICLE)

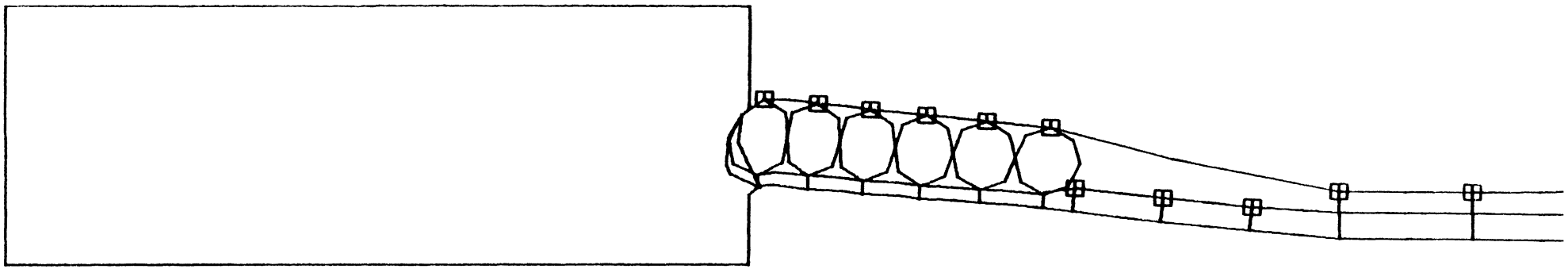

BARREL ANGLE END MOD#2 - END-ON IMPACT - ZERO DEGREES AT 60 MPH

TIME = 0.0400 SEC

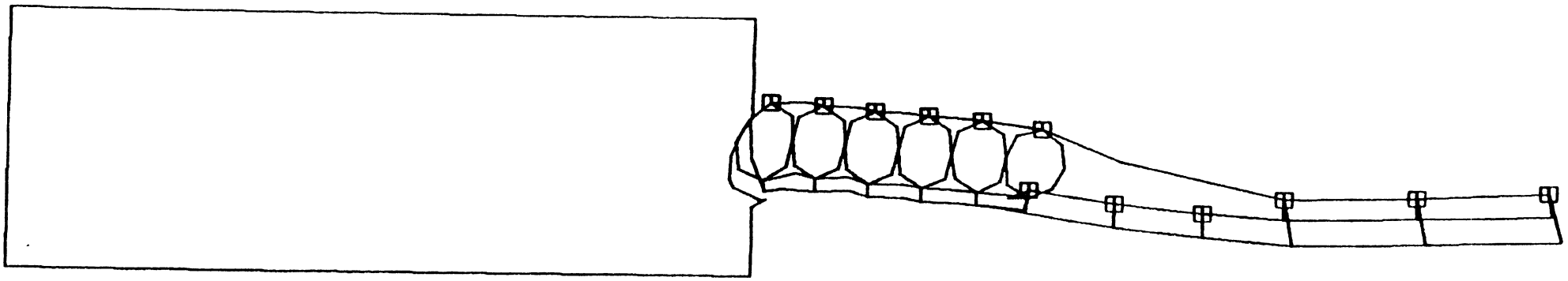

BARREL ANGLE END MOD#2 - END-ON IMPACT - ZERO DEGREES AT 60 MPH

TIME = 0.0600 SEC

FIGURE 3-14D (STIFFENED VEHICLE)

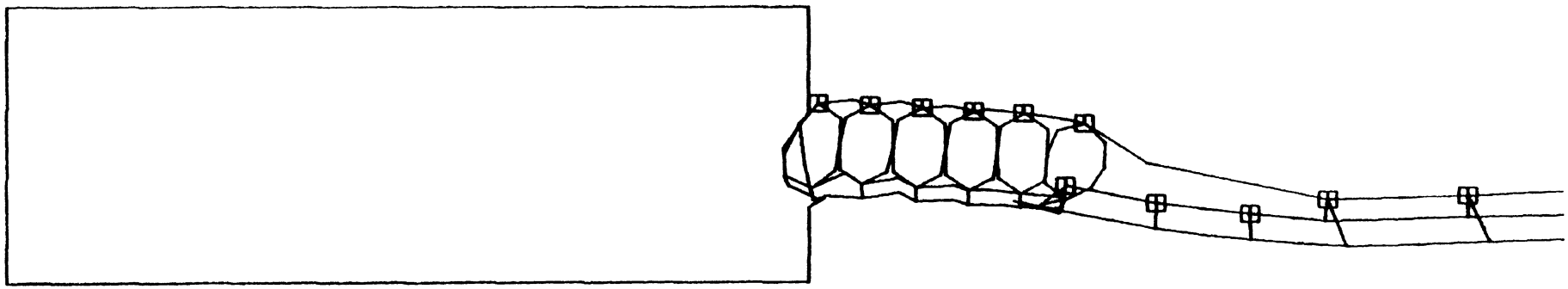

BARREL ANGLE END MOD#2 - END-ON IMPACT - ZERO DEGREES AT 60 MPH

TIME = 0.0800 SEC

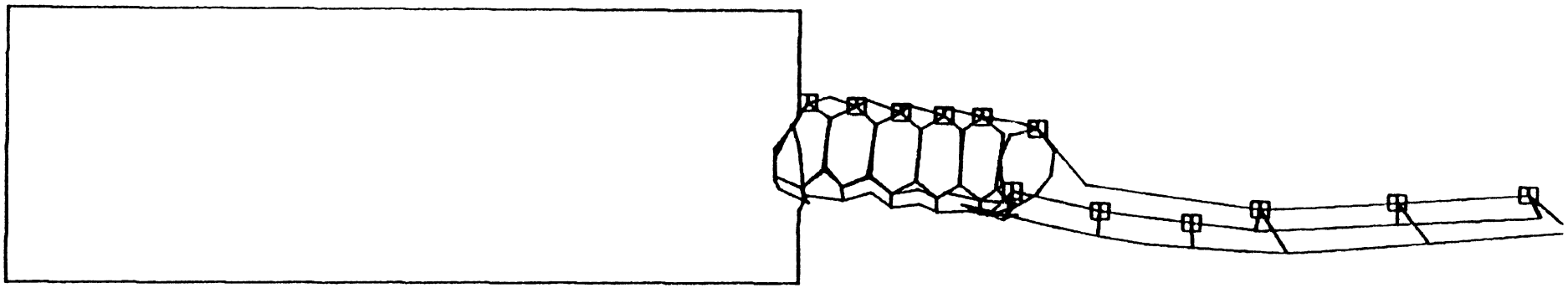

BARREL ANGLE END MØD#2 - END-ØN IMPACT - ZERØ DEGREES AT 60 MPH

TIME = 0.1000 SEC

FIGURE 3-14F (STIFFENED VEHICLE)

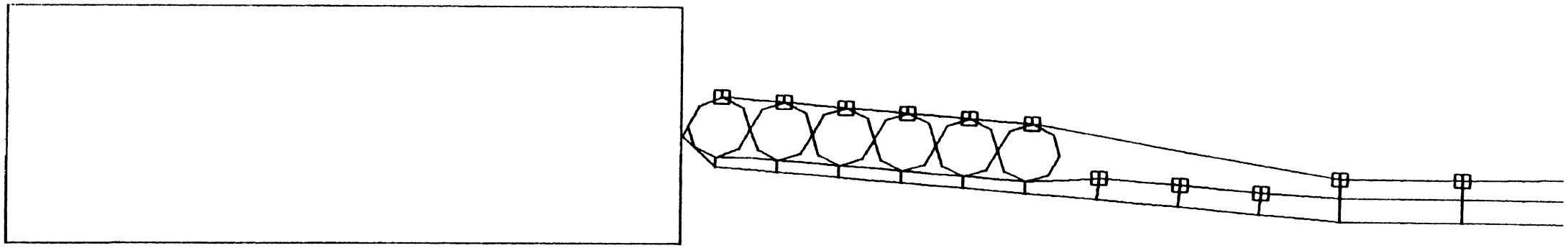

BARREL ANGLE END MOD#2 - END-ON IMPACT - ZERO DEGREES AT 60 MPH

TIME = 0.0000 SEC

FIGURE 3-15A (REALISTIC VEHICLE)

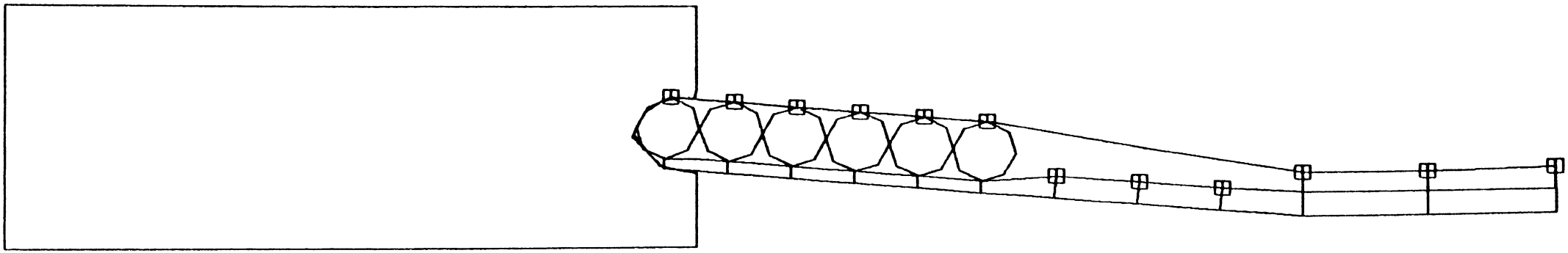

BARREL ANGLE END MOD#2 - END-ON IMPACT - ZERO DEGREES AT 60 MPH

TIME = 0.0200 SEC

FIGURE 3-15B (REALISTIC VEHICLE)

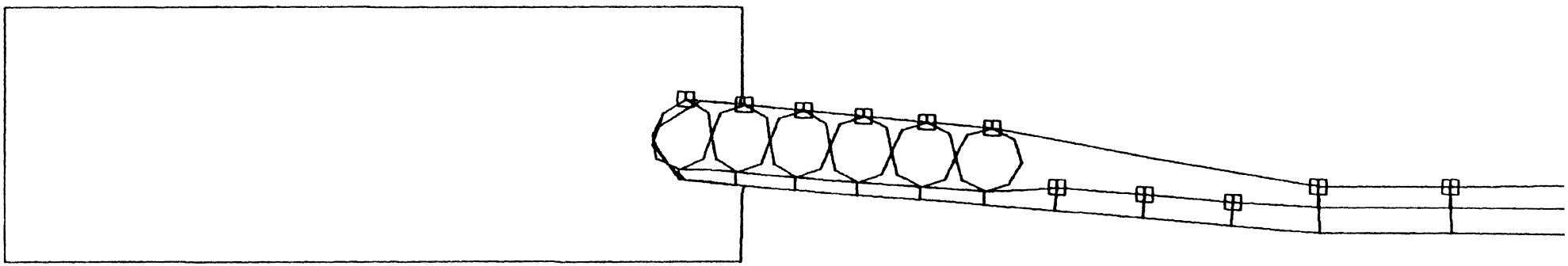

BARREL ANGLE END MØD#2 - END-ØN IMPACT - ZERØ DEGREES AT 60 MPH

TIME = 0.0400 SEC

FIGURE 3-15c (REALISTIC VEHICLE)

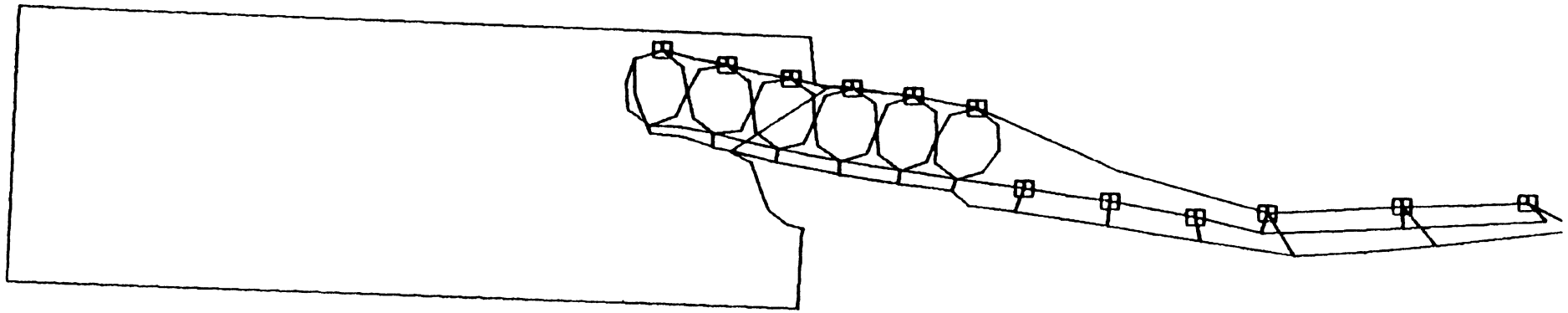

BARREL ANGLE END MOD#2 - END-ON IMPACT - ZERO DEGREES AT 60 MPH

TIME = 0.1000 SEC

FIGURE 3-16 SIMULATION BREAK DOWN THROUGH PENETRATION

barrel array is moved backward as the end is subjected to load. (Compare time 0.02 with subsequent times, in terms of relative position of barrel 6 and post 7.) Posts supporting the barrels fail completely as well as does the 8" X 3/16" steel plate surrounding the barrels. The upper W-beam (beginning at post 7 and continuing downstream) does not fail, however, and remains rigid as the barrel array is pushed past it. At the end of the run, the vehicle is traveling at 40 mph. It is very possible, therefore, that the vehicle could have continued into the structure and encountered the rigid rail end. Further research will be required to investigate this potential problem.

Longitudinal acceleration and velocity traces for the stiffer vehicle case are shown on Figure 3-17. An early part of the realistic vehicle acceleration trace is also shown. It can be noted that acceleration, as expected, builds up more rapidly for the stiffer vehicle since vehicle impact resistance is greater. After about 30 msec, however, acceleration levels are similar for the two cases. At about 50 msec, the barrier begins to penetrate the more realistic vehicle and the acceleration profile for this case is no longer representative. On the basis of these comparisons, however, it is reasonable to assume that:

1. The first 40 msec of the realistic vehicle impact are very close to what can be expected in the actual situation.
2. The remainder of the impact is not overly different from the stiffened vehicle run.

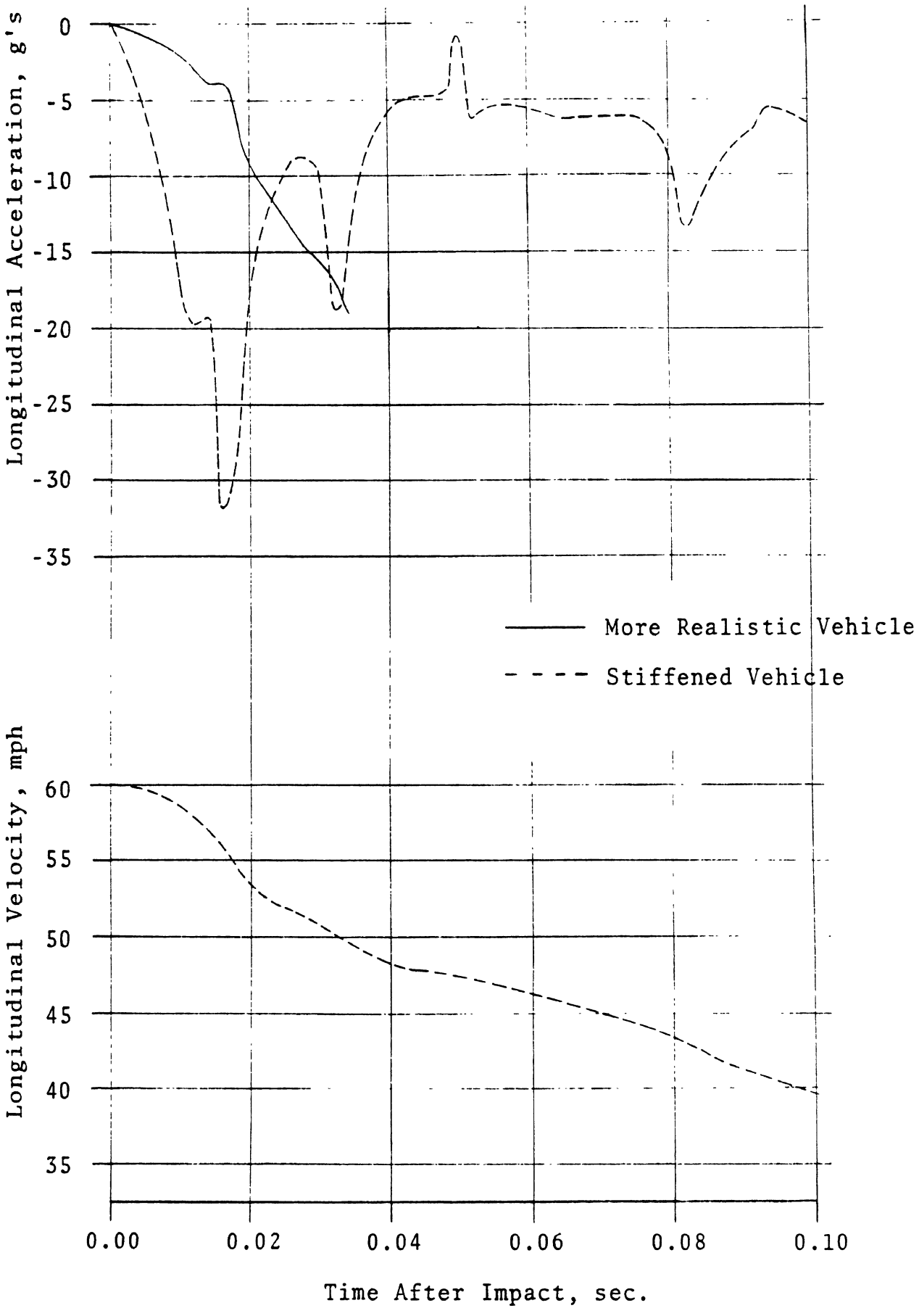

FIGURE 3-17 BARREL ANGLE END TREATMENT - 60 MPH, END ON - SIMULATION ACCELERATION AND VELOCITY HISTORIES

It could be argued that statement 2. is on less firm ground because the overshoot subroutine has been suppressed — the rationale being that in some cases structural members are unrealistically strong. This argument carries less weight, however, with increasing time into the impact. By 40 msec, all pinned link members (representing column buckling in the beam elements) have failed, all posts from the end back to three posts upstream of the barrels have failed, as well as have most of the beam elements not associated with the W-beam. In fact, the only remaining structural members are the partially crushed barrels and the W-beams. For the remainder of the run, only two of the fifteen W-beam elements enter the plastic yield region and both of these yield within 5% of the specified yield value. Therefore, it seems safe to conclude that after 40 msec, the actual impact situation is closely represented by the stiffened vehicle run.

Having established the validity of the acceleration data, an examination of the plotted values indicates that the deceleration levels are reasonably high, but not dangerously so. An unrestrained passenger would undoubtedly be injured, but one wearing a lap belt would not.

3.4.4 END TREATMENT ASSESSMENT. On the basis of the well validated simulation exercises described here, it can be concluded that the barrel angle, break-away absorber end treatment is a good beginning toward a satisfactory guardrail end, but is not yet ready for operational deployment. Redirective characteristics at 60 mph

and 10° are excellent for the region downstream from the fourth barrel. Vehicle damage can be expected to be moderate. Results are less satisfactory for the same conditions but with a 25° impact angle. Injury to an unrestrained passenger is indicated for these conditions. Vehicle damages will undoubtedly be severe. End on performance is similar to the 60 mph, 25° case in that only a passenger restrained with a lap belt could expect to escape injury. Vehicle damages approaching a total loss can be anticipated, however. In addition, the potential for spearing may exist and will require further investigation.

Angle impacts covering the region from the end downstream to barrel 4 were not simulated. Hence, performance in this region is unknown. Impacts at speeds other than 60 mph were also not made. Before embarking on these additional exercises, however, some modifications to improve the end treatment performance are in order.

As a first step, the barrier longitudinal stiffness should be reduced. This will improve the barrier's break-away characteristics in an end on impact and reduce resulting passenger loadings (particularly the high g deceleration in the first 30 msec). Second, the barrier's lateral resistance should be increased. This will improve angle impact redirective performance and reduce both vehicle and barrier damage. Finally, a means should be devised to insure that the W-beam end does not become exposed as the barrel array slides by in an end on impact.

Some suggested modifications to meet these objectives include:

1. Barrels with weaker crush characteristics,
2. Fewer barrel post supports,
3. A blocked out overlapped W-beam that telescopes longitudinal as a front for the barrels, and for a distance of about twenty to thirty feet downstream from the barrels,
4. An end anchor at the extreme upstream end that breaks away under end on impacts but holds firm for angled impacts downstream from the end.

Whatever the modifications that are ultimately made, it is strongly recommended that a simulation exercise be carried out to evaluate the prospective design before it is subjected to test.

3.5 END TREATMENT DESIGN GUIDELINES

A set of design guidelines were developed as a part of the curren research, which are suggested for use in end treatment development work. As discussed in Appendix E, the formulation of such guidelines represents the final step in a development program before arriving at a candidate design. The guidelines include considerations of costs, climatic factors, esthetics, and performance. Performance design guidelines are not as simple as would ordinarily be the case, because of the several modes in which an end treatment can function. The performance design considerations are therefore divided into four categories: a common set for all end treatments, a set for reflective treatments, and additional sets for break-away and impact absorbing ends. Considerations relating to costs, climate, and esthetics are essentially the same for all cases.

I. Performance

Common

1. The end treatment longitudinal anchorage strength shall be compatible with the tension requirements of the warranted section.

Break-away

1. The end treatment length shall be great enough to preclude a vehicle entering the hazardous area following break-through.
2. End treatment elements shall be protected such that elements which might be fractured or exposed as a result of break-through do not present a spearing hazard.
3. Structure lateral strength shall be such that (a) in the break-away end region, lateral strength shall be minimum and (b) in the transition region a positive mechanism shall exist such that the vehicle is either deflected in front of, or behind the rail so as to preclude pocketing.

Impact Absorbing

1. The end treatment length and longitudinal resistance shall be compatible with similar values for an impact absorbing barrier.
2. The end treatment lateral impact resistance shall be compatible with the warranted section of guardrail.
3. The end treatment height shall be consistent with

the warranted section of guardrail and the structure shall maintain this height throughout its design deflection range.

4. The end treatment surface shall be smooth and blocked out so as to prevent wheel snagging.

5. The elevation of the line of action of the end treatment, end on resisting force shall be compatible with the range of C.G. heights in the vehicle population so as to prevent tunneling, or ramping.

Reflective

1. The end treatment reflective characteristics shall be such as to prevent the vehicle from striking the end section regardless of impact conditions.

2. The end treatment design shall be such as to preclude the vehicle from entering the hazardous area following reflection behind the rail.

3. The end on approach profile shall be such as to prevent the vehicle from mounting the guardrail and riding along its upper surface.

4. The end on profile shall be such as to preclude the vehicle from being launched into the air and pitched, or rolled over.

II. Climatic

1. The end treatment functional design shall be such as to minimize variations in performance resulting from seasonal weather changes.

2. End treatment materials shall be chosen such that corrosion, rot, sunlight deterioration, and other age and deterioration factors are minimized.

III. Cost

1. The end treatment shall be capable of quick, safe, and easy repair.
2. Installation and materials costs shall be kept reasonably low.
3. Maintenance costs shall be kept to a minimum.
4. Vehicle damage cost shall be kept to a compatible minimum.

IV. Esthetics

1. The end treatment shall permit adequate lateral visibility.
2. The end treatment shall have a pleasing appearance.

V. Traffic Control

1. The end treatment shall permit adequate site distance visibility.
2. The end treatment shall not be so imposing as to cause traffic to veer from the road edge.

3.6 CONCLUSIONS AND RECOMMENDATIONS

The historical evaluation of guardrail ends has shown that bare ends terminated at standard guardrail height can cause spearing in end on impacts. Ramped rail ends, on the other hand, have been found to vault vehicles into the air and cause roll over. While no as bad as spearing, vaulting and roll over also represent

unsatisfactory end treatment performance.

In the research activities described here, both an earth mound and a break-away absorber end treatment were evaluated. The first was found to act very much like a ramped rail end in vaulting the test vehicle and causing it to roll over. Recommendations for a modified design are presented, but even these have obvious deficiencies The main problem area is in producing a transition between road shoulder level and guardrail height without creating a ramp. A validated simulation program (CALSVA) will allow evaluation of modified earthen end treatments should a satisfactory design be developed. This step is not recommended for any of the current designs, however.

The break-away, absorber end treatment was found to perform satisfactorily for low angle (10°, or less) side impacts. Performance was less satisfactory for high angle (25°) side impacts, and end on impacts. Before further analysis or testing of this end treatment is undertaken, it is recommended that several design modifications be considered. These are listed in Section 3.4. In addition, it is recommended that the BARRIER simulation program be modified such that the vehicle crush representati does not allow penetration between the springs arrayed around the vehicle boundary. This modification would greatly facilitate studies of guardrail end configurations.

The design guidelines provide a rational means of developing an effective end treatment. It is recommended that they be used in future end treatment development exercises.

4. CURB INVESTIGATIONS

The curb investigations described here include a state-of-the-art review and a discussion of the simulation exercises carried on at HSRI. These latter exercises are used to evaluate the impact performance of MDSH curbs A, B, C, D and K. Comparisons, where possible, are made between the simulation results and the results from tests conducted by other organizations. A statistical analysis is used to evaluate the redirection effectiveness of two optimized barrier curbs which were developed in Europe. Design guidelines are presented as an aid in developing more effective barrier curbs.

4.1 DEFINITIONS

Curbs in current highway design practice serve the following functions [11]:

1. Control rainfall drainage
2. Deter vehicles from leaving the pavement
3. Delineate the road edge
4. Present a finished appearance
5. Assist in orderly development of the roadside.

The discussion that follows will be centered on the second of these, i.e., the effect that curbs have on redirecting vehicles which leave the roadway. The curbs under consideration are of two types: mountable or barrier.

Mountable curbs are designed so that vehicles can cross when required. These are low and have flat or round sloping faces. Curb heights are usually on the order of six inches, or less. Mountable curbs are generally used in areas where the road edge can be used for emergency pull-offs.

Barrier curbs are relatively high and steep-faced and are designed to inhibit vehicles from leaving the pavement. Heights most frequently range between six and twelve inches. The face, if it slopes, does not exceed one inch per three inches of height. The upper corner is often rounded or chamfered to discourage the wheel rim from biting into the curb face.

4.2 HISTORICAL REVIEW

The first published research on curb mounting and redirection was carried out in 1953 by the California Division of Highways [12]. The research consisted of 149 full-scale impact tests on eleven different curb cross-sections (see Figure 4-1). Impact speeds ranged from 5 to 50 mph at angles between five and thirty degrees. All curbs except one in the series were considered to be barrier curbs. The one mountable curb was Curb X. Of the eleven curbs, eight were nine inches high, one was six inches, and two were twelve inches high. The two nine-inch curbs found to most efficient in redirection were Curbs V and VI-M. Both curbs were rounded at the top and

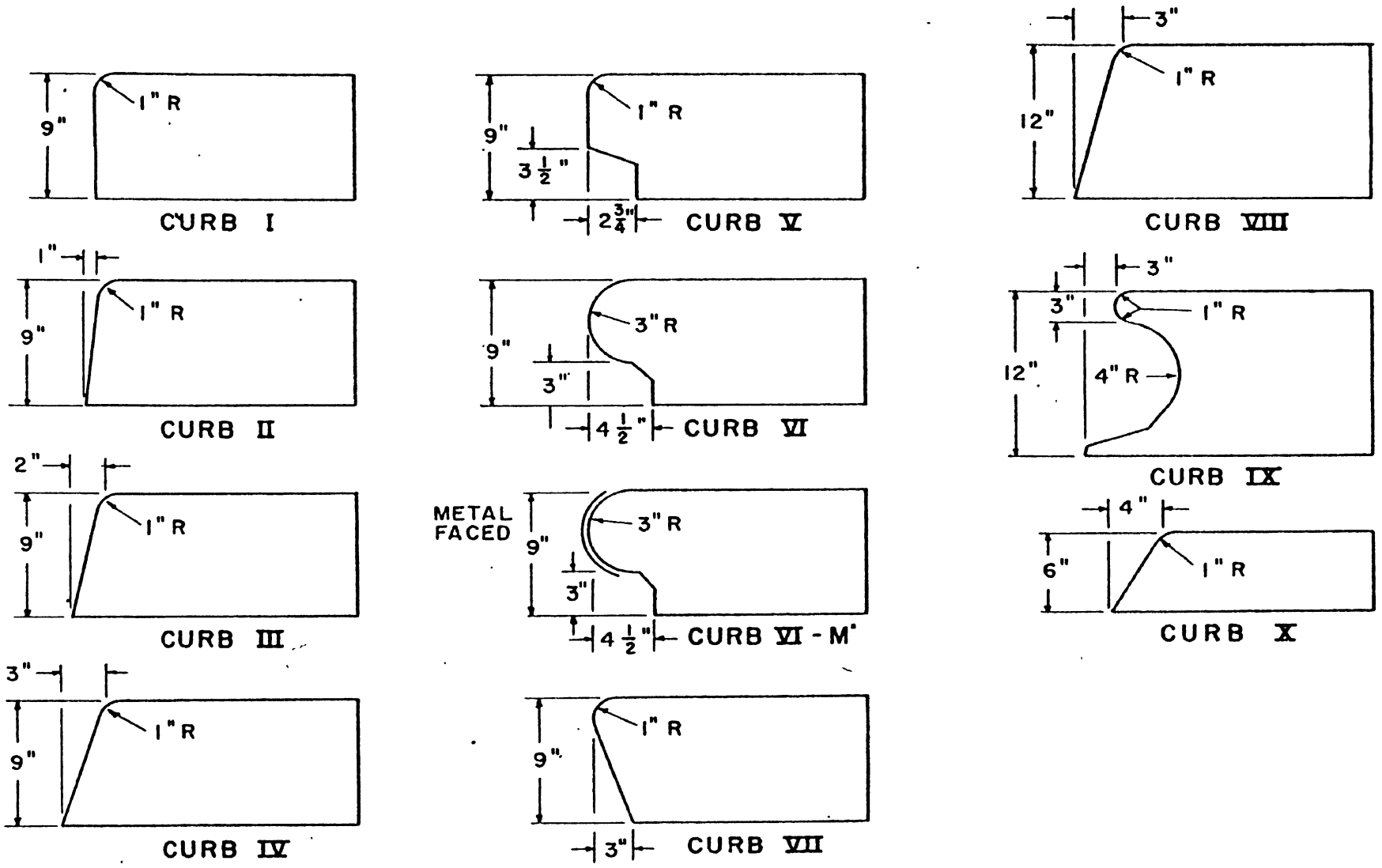

FIGURE 4-1. 1953 STATE OF CALIFORNIA TEST CURBS.

undercut. Curb VI-M was fitted with a metal facing to reduce tire/curb friction forces, and thus reduce the tendency for mounting. All curbs in the test series were standard cross-sections then in use on California highways. A summary of the test results is given on Figures 4-5 through 4-13 and 4-18 and 4-19 of Section 4.4.

As the result of these tests, a second series of barrier curb tests was undertaken in 1955 so that specific recommendations could be made for the design of more efficient barrier curbs [13]. Four basic cross sections were tested, with shims being used to achieve a desired height as indicated on Figure 4-2. The designs were essentially modifications of the V and VI-M designs tested earlier. Test results are shown on Figures 4-14 through 4-16 and 4-20.

Conclusions from the two test series indicate that an efficient barrier curb should be at least ten inches high and that it should be undercut. The curb surface texture should be neither smooth nor rough. A smooth surface tends to redirect a vehicle back into traffic at a relatively high angle, whereas an overly rough surface enhances mounting. Finally, the upper corner should be rounded so as to reduce the tendency of the wheel rim to grab onto the curb top. The recommended curb design which incorporates all these features is shown on Figure 4-3a. Unfortunately, the design was never evaluated.

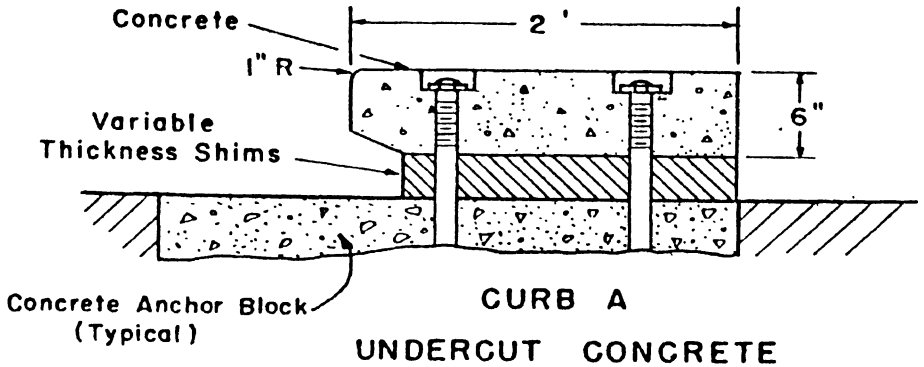

CURB A

UNDERCUT CONCRETE

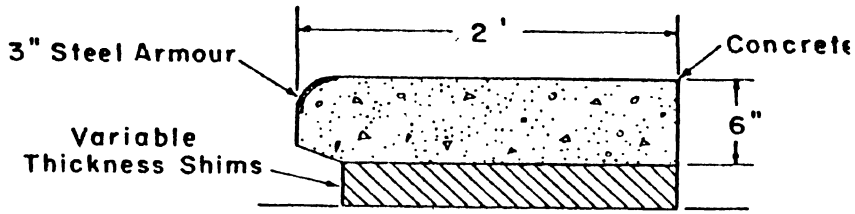

CURB B

ARMOURED UNDERCUT CONCRETE

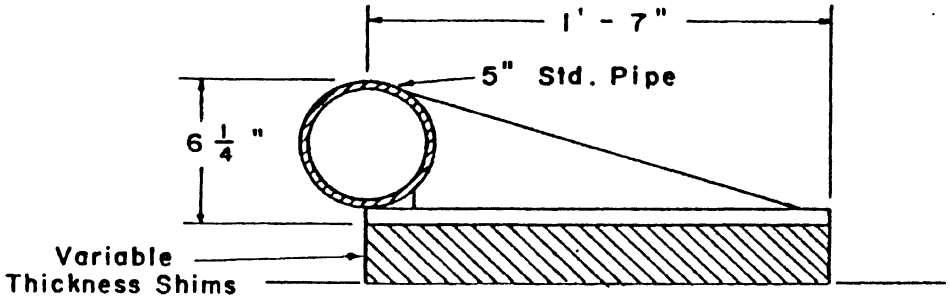

CURB C

STEEL PIPE

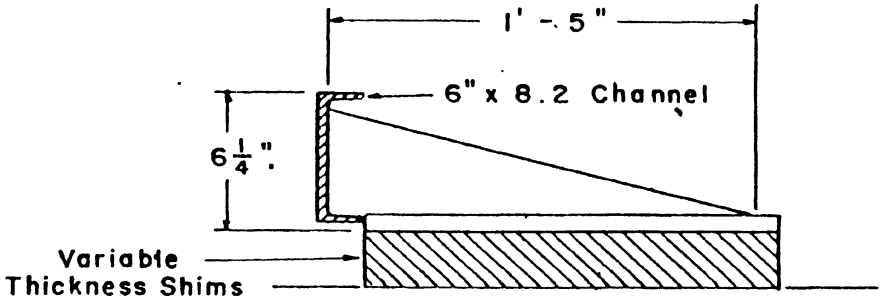

CURB D

STEEL CHANNEL

FIGURE 4-2. 1953 STATE OF CALIFORNIA TEST CURBS.

Curbs somewhat similar to the recommended California cross-section have been tested in Canada and West Germany, however. The Canadian test [14] was conducted as part of a larger study to determine the efficiency of the curb in combination with various guardrails as a redirection system. Only a single test was made, at a velocity and angle of 64 mph and 20°, respectively. As indicated on Figure 4-17 (Curb D), redirection did not occur. The cross-section is shown on Figure 4-3b.

The West German cross section [15] is shown on Figure 4-3c. Five tests were made on the curb, with various vehicles, at speeds ranging between 29 and 48 mph and at angles of ten and fifteen degrees. All cases resulted in a redirection except one involving a VW at 48 mph and 15°. The vehicle mounted in this test, but this was attributed in some degree to the rear engine configuration of the vehicle and its low total mass. Test results are summarized on Figure 4-16 (Curb F).

The Trief curb (Figure 4-17) developed in Belgium is another example of a barrier curb with specific design features to enhance redirection. In an interesting series of tests conducted in England [16], the redirective character of the Trief curb was found to conform to the equation:

$$V \sin \alpha = \text{Constant} \qquad (4\text{-}1)$$

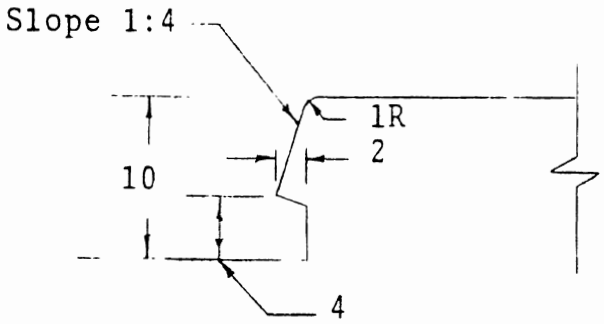

FIGURE 4-3A. OPTIMIZED CALIFORNIA CURB [13]

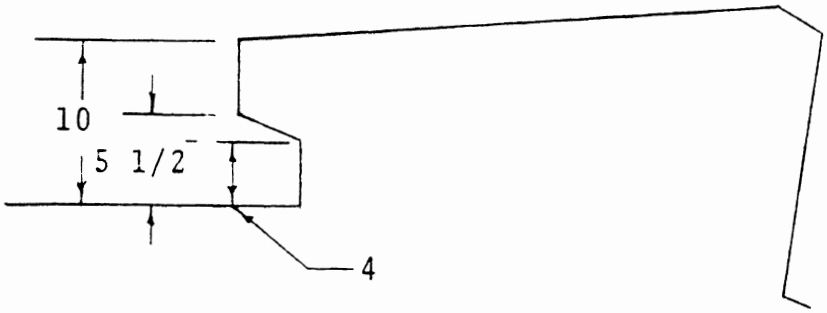

FIGURE 4-3B. CANADIAN UNDERCUT CURB [14]

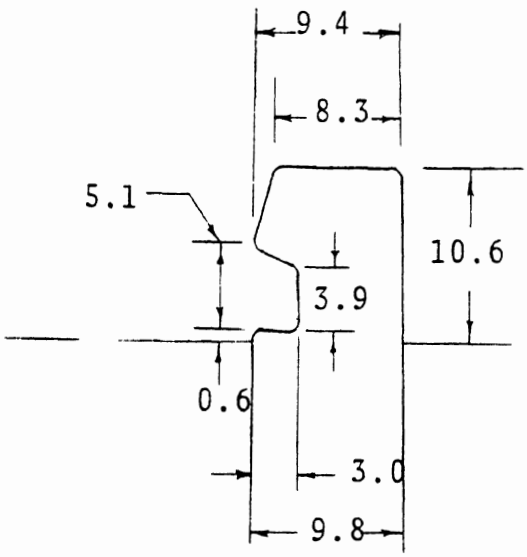

FIGURE 4-3c. WEST GERMAN (ELSHOLZ) UNDERCUT CURB [15]

where V = velocity

α = impact incidence angle

In effect, it was found that whenever the component of vehicle velocity normal to the curb was larger than a fixed value, the vehicle would mount. Below this value redirection would occur. For the Trief curb, the constant was about 3 mph. The results in graphical form are reproduced on Figure 4-17. The influence of tire/curb friction on mounting was confirmed in these tests, in that the mounting velocity increased from 12 mph to 20 mph when the tire and curb were wet.

An additional class of higher curbs, which could more properly be called concrete guardrails, has also received research attention in the last decade. Among the various designs that have arisen are the GM and New Jersey reflecting barriers. These are two barriers of fairly similar dimensions (see Figures 4-24 and 4-25) which redirect a vehicle by first causing it to ride up on the lower face. This motion causes the vehicle to bank and forces the front wheels to turn away from the barrier [17]. In general, these barriers function well at impact angles below ten or twelve degrees. At higher angles, extensive vehicle damage occurs [18, 19], but the nature of the damage is such that the vehicle is not usually redirected back into the traffic stream. The structures have therefore been used extensively in several states, and modifications of the reflecting shape has been incorporated into bridge railings [17, 20].

Other higher curbs include the Sabla curb of France [21] (Figure 4-23), the reinforced 36-inch vertical wall of California [22] (Figure 4-26), and the various DAV (Dansk Auto Vaern) configurations (Figure 4-21) used in Europe and Japan [23, 24, 25, 26, 27]. In general, most of these curbs (concrete guardrails) are not highly regarded and hence are being used less because of:

1. Most are too low in relation to the vehicle's c.g.
2. Some have structural integrity problems.
3. Those that are rigid impart higher decelerations to a vehicle than semi-rigid metal guardrails which tend to deflect under impact.

4.3 EVALUATION EXERCISES

Curb evaluation was carried out in two ways. First, curb test data from all available test programs conducted by other organizations was assembled. This was synthesized and grouped according to curb height.

Second, simulation exercises were carried out on specific curb configurations. These were curbs which were either recommended for evaluation by the Michigan Department of State Highways [46], or which had been tested by other organizations. The latter curbs were similar to MDSH designs, but in no case exactly the same. Simulations were made on these designs so as to acheive a point of reference for the test exercises.

4.4 CURB TEST DATA

Available test data for curbs ranging in height from two to thirty-six inches are shown on Figures 4-4 through 4-26. The data are for a variety of test conditions, and for all manner of curb shapes. It is therefore difficult to synthesize specific conclusions. The discussions which follow cover the few areas where detailed comments are possible. These comments pertain to the effects that curb height and face slope have on mounting performance.

In the first series of curb tests made by the California Division of Highways [12], the slope of the curb face was made a parameter. Before the test series, it was thought that making the curb face more vertical would discourage mounting and enhance redirection. (That is, making the curb face flatter would make the curb more easily mountable,and vice versa.) As it turned out, however, this was only true for impact angles above 15 to 20°. At lower angles a vertical curb face actually enhanced mounting by providing a surface for the wheel rim to catch and bite into. It was found, therefore, that flattening the curb face (within limits, that is) actually reduced the tendency to mount.

As illustrated on Figure 4-27, the trade-off occurs at a slope of about 2:9 (i.e., two inches of slope set back in nine inches of height). The boundary between mounting and

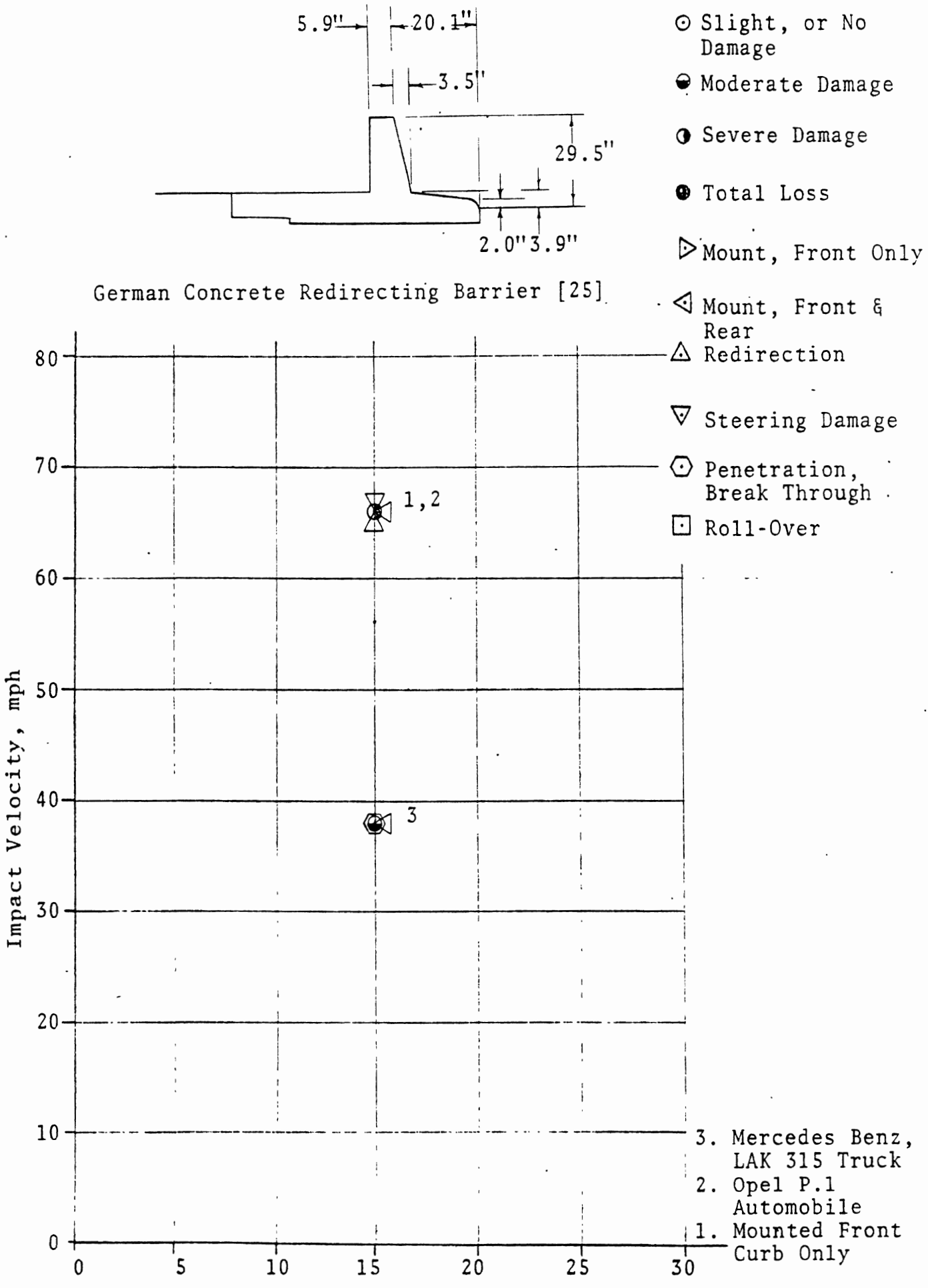

FIGURE 4-4. TWO INCH CURB TEST RESULTS SUMMARY.

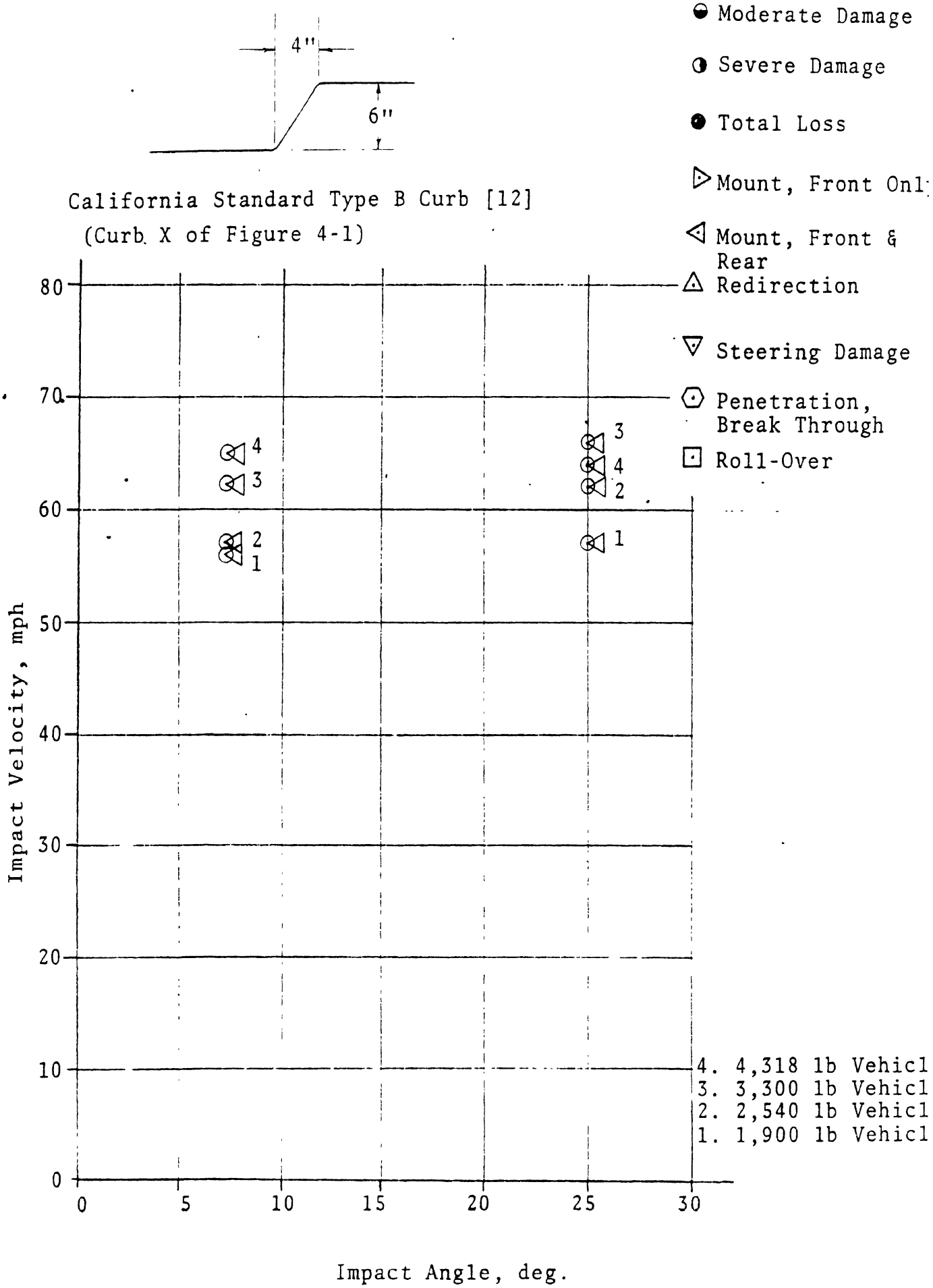

FIGURE 4-5. SIX INCH CURB TEST RESULTS SUMMARY

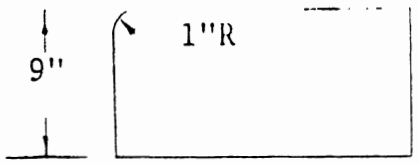

California Curb I [12]

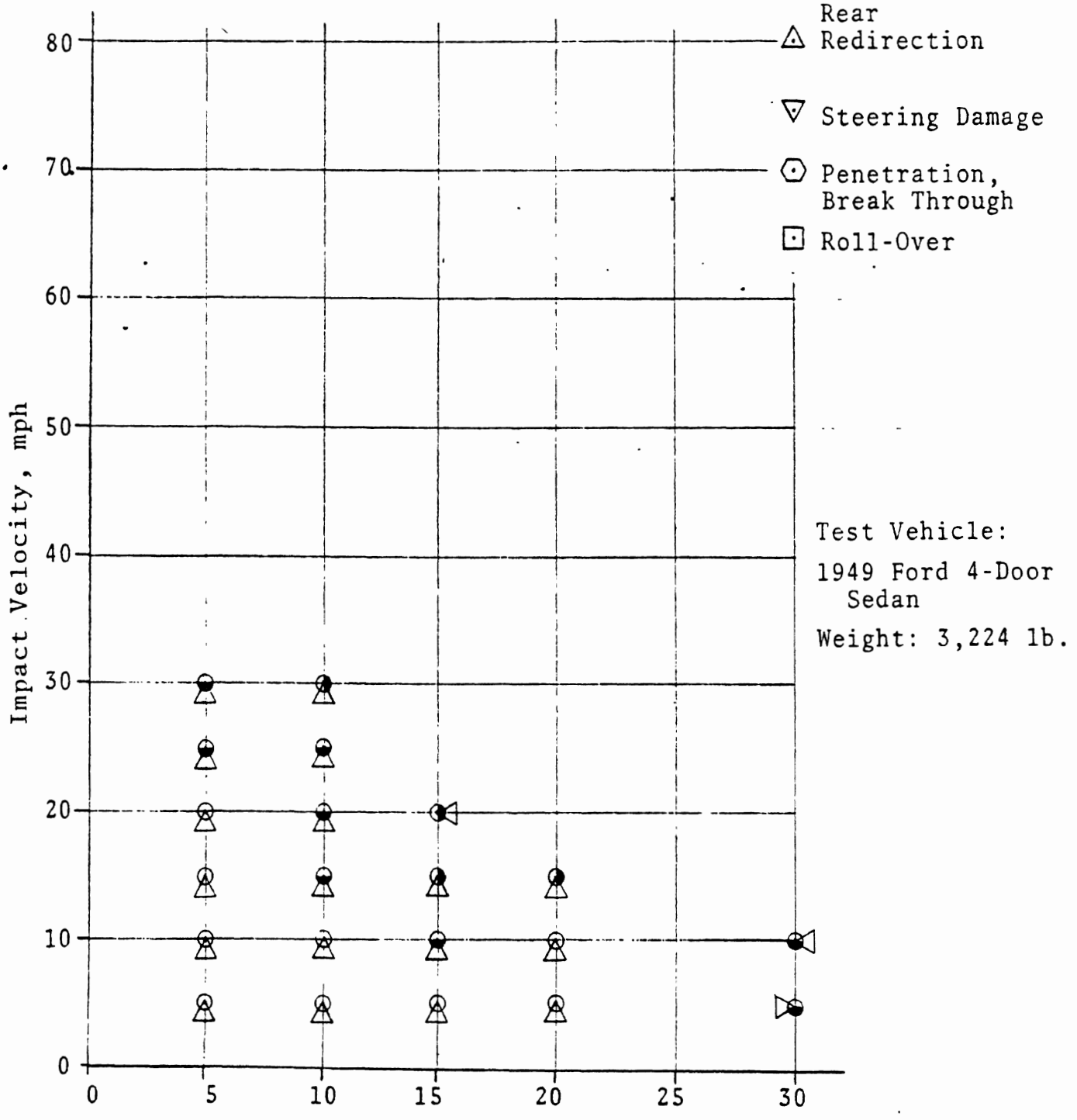

FIGURE 4-6. CALIFORNIA CURB I TEST RESULTS SUMMARY.

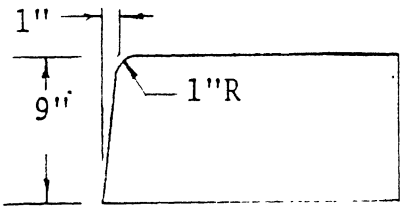

California Curb II [12]

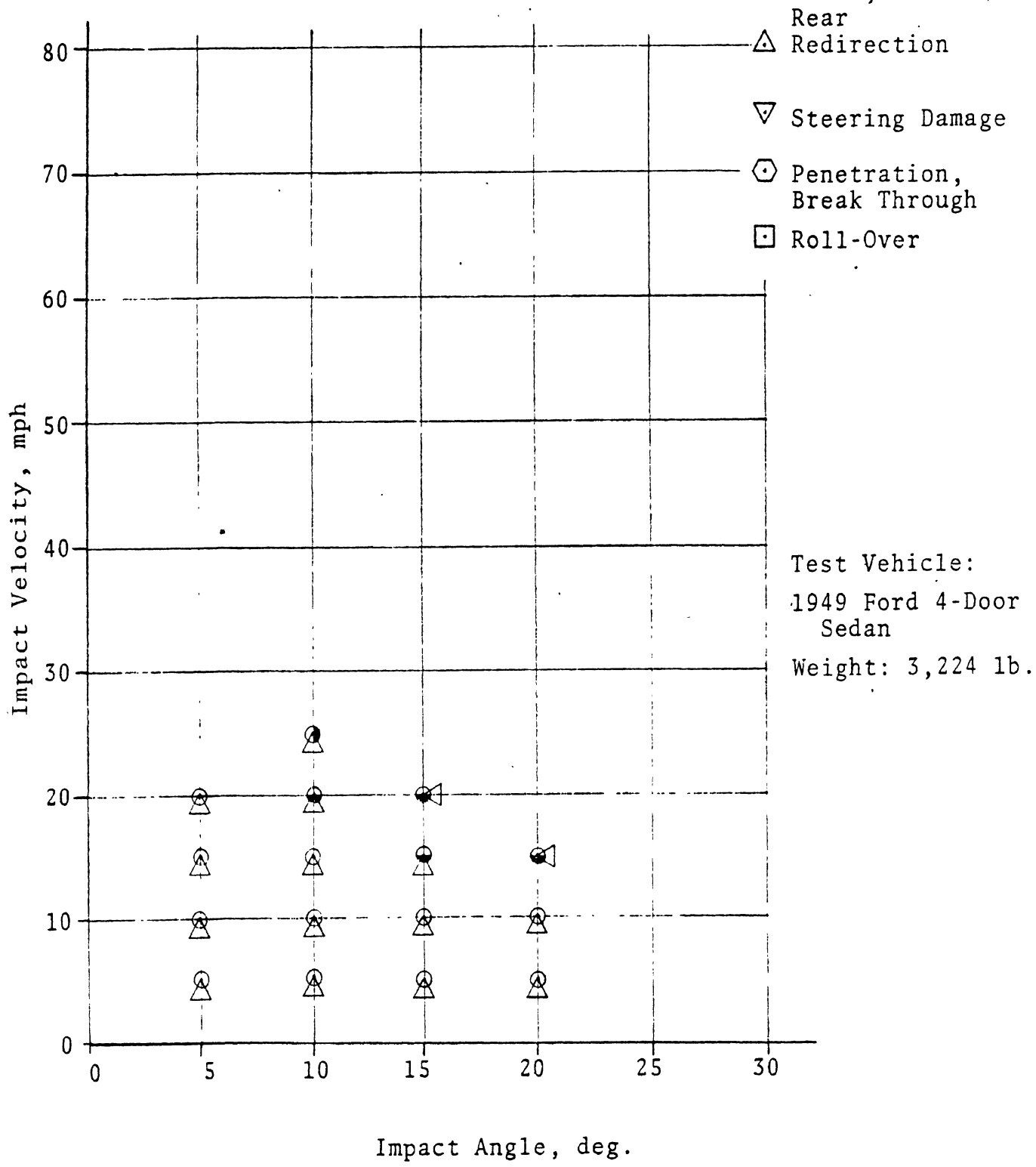

FIGURE 4-7. CALIFORNIA CURB II TEST RESULTS SUMMARY

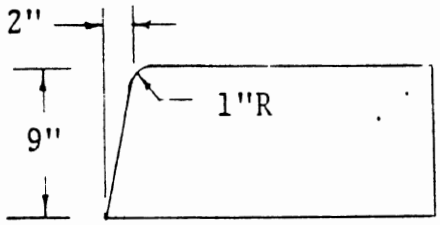

California Curb III [12]

FIGURE 4-8. CALIFORNIA CURB III TEST RESULTS SUMMARY.

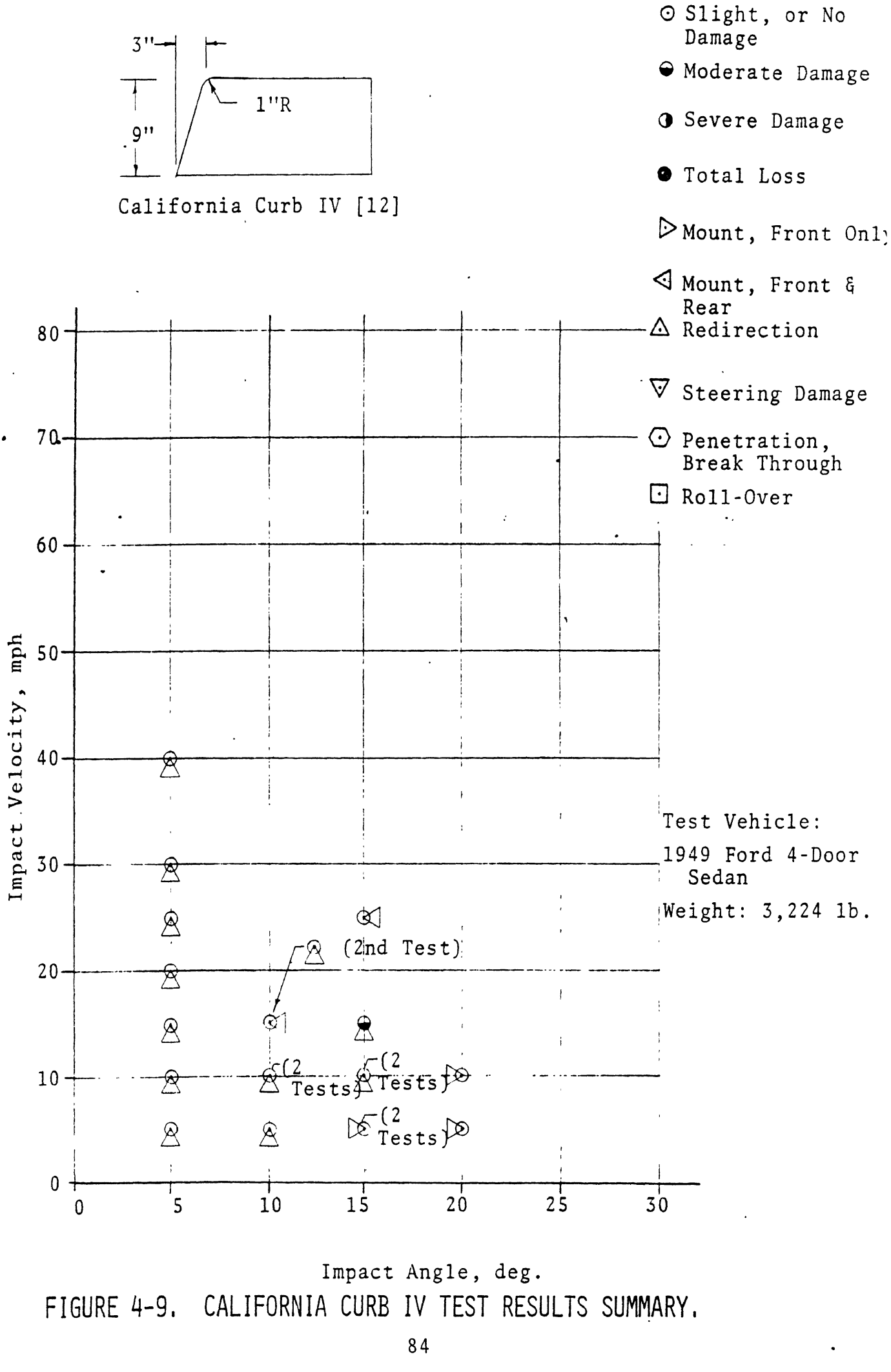

FIGURE 4-9. CALIFORNIA CURB IV TEST RESULTS SUMMARY.

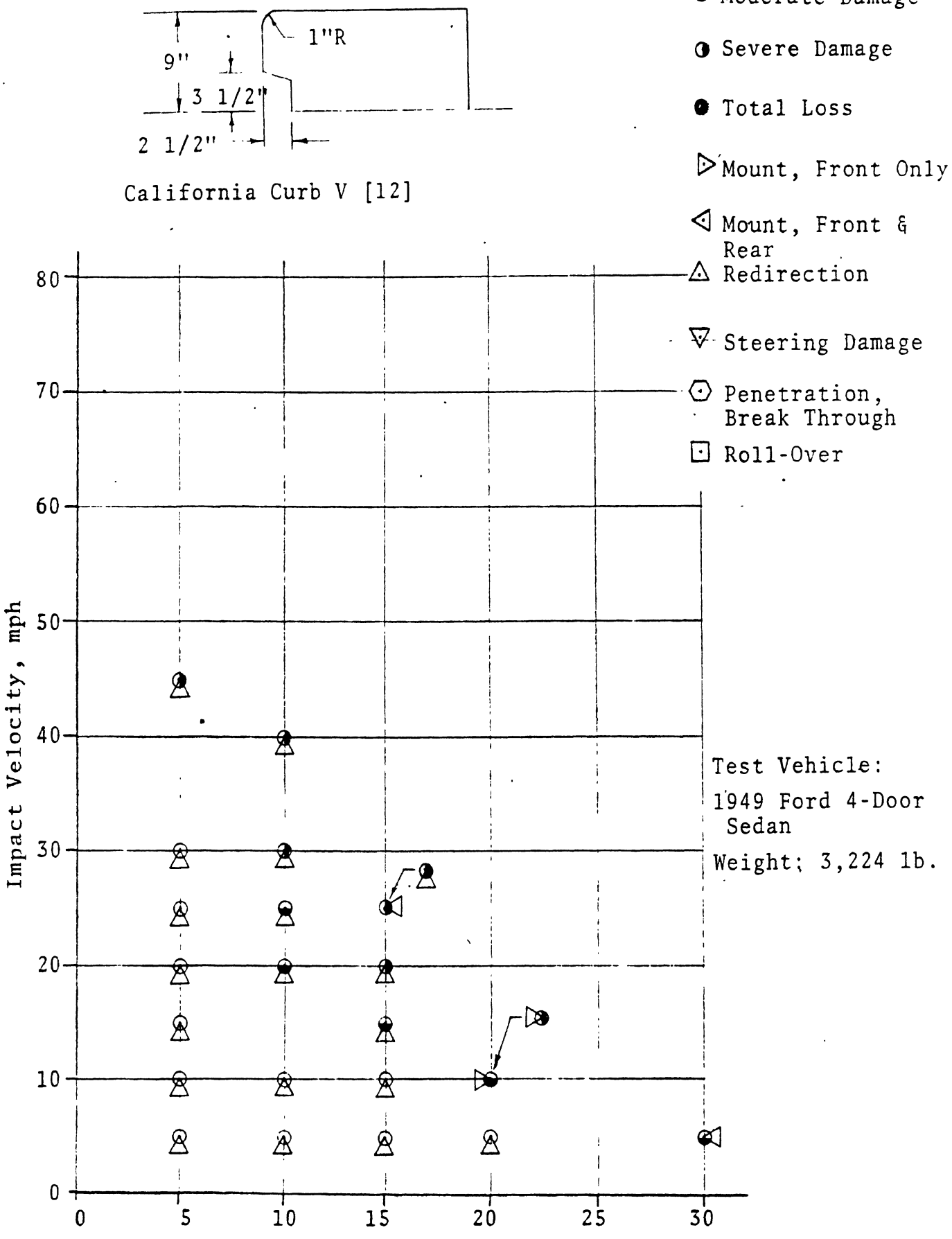

FIGURE 4-10. CALIFORNIA CURB V TEST RESULTS SUMMARY.

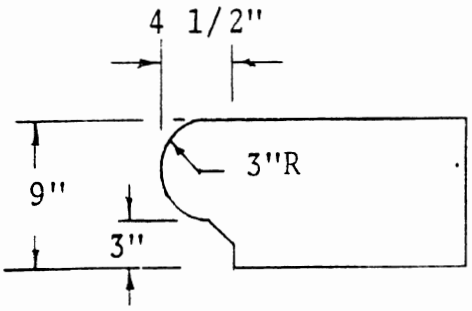

California Curb VI [12]

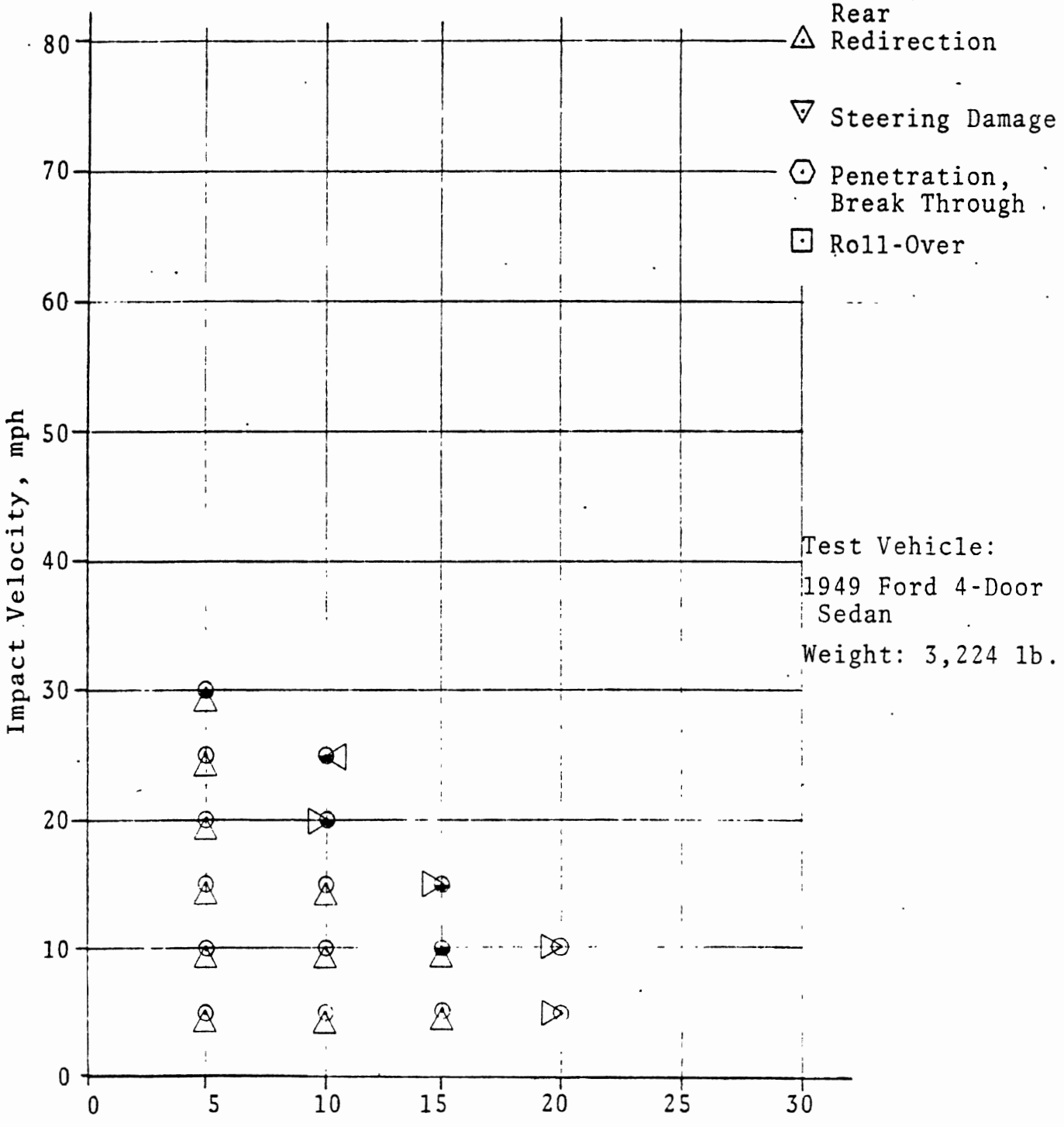

FIGURE 4-11. CALIFORNIA CURB VI TEST RESULTS SUMMARY

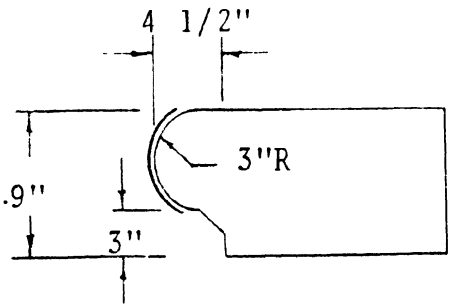

California Curb VI-M (Metal Faced) [12]

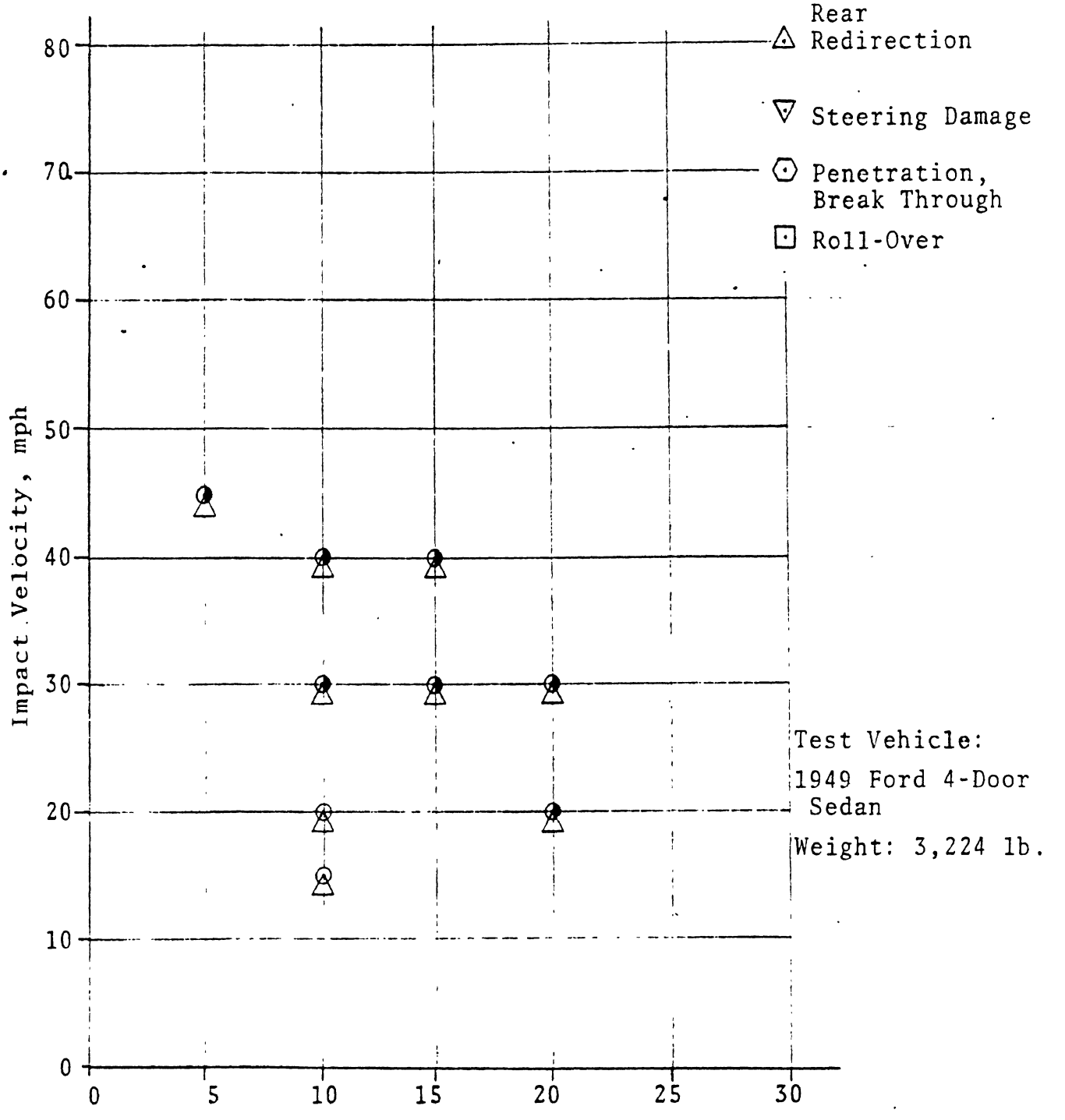

FIGURE 4-12. CALIFORNIA CURB VI-M TEST RESULTS SUMMARY

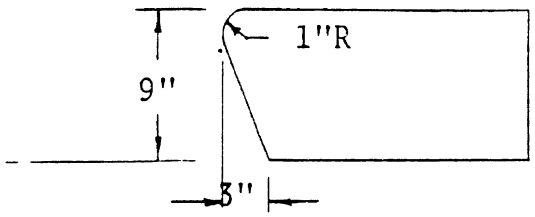

California Curb VII [12]

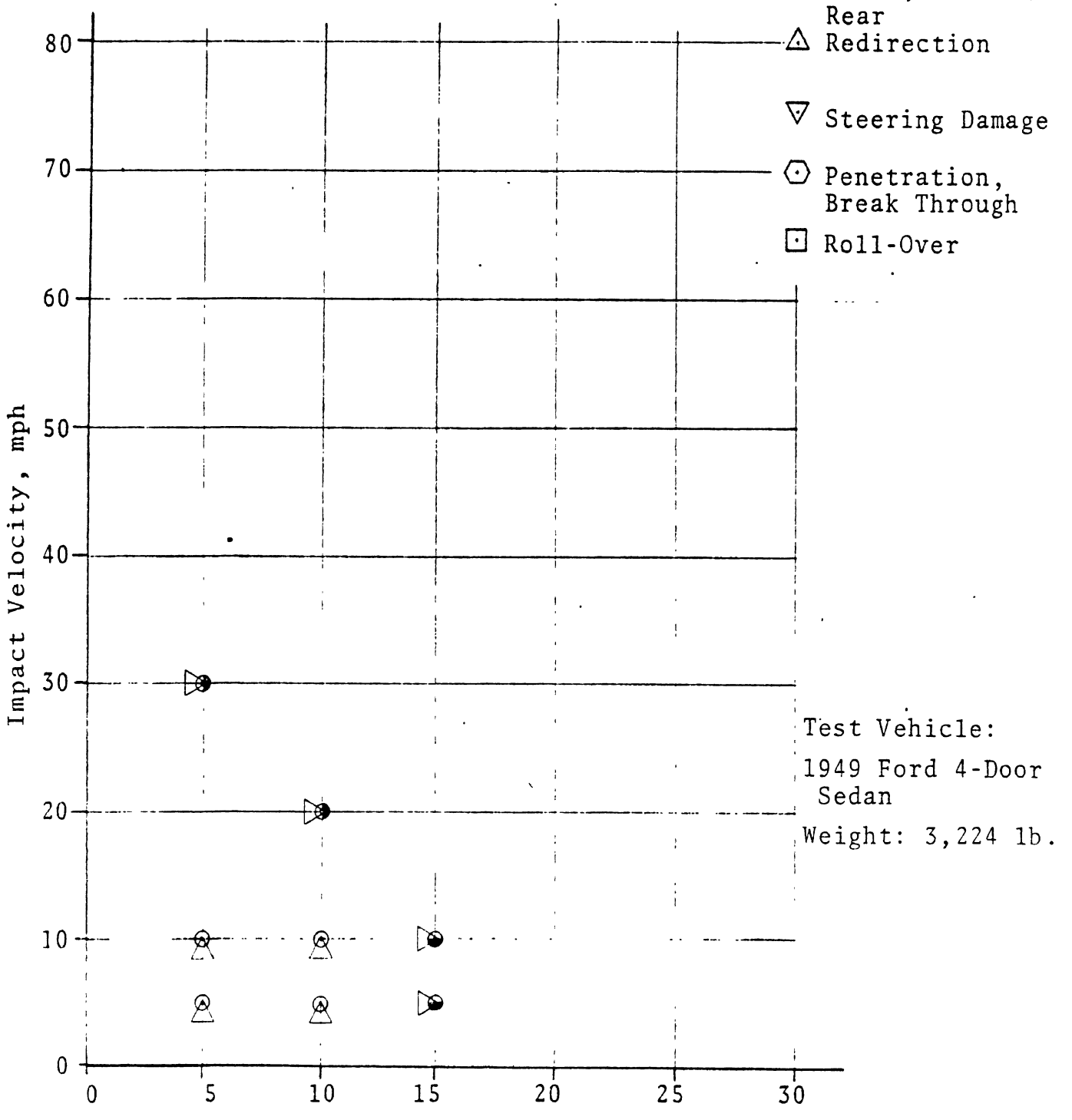

FIGURE 4-13. CALIFORNIA CURB VII TEST RESULTS SUMMARY

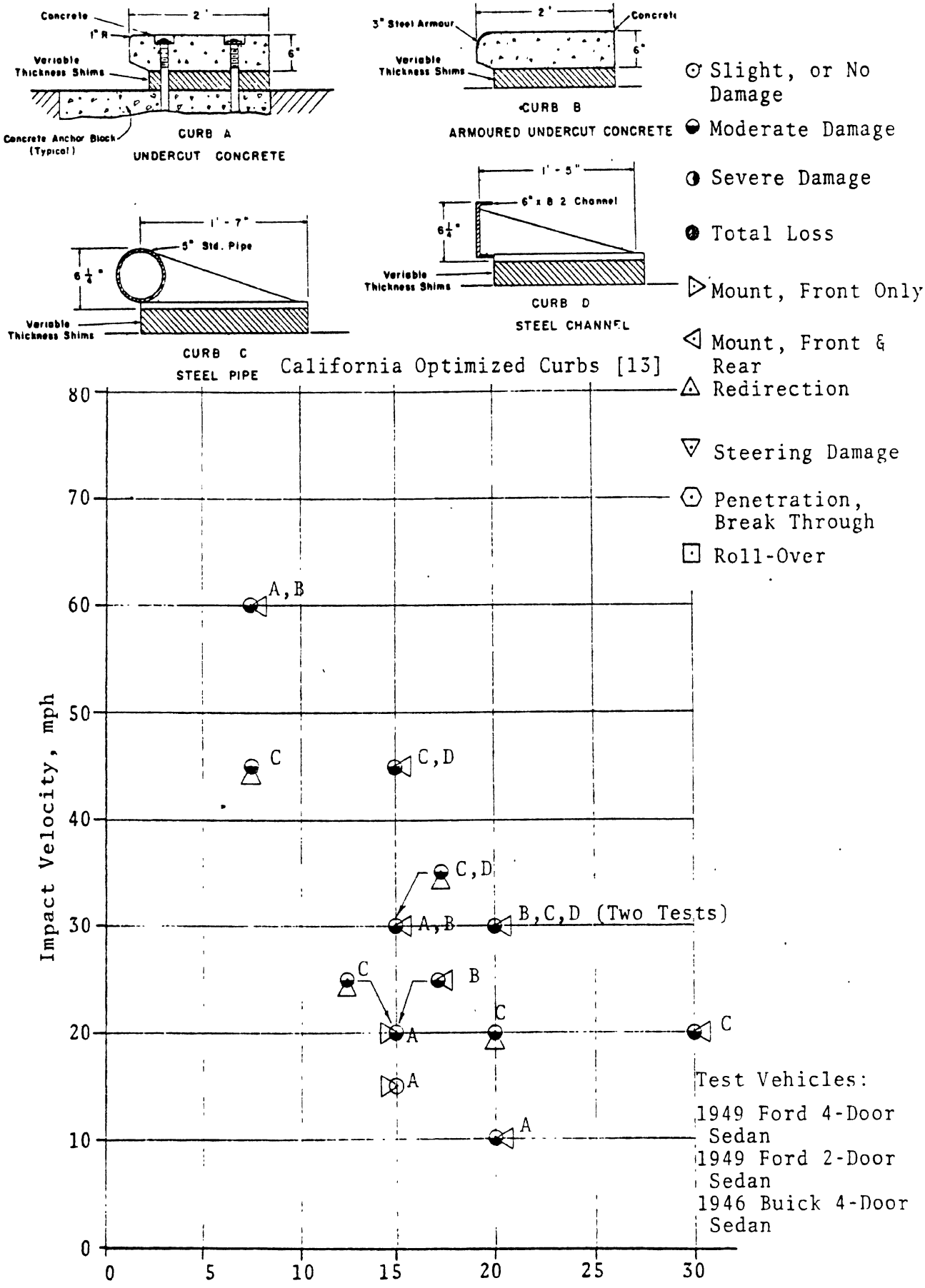

FIGURE 4-14. OPTIMIZED CALIFORNIA NINE-INCH CURB TEST RESULTS SUMMARY

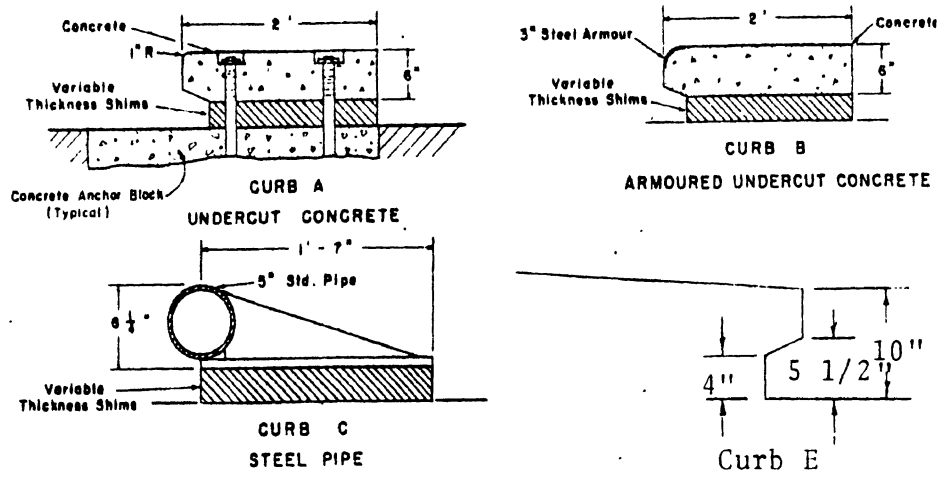

California Optimized Curbs [13]

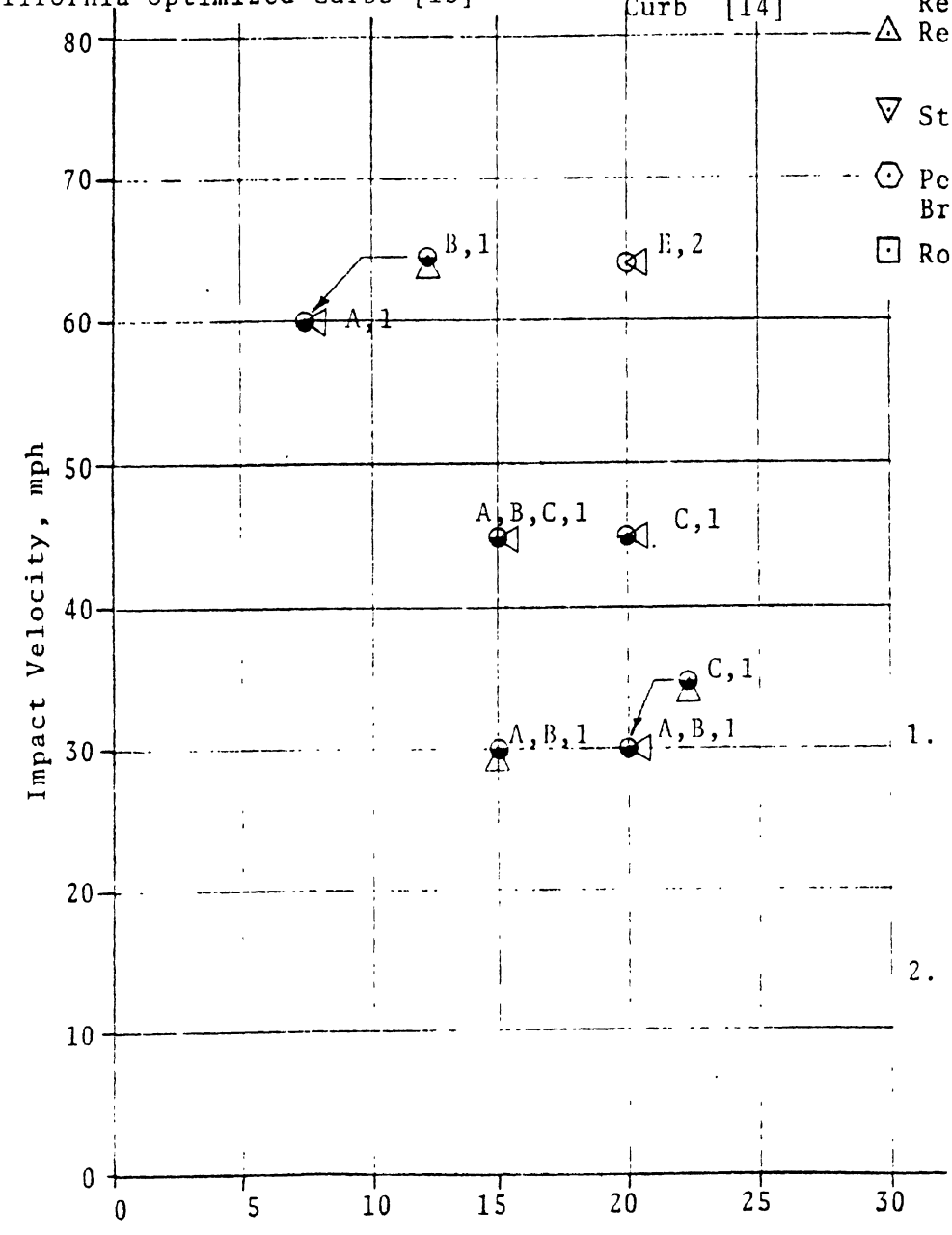

⊙ Slight, or No Damage

◒ Moderate Damage

◑ Severe Damage

● Total Loss

▷ Mount, Front Only

◁ Mount, Front & Rear

△ Redirection

▽ Steering Damage

⊙ Penetration, Break Through

⊡ Roll-Over

1. Test Vehicles:
   - 1949 Ford 4-Door Sedan
   - 1949 Ford 2-Door Sedan
   - 1946 Buick 4-Door Sedan
2. 3,700 lb Vehicle

FIGURE 4-15. TEN-INCH CURB TEST RESULTS SUMMARY

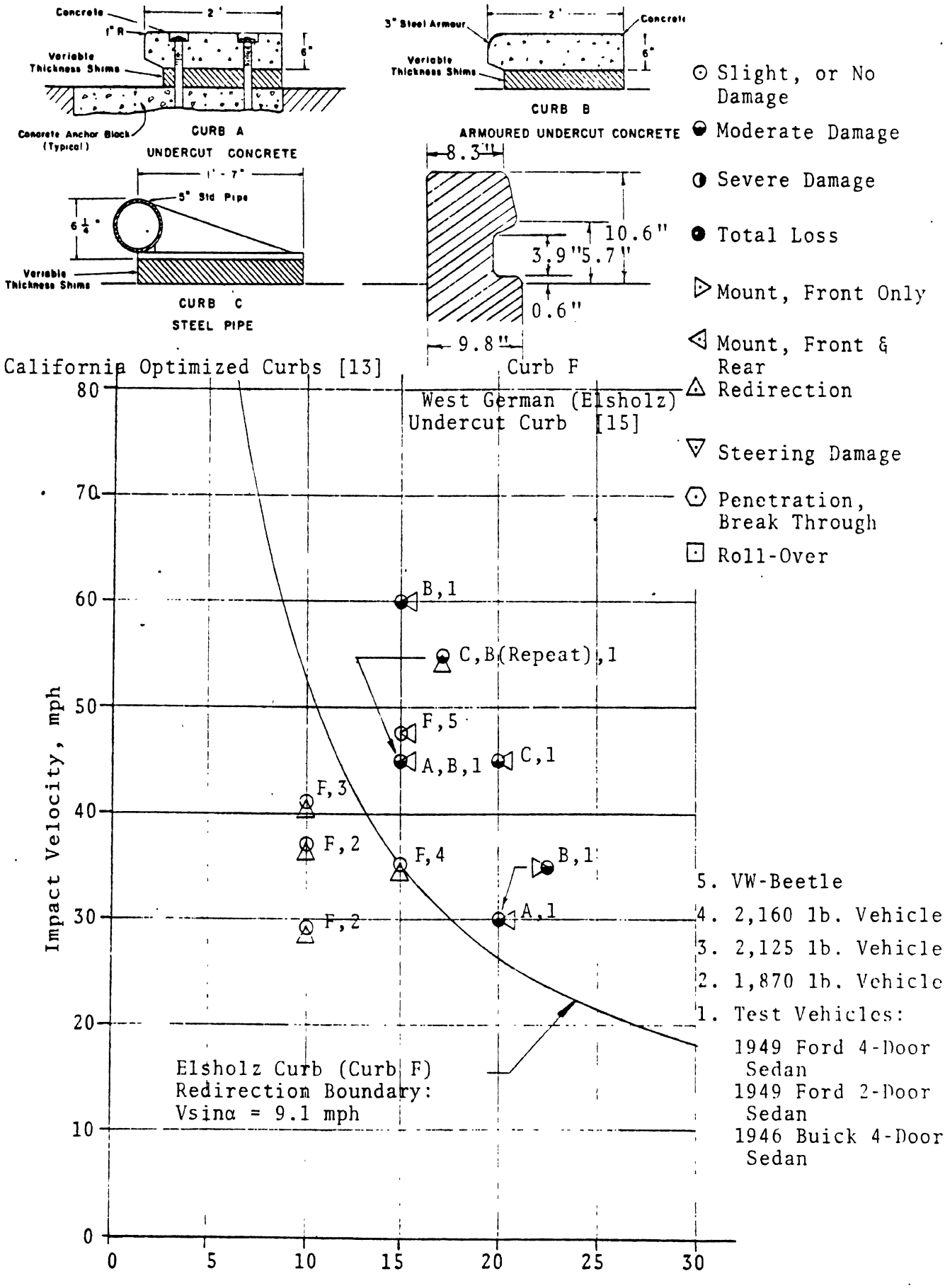

FIGURE 4-16. ELEVEN-INCH CURB TEST RESULTS SUMMARY

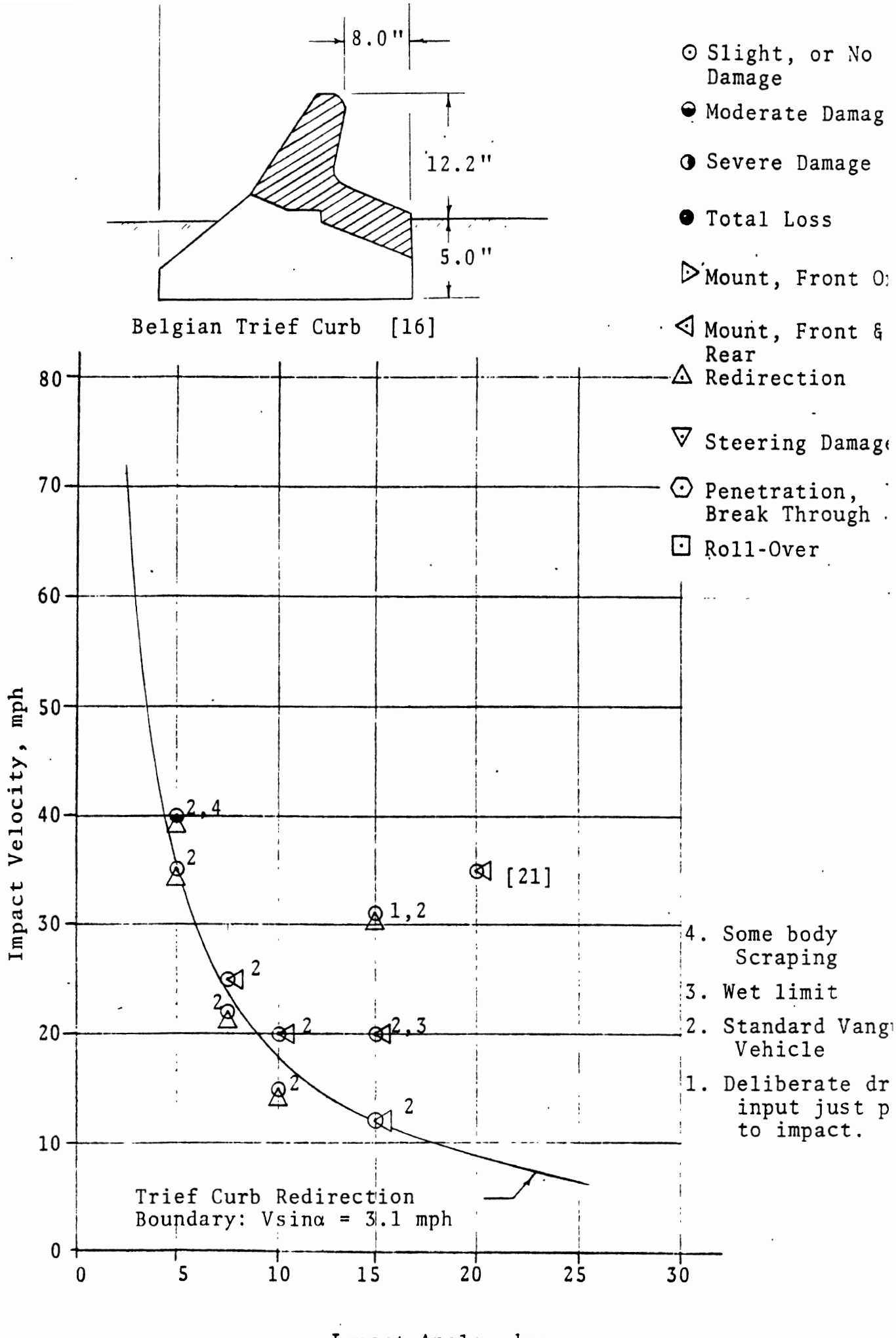

FIGURE 4-17. TWELVE-INCH TRIEF CURB TEST RESULTS SUMMARY

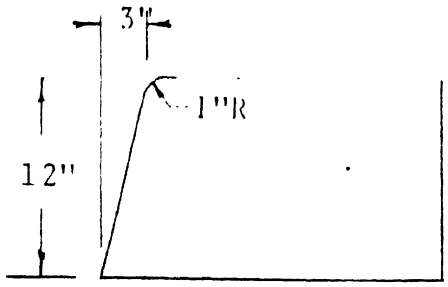

California Curb VIII [12]

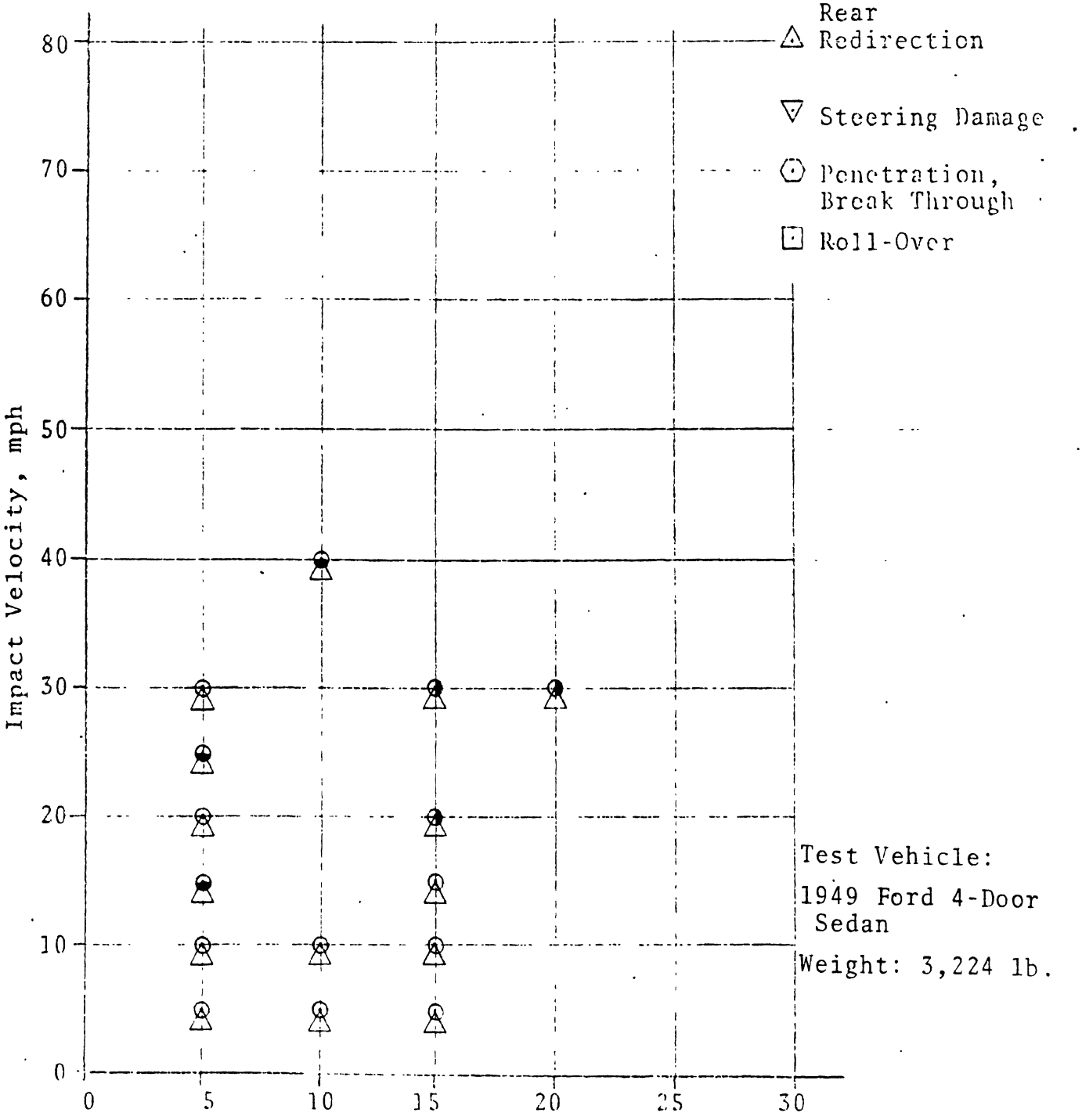

FIGURE 4-18. CALIFORNIA CURB VIII TEST RESULTS SUMMARY

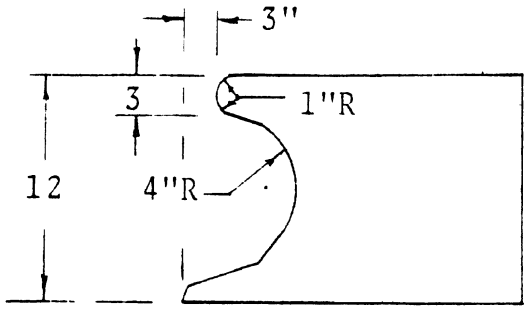

California Curb IX [12]

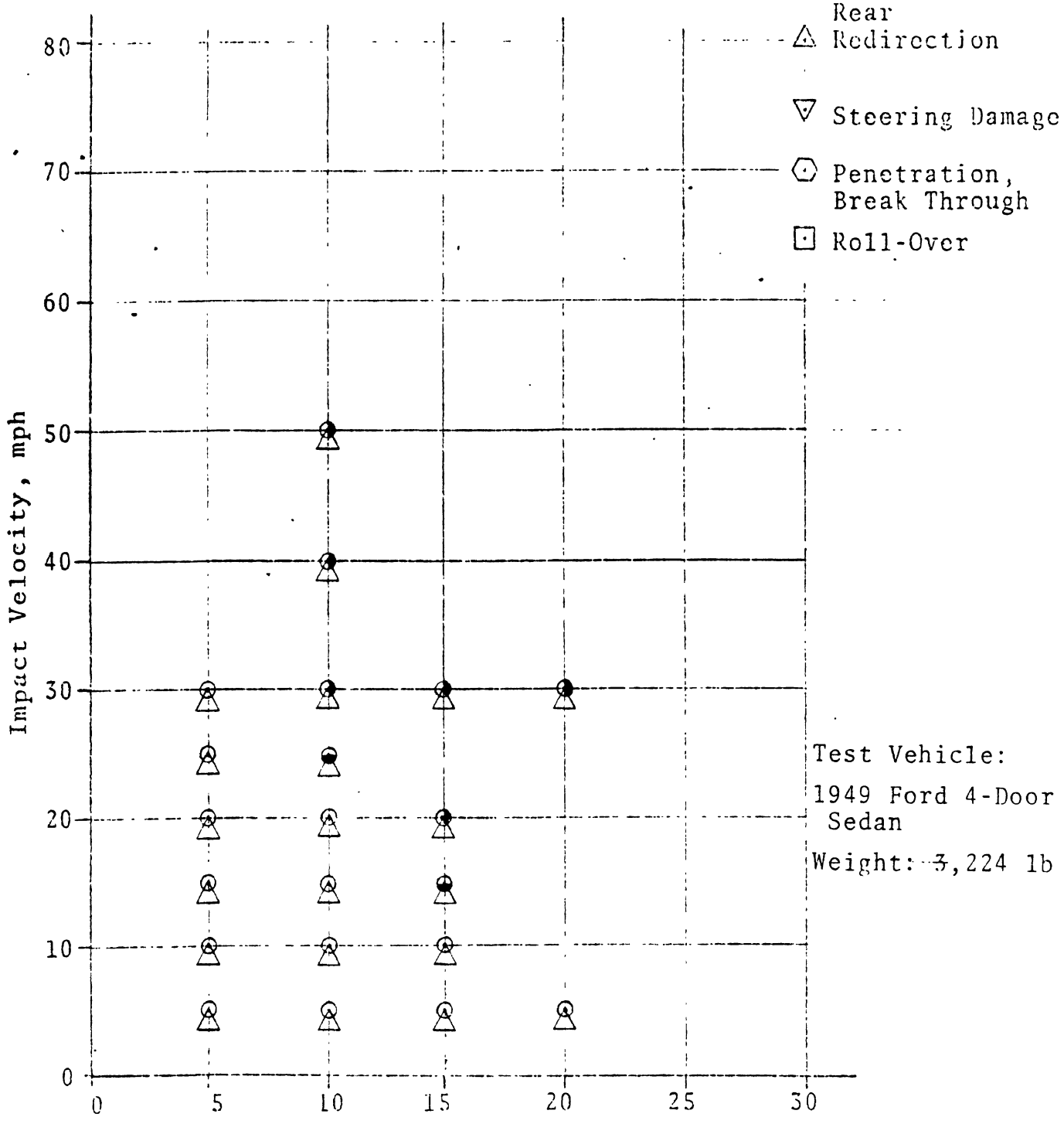

FIGURE 4-19. CALIFORNIA CURB IX TEST RESULTS SUMMARY

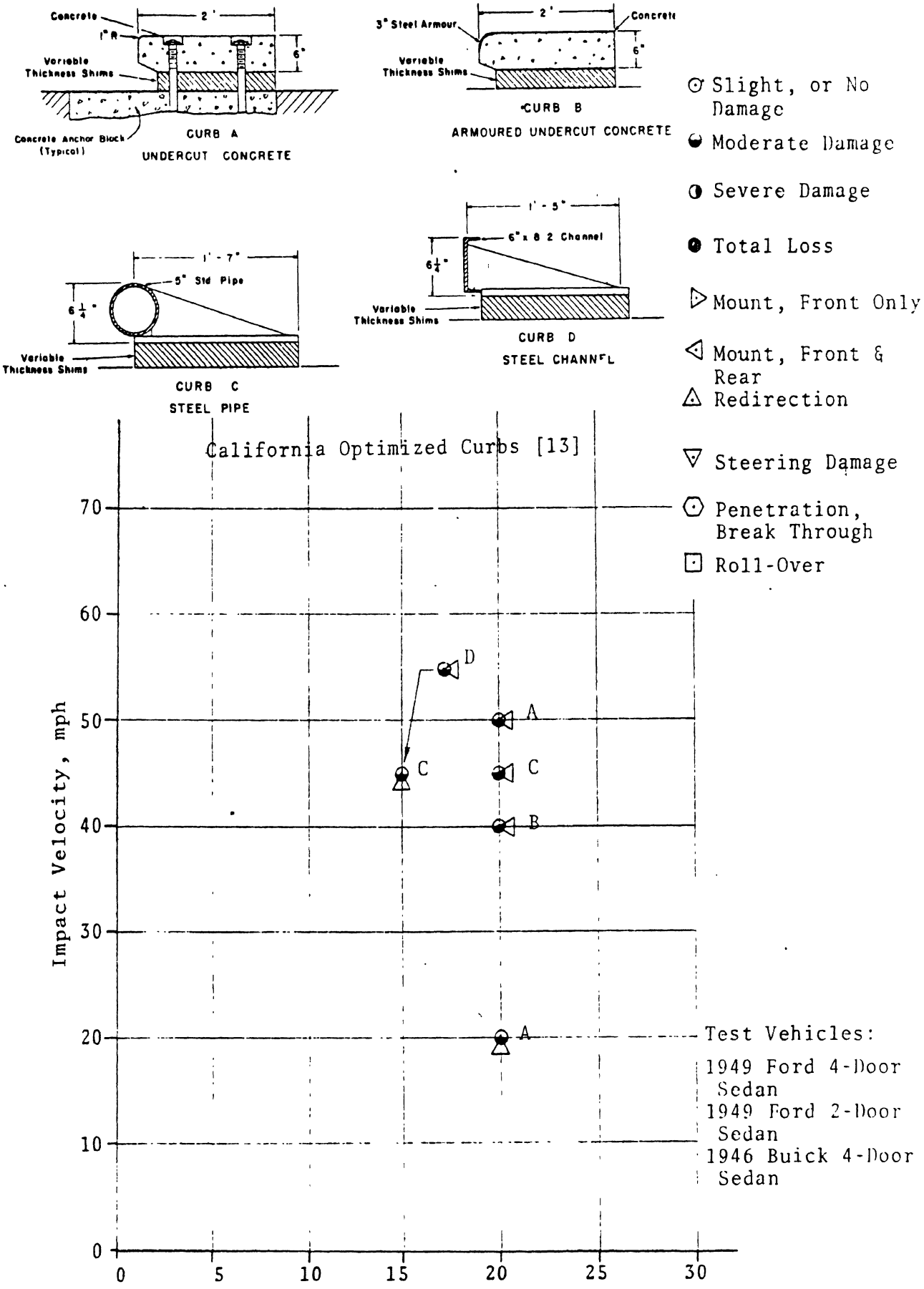

FIGURE 4-20. OPTIMIZED CALIFORNIA TWELVE-INCH TEST RESULTS SUMMARY

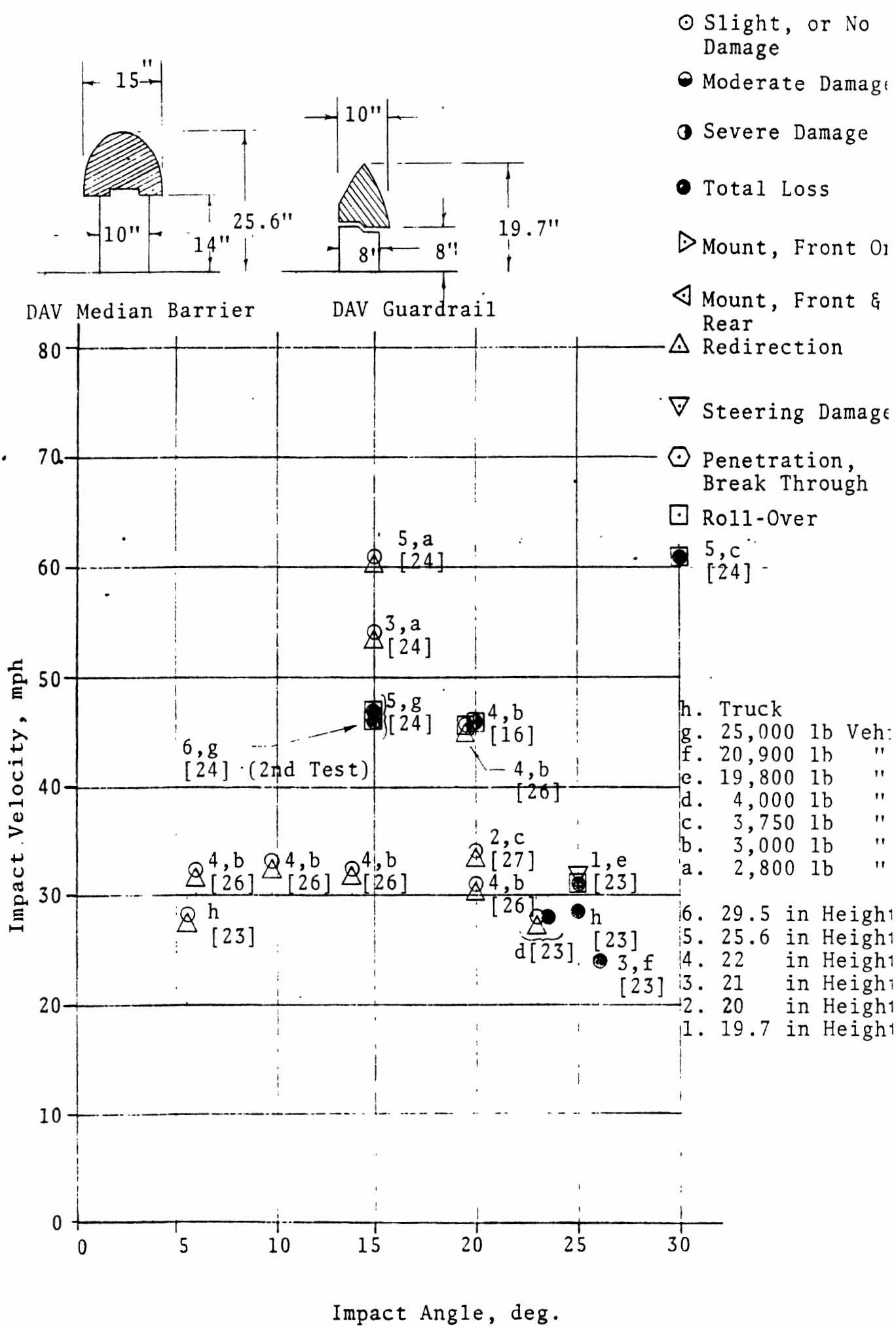

FIGURE 4-21. DAV BARRIER TEST RESULTS SUMMARY

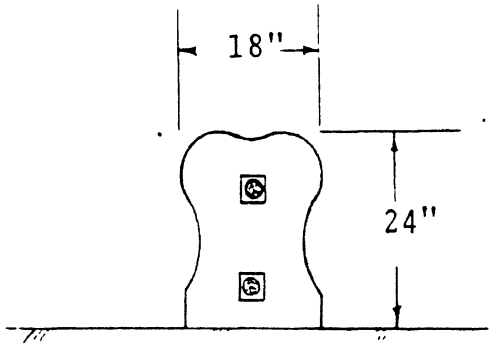

Vianini-Autostrade Median Barrier [49]

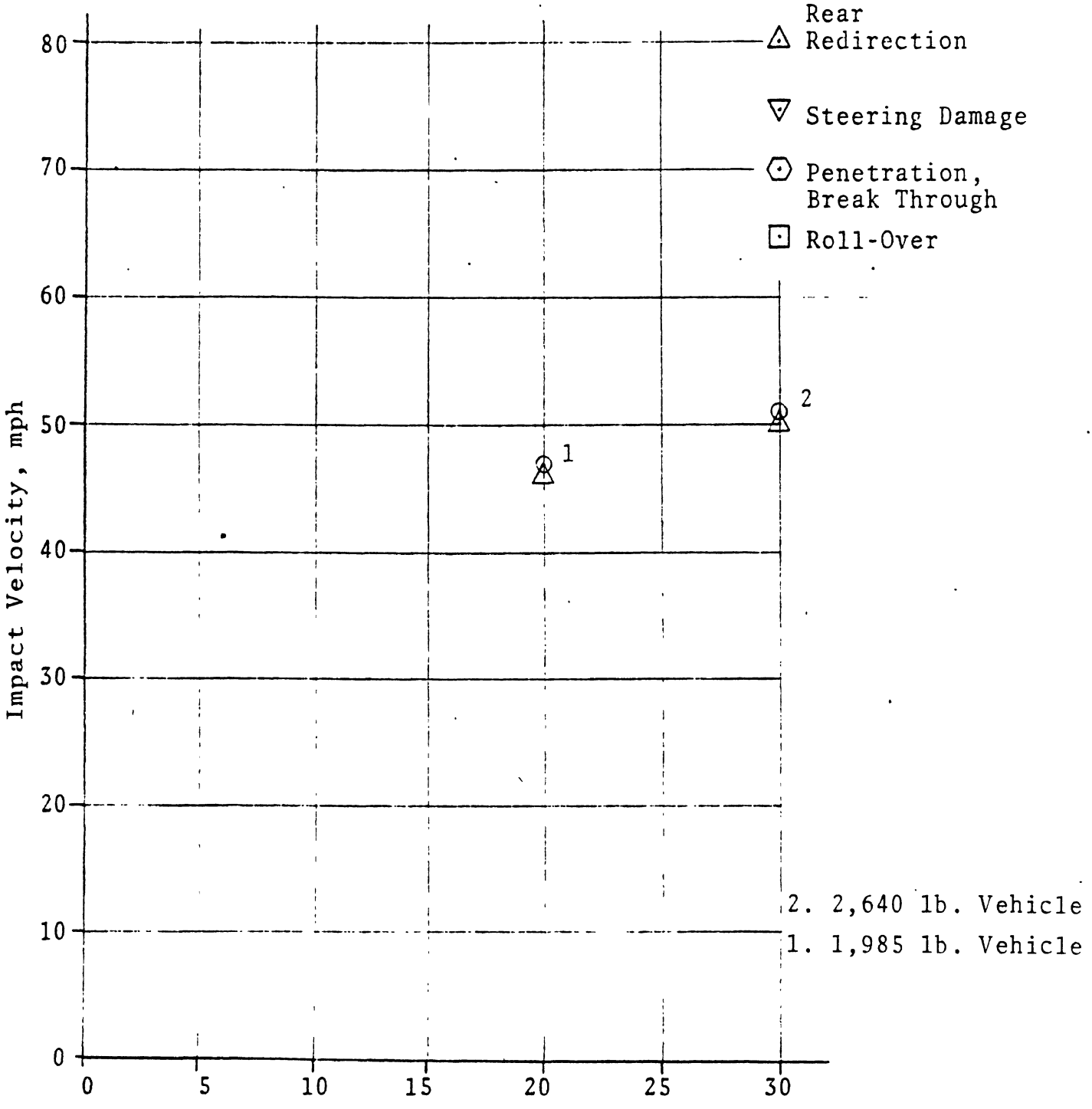

FIGURE 4-22. VIANINI-AUTOSTRADE BARRIER STEST RESULTS SUMMARY

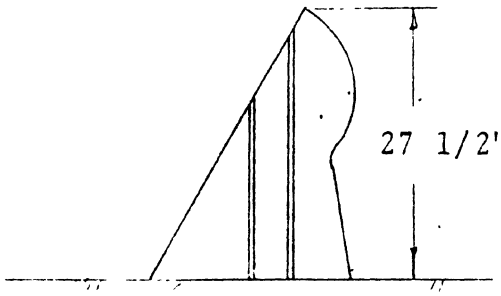

Sabla Curb Guardrail

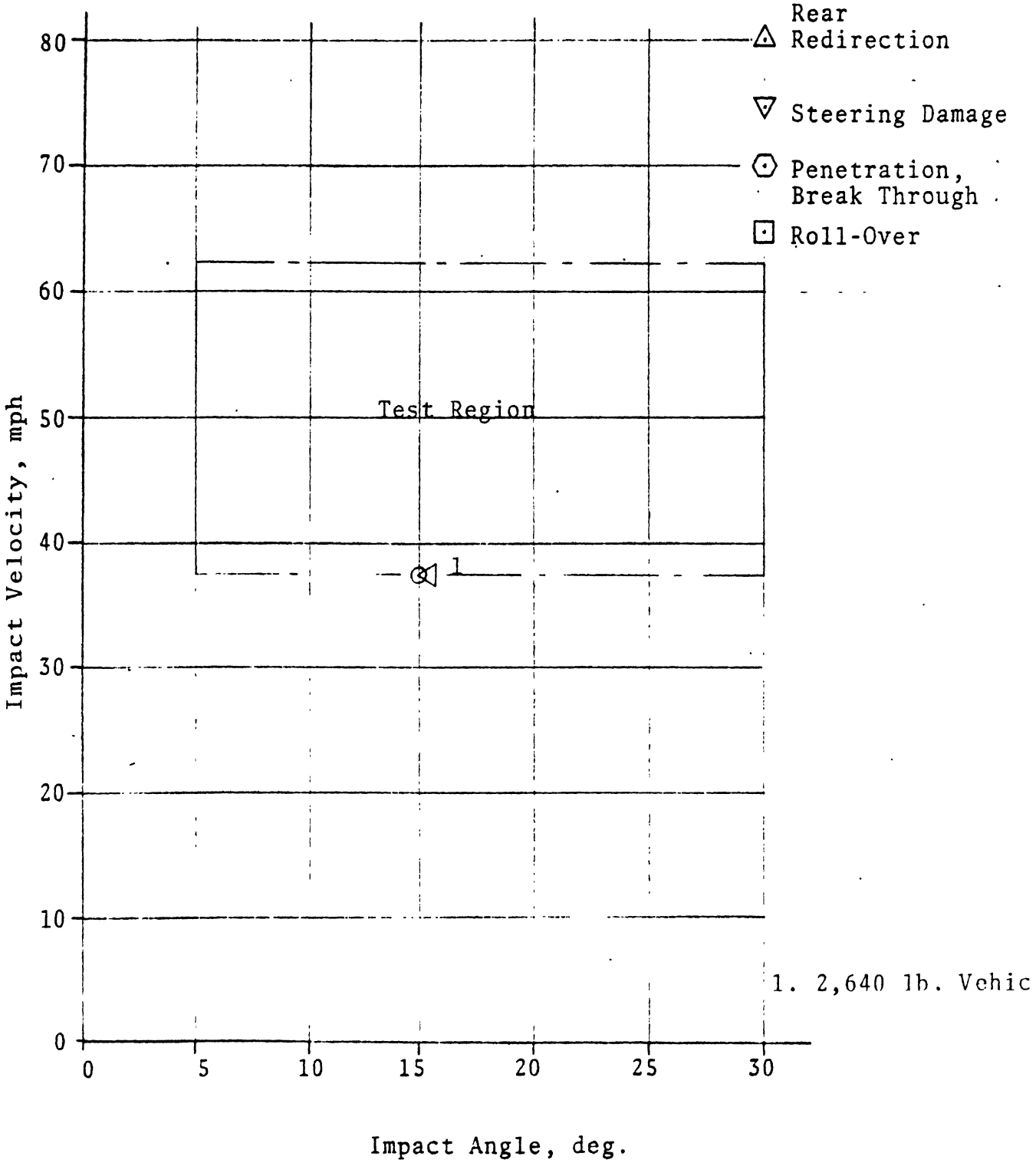

FIGURE 4-23. SABLA CURB TEST RESULTS SUMMARY

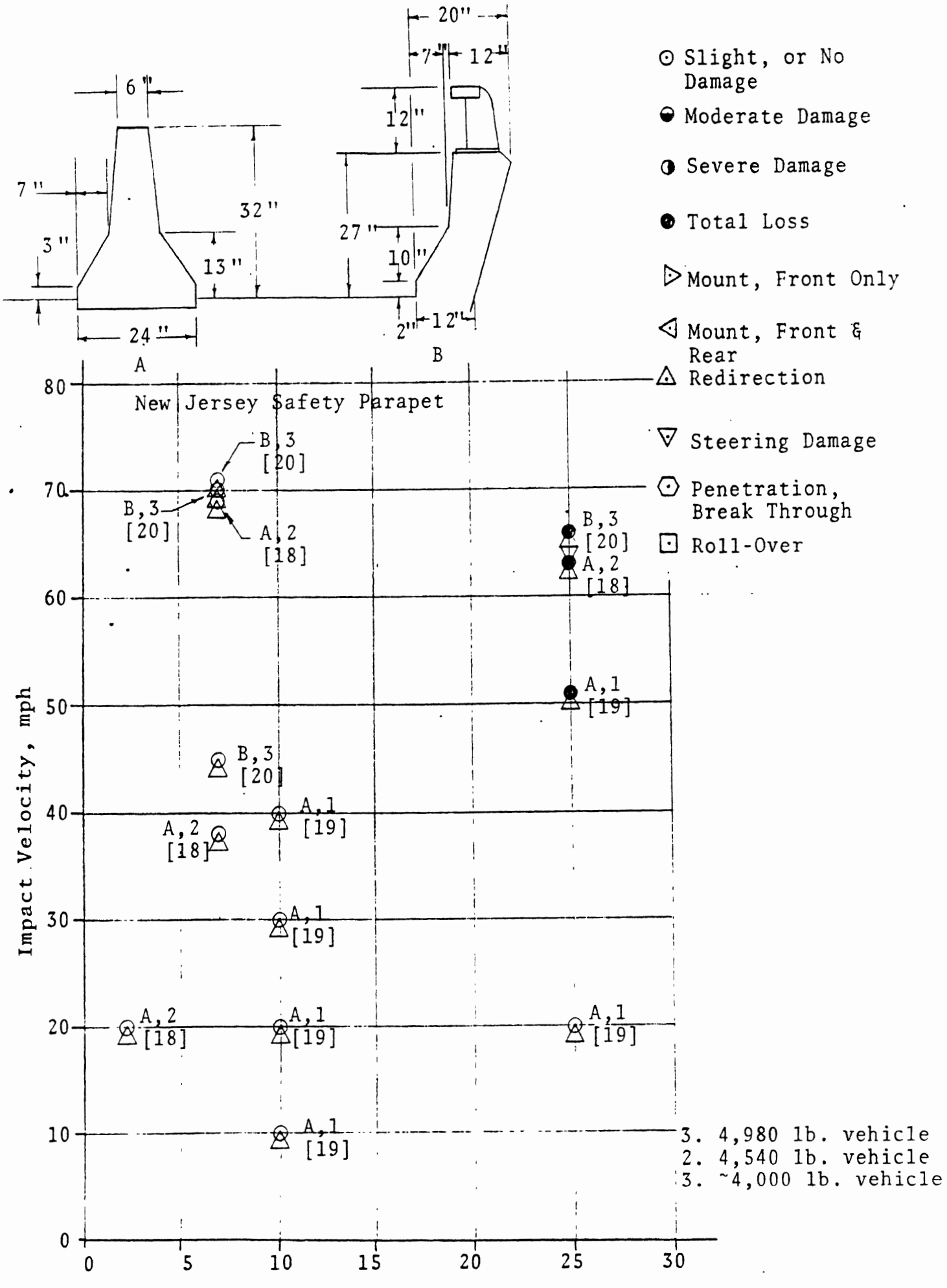

FIGURE 4-24. NEW JERSEY SAFETY PARAPET TEST RESULTS SUMMARY

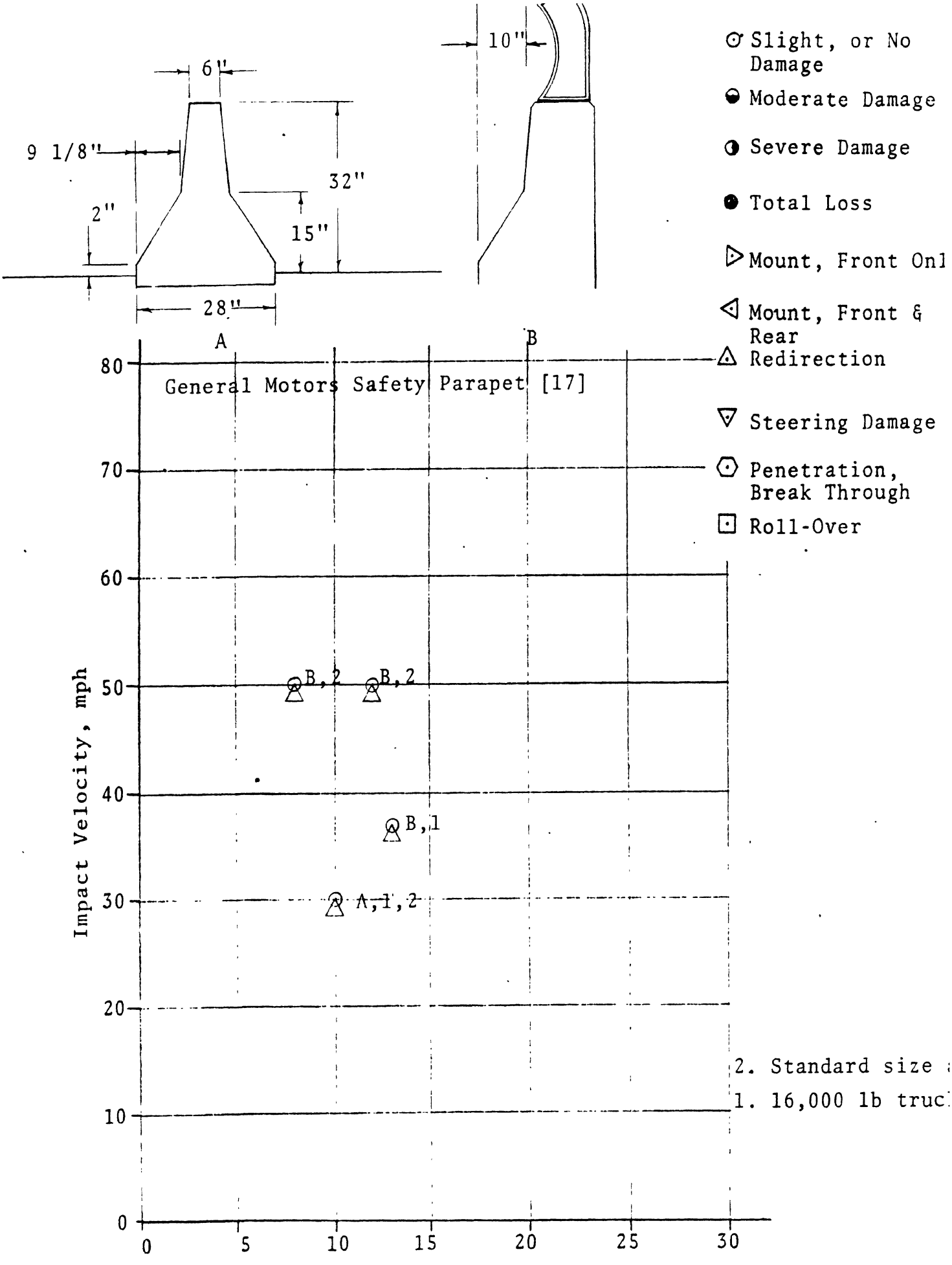

FIGURE 4-25. GENERAL MOTORS SAFETY PARAPET TEST RESULTS SUMMARY

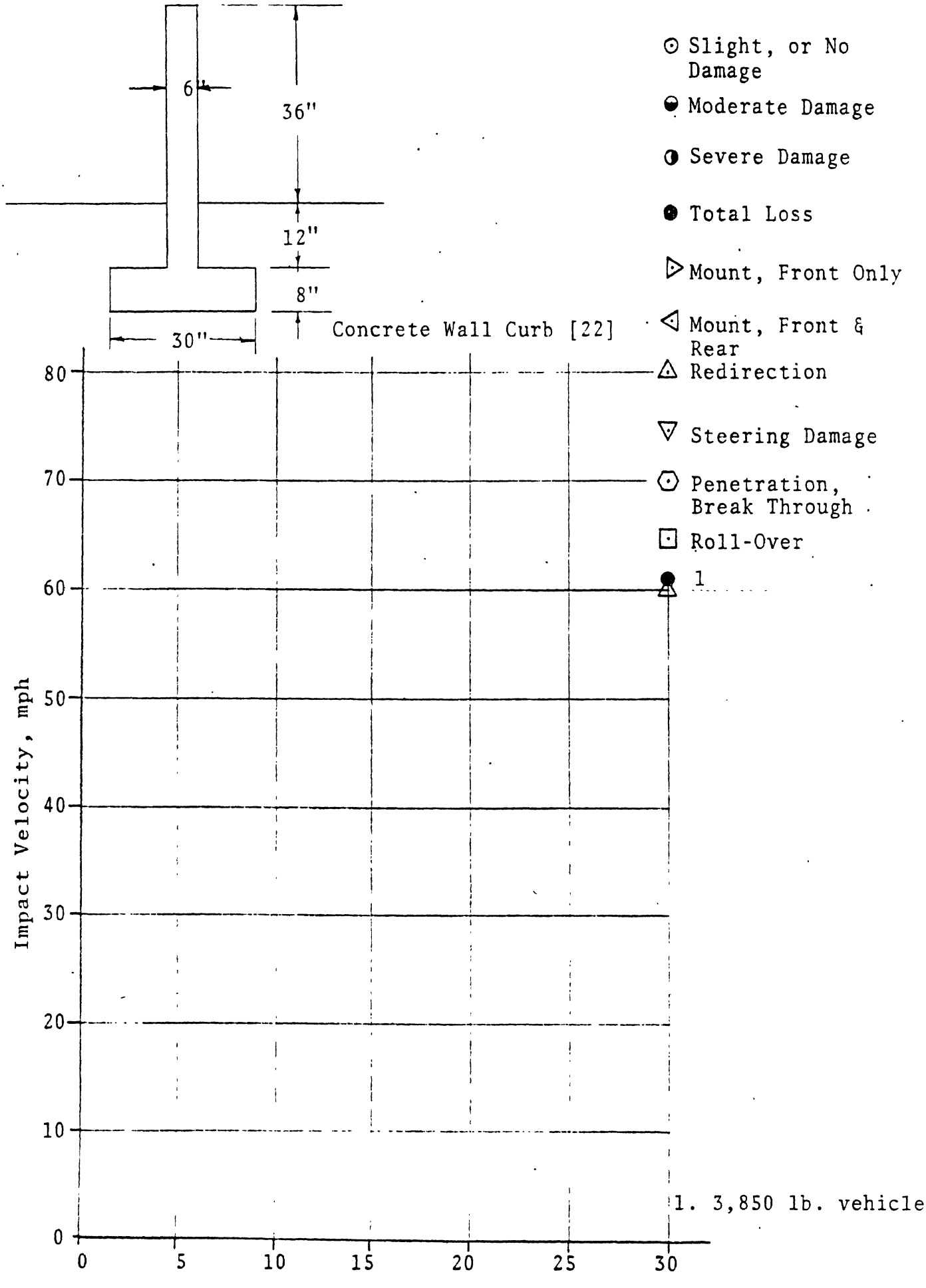

FIGURE 4-26. THIRTY-SIX INCH CURB TEST RESULTS SUMMARY

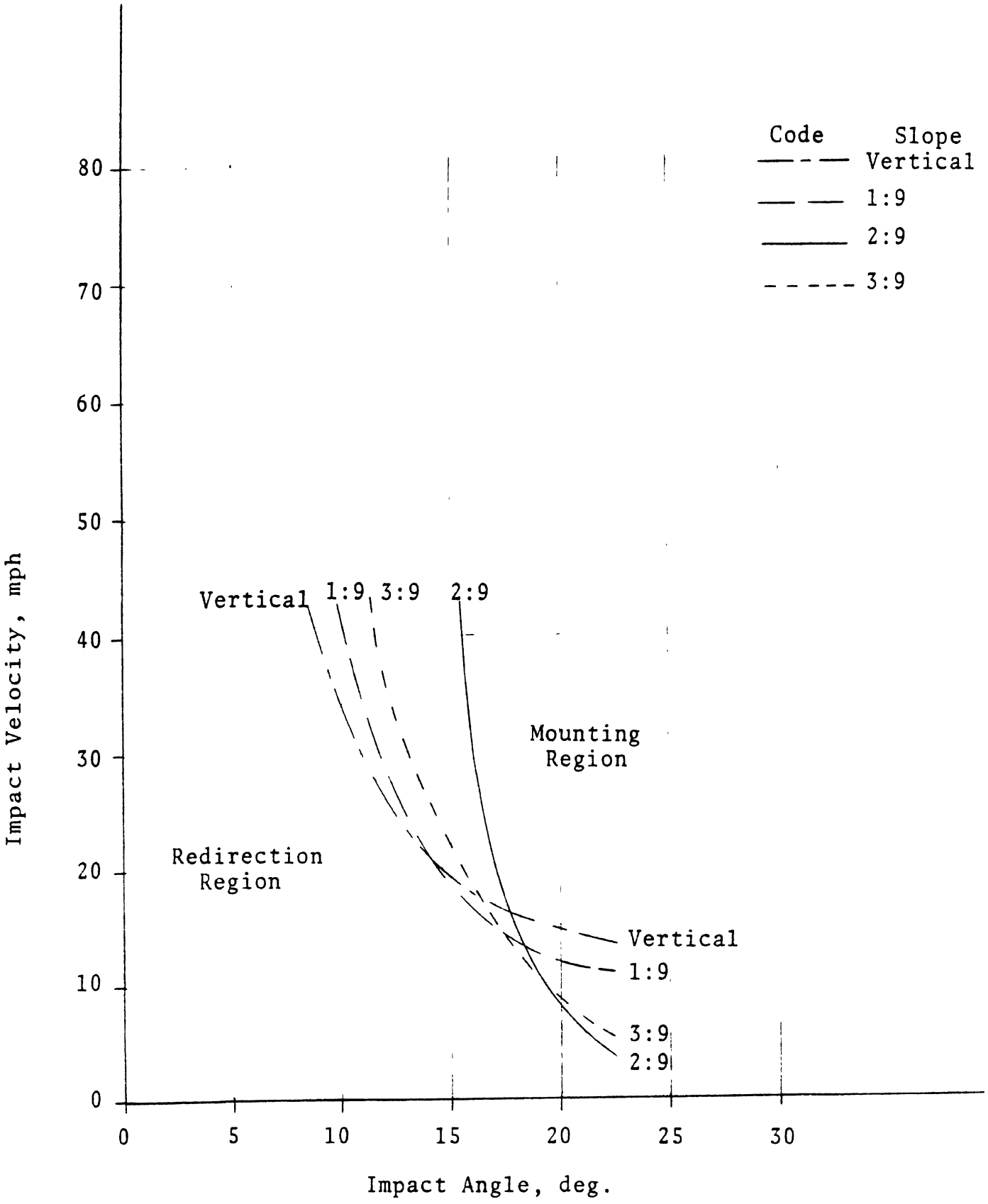

FIGURE 4-27. THE INFLUENCE OF CURB FACE SLOPE ON REDIRECTION PERFORMANCE

redirection is the farthest to the right for this slope, indicating the highest redirection efficiency. Slopes more steep than 2:9 tend to enhance mounting through rim contact while those with flatter slopes do so by providing a ramp for the tire.

In the second California test series, curb height was made a test parameter [13]. Four curb configurations with adjustable shims for height control were tested as indicated earlier on Figures 4-14 through 4-16 and 4-20. Enough data are available for the curbs A, B, and C shown on these figures to conclusively show that increasing curb height, as would intuitively be expected, does indeed enhance redirection. Data for curbs A and C, illustrating this conclusion, are shown on Figures 4-28 and 4-29, respectively. The lines labeled with constant curb height indicate the redirection boundary for the indicated height. Above the line mounting is likely to occur and below it redirection. (Note the differences in slope that the redirection boundaries have for these two varieties of curb faces.)

While it is clear, then, that increasing barrier curb height enhances redirection, it is also true that increased height increases vehicle body damage. Therefore, improved redirection is not gained without a price.

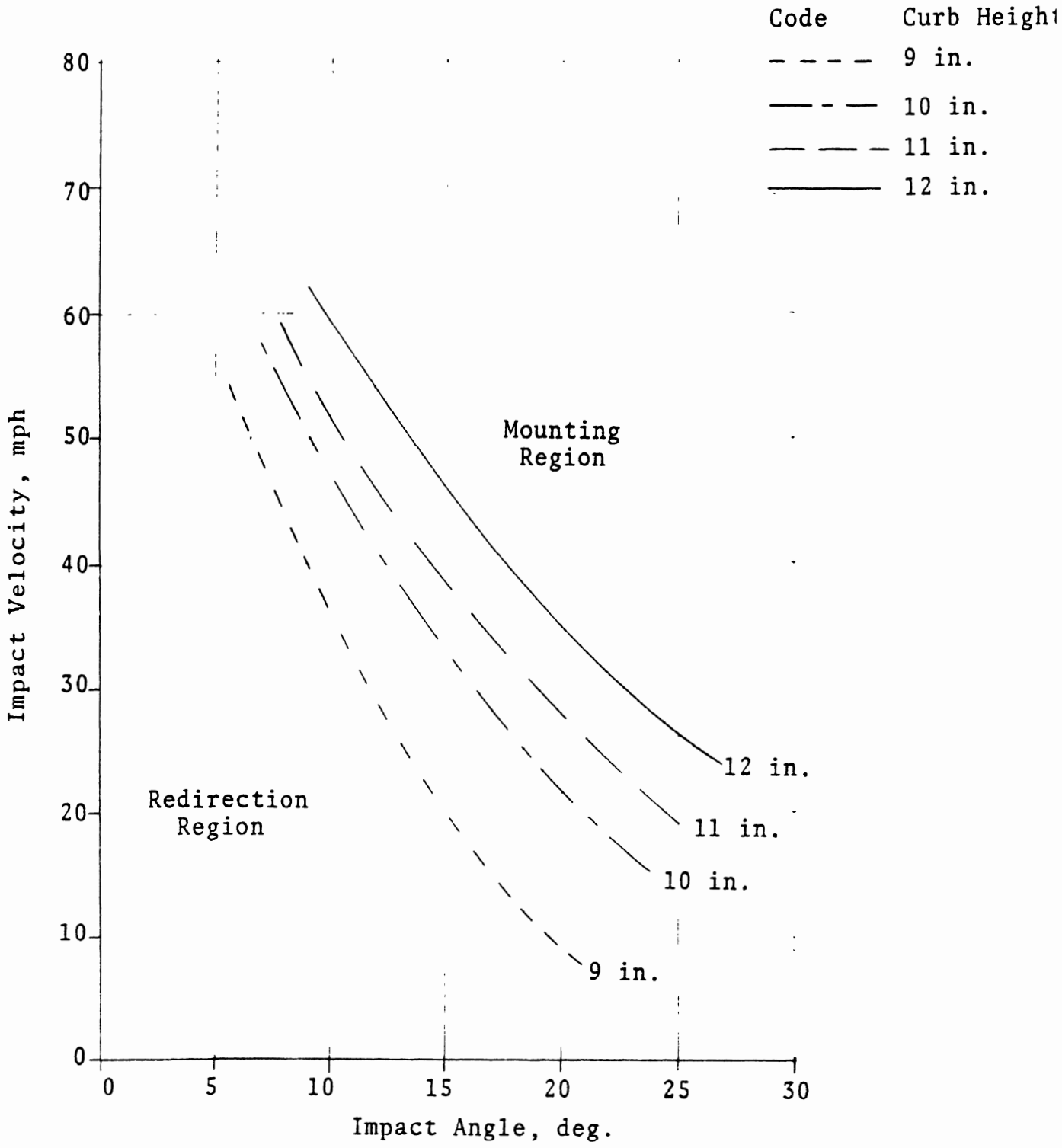

FIGURE 4-28. OPTIMIZED CALIFORNIA CURB A HEIGHT INFLUENCE ON REDIRECTION PERFORMANCE.

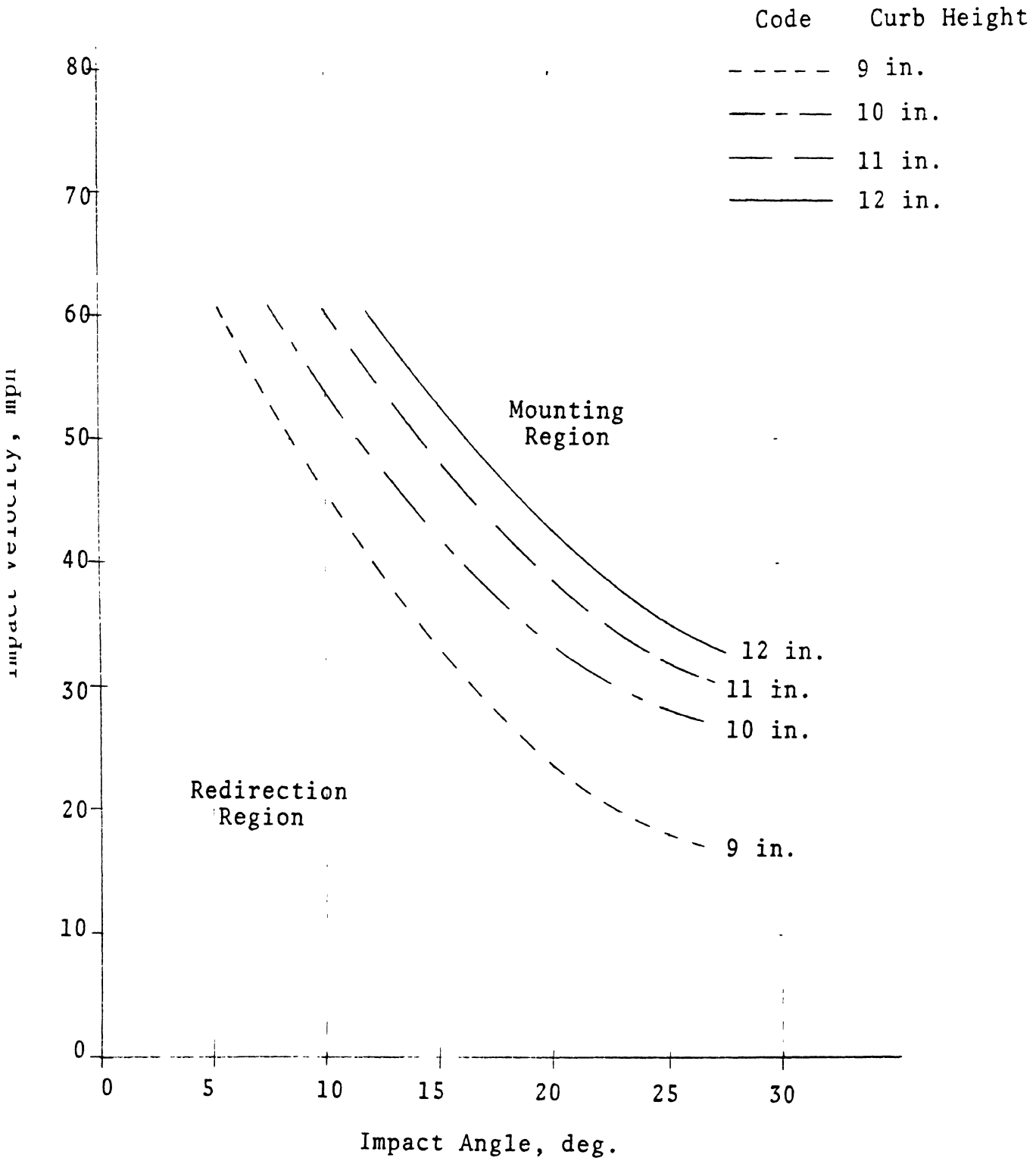

FIGURE 4-29. OPTIMIZED CALIFORNIA CURB C HEIGHT INFLUENCE ON REDIRECTION PERFORMANCE.

4.5 CURB IMPACT SIMULATION

The simulation exercises were carried out to evaluate the curb configurations recommended by the Michigan Department of State Highways [46]. Computer impact runs were therefore made on these designs as well as on designs which were similar and for which test data is available. The latter runs were made as a simulation/test correlation exercise. The parameters used in the exercises were approach velocity and angle, and median surface slope.

4.5.1 SIMULATION PROGRAM. The digital computer simulation program used in the exercises was the Cornell Aeronautical Laboratory Single Vehicle Accident (CALSVA) program which is described in Appendix A. In terms of curb impacts, the program is best suited to determining the vehicle dynamic reaction as it mounts the curb. The spring-mass representations of the tire, suspension and vehicle body, faithfully simulate the motions of an actual vehicle in this kind of situation.

The actual mechanics of curb mounting, e.g., the tire sidewall/curb face friction interaction, are not well represented. The tire is represented as a thin disc with springs emanating radially outward from its center. Friction forces on the sidewall are not calculated, since the program was not developed for that purpose. Situations where the tire

strikes the curb at a high enough angle and where scrubbing is not a factor are well simulated, however. This kind of situation (i.e., where the impact angle is 10° or more) is the type which was examined in these exercises.

4.5.2 SIMULATION EXERCISES. The simulation exercise runs for the various curb configurations which were evaluated are described in this subsection. Parameters and variables which were held constant for these runs are:

1. An unpowered, unbraked vehicle
2. A fixed steering wheel position
3. Up to 75 parameters defining the vehicle's dynamic properties.

The standard Michigan Department of State Highways curbs which were evaluated are shown on Figure 4-30. Results are presented in the form of kinematic data for each configuration.

4.5.2.1 Curb A. The simulation runs made on the MDSH concrete curb and gutter design A are shown in Table 4-1. As indicated on Figure 4-30 [47], curb A is a barrier curb since the curb face slope is 1.5:9.

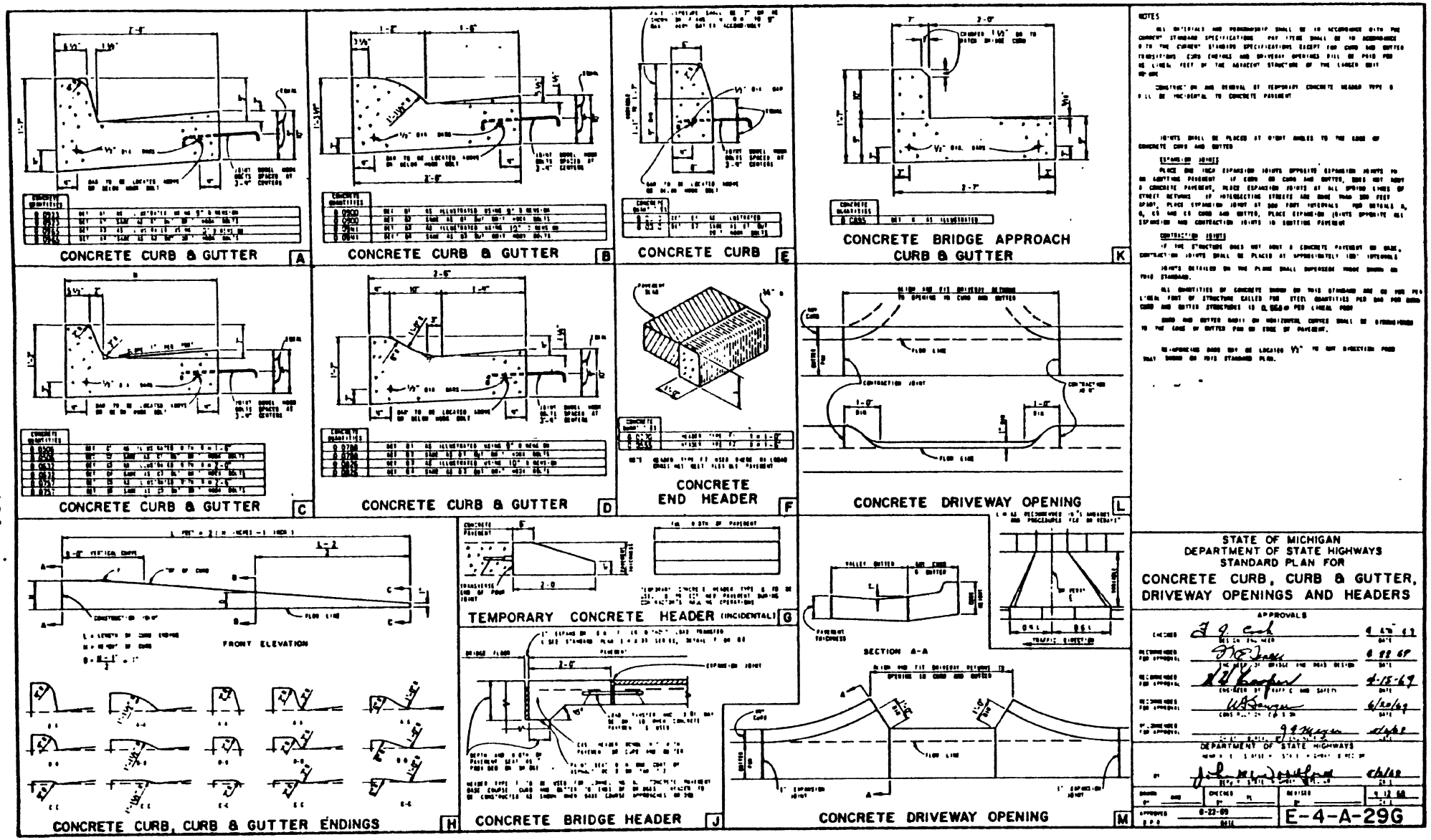
CONCRETE CURB & GUTTER A
CONCRETE CURB & GUTTER B
CONCRETE CURB E
CONCRETE BRIDGE APPROACH CURB & GUTTER K
CONCRETE CURB & GUTTER C
CONCRETE CURB & GUTTER D
CONCRETE END HEADER F
CONCRETE DRIVEWAY OPENING L
NOTES
STATE OF MICHIGAN
DEPARTMENT OF STATE HIGHWAYS
STANDARD PLAN FOR
CONCRETE CURB, CURB & GUTTER, DRIVEWAY OPENINGS AND HEADERS
APPROVALS
DEPARTMENT OF STATE HIGHWAYS
E-4-A-29G
FRONT ELEVATION
CONCRETE CURB, CURB & GUTTER ENDINGS H
TEMPORARY CONCRETE HEADER (INCIDENTAL) G
CONCRETE BRIDGE HEADER J
SECTION A-A
CONCRETE DRIVEWAY OPENING M

FIGURE 4-30.

TABLE 4-1

CURB A SIMULATION RUNS

Run	Velocity	Angle	Median Slope	Vehicle
CG-20	40 mph	25°	1/2" per ft.	1966 Ford Custom
CG-11	60 mph	10°	1/2" per ft.	1966 Ford Custom
CG-1	60 mph	25°	1/2" per ft.	1966 Ford Custom
CG-16	80 mph	10°	1/2" per ft.	1966 Ford Custom

Plan view results of the four simulation runs are shown on Figures 4-31, 4-32, 4-34, and 4-35. In all cases the vehicle mounted the curb, but the tendency toward redirection was more pronounced for the lower velocities and angles. In the 40 mph, 25° case shown on Figure 4-31, for example, it is apparent that the vehicle will eventually return to the roadway even though all four wheels initially mounted the curb.

A different effect is indicated on Figure 4-32 for the 60 mph, 10° case. As the left front wheel initially strikes the curb a yawing moment is applied to the vehicle which causes it to turn toward the road. The front wheels are also deflected toward the road at this time, further tending to produce a redirecting action. The wheel mounts the curb,

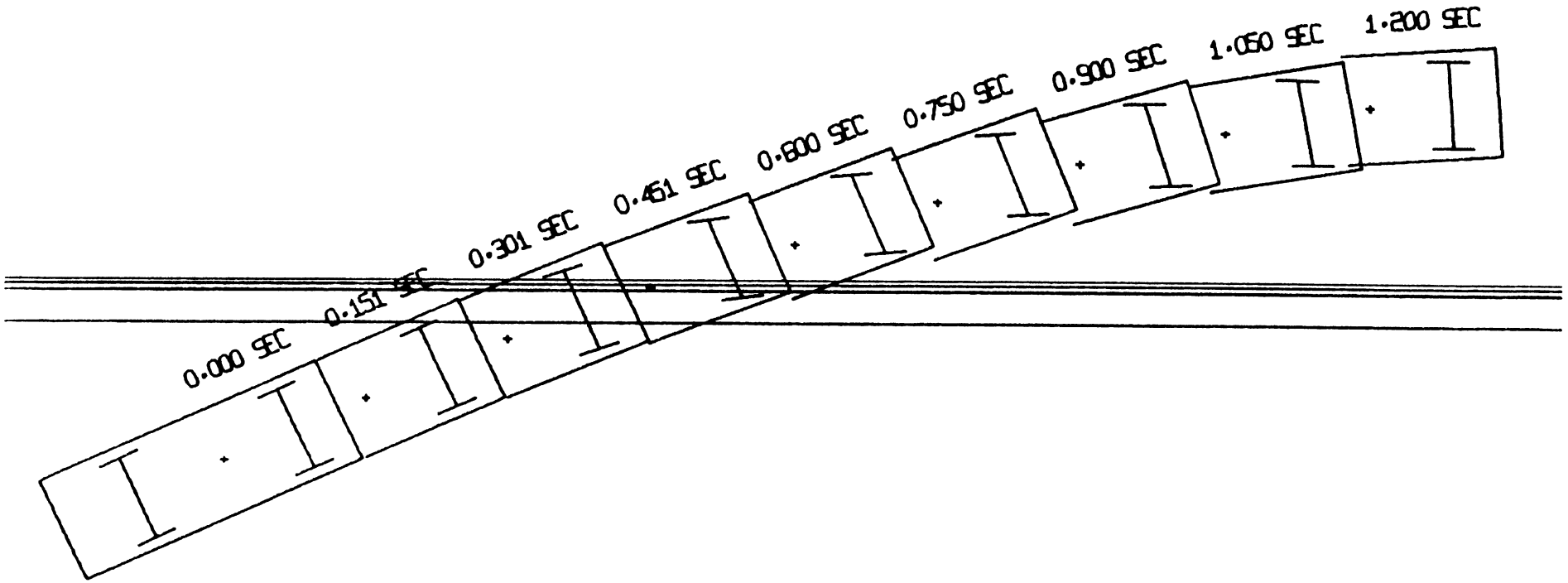

SCALE 0 10 20 FEET

EVALUATION OF MSHO CURBS

FIGURE 4-31

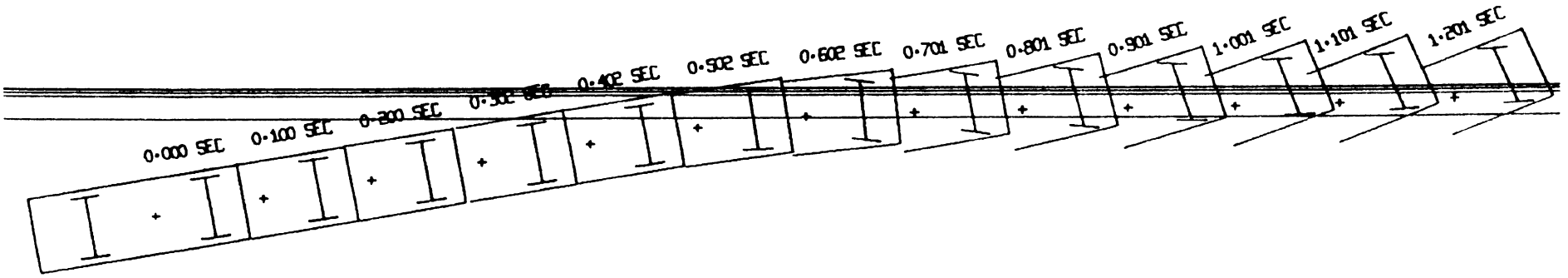

SCALE 0 10 20 FEET

EVALUATION OF MSHO CURBS

FIGURE 4-32

RUN CG-11 - CURB TYPE A - 1966 CUSTOM - 60 MPH - 10 DEG - SLOPED MEDIAN

however, and the net result of the turning action is to cause the left rear wheel to strike the curb at a shallower angle. This latter action produces a yawing moment in the opposite direction which causes the vehicle to go into a mild spin. The angle of the vehicle relative to the curb becomes larger and the rear wheels scrub along the pavement as the vehicle moves sideways. Eventually, the steer angle of the front wheels nulls the skid, however, bringing the yaw rate to zero and stabilizing the yaw angle. Time histories of both yaw rate and angle are shown on Figure 4-33.

The conditions of this simulated run (i.e., 60 mph and 10°) are fairly close to two tests made in California in 1957 [13], which are summarized on Figure 4-15. Impact tests on two similar nine-inch curbs, both at 60 mph and 7.5°, showed mounting by both the front and rear wheels. Evidently mounting occurred in these tests without the skidding action which occurred in the simulation runs. This can be explained by the fact that tire sidewall/curb face friction is present in the test and not in the simulation. Also, the test vehicle was somewhat different than the one used in the simulation.

The remaining two runs at higher angles and velocities (Figures 4-34 and 4-35) exhibit mounting phenomena which are generally predictable for this type of curb.

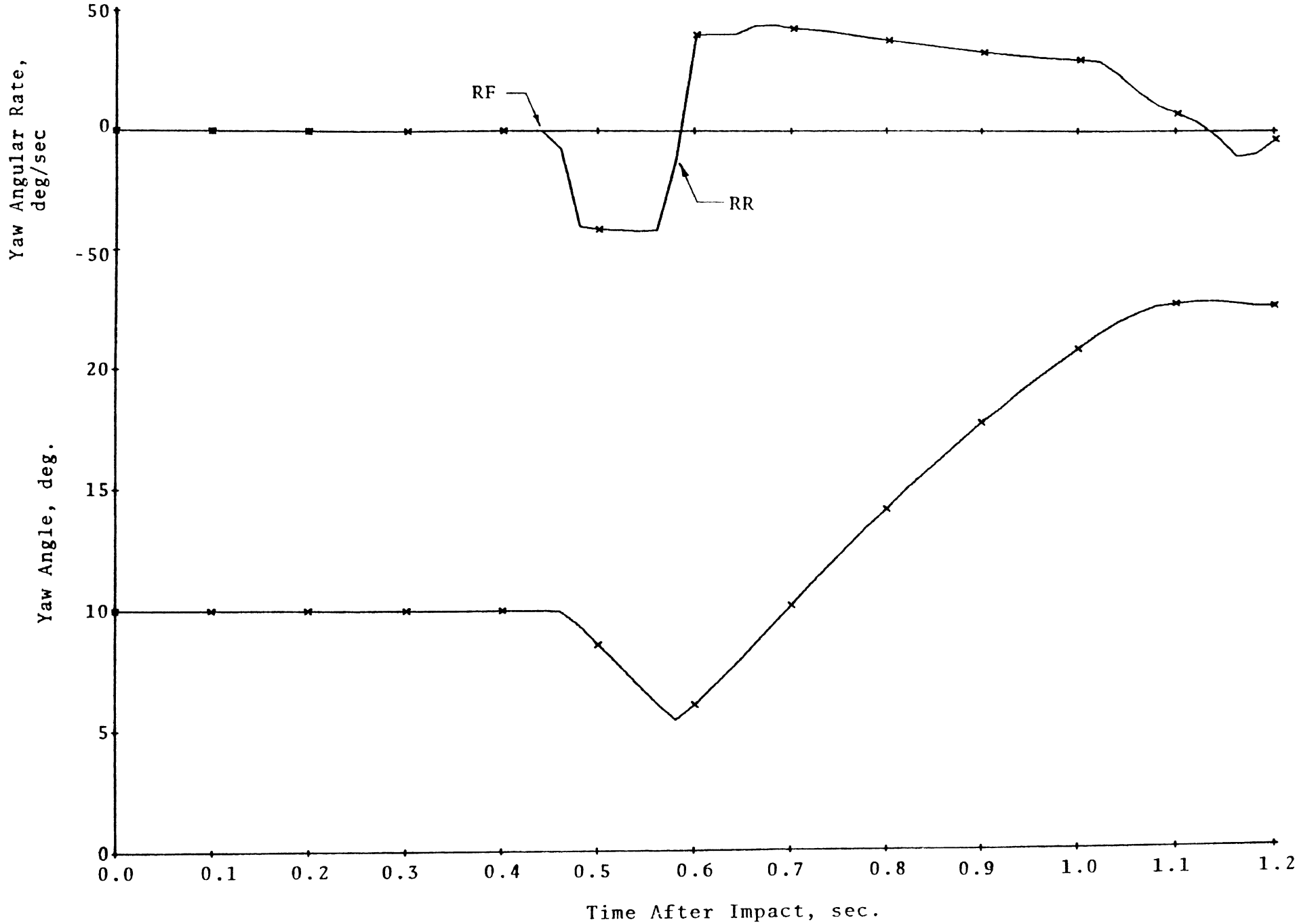

FIGURE 4-33. RUN CG-11 - CURB A, 60 MPH, 10 DEG. IMPACT-YAW ANGLE AND ANGULAR RATE HISTORIES

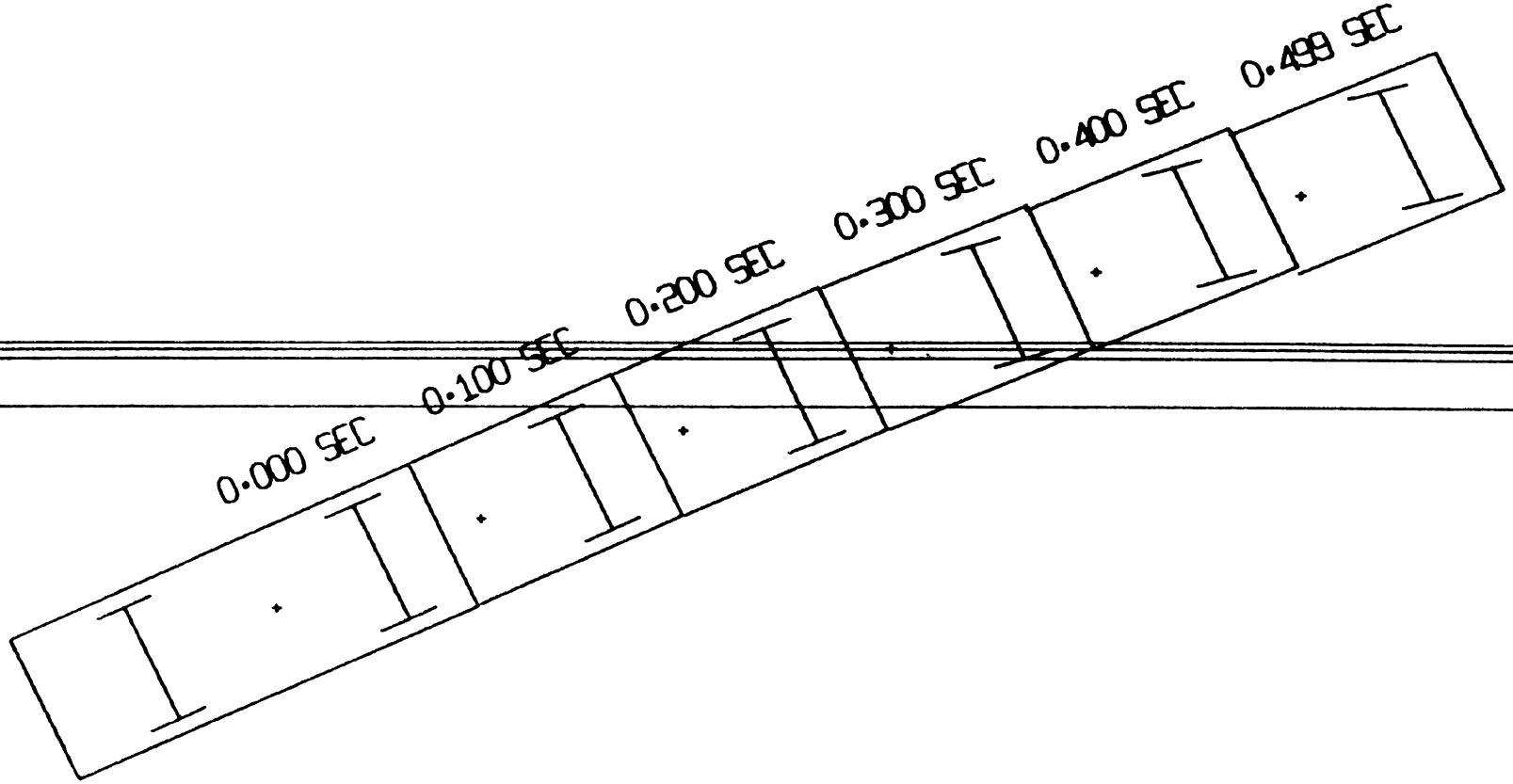

SCALE 0 10 20
FEET

EVALUATION OF MOSH CURBS

FIGURE 4-34

RUN CG-1 - CURB TYPE A - 1966 CUSTOM - 60 MPH - 25 DEG IMPACT

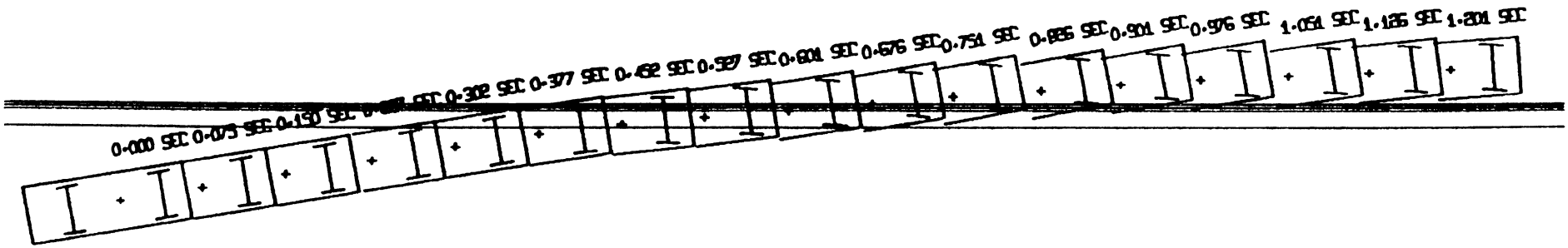

SCALE 0 10 20

FEET

EVALUATION OF MSHO CURBS

FIGURE 4-35

RUN CG-16 - CURB TYPE A - 1966 CUSTOM - 80 MPH - 10 DEG - SLOPED MEDIAN

In order to insure additional compatability between test and simulation results, a simulation run at 60 mph and 25° was made on the California nine-inch curb listed as curb A on Figure 4-15. The results in plan view are shown on Figure 4-36 and can be compared with similar results for the MDSH curb A on Figure 4-34.

Acceleration data is not given for any of the runs since calculated values are always well below the tolerance levels described in Appendix E.

4.5.2.2 Curb B. The MDSH concrete curb and gutter design B shown on Figure 4-30 indicates that curb B is a mountable curb. The simulation runs made on the curb are given in Table 4-2.

TABLE 4-2

CURB B SIMULATION RUNS

Run	Velocity	Angle	Median Slope	Vehicle
CG-21	40 mph	25°	1/2" per ft.	1966 Ford Custom
CG-12	60 mph	10°	1/2" per ft.	1966 Ford Custom
CG-2	60 mph	25°	1/2" per ft.	1966 Ford Custom
CG-17	80 mph	10°	1/2" per ft.	1966 Ford Custom

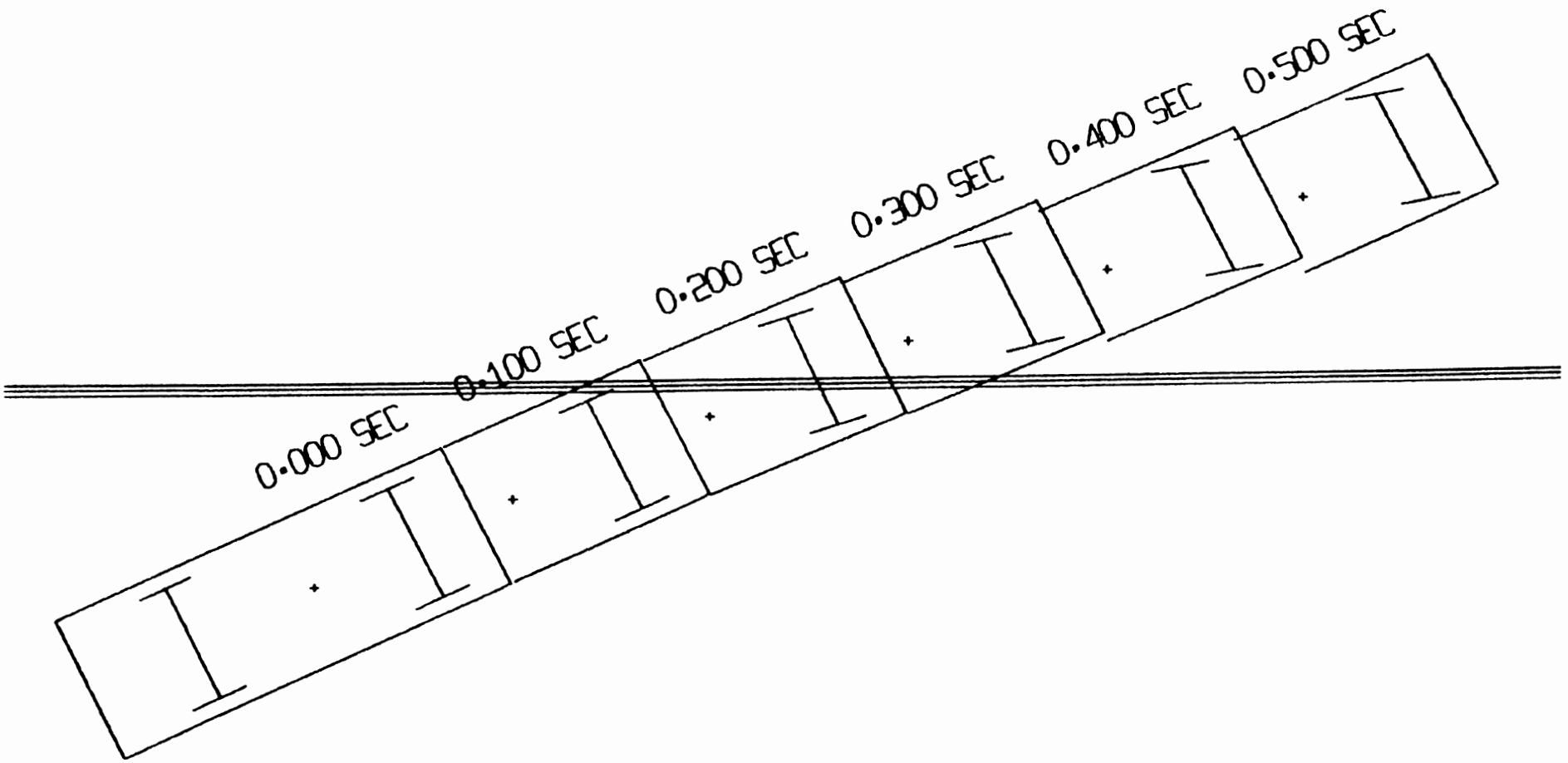

SCALE 0 10 20 FEET

EVALUATION OF MSHD CURBS

FIGURE 4-36

RUN CG-8 - CAL 9 IN - 1966 CUSTOM - 60 MPH - 25 DEG - SLOPED MEDIAN

Plan view results for the runs are shown on Figures 4-37 through 4-40. In all cases the vehicle mounted the curb without any essential tendency toward redirection. The largest change in vehicle heading angle occurred in the 40 mph, 25° case where the angle changed from 25° to just over 20° at the end of the run. In all other cases the heading angle changed no more than one degree.

In comparing the curb B simulation results with test results, the design nearest to curb B that has been tested is the California six-inch mountable curb shown on Figure 4-5. As indicated on that figure, all tests show the California curb to be easily mountable. Since the MDSH curb B is only 5 1/2 inch high and somewhat flatter in cross-section, the tests would suggest that it also can be expected to be easily mountable. A simulation run for the California six-inch curb was made to confirm this expectation and this is shown on Figure 4-41. Run conditions are the same as for the MDSH curb B shown on Figure 4-39.

Accelerations imparted to the vehicle were never larger than one g in any direction. It can be concluded, therefore, that curb B will have little influence on vehicle motions during a vehicle/curb impact.

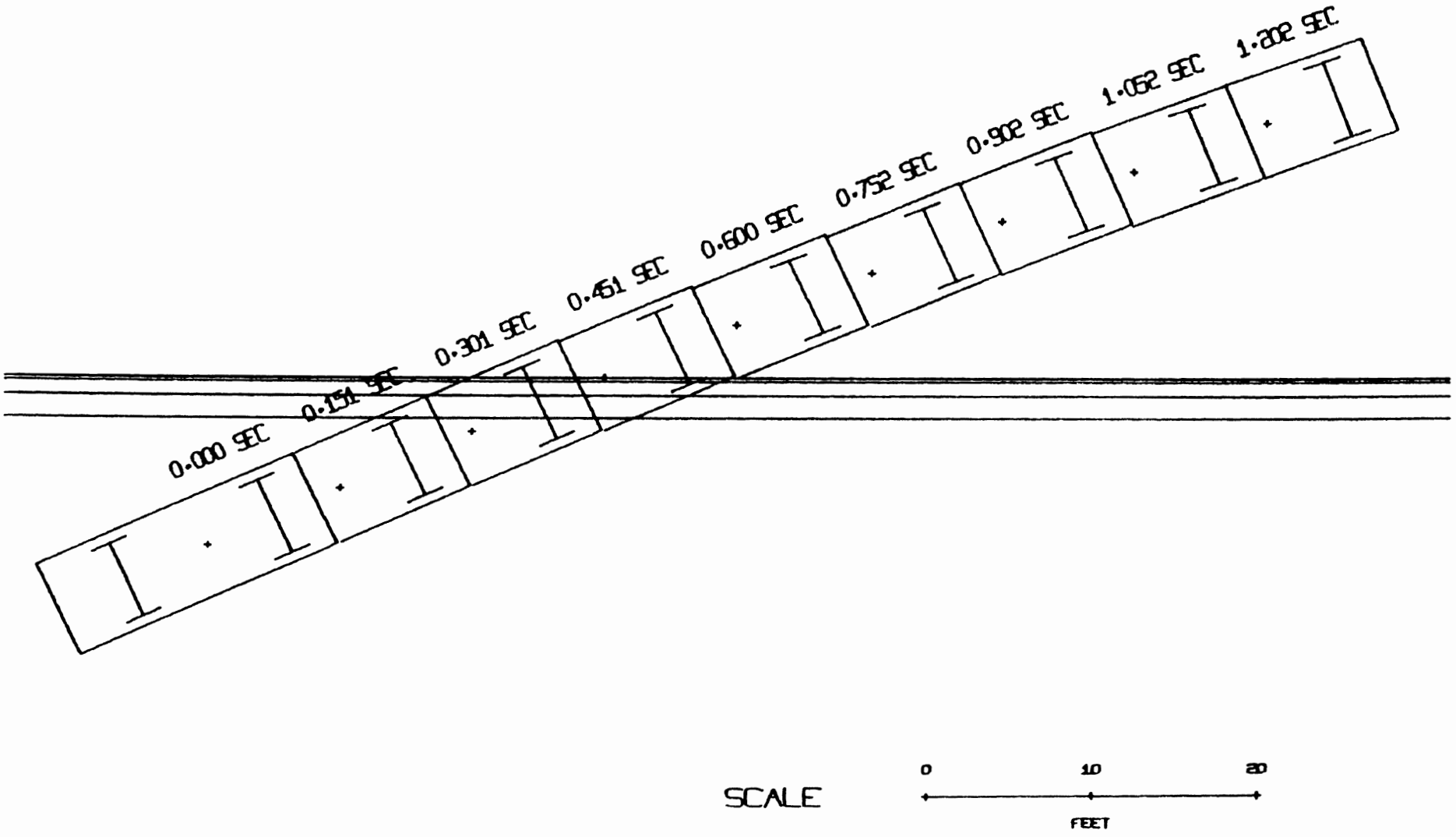

FIGURE 4-37

EVALUATION OF MSHD CURBS

RUN CG-21 - CURB TYPE B - 1966 CUSTOM - 40 MPH - 25 DEG - SLOPED MEDIAN

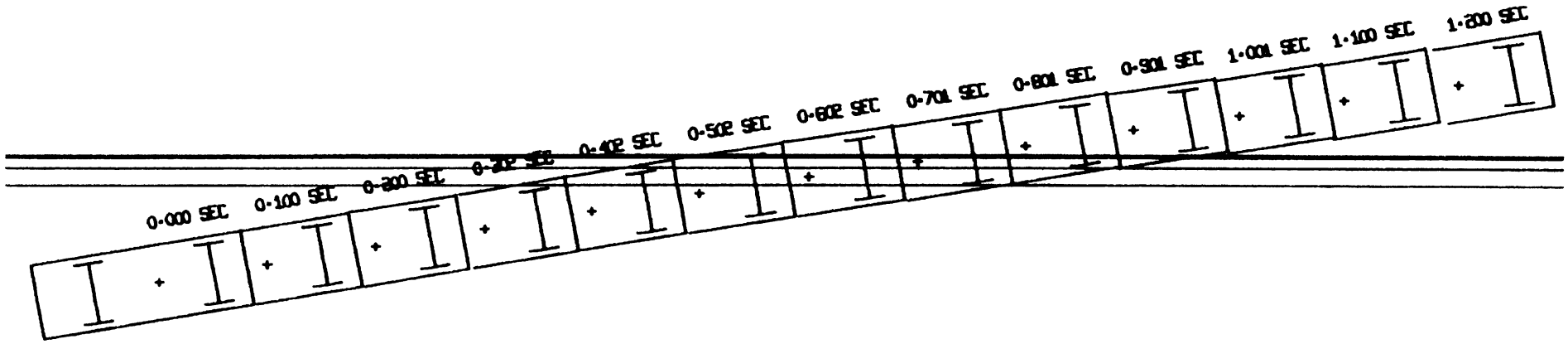

SCALE 0 10 20 FEET

EVALUATION OF MSHO CURBS

FIGURE 4.29

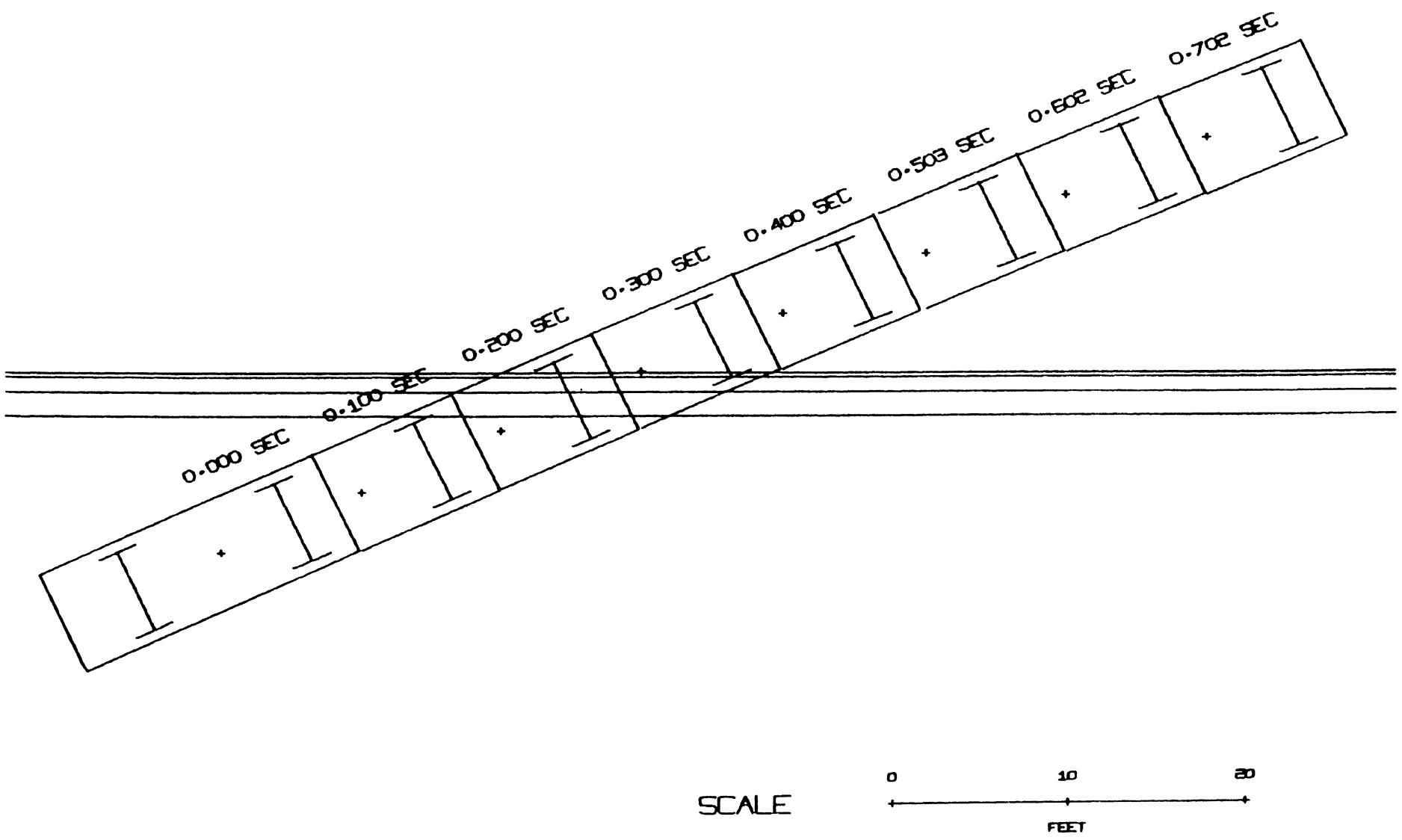

EVALUATION OF MSHO CURBS

FIGURE 4-39

RUN CG-2 - CURB TYPE B - 1966 CUSTOM - 60 MPH - 25 DEG IMPACT

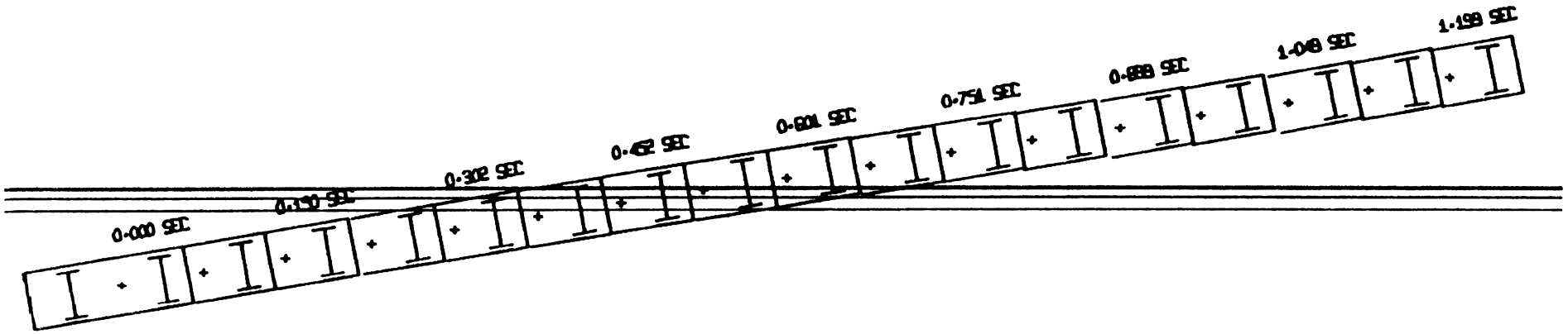

SCALE 0 10 20 FEET

FIGURE 4-40 EVALUATION OF MSHD CURBS

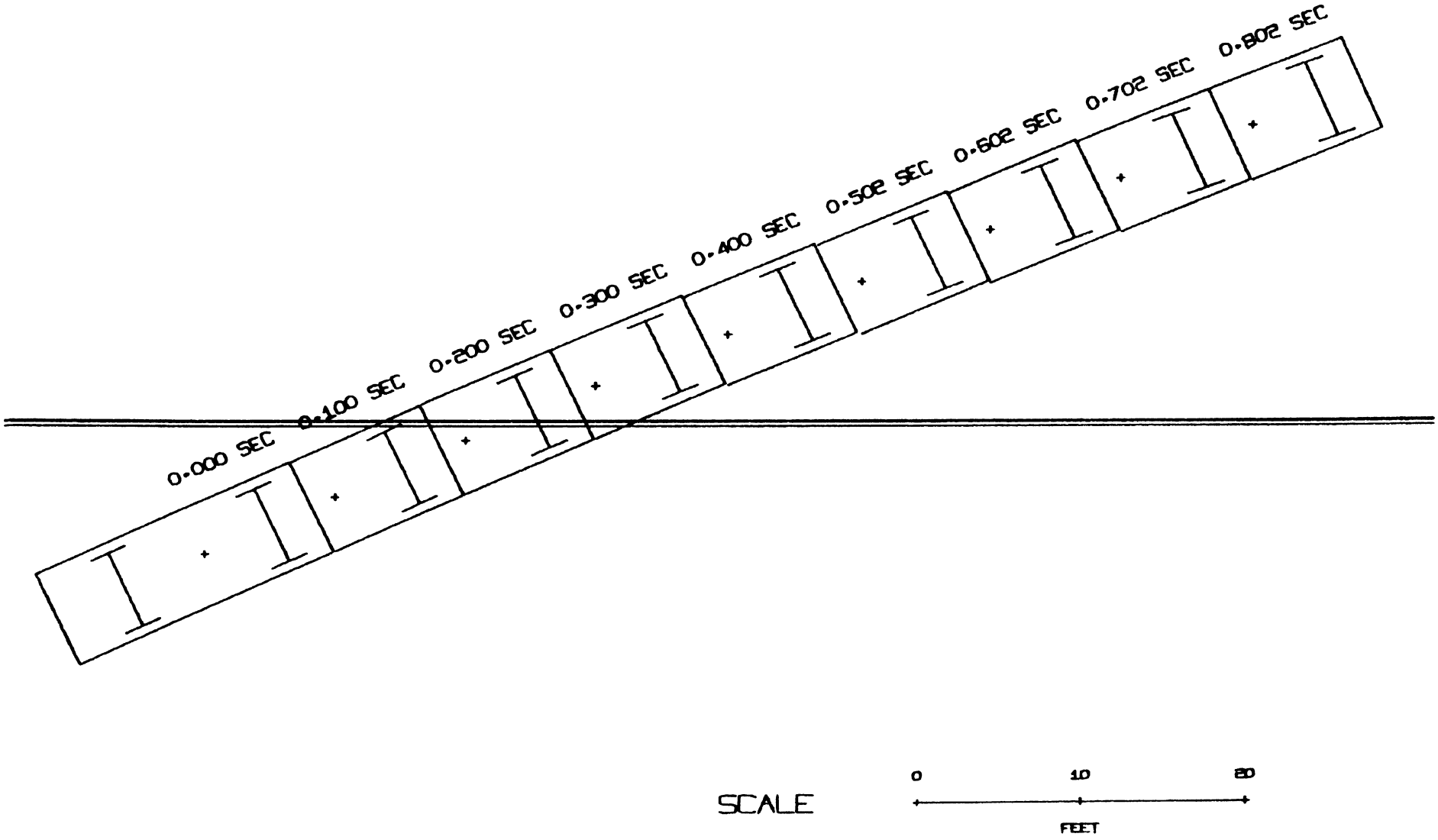

EVALUATION OF MSHD CURBS

FIGURE 4-41

RUN CG-4 - CAL 6 IN - 1966 CUSTOM - 60 MPH - 25 DEG - SLOPED MEDIAN

4.5.2.3 Curb C. The curb C configuration shown on Figure 4-30 is, by the California definition [47], a barrier curb. The design is on the borderline of being classified as mountable, however, since the face slope is 2:7. (A mountable face slope would be 1:3, or flatter.)

The simulation runs made on curb C are given in Table 4-3. Note that the impact velocities for this curb are somewhat lower than for curbs A and B. These lower values were chosen because speeds on roads where curb C is used are usually 50 mph, or less [46].

TABLE 4-3

CURB C SIMULATION RUNS

Run	Velocity	Angle	Median Slope	Vehicle
CG-22	30 mph	25°	Flat	1966 Ford Custom
CG-13	50 mph	10°	Flat	1966 Ford Custom
CG-7	50 mph	25°	Flat	1966 Ford Custom

Plan view results of the three simulation runs are shown on Figures 4-42 through 4-44. In all three cases, the vehicle easily mounted the curb with a mild tendency toward redirection resulting from the steering action of the front wheels; the

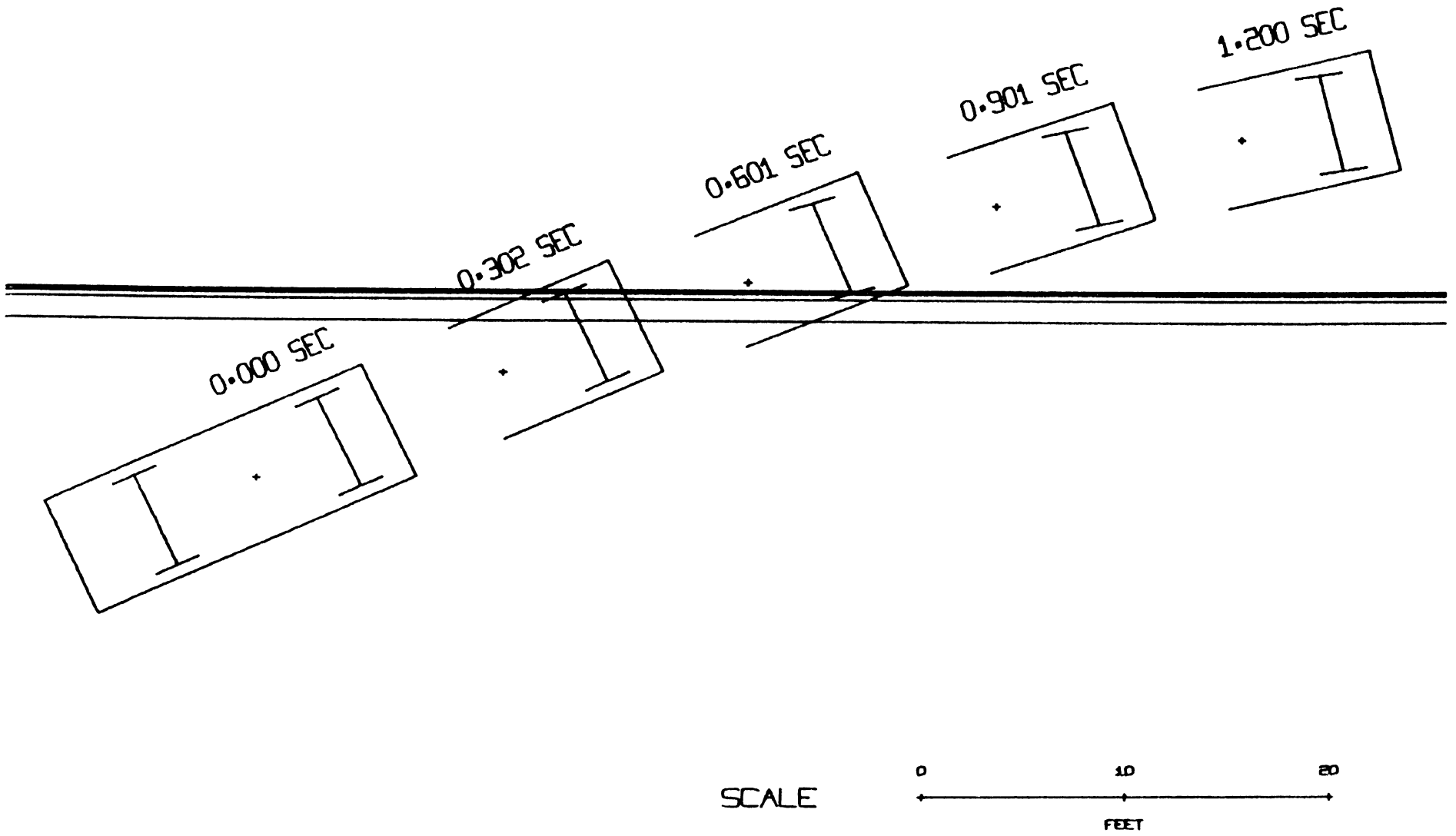

EVALUATION OF MSHO CURBS

FIGURE 4-42

RUN CG-22 - CURB TYPE C - 1966 CUSTOM - 30 MPH - 25 DEG - FLAT MEDIAN

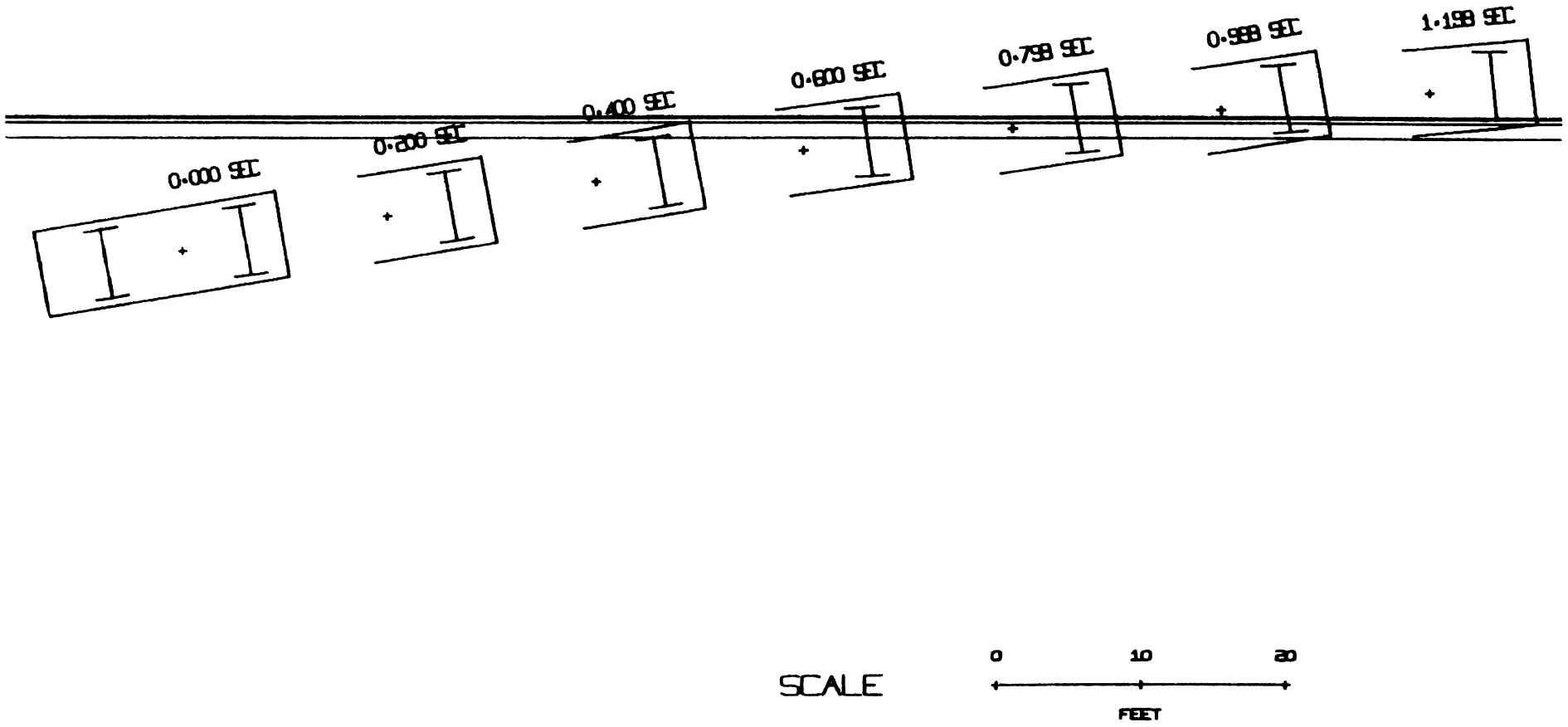

EVALUATION OF MSHO CURBS

FIGURE 4-43

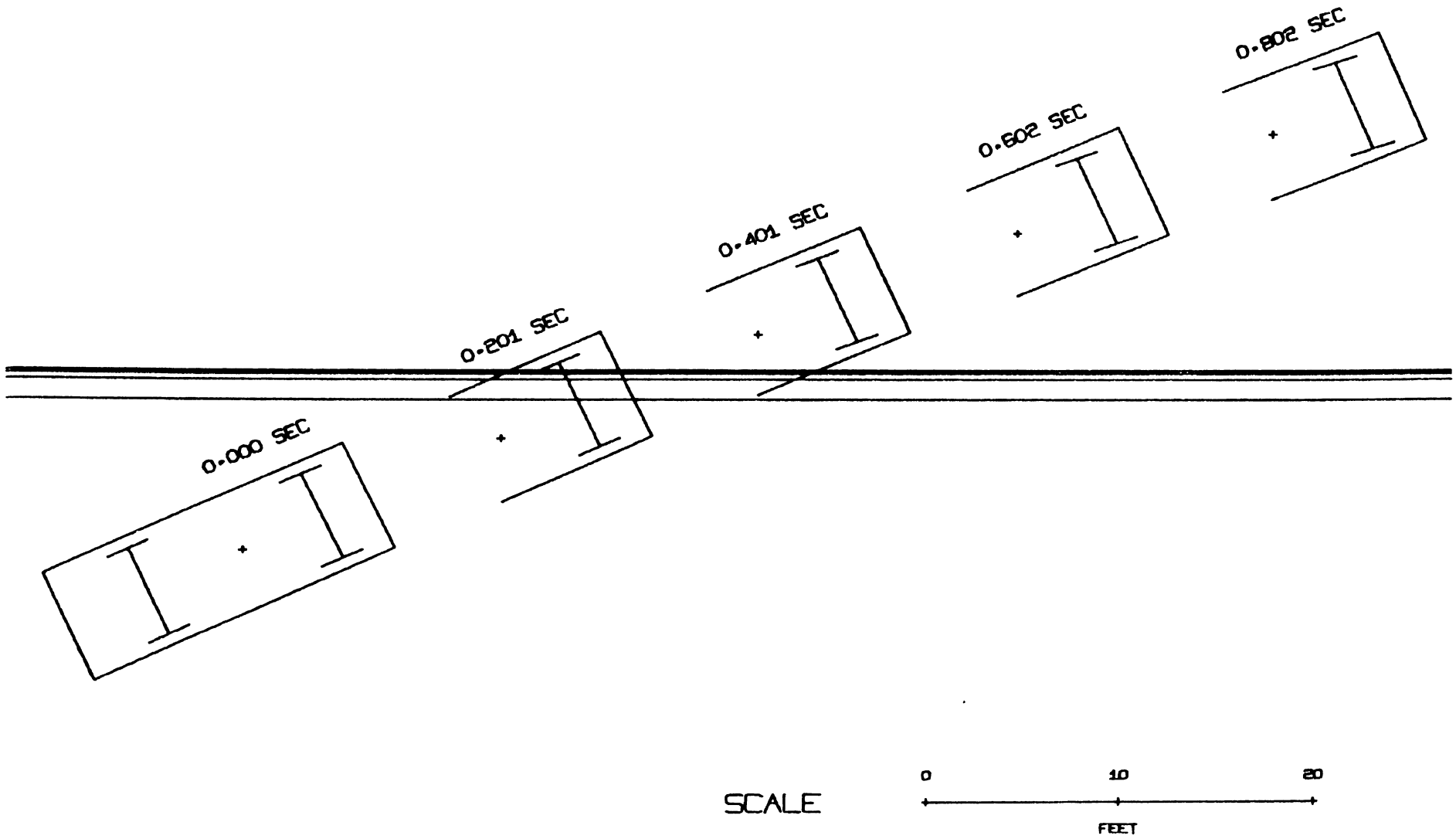

EVALUATION OF MSHO CURBS

FIGURE 4-44

RUN CG-7 - CURB TYPE C - 1966 CUSTOM - 50 MPH - 25 DEG - FLAT MEDIAN

front wheels acquiring a steer angle during the initial contact. The 30 mph run tended to show more redirection than the two 50 mph runs, with the heading angle changing from 25° to 13°. Heading changes of no more than three or four degrees were recorded for the 50 mph runs. This effect is to be expected since, at the higher velocity, more side force that is required to deflect the vehicle velocity vector.

In no case were accelerations imparted to the vehicle sufficient to endanger vehicle occupants.

The only curb design that has been tested which is even remotely comparable to curb C is the California six-inch curb described in the discussion of curb B. The face of the MDSH curb C is more steep than the California curb, however, and the curb C design is one inch higher. Comparisons, therefore, can only be general.

4.5.2.4 Curb D. The curb D concrete curb and gutter design shown on Figure 4-30 is clearly a mountable curb. Simulation runs for the curb are given in Table 4-4.

Plan view simulation results are shown on Figures 4-45 through 4-48. In no case was the vehicle deflected more than 2.5° by the curb, nor did accelerations imparted to the vehicle ever exceed one g, in any direction.

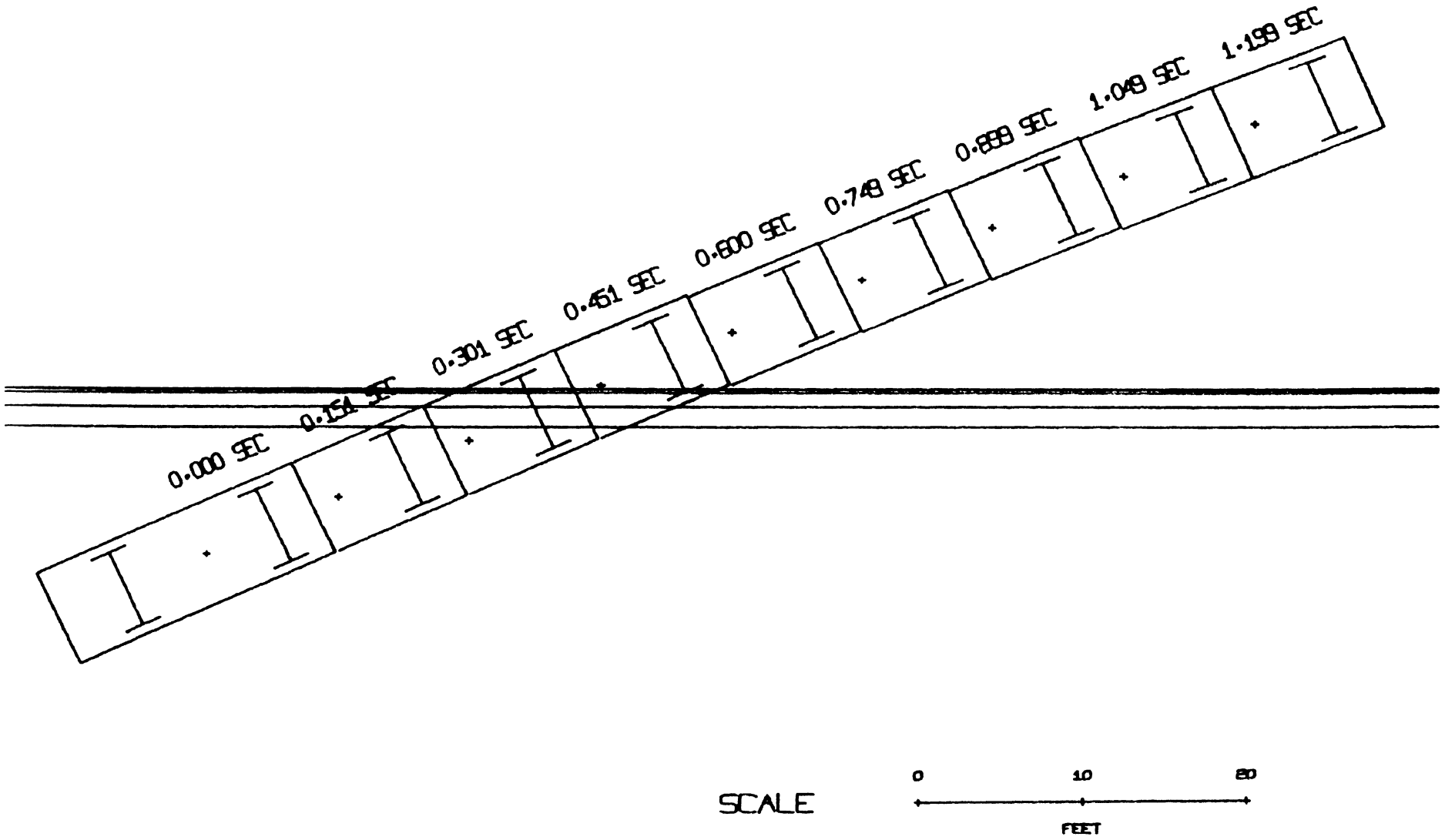

EVALUATION OF MSHO CURBS

FIGURE 4-45

RUN CG-23 - CURB TYPE D - 1966 CUSTOM - 40 MPH - 25 DEG - SLOPED MEDIAN

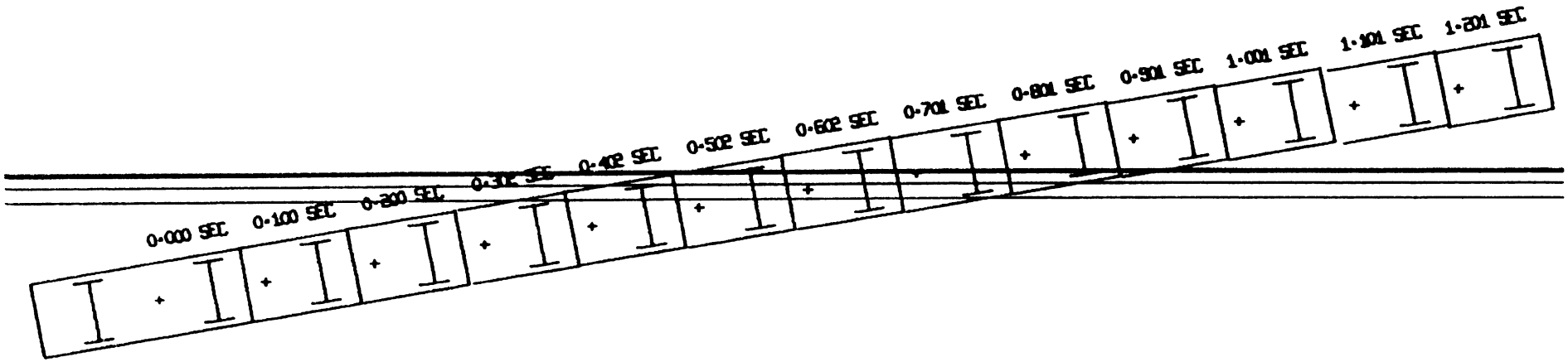

SCALE

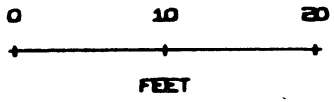

EVALUATION OF MSHO CURBS

FIGURE 4-46

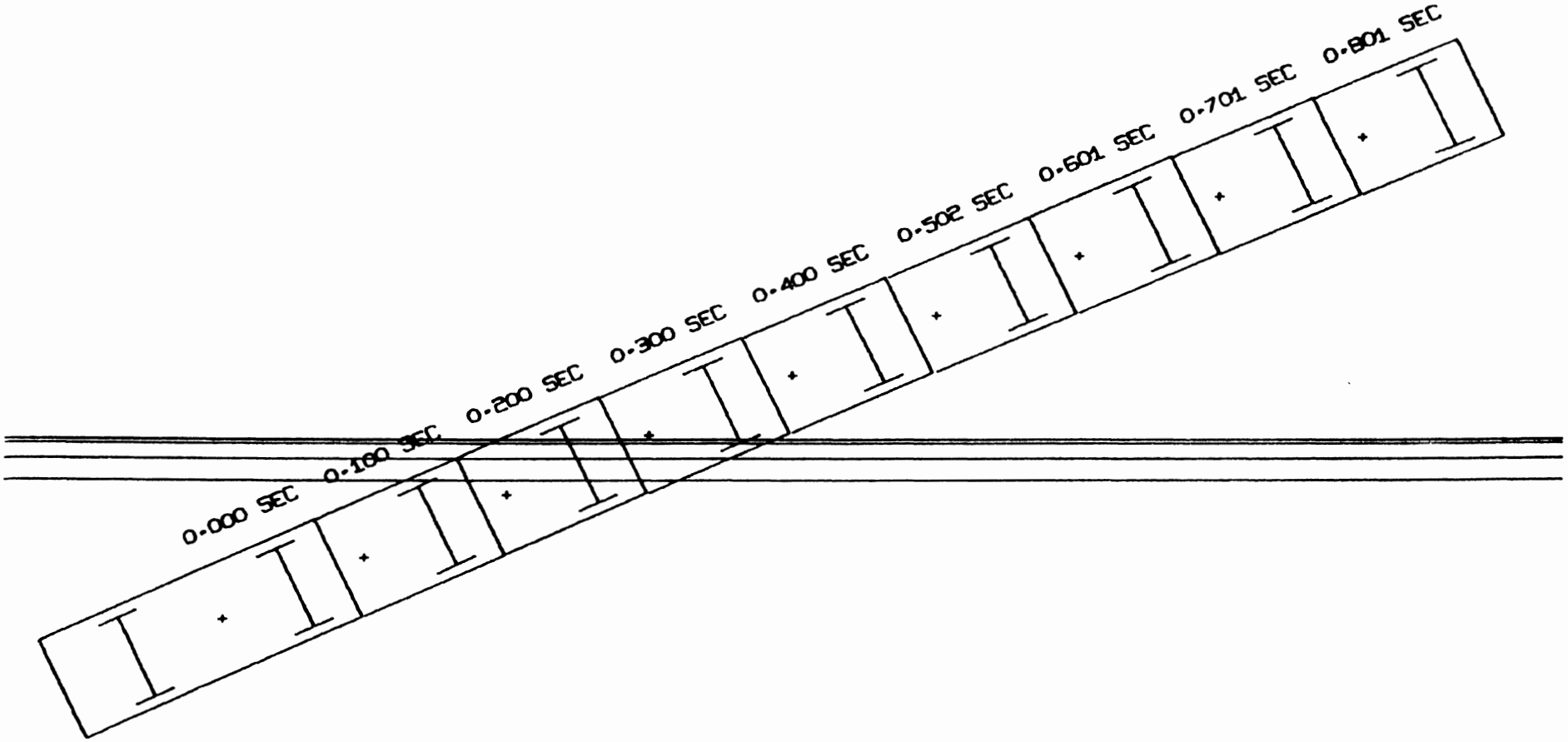

SCALE 0 10 20 FEET

EVALUATION OF MSHD CURBS

FIGURE 4-47

RUN CG-3 - CURB TYPE D - 1966 CUSTOM - 60 MPH - 25 DEG - SLOPED MEDIAN

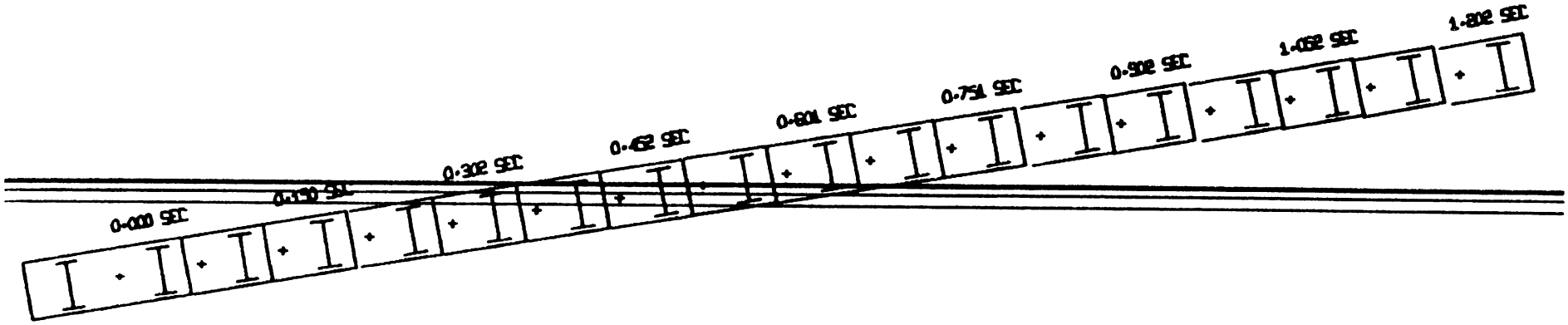

SCALE 0 10 20 FEET

FIGURE 4-48

EVALUATION OF MSHD CURBS

No test data exists for a curb comparable to curb D. It can be concluded, however, that curb D will have little influence on vehicle dynamics. This conclusion is supported both by these simulation exercises and by tests on curbs of more formidable cross-section.

TABLE 4-4

CURB D SIMULATION RUNS

Run	Velocity	Angle	Median Slope	Vehicle
CG-23	40 mph	25°	1/2" per ft.	1966 Ford Custom
CG-14	60 mph	10°	1/2" per ft.	1966 Ford Custom
CG-3	60 mph	25°	1/2" per ft.	1966 Ford Custom
CG-18	80 mph	10°	1/2" per ft.	1966 Ford Custom

4.5.2.5 Curb K. The curb K concrete bridge approach curb and gutter, shown on Figure 4-30, is a barrier curb. Simulated impact runs made on the curb are given in Table 4-5.

Plan view impact results are shown on Figures 4-49 through 4-52. Mounting in the ordinary sense occurred in both the 25° impact cases. A partial mounting occurred in the 60 mph, 10° case with the left side of the vehicle going up on the curb before the vehicle is redirected. In the 80 mph, 10° case, the vehicle went into a lateral skid

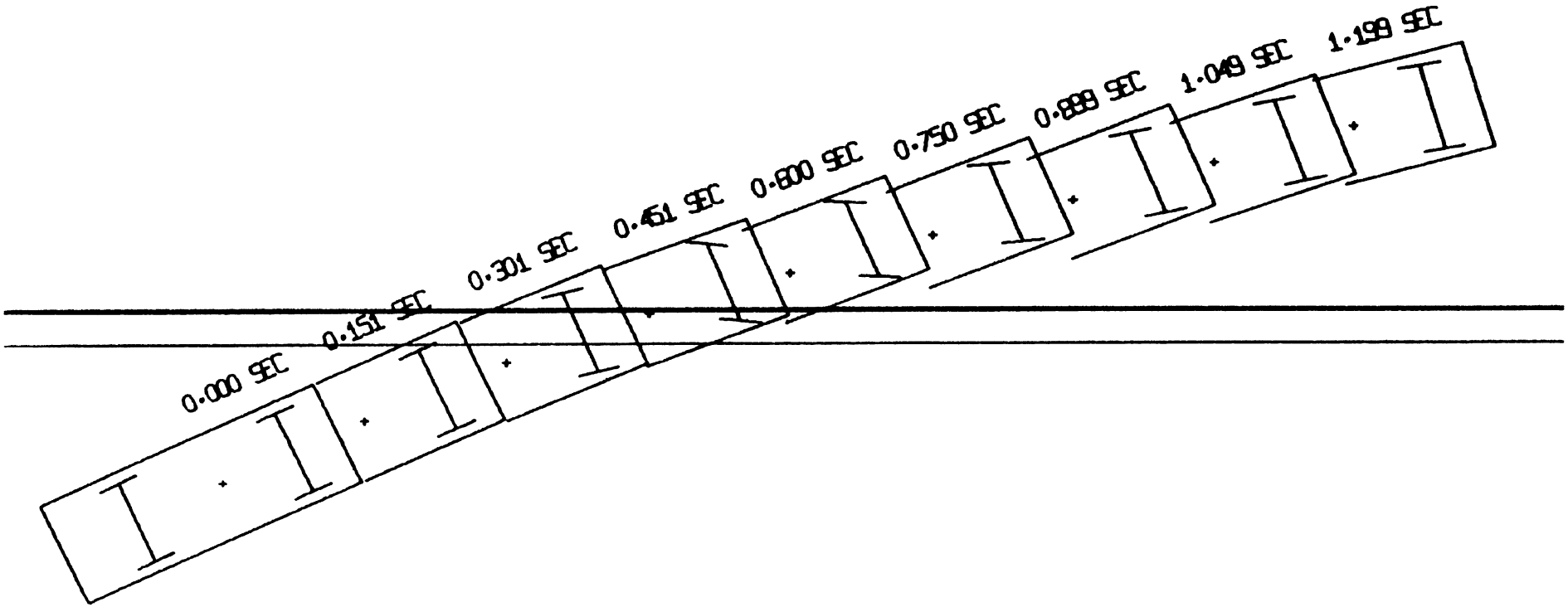

SCALE 0 10 20 FEET

EVALUATION OF MSHO CURBS

FIGURE 4-49

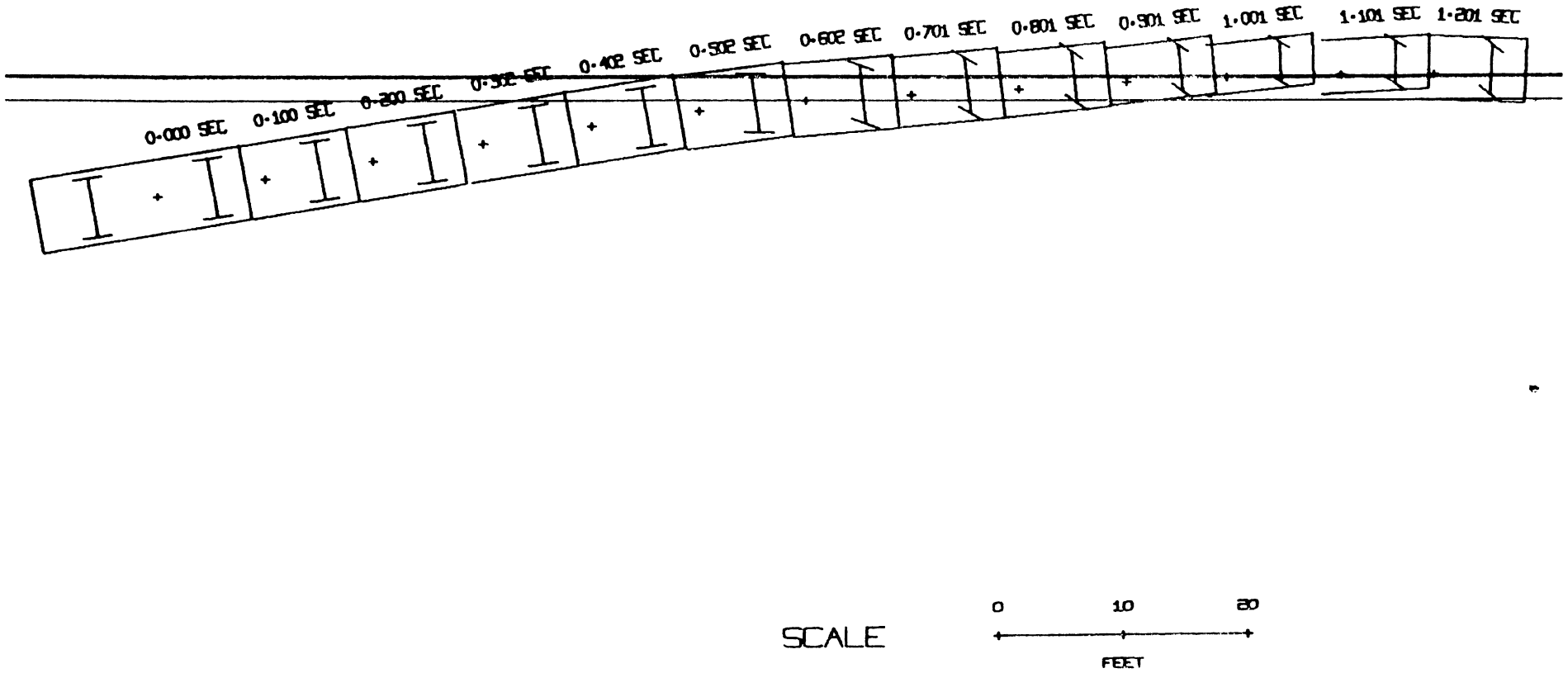

EVALUATION OF MSHO CURBS

FIGURE 4-50

RUN CG-10 - CURB TYPE K - 1966 CUSTOM - 60 MPH - 10 DEG - FLAT MEDIAN

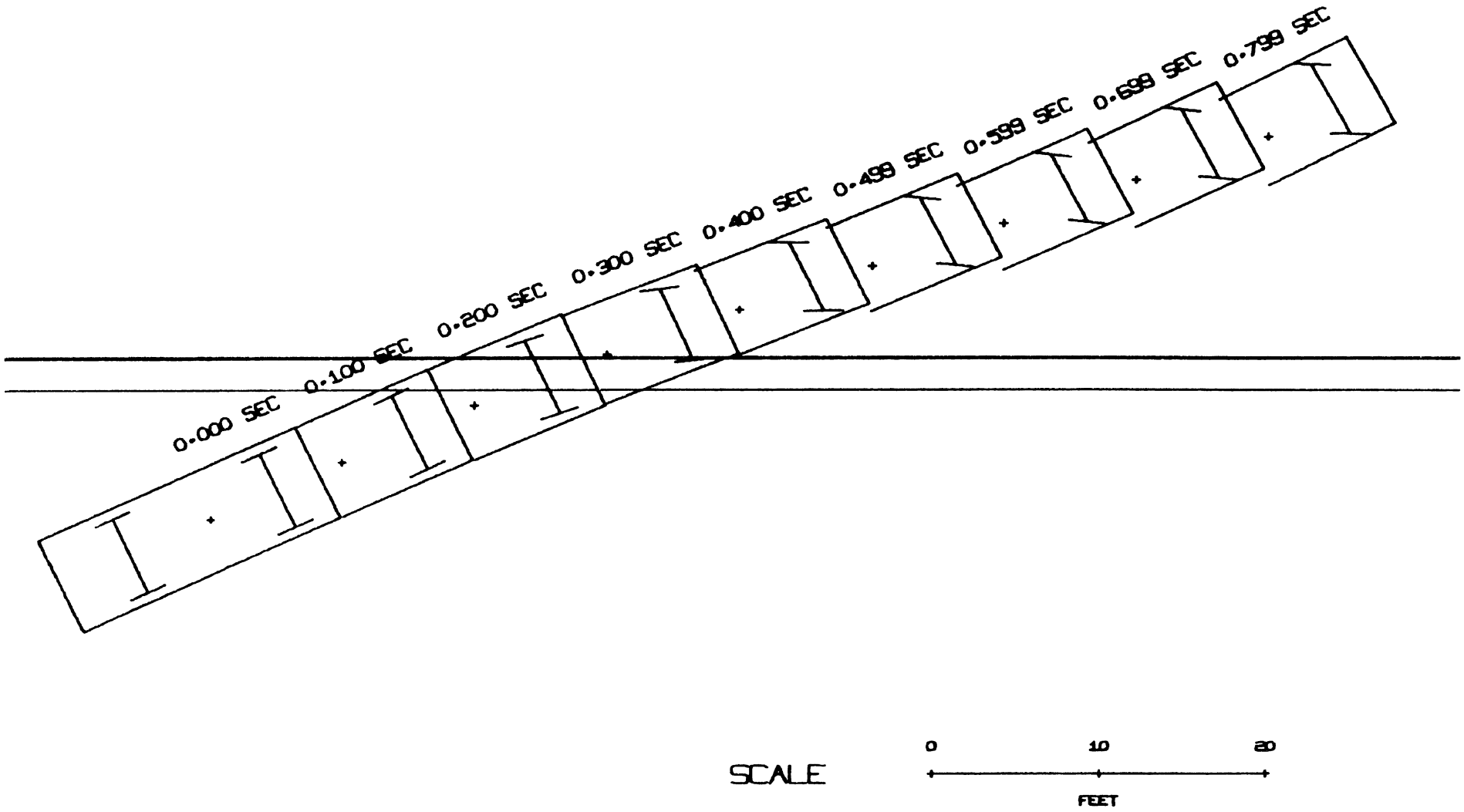

FIGURE 4-51 EVALUATION OF MSHO CURBS

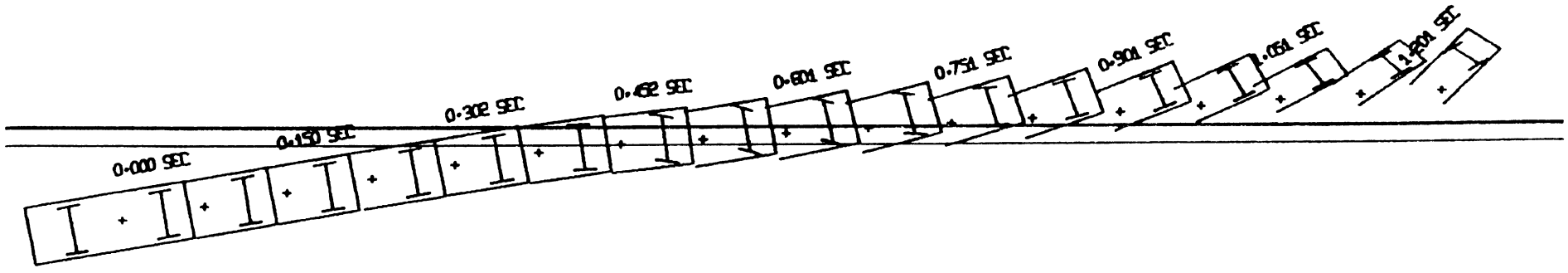

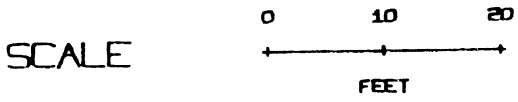

EVALUATION OF MSHO CURBS

FIGURE 4-52

RUN CG-15 - CURB TYPE K - 1966 CUSTOM - 80 MPH - 10 DEG - FLAT MEDIAN

following mounting. This latter case and the two 60 mph cases will be discussed more thoroughly.

TABLE 4-5

CURB K SIMULATION RUNS

Run	Velocity	Angle	Median Slope	Vehicle
CG-19	40 mph	25°	Flat	1966 Ford Custom
CG-10	60 mph	10°	Flat	1966 Ford Custom
CG-6	60 mph	25°	Flat	1966 Ford Custom
CG-15	80 mph	10°	Flat	1966 Ford Custom

For the 60 mph, 10° case, the redirective action is due to the large steer angles that are produced in the front wheels as a result of the initial impact of the left front wheel with the curb. When the left rear wheel mounts the curb, the resulting yaw motion is surprisingly small. This small effect is due to the fact that at this point the angle between the vehicle and curb is less than five degrees. Histories of yaw angle and angular rate for this case are shown on Figure 4-53, with pertinent events noted.

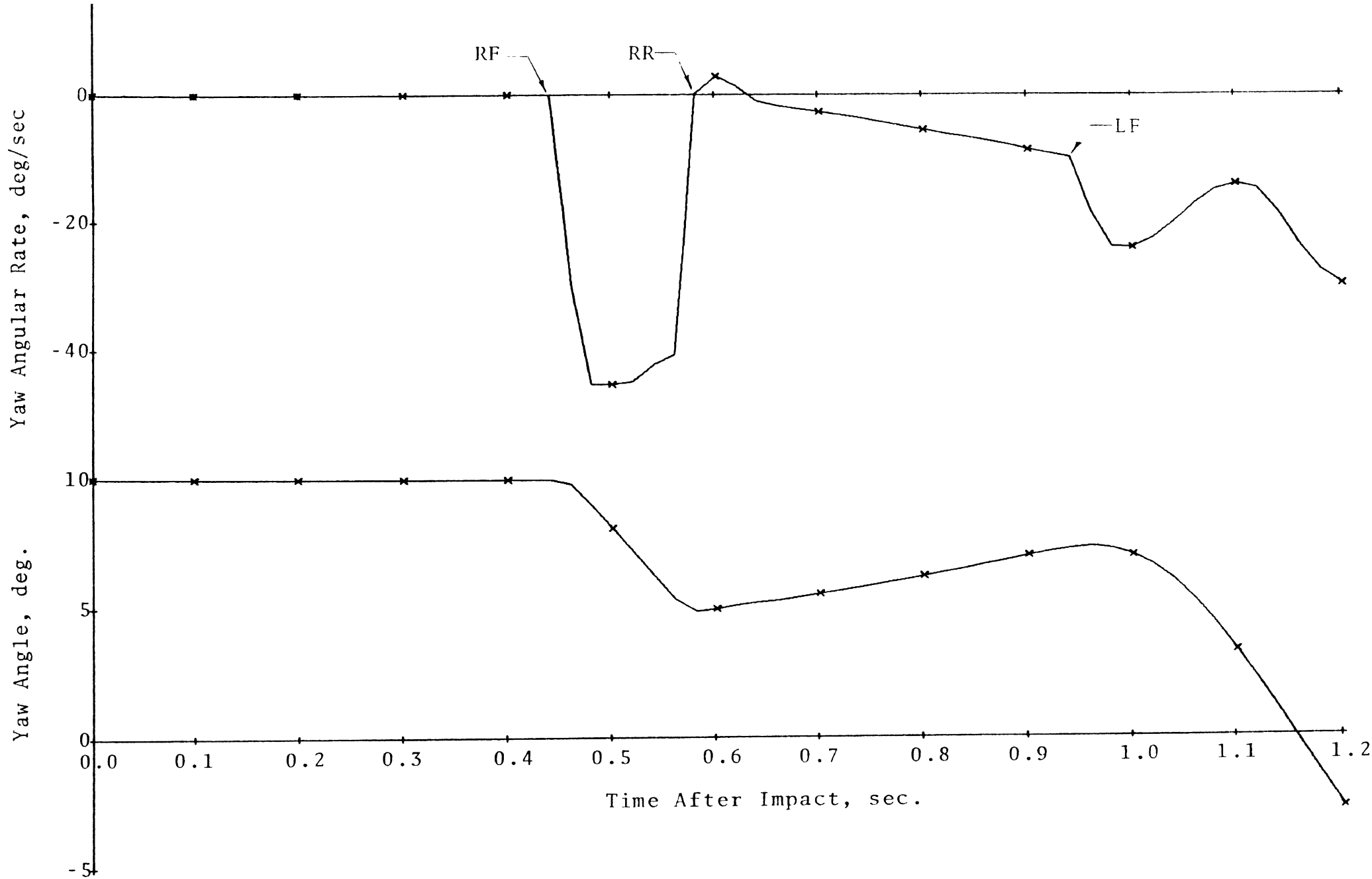

FIGURE 4-53. RUN CG-10 - CURB K, 60 MPH, 10 DEG. IMPACT-YAW ANGLE AND ANGULAR RATE HISTORIES

The initial impact of the left front wheel also produces a violent rolling action away from the curb. The resulting roll angle reaches about 48° before the vehicle begins to right itself. Roll angle and angular rate histories are shown on Figure 4-54.

The history of the vehicle center of gravity height during the impact is shown on Figure 4-55. The interval where the vehicle is completely airborne is noted. In no case are vehicle accelerations, experienced in the impact, likely to cause passenger injury.

For the 60 mph, 25° case vehicle motions are much less violent. As each of the four wheels mounts the curb, lateral accelerations are imparted to the vehicle which are of a similar order of magnitude. Because of the positions of the wheels with respect to the vehicle C.G. (the result of the 25° impact angle), the resulting yaw motions tend to cancel each other. By virtue of this canceling effect, vehicle yaw angle varies less than three degrees throughout the run. This is indicated on the yaw angle and angular rate histories shown on Figure 4-56. (The designations of RF, RR, LF, and LR refer to the wheel impact events.) These histories can be compared with similar histories for the 60 mph, 10° case on Figure 4-53.

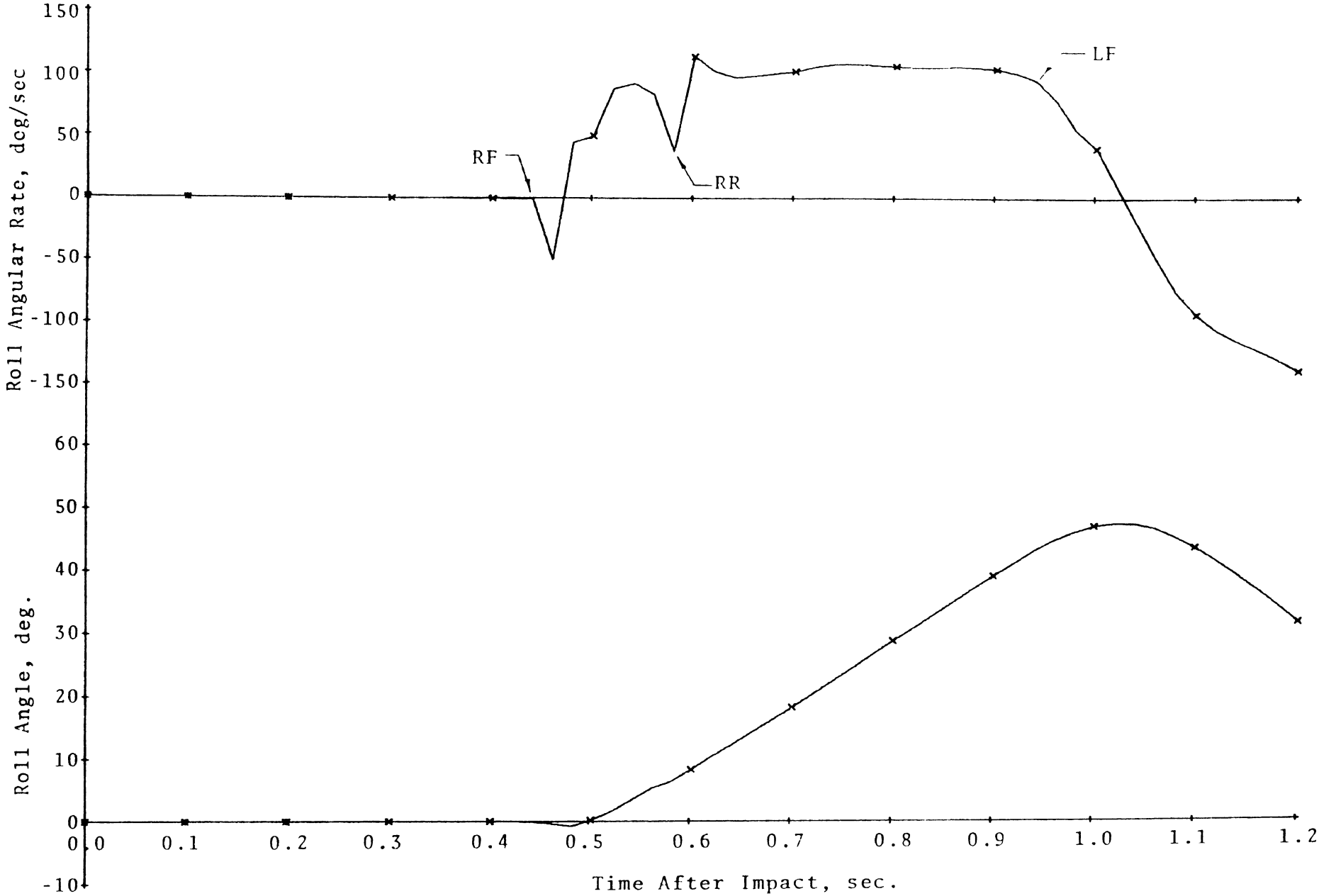

FIGURE 4-54. RUN CG-10 - CURB K, 60 MPH, 10 DEG. IMPACT-ROLL ANGLE AND ANGULAR RATE HISTORIES.

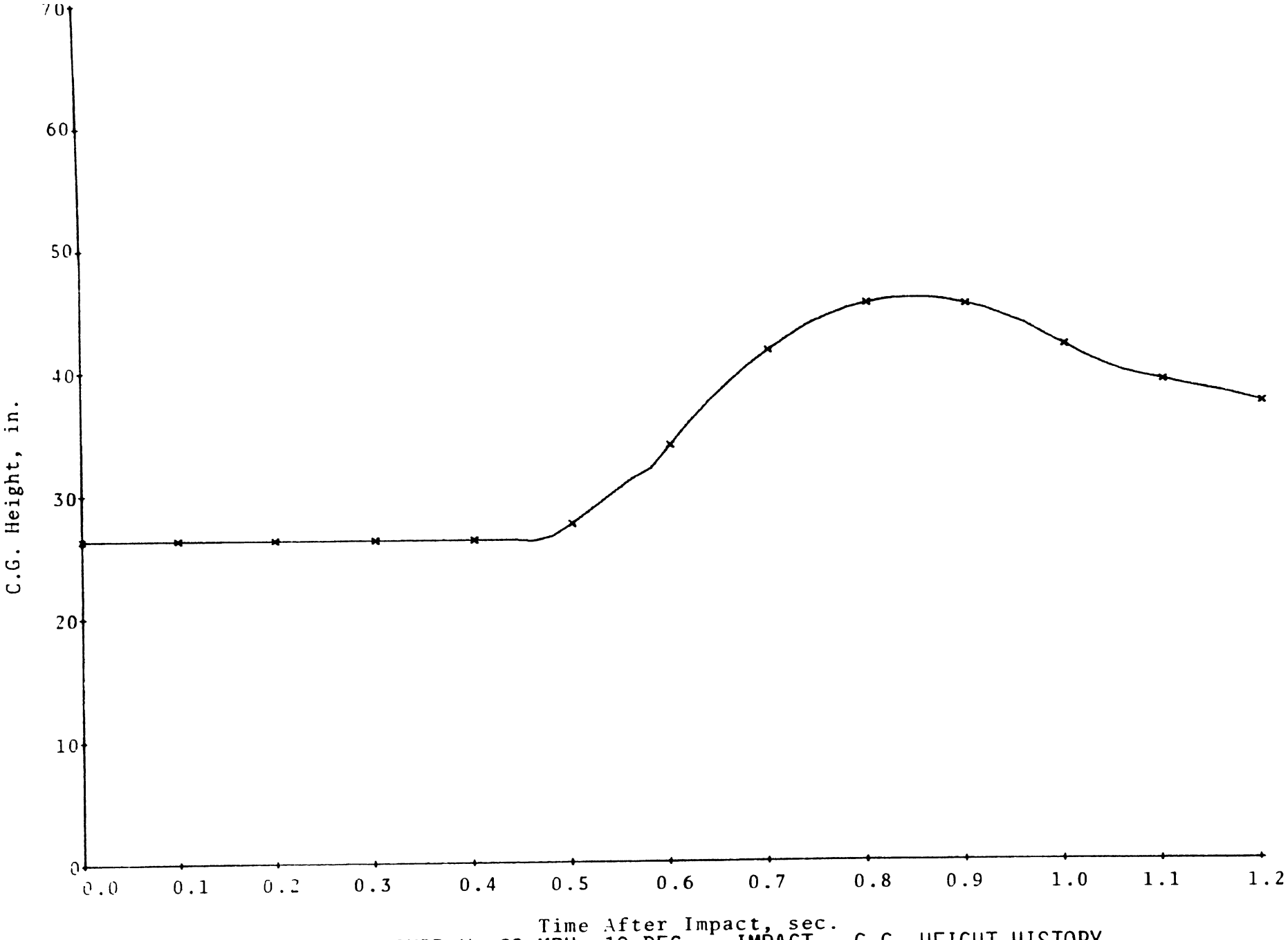

FIGURE 4-55. RUN CG-10 - CURB K, 60 MPH, 10 DEG. - IMPACT - C.G. HEIGHT HISTORY.

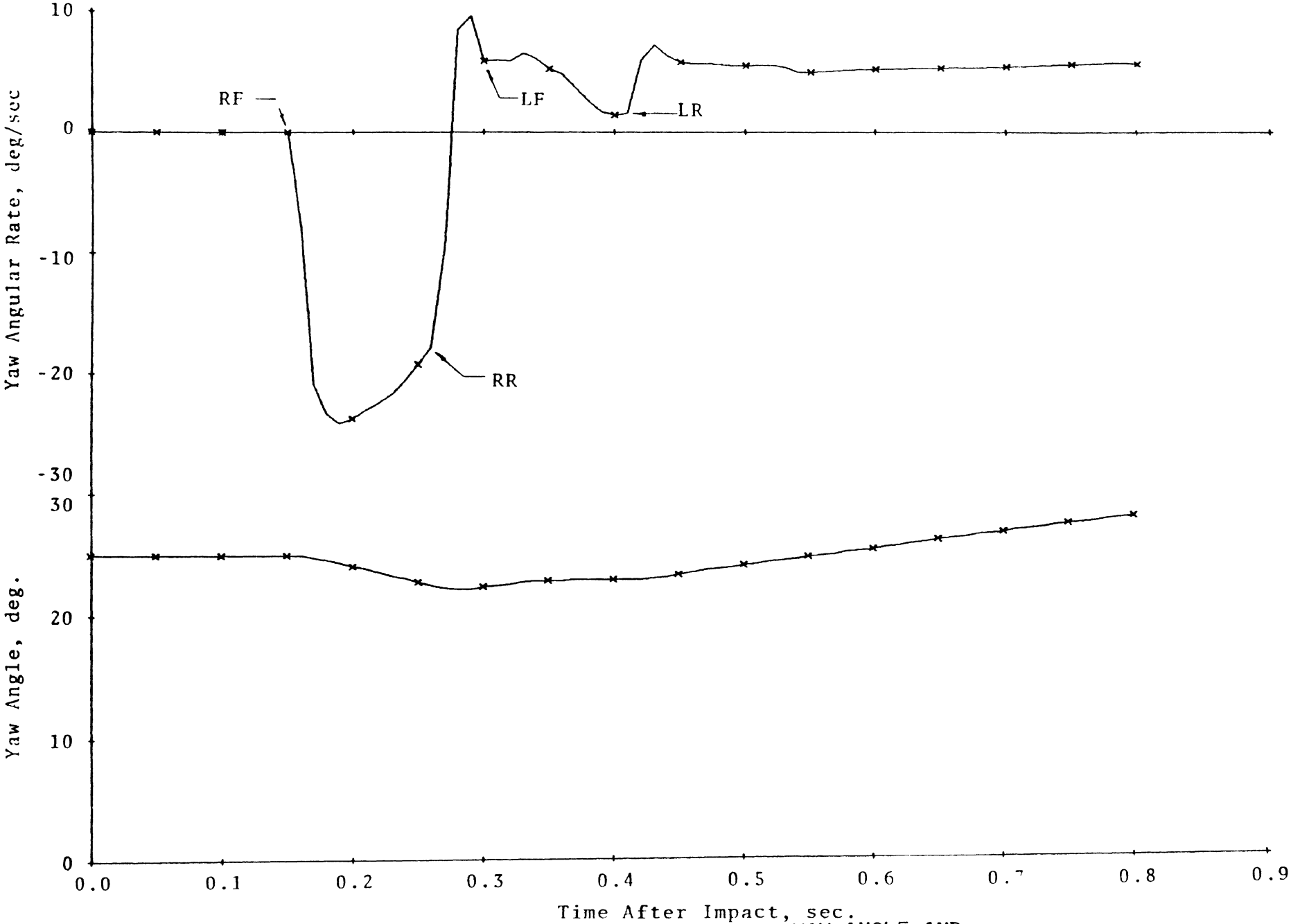

FIGURE 4-56. RUN CG-6-CURB K, 60 MPH, 25 DEG. IMPACT - YAW ANGLE AND ANGULAR RATE HISTORIES

The canceling effect of the wheel impacts also tends to keep the roll angle relatively small--reaching a maximum value of about 22° away from the curb (Figure 4-57). Vehicle C.G. height rises over 28 inches, however, since all four wheels act in concert in imparting vertical forces to the vehicle. The C.G. height history is shown on Figure 4-58 with impact points and the airborne interval noted.

The 80 mph, 10° case produced the most unusual vehicle motion of the four cases. Three of the four wheels mounted the curb, but the right rear wheel did not. At the time the run was terminated, the right rear wheel was sliding along the curb face while the vehicle was in a lateral spin. Vehicle heading angle with respect to the curb had increased from 10° to over 45° by this time. Forward velocity had decreased from 80 to 54 mph, lateral velocity had increased from 0 to 40 mph, and vertical velocity from 0 to 36 mph. Time histories of the various quantities are shown on Figures 4-59 (yaw angle and angular rate) and 4-60 (roll angle and angular rate). The C.G. height history is shown on Figure 4-61. Despite the relatively wild motions, vehicle accelerations are well within passenger tolerance levels.

Test data for ten-inch curbs is summarized on Figure 4-15. No curb which has been tested is exactly like the MDSH curb K. The nearest in design are curbs A, B, and E on Figure 4-15,

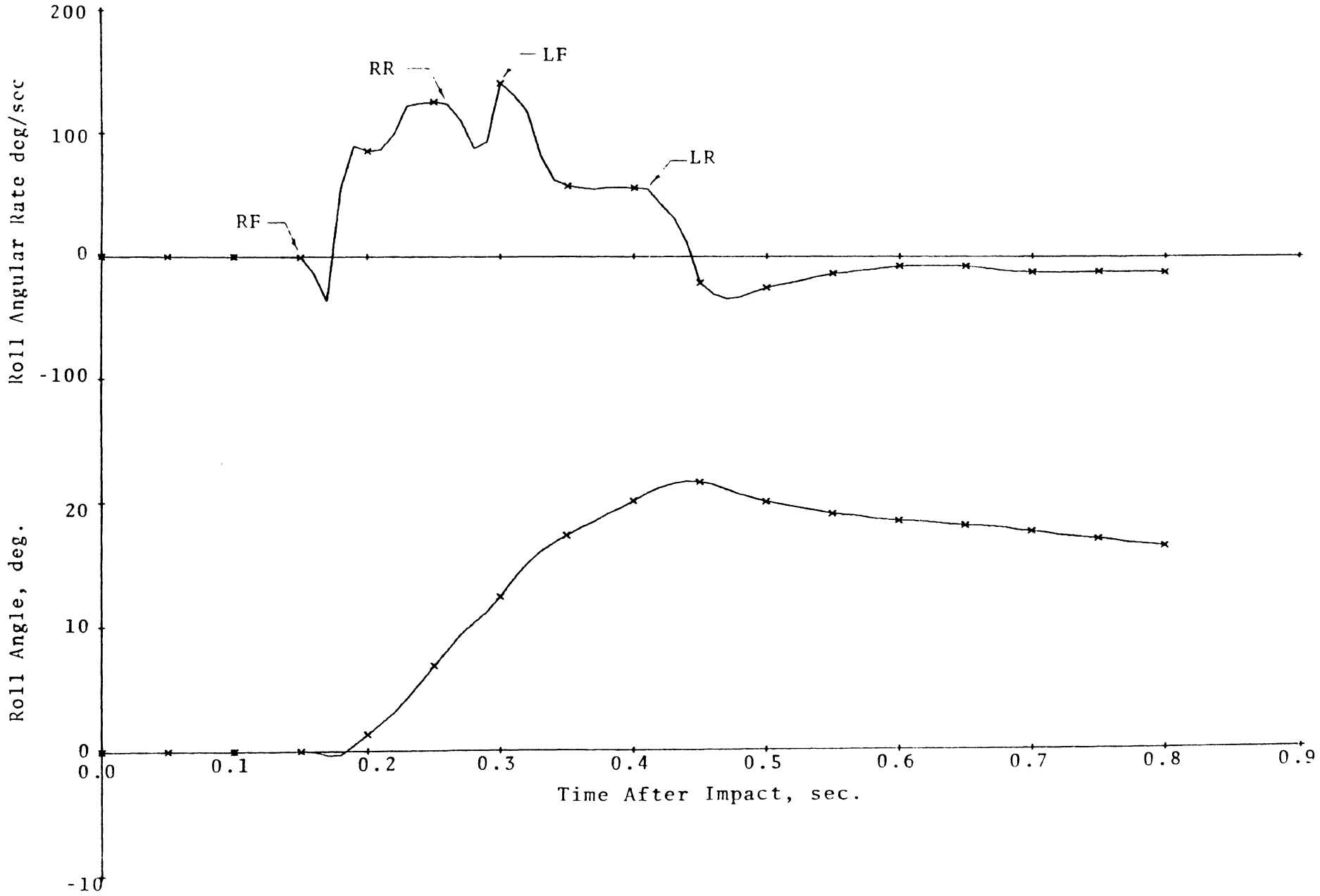

FIGURE 4-57. RUN CG-6 - CURB K, 60 MPH, 25 DEG. IMPACT - ROLL ANGLE AND ANGULAR RATE HISTORIES.

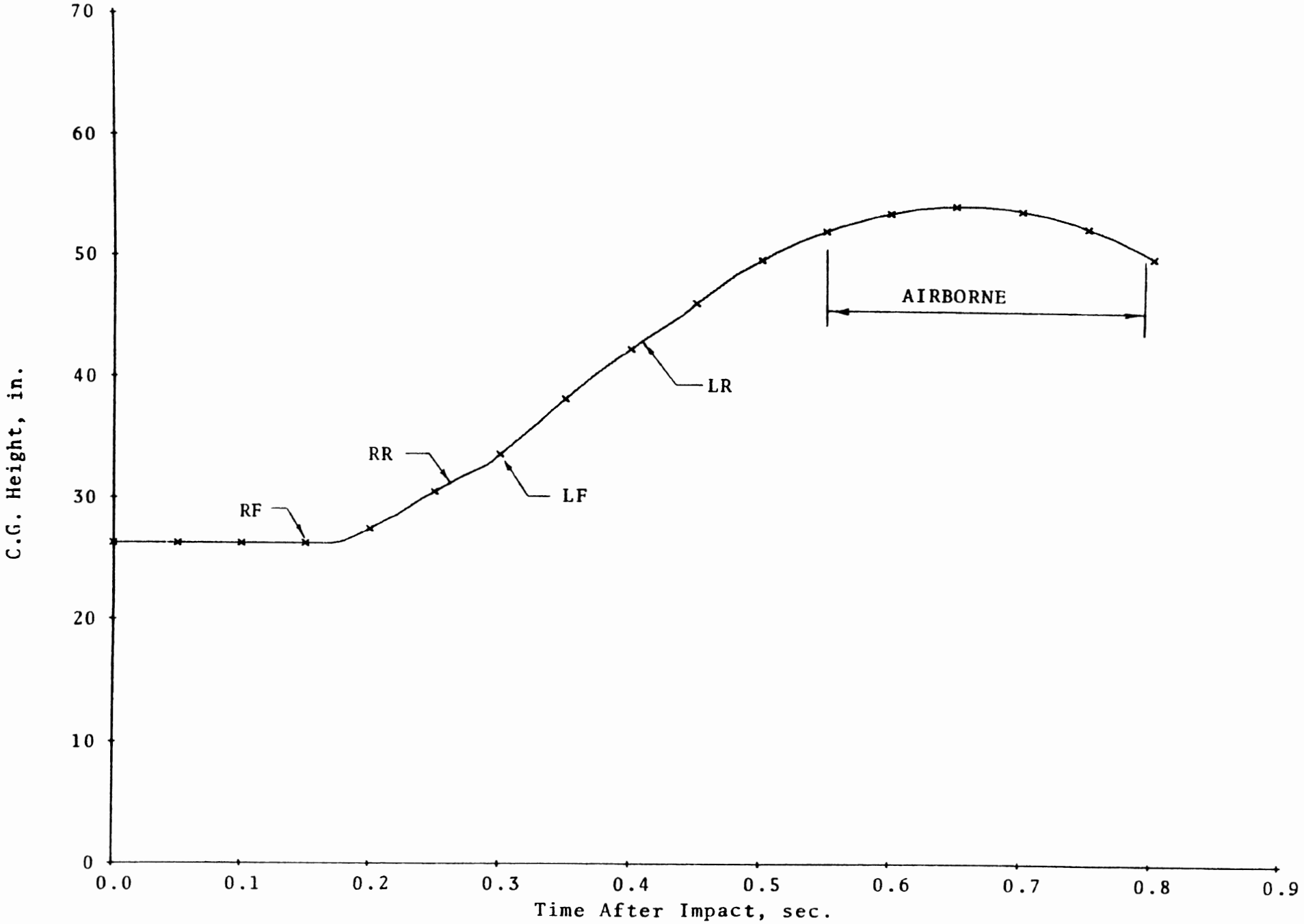

FIGURE 4-58. RUN CG-6 - CURB K, 60 MPH, 25 DEG. IMPACT - C.G. HEIGHT HISTORY

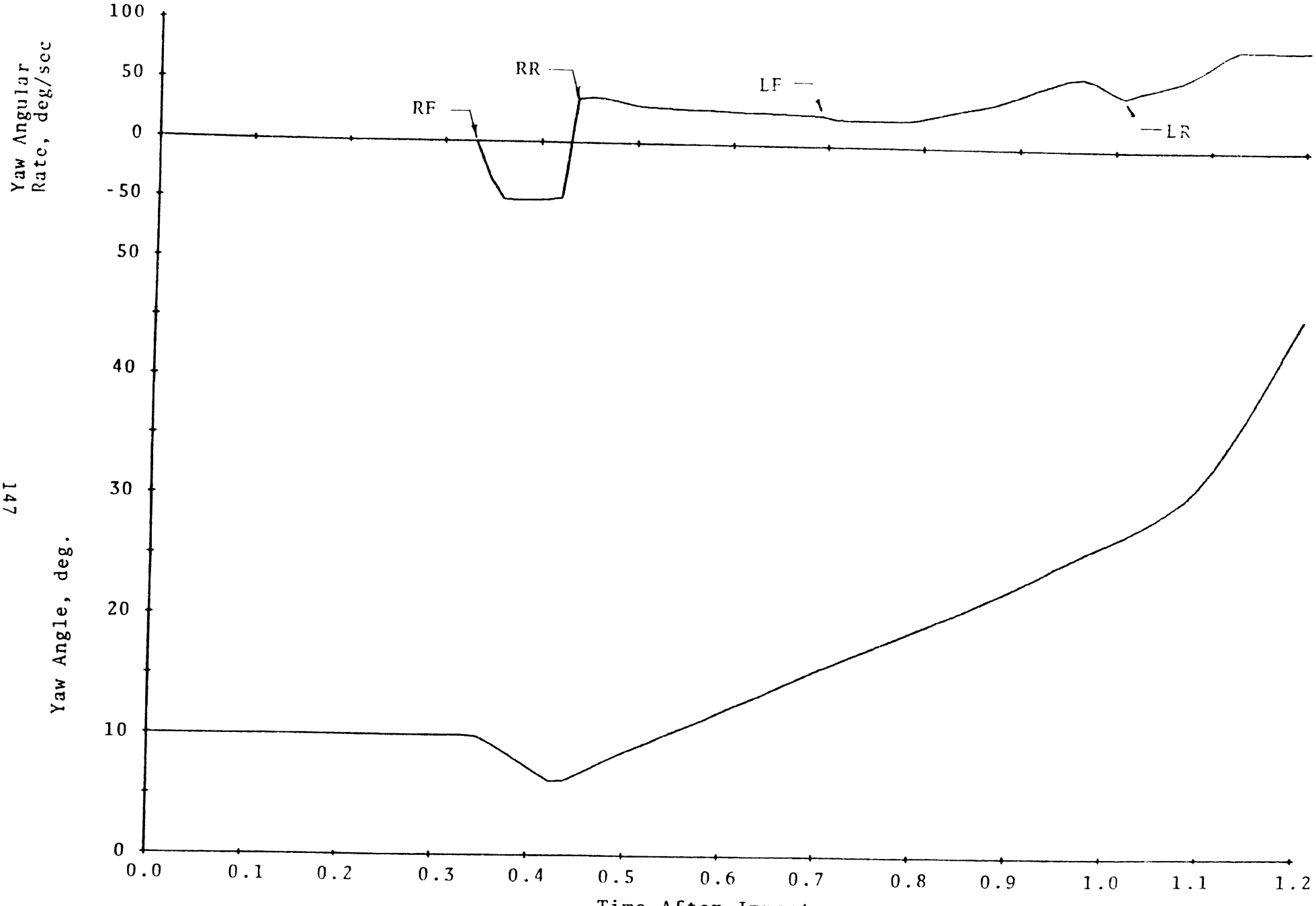

FIGURE 4-59. RUN CG-15 - CURB K, 80 MPH, 10 DEG. IMPACT - YAW ANGLE AND ANGULAR RATE HISTORIES

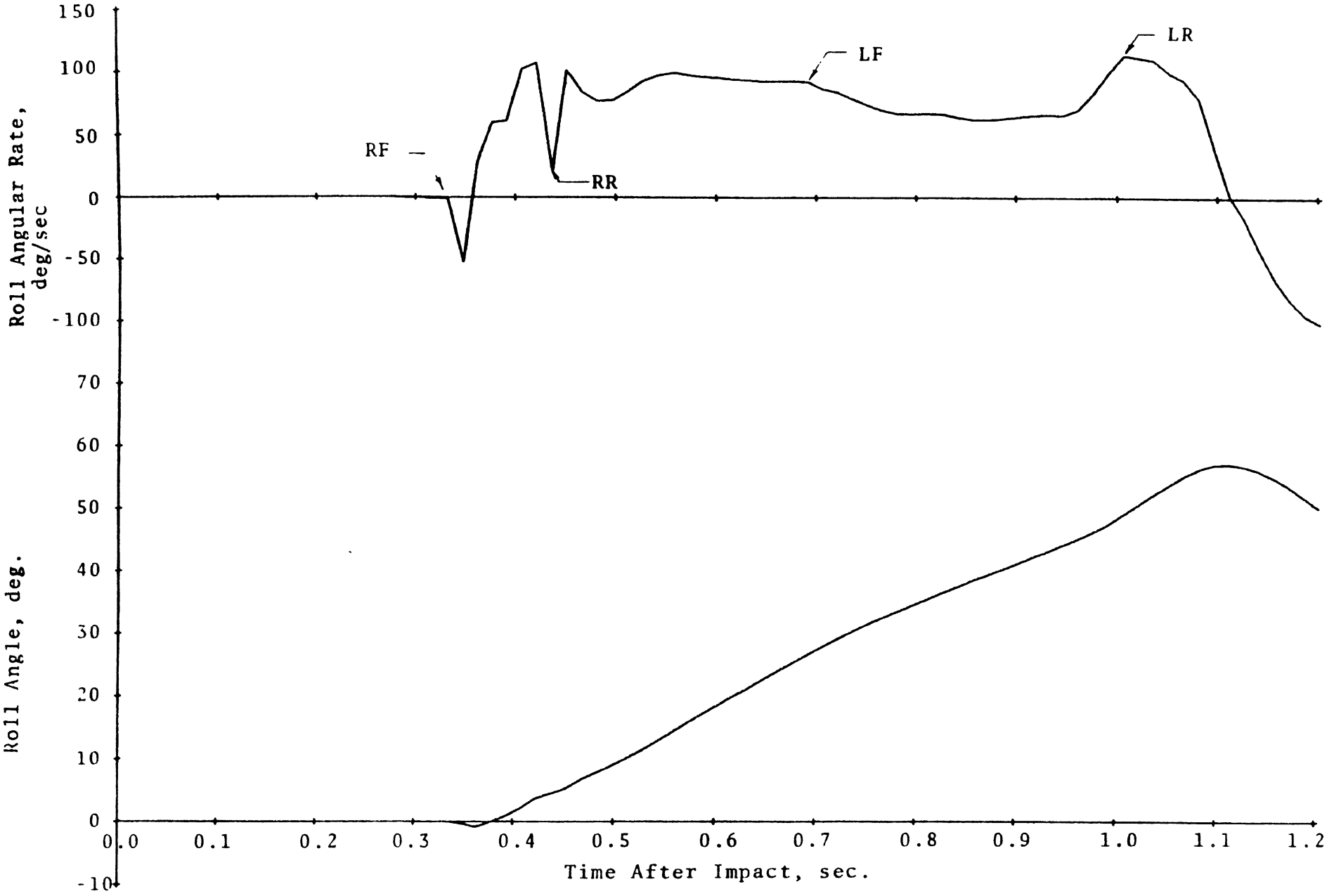

FIGURE 4-60. RUN CG-15 - CURB K, 80 MPH, 10 DEG. IMPACT - ROLL ANGLE AND ANGULAR RATE HISTORIES

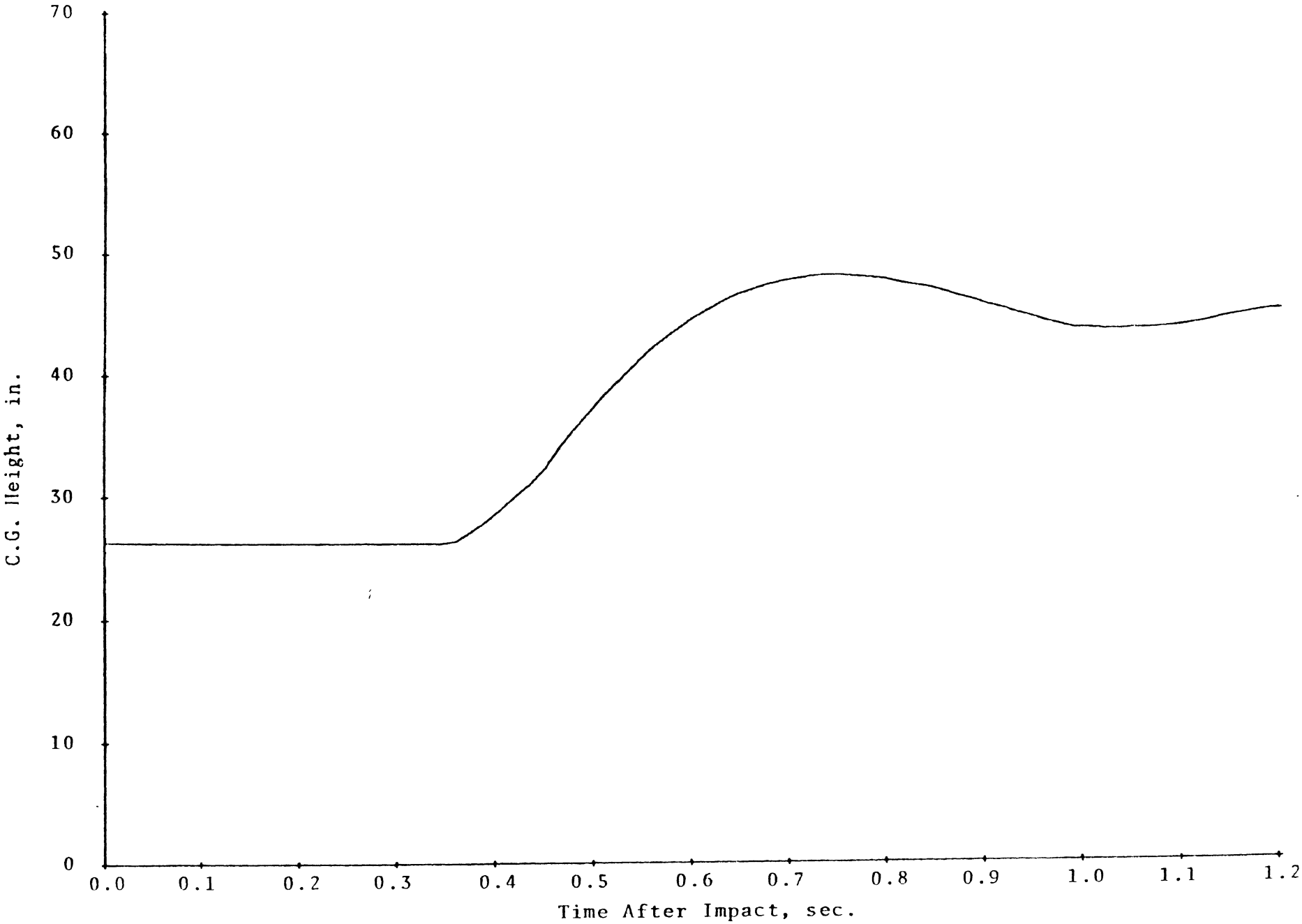

FIGURE 4-61. RUN CG-15 - CURB K, 80 MPH, 10 DEG. IMPACT - C.G. HEIGHT HISTORY

although each differs from MDSH curb K in the way that the curb face is undercut. Four tests were made on these three curbs in the range of the simulated impact conditions. Mounting occurred in all cases except the one involving the metal curb face (California curb B) at 60 mph and 7.5°. (As noted earlier, this is a special design which was developed to promote redirection and discourage mounting.) Comparative results for the test and simulation exercises are shown on Table 4-6. Results are obviously in general agreement despite the differences in designs and the absence of tire sidewall/curb face friction forces in the simulation.

As an additional correlation, a simulated run at 60 mph and 25° was made against the California curb A design shown on Figure 4-15. The plan view trajectory is shown on Figure 4-62. Plots of yaw angle and angular rate (Figure 4-63), roll angle and angular rate (Figure 4-64) and C.G. height (Figure 4-65) versus time can be compared with respective counterparts for the 60 mph, 26° run on curb K. General agreement can be noted, although differences resulting from the different curb designs are apparent.

TABLE 4-6

TEN-INCH CURB TEST AND SIMULATION COMPARISON

Curb	Exercise	Velocity	Angle	Action	Reference
Curb A	Test	60 mph	7.5°	Mounting F and R	13
Curb A	Test	45 mph	15°	Mounting F and R	13
Curb B	Test	60 mph	7.5°	Redirection	13
Curb B	Test	45 mph	15°	Mounting F and R	13
Curb C	Test	45 mph	15°	Mounting F and R	13
Curb C	Test	45 mph	20°	Mounting F and R	13
Curb E	Test	64 mph	20°	Mounting F and R	14
Curb K	Simulation	40 mph	25°	Mounting F and R	
Curb K	Simulation	60 mph	10°	Mounting F and R on one side with subsequent redirection.	
Curb K	Simulation	60 mph	25°	Mounting F and R	
Curb K	Simulation	80 mph	10°	Mounting F and R on one side, F only on the other, with subsequent spin-out	

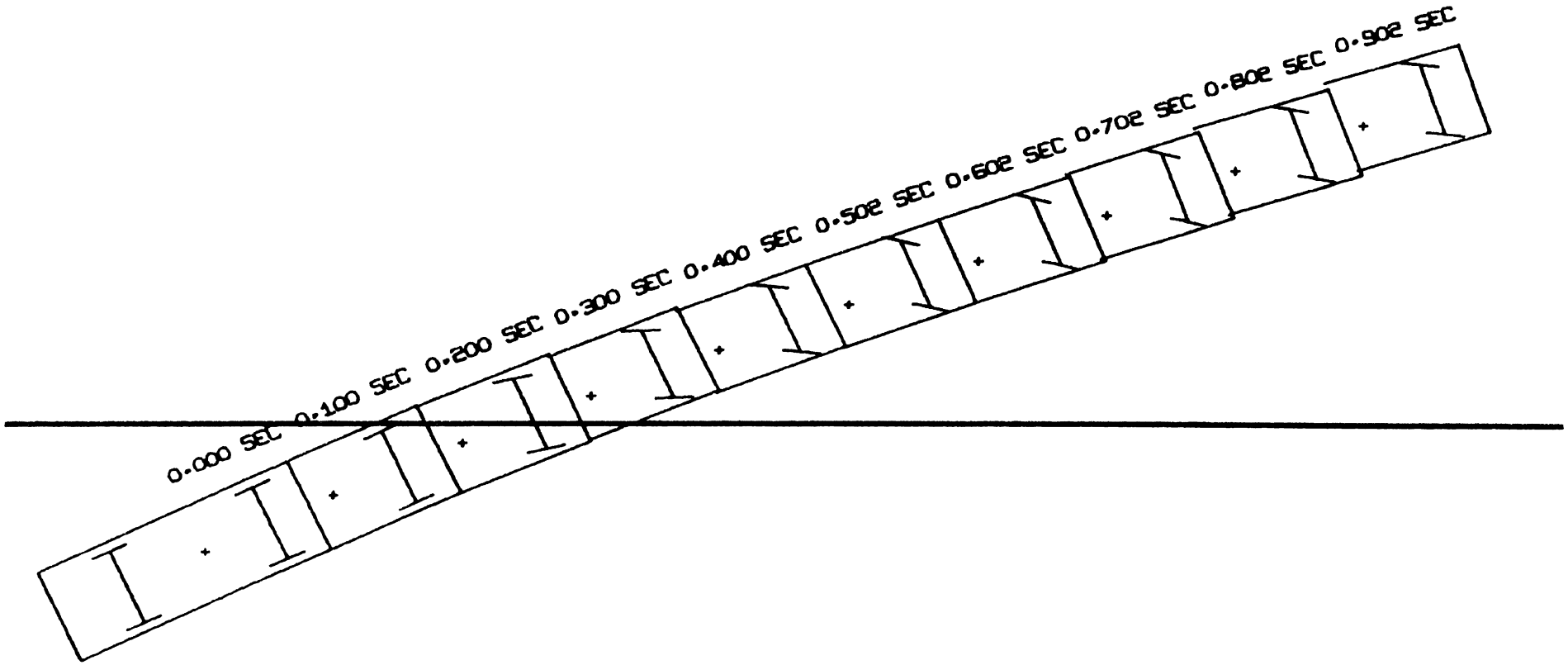

SCALE 0 10 20

FEET

EVALUATION OF MSHO CURBS

FIGURE 4-62

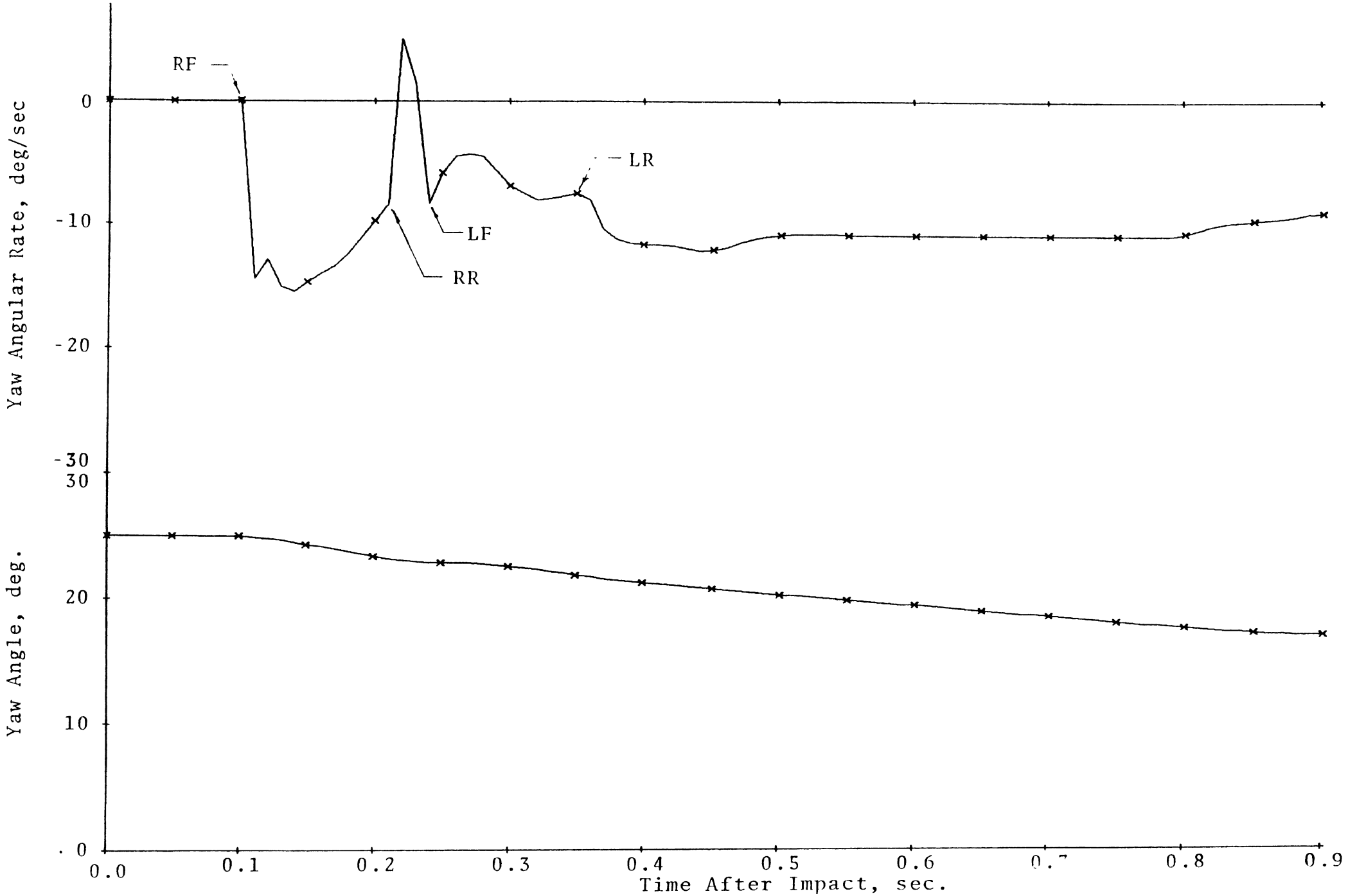

FIGURE 4-63. RUN CG-9 - CAL 10 IN. CURB, 60 MPH, 25 DEG. IMPACT - YAW ANGLE AND ANGULAR RATE HISTORIES

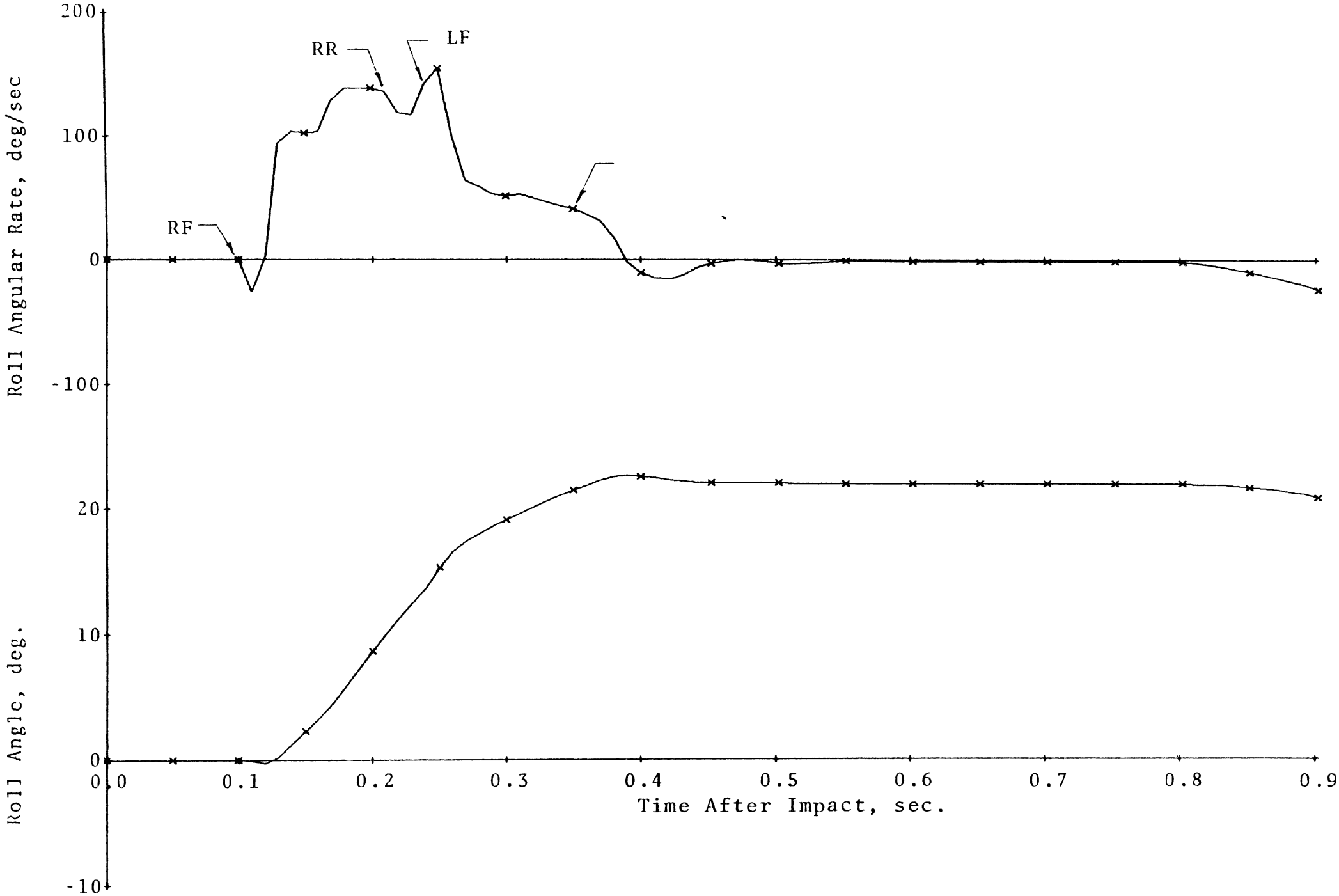

FIGURE 4-64. RUN CG-9 - CAL 10 IN. CURB, 60 MPH, 25 DEG. IMPACT - ROLL ANGLE

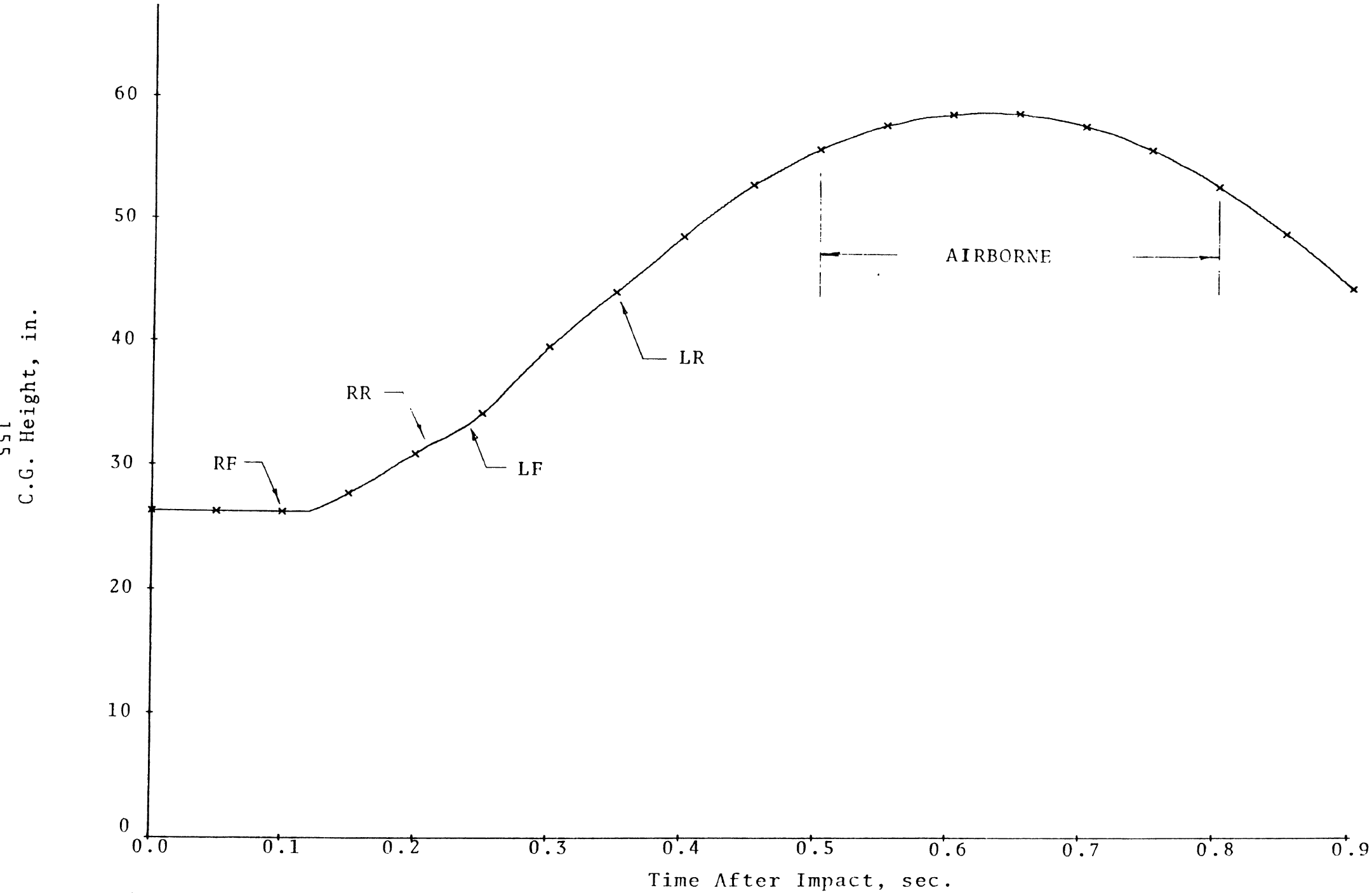

FIGURE 4-65. RUN CG-9 - CAL 10 IN. CURB, 60 MPH, 25 DEG. - C.G. HEIGHT HISTORY

4.6 BARRIER CURB REDIRECTION EFFECTIVENESS

Using a curb as an errant vehicle redirection device has probably been considered by highway designers as far back as when curbs were first placed along paved motor highways. Using curbs for redirection purposes has never been universal, however, and in recent years has grown into disfavor (particularly in front of guardrails [48]). In current practice, therefore, low barrier curbs (twelve inches in height or less) are usually not used for redirection. Rather, curbs, when used, are primarily designed for drainage control and delineation, and are of the mountable type. This is particularly true along high-speed urban highways where mountable curbs are used to allow disabled vehicles easy access to the shoulder [11].

One of the main objections to using barrier curbs along roadways is that such curbs tend to effect the lateral placement of traffic and reduce the effective road width. Evidently, drivers tend to veer away from structures having a formidable appearance. Conflicting evidence suggests that drivers soon become used to such structures, however, and after a reasonable period use the road width in the same manner that it was used previously, without the structure [59]. In any case, experience has generally shown that curbs placed four to six feet beyond the traffic pavement edge cause little

reduction in effective lane width [11]. Having discussed the possible negative factors related to using barrier curbs, the remaining part of the section will be centered upon the benefits which can be expected from their use.

First of all, it is obvious that a curb whose height is below the center of mass of a vehicle will cause an overturning moment upon impact. Therefore, a barrier curb of limited height can never be expected to redirect vehicles over the full range of operational impact conditions. On the other hand, for the range of impact conditions where a curb can be effective in redirection, vehicle damage resulting from striking the curb will be far less than that which would result from striking a guardrail.

In order to determine the efficiency of a barrier curb as a redirective device, a measure of effectiveness is required. In this exercise, the measure was chosen to be the percentage of the total errant vehicle population which could be expected to be redirected by a given barrier curb. To arrive at this percentage, four kinds of data are required:

1. The redirective performance of particular barrier curbs in terms of speed and angle.
2. The distribution of vehicle speeds in the operational traffic environment.

3. The distribution of ran-off-the-road angles in the operational traffic environment.

4. The statistical correlation between the data in 2 and 3.

Fortunately, all four kinds of data are available.

In generalized mathematical terms, the desired percentage measure can be written in the following form:

$$P[V < V_p(\alpha)] = \int_0^{\pi/2} \int_0^{V_p(\alpha)} f(V, \alpha) dV \, d\alpha \qquad (4\text{-}2)$$

where:

V = velocity

α = angle

$V_p(\alpha)$ = A specific curb redirective performance limit expressed in terms of α.

$f(V,\alpha)$ = The joint frequency function of velocity and angle for ran-off-the-road vehicles.

This equation expresses the probability that a vehicle leaving the roadway will be within the redirective performance limits of a specific barrier curb.

In practical terms, research with the Trief curb, mentioned in Section 4.1, indicates that the redirective performance of a curb can be expressed in the form:

$$V \sin \alpha = \text{constant} = K \qquad (4\text{-}1)$$

For the Trief curb, the constant is about 3.1 mph. Impact data for the special redirective curb tested by Elsholz [15] (Figure 4-16) indicates a constant of about 9.1 mph. The two performance boundaries are shown on Figure 4-66.

Also shown on Figure 4-66 is a curve which indicates the boundary below which vehicle speed and impact angle can be expected to be uncorrelated. The equation for the curve is given as follows [49]:

$$\alpha = \cos^{-1}\left[1 - \frac{gy\mu}{V^2}\right] \qquad (4\text{-}3)$$

where:

g = gravitational constant

y = distance from initial vehicle C.G. straight ahead path to curb

μ = tire/road friction coefficient.

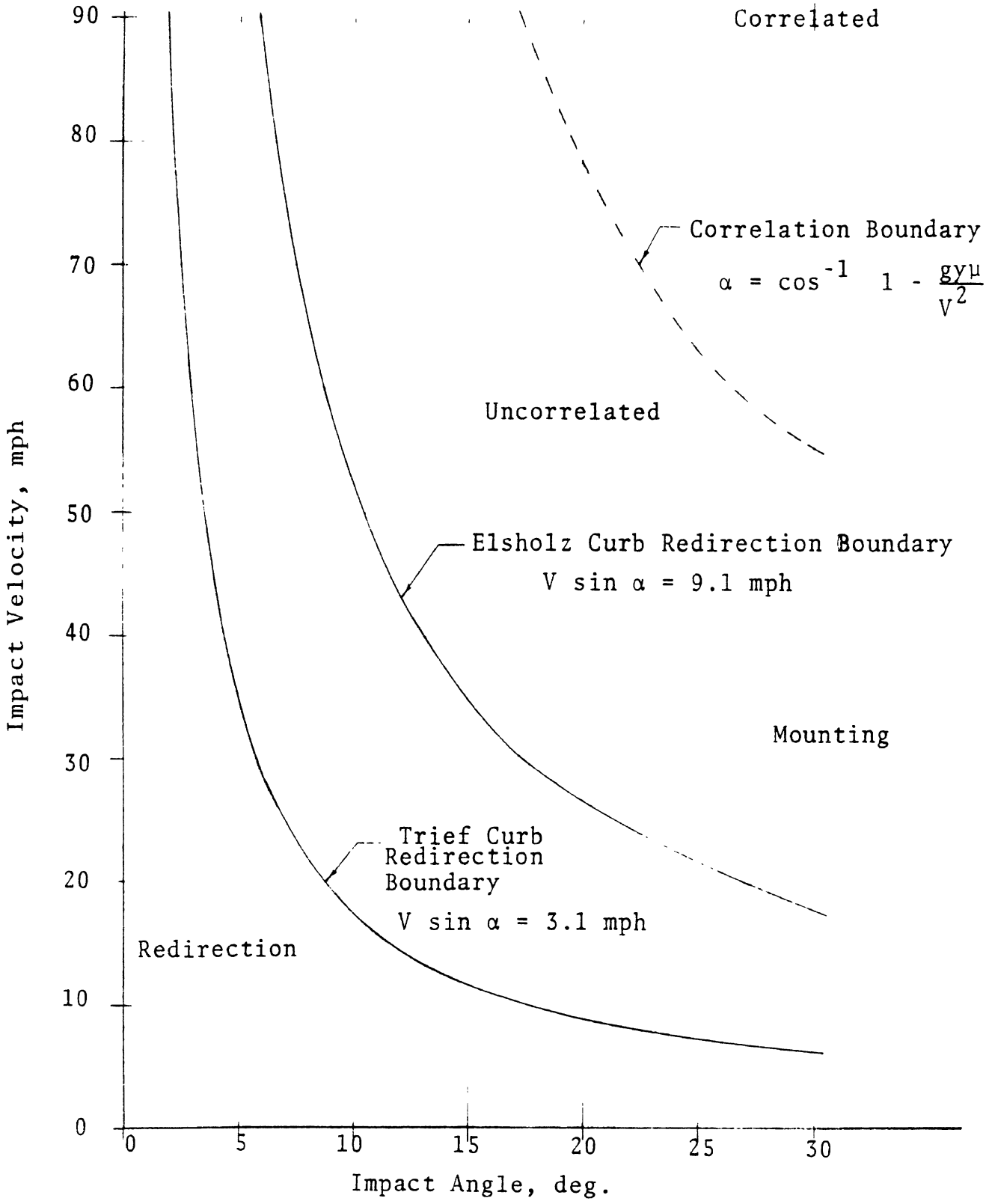

FIGURE 4-66. REDIRECTION AND CORRELATION BOUNDARIES

This equation yields the maximum vehicle path angle (impact angle in this case) that can be achieved for given road width and friction characteristics as a function of velocity. The curve on Figure 4-66 is for values of y and μ of 19 feet and 0.6, respectively. All combinations of velocity and angle under this curve are achievable and hence can be expected to be uncorrelated. This being the case, the joint velocity, angle frequency function can now be written as:

$$f(V, \alpha) = g(V)h(\alpha) \qquad (4\text{-}4)$$

Thus, distributions of angle and velocity can be considered separately.

Velocity distribution data was chosen to represent urban traffic conditions. It was felt that urban data would be the most meaningful in evaluating barrier curbs since curb use is primarily in urban areas. The specific data was taken from Michigan Department of State Highways Survey Station 010. The station is located along M-43 in Ingham County and has a posted speed limit of 40 mph [50]. Ran-off-the-road angle data was taken from the Hutchinson study [44].

With the changes discussed above, Equation (4-2) can now be rewritten as follows:

$$P(V < \frac{K}{\sin \alpha}) = \int_0^{\pi/2} \int_0^{\frac{K}{\sin\alpha}} h(\alpha)g(V)dVd$$

$$= \int_0^{\pi/2} \left[G(\frac{K}{\sin \alpha}) - G(0)\right] h(\alpha)d\alpha$$

$$= \int_0^{\pi/2} G(\frac{K}{\sin \alpha})h(\alpha)d\alpha \qquad (4\text{-}5)$$

where $G(V)$ is the distribution function corresponding to $g(V)$ and

$$G(0) = 0 \qquad (4\text{-}6)$$

Equation (4-5) in its present form requires that $G(\frac{K}{\sin \alpha})$ and $h(\alpha)$ be described analytically. Since both the speed and angle data are in tabular form, it was found that a discrete summation process worked more readily than the indicated integration. In mathematical terms, the discrete process can be written as follows:

$$P(V < \frac{K}{\sin \alpha}) = \sum_{i=1}^{h} G(\frac{K}{\sin\alpha_i})h(\alpha_i)\Delta\alpha_i$$

$$= \sum_{i=1}^{h} G(\frac{K}{\sin\alpha_i})h(\alpha_i, \Delta\alpha_i) \qquad (4\text{-}7)$$

where

$$h(\alpha_i, \Delta\alpha_i) = h(\alpha_i)\Delta\alpha_i \cong \int_{\alpha_i - \frac{\Delta\alpha_i}{2}}^{\alpha_i + \frac{\Delta\alpha_i}{2}} h(\alpha)d\alpha \qquad (4\text{-}8)$$

The quantity $h(\alpha_i, \Delta\alpha_i)$ turns out to be the percentage of the total sample space of ran-off-the-road angles that occur within the interval $\Delta\alpha_i$.

Using a value of K for the Elsholz curb of 9.1 mph, the summation process defined by Equation (4-7) yields a value of .704 for $P(V < \frac{K}{\sin \alpha})$. (The specific calculations are given in Table 4-7.) In other words, 70.4% of all vehicles striking the Elsholz curb would be redirected under urban traffic conditions. The corresponding value for the Trief curb under the same circumstances is 27.4%.

It is evident, then, that a barrier curb in certain situations can be an effective redirection device. The critical factors are curb height, shape, and facing material. These will be discussed more thoroughly in the next section.

TABLE 4-7

BARRIER CURB REDIRECTION EFFECTIVENESS CALCULATIONS

Hutchinson Incursion Angle Data [44]					Ilsholz Curb [15]				Trief Curb [16]			
α Interval	α_i	Incursion Events	% Total Events $h(\alpha_i, \Delta\alpha_i)$	sin α_i	K_1	$V_i = \frac{K_1}{\sin\alpha_i}$	$G(\frac{K_1}{\sin\alpha_i})$ [50]	$P(V<\frac{K_1}{\sin\alpha_i})\times 100$	K_2	$V_i = \frac{K_2}{\sin\alpha_i}$	$G(\frac{K_2}{\sin\alpha_i})$ [50]	$P(V<\frac{K_2}{\sin\alpha_i})\times 100$
0-0.5(-)	0.25	1	.318	.00436	9.1mph	2090	1.000	0.32	3.1mph	711	1.000	0.32
0.5-1.0(-)	0.75	4	1.27	.01309	9.1mph	696	1.000	1.27	3.1mph	237	1.000	1.27
1.0-1.5(-)	1.25	11	3.50	.0218	9.1mph	417	1.000	3.50	3.1mph	142	1.000	3.50
1.5-2.0(-)	1.75	7	2.23	.0305	9.1mph	298	1.000	2.23	3.1mph	102	1.000	2.23
2.0-2.5(-)	2.25	12	3.82	.0393	9.1mph	232	1.000	3.82	3.1mph	78.9	1.000	3.82
2.5-3.0(-)	2.75	11	3.50	.0480	9.1mph	190	1.000	3.50	3.1mph	64.6	1.000	3.50
3.0-3.5(-)	3.25	16	5.10	.0567	9.1mph	161	1.000	5.10	3.1mph	54.6	.986	5.02
3.5-4.0(-)	3.75	22	7.01	.0654	9.1mph	139	1.000	7.01	3.1mph	47.4	.776	5.44
4.0-4.5(-)	4.25	14	4.46	.0741	9.1mph	123	1.000	4.46	3.1mph	41.9	.371	1.66
4.5-5.0(-)	4.75	13	4.14	.0828	9.1mph	110	1.000	4.14	3.1mph	37.5	.128	0.53
5.0-5.5(-)	5.25	8	2.55	.0915	9.1mph	99.5	1.000	2.55	3.1mph	33.9	.0323	0.08
5.5-6.0(-)	5.75	15	4.78	.1002	9.1mph	90.6	1.000	4.78	3.1mph	31.0	.0085	0.04
6.0-7.0(-)	6.5	15	4.78	.1132	9.1mph	80.3	1.000	4.78	3.1mph	27.4	.0024	0.01
7.0-8.0(-)	7.5	9	2.87	.1305	9.1mph	69.7	1.000	2.87	3.1mph	23.8	0	0
8.0-9.0(-)	8.5	19	6.05	.1478	9.1mph	61.6	1.000	6.05	3.1mph	21.0	0	0
9.0-10.0(-)	9.5	20	6.37	.1651	9.1mph	55.1	.996	6.35	3.1mph	18.8	0	0
10.0-11.0(-)	10.5	0	0	.1822	9.1mph	49.9	.933	0	3.1mph	17.0	0	0
11.0-12.0(-)	11.5	34	10.83	.1994	9.1mph	45.6	.663	7.19	3.1mph	15.5	0	0
12.0-14.0(-)	13.0	0	0	.225	9.1mph	40.4	.248	0	3.1mph	13.8	0	0
14.0-15.0(-)	14.5	17	5.41	.250	9.1mph	36.4	.089	0.48	3.1mph	12.4	0	0
15.0-18.0(-)	16.5	0	0	.284	9.1mph	32.0	.019	0	3.1mph	10.9	0	0
18.0-19.0(-)	18.5	27	8.60	.317	9.1mph	28.7	.0037	0.03	3.1mph	9.8	0	0
19.0-20.0(-)	19.5	5	1.592	.334	9.1mph	27.3	.0023	--	3.1mph	9.3	0	0
20.0-21.0(-)	20.5	1	.318	.350	9.1mph	26.0	.0010	--	3.1mph	8.9	0	0
21.0-23.0(-)	22.0	0	0	.375	9.1mph	24.3	0	0	3.1mph	8.3	0	0
23.0-24.0(-)	23.5	2	.637	.399	9.1mph	22.8	0	0	3.1mph	7.8		
24.0-26.0(-)	25.0	0	0	.423	9.1mph	21.3	0	0	3.1mph	7.3	0	0
26.0-27.0(-)	26.5	13	4.14	.446	9.1mph	20.4	0	0	3.1mph	6.9	0	0
27.0-28.0(-)	27.5	2	.637	.462	9.1mph	19.7	0	0	3.1mph	6.7	0	0
28.0-38.0(-)	33.0	0	0	.545	9.1mph	16.7	0	0	3.1mph	5.7	0	0
38.0-39.0(-)	38.5	1	.318	.623	9.1mph	14.6	0	0	3.1mph	5.0	0	0
39.0-45.0(-)	42.0	0	0	.669	9.1mph	13.6	0	0	3.1mph	4.6	0	0
45.0-46.0(-)	45.5	14	4.46	.713	9.1mph	12.8	0	0	3.1mph	4.3	0	0
46.0-89.0(-)	67.5	0	0	.924	9.1mph	9.9	0	0	3.1mph	3.4	0	0
89.0-90.0(-)	89.5	1	.318	1.000	9.1mph	9.1	0	0	3.1mph	3.1	0	0
Totals		314	100.0					70.4				27.4

4.7 BARRIER CURB DESIGN CONSIDERATIONS

The primary objective in barrier curb design is to redirect errant vehicles. Other curb functions such as drainage control, delineation, etc., do not appear to constrain this objective to any appreciable extent. The imposing appearance of the barrier curb may be a factor in reducing the effective lane width of the curb side lane, however.

4.7.1 CURB HEIGHT. Since the primary advantage of a barrier curb over a guardrail is in lower expected vehicle damage, curb height should be chosen to optimize the ratio of redirective effectiveness to damage cost. A complete analysis of the factors involved in the ratio would be rather complicated and probably could not be done with presently available information. Some insight can be gained by examining certain of the factors, however.

The range and mean value of various vehicle dimensions which are pertinent to barrier curb damage are shown on Figure 4-67 [51]. The values given are for 1971 passenger vehicles. It is evident from the running ground clearance dimension that some body contact is possible for barrier curbs as low as four inches. Further, contact is virtually certain for curbs eight inches and up. Body damage, in turn, can be expected to become more severe with increasing curb height.

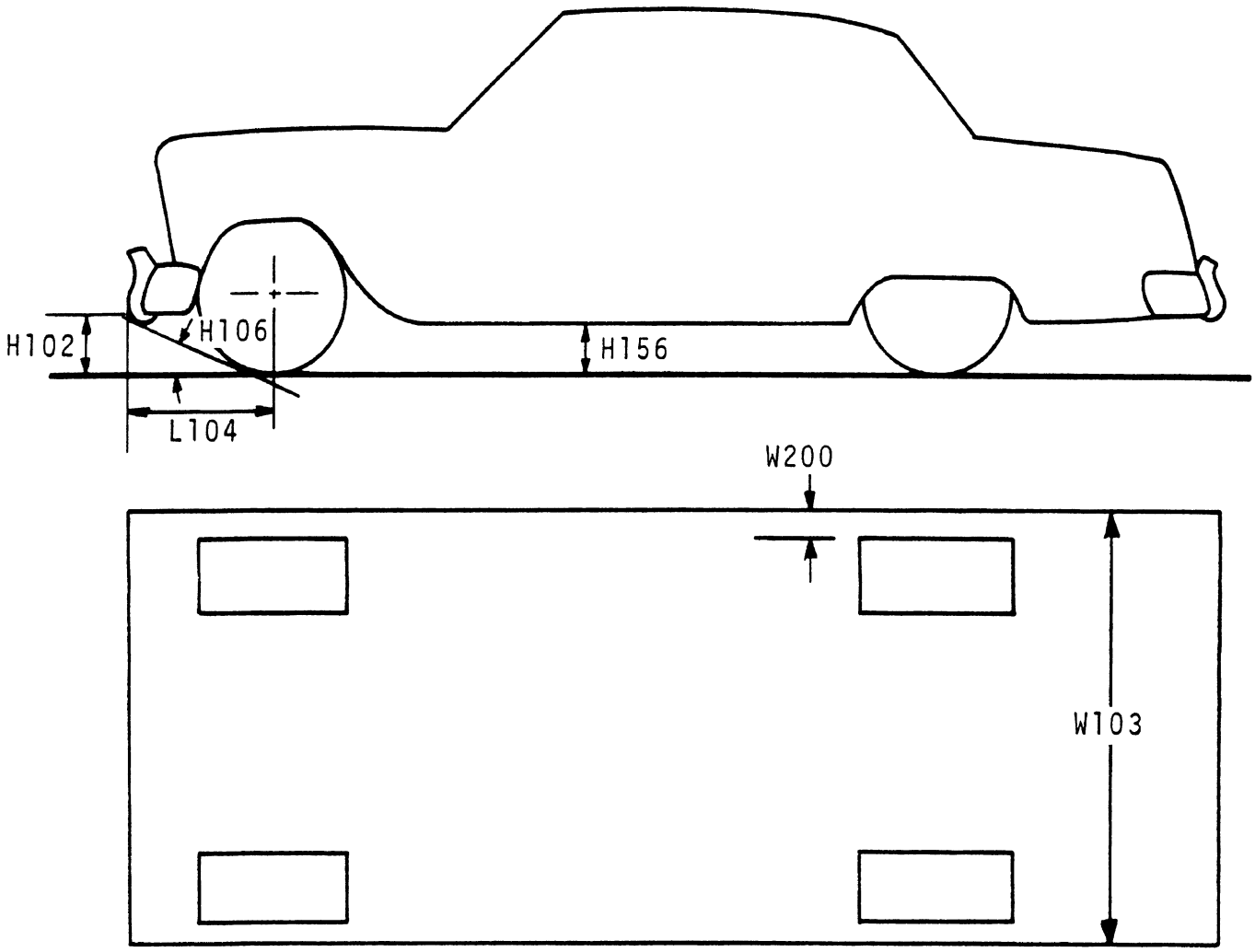

	Max.	Min.	Avg.
Bottom of Front Bumper to Ground (H102)	20.7	10.6	13.0
Overhang, Front (L104)	45.0	23.0	41.0
Angle of Approach (H106) (degrees)	10.3	46.8	21.0
Minimum Running Ground Clearance (H156)	7.8	4.2	5.5
Overall Width (W103)	79.9	65.2	79.0
Inset of Front Tire (W200)	5.0	1.0	3.0

All figures in inches, except where noted

FIGURE 4-67 1971 AUTOMOBILE DIMENSION RANGES

A barrier curb does not really become effective as a redirective device, however, until the curb height is eight or nine inches. As noted earlier in Section 4.2, a ten-inch barrier curb height was recommended on the basis of the 1957 California test series. In addition, the Trief curb and the very effective Elsholz curbs are 12.2 inches and 10.6 inches high, respectively. The final curb height choice should therefore be made on the basis of the variation in the ratio of redirective effectiveness to damage cost for each additional inch of curb height.

A sample of what such curves might look like and how a curb height might be determined from their use is shown on Figure 4-68. Using the rationale that the design point should be in the region where the effectiveness/cost curves begin to level off, the optimum height for curb #1 is about twelve inches and curb #2 about eighteen inches. In choosing between curbs, however, one would obviously choose curb #1.

4.7.2 CURB PROFILE SHAPE. As discussed in Section 4.2, an optimum barrier curb profile was recommended after the 1957 California test series. This is shown on Figure 4-3a. Although this curb was never tested, curbs similar to it have been evaluated in both Canada and Germany. The German tests in particular were very impressive and, as indicated in Section 4.6, suggest that the Elsholz curb would redirect over 70% of ran-off-the-road vehicles in urban traffic conditions.

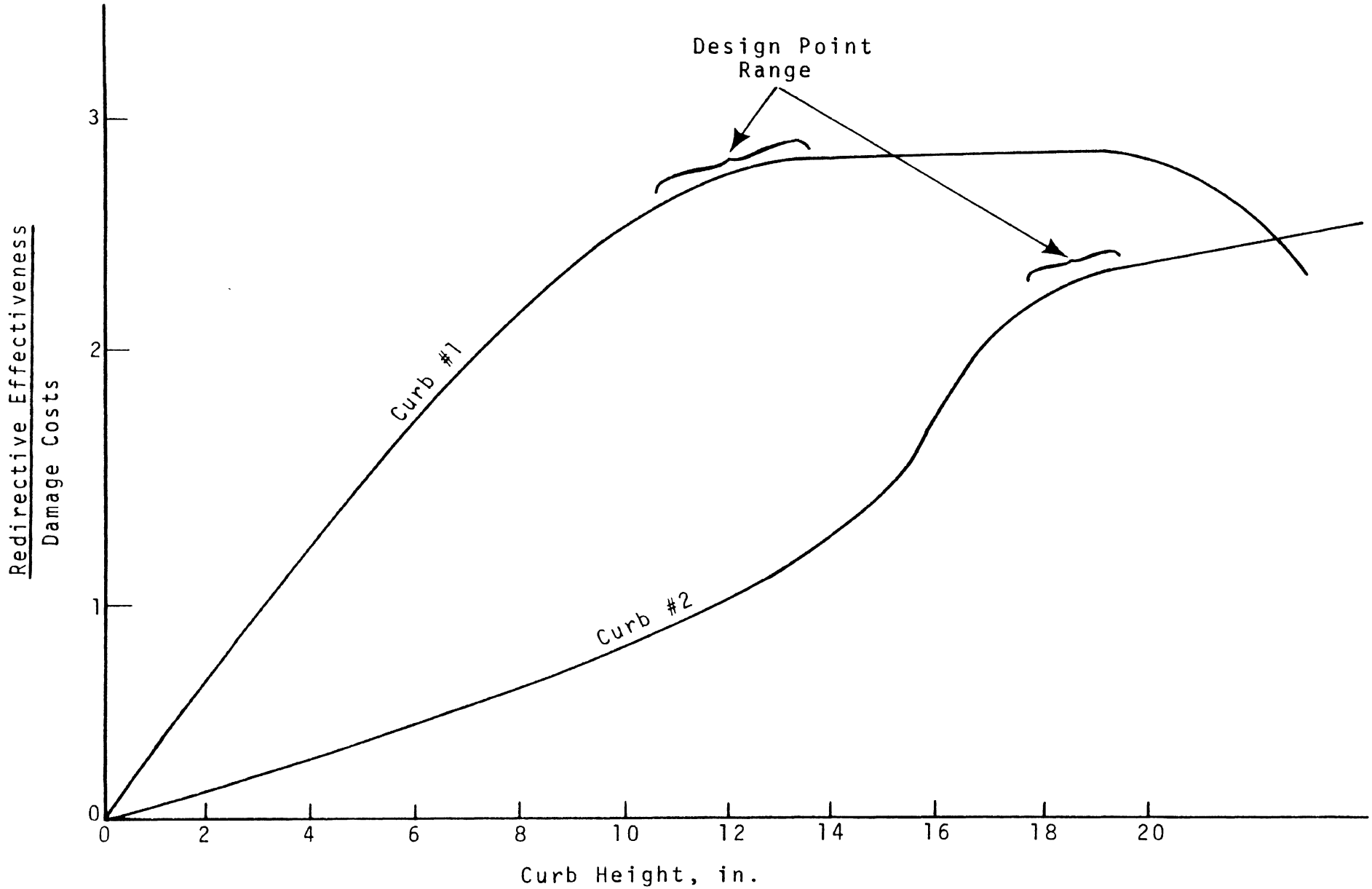
Design Point
Range
Curb #1
Curb #2
Redirective Effectiveness
Damage Costs
0
1
2
3
0
2
4
6
8
10
12
14
16
18
20
Curb Height, in.

It is evident, then, that an optimum barrier curb profile is very probably quite similar to the California and Elsholz configurations.

4.7.3 CURB FACE. The barrier curb face should discourage wheel mounting through the mechanism of induced tire sidewall/curb face friction. For best performance, the curb face should have a smooth texture and should be made of a hard material with low friction properties. In the 1953 California tests, for example, the metal facing on curb VI-M was found to produce a substantial improvement in redirective performance over curb VI with a concrete facing.

A possible curb face material is the epoxy sand mix which has been experimentally tested as a wear resistant paving material [54]. The material is hard, fine textured, and low in friction coefficient. The latter property, unfortunately, makes it unsuitable for a pavement surface.

4.7.4 BARRIER CURB DESIGN GUIDELINES. As discussed in Appendix A under barrier development procedures, the final step before arriving at a candidate design is to produce a set of design guidelines. The specific guidelines for a barrier curb, which have been arrived at as a result of the current research, are listed as follows:

I. Performance

1. The barrier curb height shall be high enough for maximum redirection properties, and low enough to minimize vehicle damage (at this writing about ten inches).

2. The barrier curb face shall be undercut so that the cut-out portion will trap the tire bulge in a hold down manner while at the same time minimizing curb face/tire sidewall friction forces.

3. The upper corner of the barrier curb shall be rounded with a radius of at least one inch so as to minimize the possibility of the corner acting as a mounting fulcum for the wheel rim.

4. The barrier curb facing material shall be chosen to produce a low coefficient of friction when in contact with the tire sidewall.

5. The barrier curb face shall slope back no more than one inch for each three inches of height.

II. Climatic

1. The barrier curb face design shall be such that it does not act as a snow, ice, or dirt accumulation repository.

2. Curb face material shall be chosen such that corrosion, rot, sunlight deterioration, and other age and deterioration factors are minimized.

III. Cost

1. Installation and materials cost shall be kept to a reasonable minimum.
2. Maintenance costs, including curb face cleaning, shall be minimized.
3. Vehicle damage shall be limited to minor body scraping.

IV. Esthetics

1. The barrier curb shall present a pleasing finished appearance.
2. The barrier curb shall assist in the orderly development of the roadside.

V. Traffic Control

1. The barrier curb shall delineate the road edge.
2. The barrier curb shall not be so imposing as to cause traffic to veer from the road edge and reduce the effective right-of-way.

VI. Drainage Control

1. The barrier curb shall act as one bank of a channel for surface water run-off.

4.8 CONCLUSIONS AND RECOMMENDATIONS

The redirective properties of barrier curbs are directly related to height, face profile, face material, and face surface texture. The best shapes yet produced are between nine and twelve inches high, have an undercut face, slope backward at a rate of 2:9 from the road edge, and have a smooth, low friction surface. Redirective performance of curbs has been found to be determined by the vehicle velocity component normal to the curb face when shape parameters are fixed.

Of the five MDSH barrier curbs evaluated, only the higher curbs (A, K, and to a lesser extent C) had a significant influence on the vehicle path. Curb A had the most effect for low speed, low angle impacts. For 40 mph, 25° case the vehicle was redirected after it had mounted the curb. At 60 mph and 10° the vehicle spun out in a direction to increase the incidence angle. For the 60 mph, 25°, and 80 mph, 10° cases the vehicle was largely unaffected by the curb.

The results for curb K are similar to those found for curb A, except that a spin out occurred for the 80 mph and 10° case. Eventual redirection again occurs at 60 mph and 10°, and at 40 mph and 25°, while curb influence is small for the 60 mph 25° case.

As predicted from test results, combinations of lower speeds and small angles tend to produce the greatest effect on the vehicle path. The fact that curb face/sidewall forces were not present in the simulation undoubtedly influenced the results to some extent. Comparisons between test and simulation results proved to be good, however.

Using urban speed and ran-off-the-road exit angle distributions, it was found that the Trief curb would redirect about 27% of the vehicles accidently leaving the roadway. Similar calculations for a curb tested by Elsholz in Germany produced a figure of 70%. It is apparent, then, that in certain circumstances a barrier curb can be an effective redirection device. It is recommended, therefore, that those MDSH curb designs which are considered to be barrier curbs be evaluated with respect to the design guidelines presented in Section 4.7. Particular attention should be given to curb height, profile, facing material and texture.

5. CURB/GUARDRAIL INVESTIGATIONS

The curb/guardrail investigations include a state-of-the-art review and a description of the analysis and simulation activities carried on at HSRI. These latter activities involved the evaluation of several in service curb-guardrail configurations, which were considered by the Michigan Department of State Highways to have questionable impact performance behavior. Comparisons between the results achieved by simulation and analysis are made wherever possible with test results. Design guidelines, based on the research findings presented here, are included as an aid in developing sound curb/guardrail installation practices.

5.1 HISTORICAL REVIEW

The first published research on curb/guardrail impact investigations was carried out by the California Division of Highways in 1955 [13]. The studies were concerned with evaluating a concrete guardrail (in this case a bridge rail) fronted by a nine-inch undercut curb. In all, three configurations were tested, with the rail setback ranging from 1 5/8 inches to eighteen inches. Impact conditions were relatively severe in all cases, with velocities varying between 48 and 57 mph, and angles between 20° and 30°. In all cases, the vehicle mounted the curb and caused a fracture in the backup concrete rail. In only one case, however, where the rail was but 21 inches high, did the vehicle penetrate. The results of the test series are summarized on Figure 5-7 in Section 5.3.

A most important part of this early publication was the inclusion of the first reference to the "dynamic jump" phenomenon. This phenomenon is associated with the jumping motion of the vehicle as it mounts the curb and is bounced into the air. The dynamic jump curves published at that time are shown on Figures 5-1, 5-2, and 5-3. The curbs referred to are shown on Figure 4-2 of Section 4.2.

Using these jump curves, it was concluded that guardrails (in this case bridge rails) used in combination with a curb and set back further than five inches from the curb face, must be higher than guardrails used without a curb. The formula arrived at for barrier curbs between nine and twelve inches high, required that the barrier height be increased five inches for each one foot of setback up to a maximum height of 48 inches.

The first tests of metal beam guardrail condigurations fronted by curbs were also conducted by the California Division of Highways [28]. The two designs shown on Figure 5-4 were tested, once each. Although the six-inch curb was offset 48 inches from the guardrail, no apparent adverse effect on the collision mechanics was noted. In one of the tests the impact vehicle actually went under the rail following contact with the curb. The six inch curb, which is shown in cross-section on Figure 4-1 (Curb X) and which would be classed as mountable, evidently had very little effect on either the rise, or redirection of the vehicle prior to contact with the barrier.

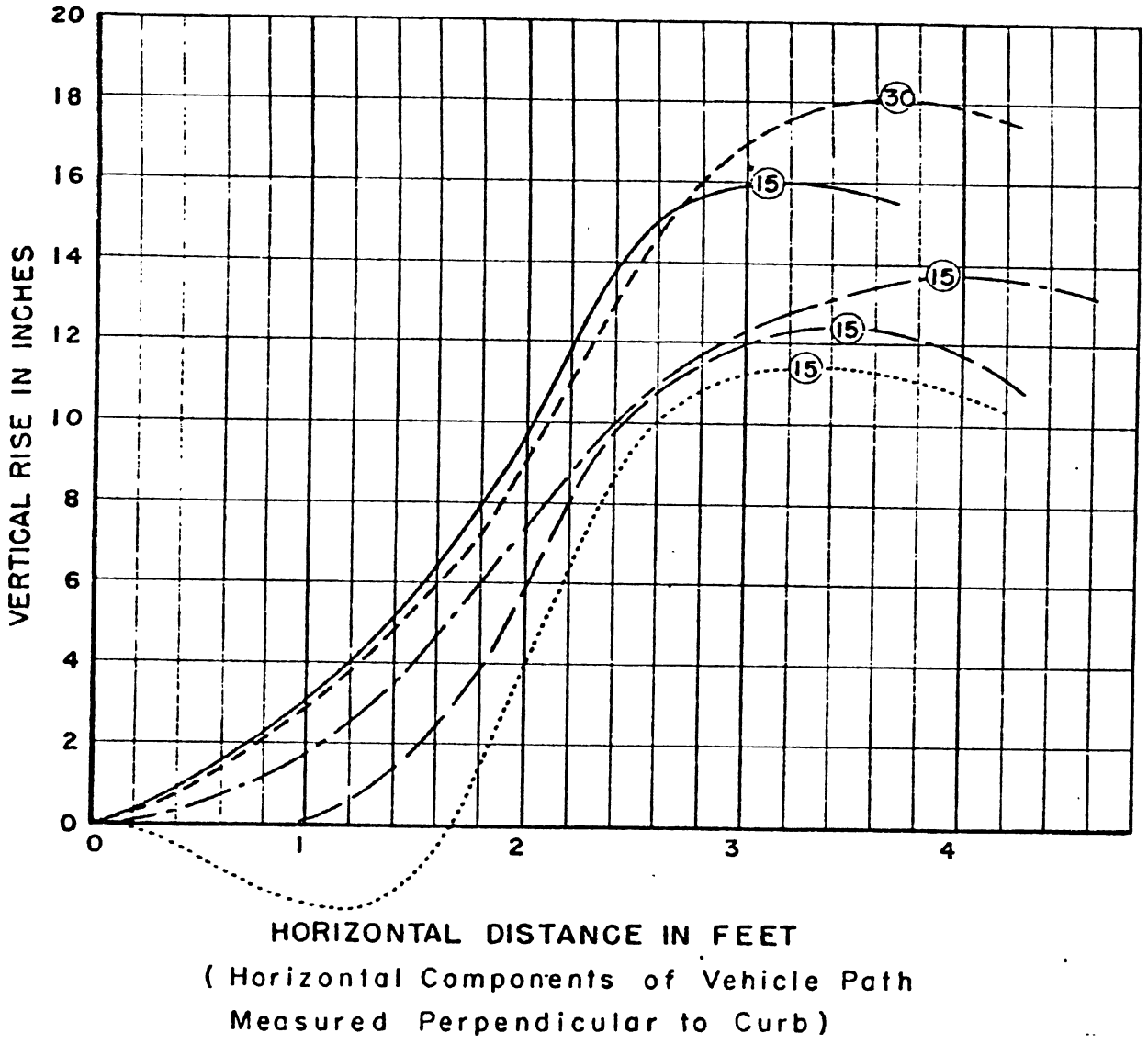

Curb	Angle	Speed	Curve
A 9	7.5°	60	– – – –
A 9	15°	30	—— ——
A 10	15°	45	—— · ——
A 10	20°	30	·····
A 11	20°	30	——

Note: Circled numbers indicate distance in feet along vehicle path from point of impact to crest of jump.

Vertical rise is referenced to right front of car frame.

FIGURE 5-1. CALIFORNIA CURB A DYNAMIC JUMP CURVES

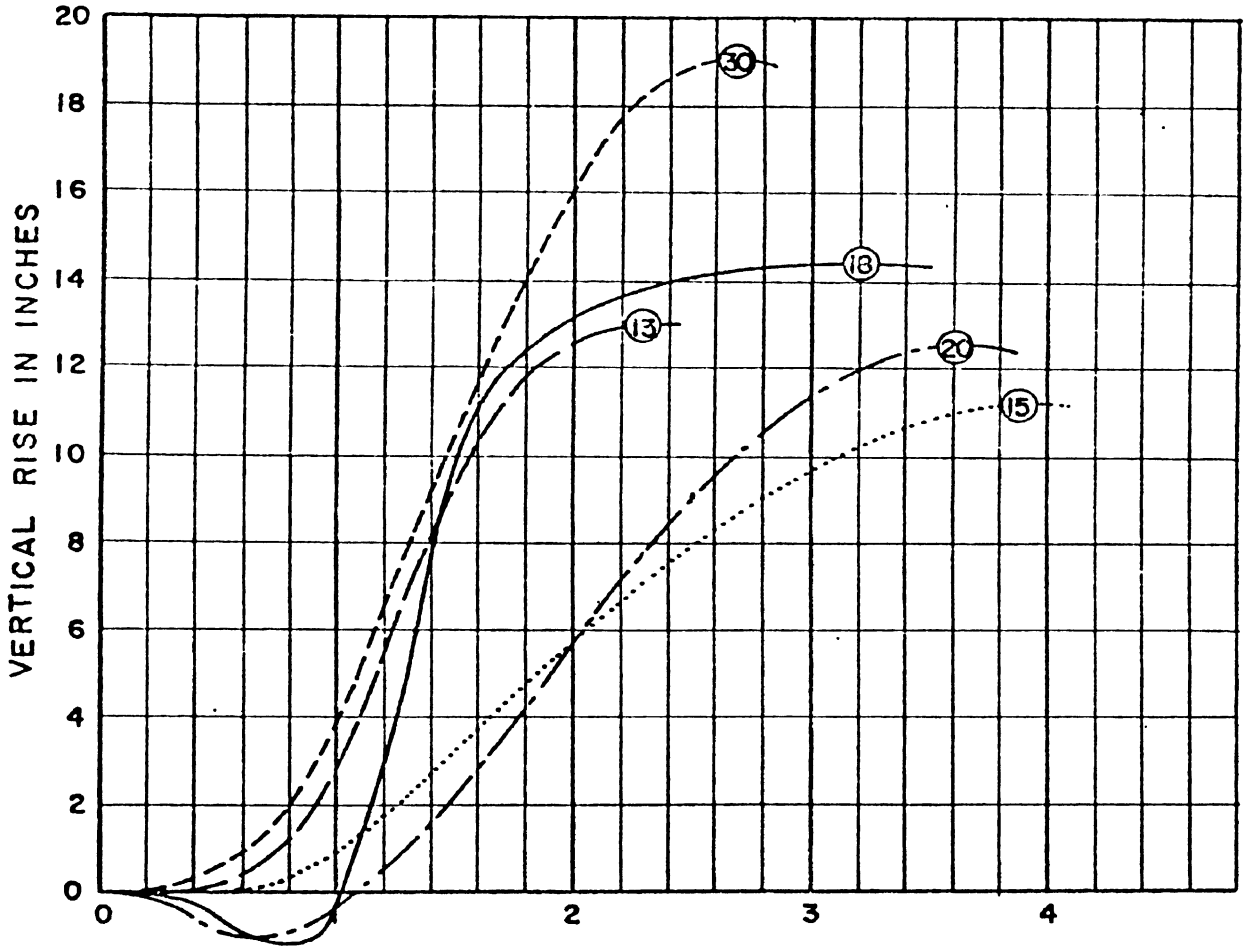

Curb	Angle	Speed	Curve
B 9	7.5 °	60	— — — —
B 9	15 °	20	—— ——
B 9	15 °	30	—— · ——
B 9	20 °	30	·····
B 11	15 °	45	——

Note: Circled numbers indicate distance in feet along vehicle path from point of impact to crest of jump.
Vertical rise is referenced to right front of car frame.

FIGURE 5-2. CALIFORNIA CURB B DYNAMIC JUMP CURVES

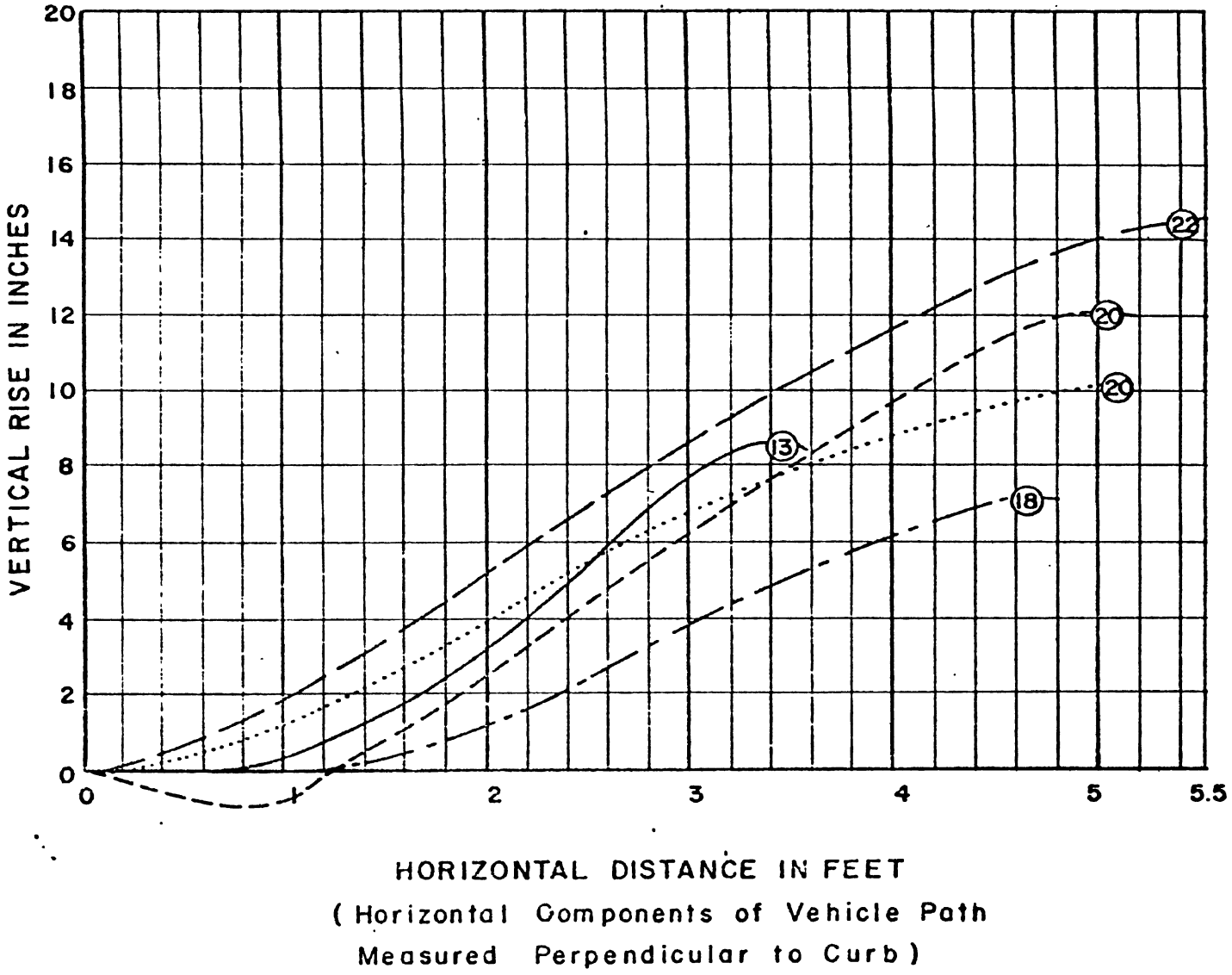

Curb	Angle	Speed	Curve
C12	20°	45	— —
C 9	20°	30	———
C10	15°	45	- - - -
C11	20°	45	.....
C10	20°	45	— · —

Note: Circled numbers indicate distance in feet along vehicle path from point of impact to crest of jump.
Vertical rise is referenced to right front of car frame.

FIGURE 5-3. CALIFORNIA CURB C DYNAMIC JUMP CURVES

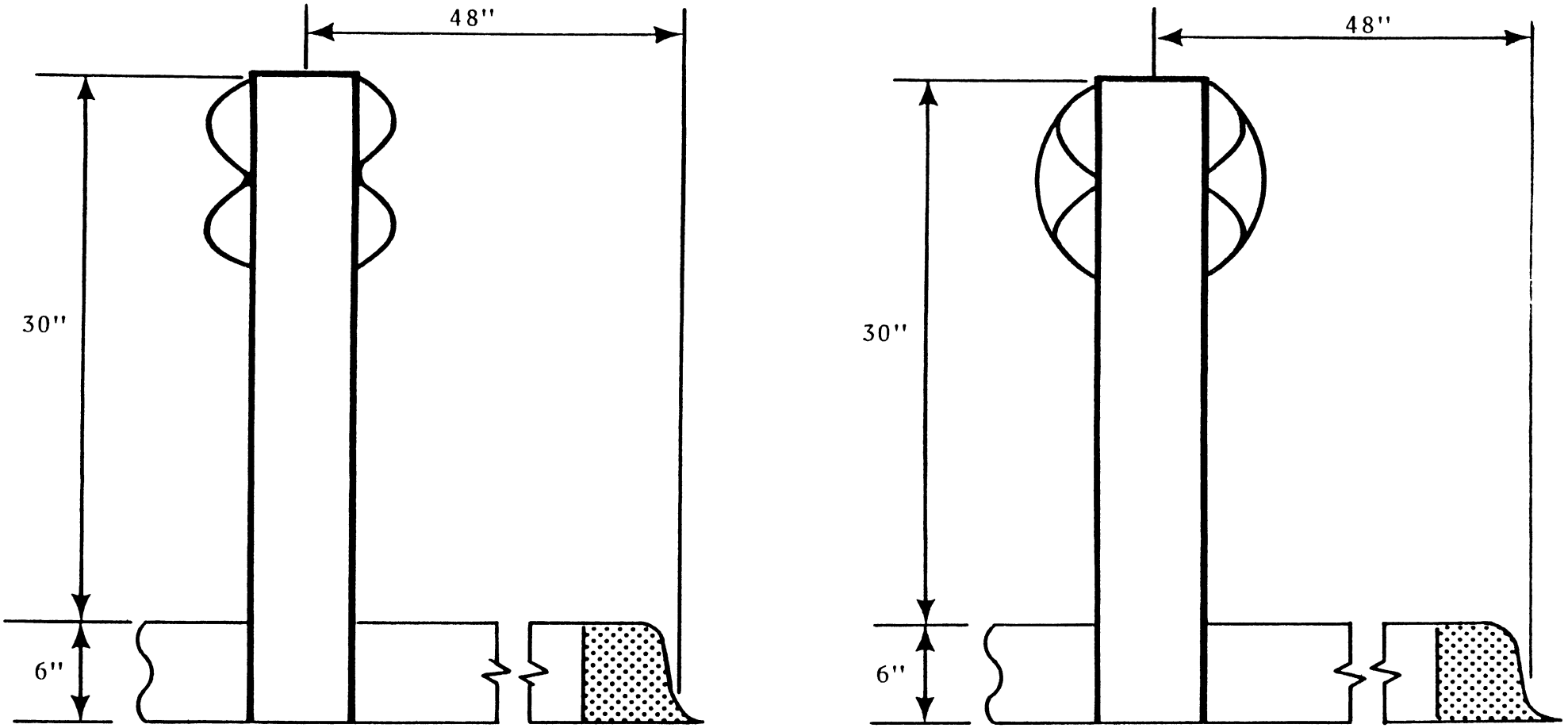

FIGURE 5-4 CURB GUARDRAIL COMBINATIONS TESTED IN CALIFORNIA

An additional set of tests on concrete guardrails (again bridge rails) fronted by curbs was conducted in California in 1959 [29]. The first configuration, shown on Figure 5-7 (Item E), was fronted by a sloping nine-inch barrier curb offset 19 inches from the rail facing. A second design, shown on Figure 5-9 (Item J) was fronted by a ten-inch undercut barrier curb which was offset four inches.

In a single test of the first configuration, the backup rail failed structurally and the vehicle broke through. The curb caused the vehicle to rise about nine inches before impacting the rail. No evidence indicates the curb was a factor in the breakthrough, however.

In three tests of the second design, two involved automobiles while the third involved a 17,500-pound city bus. The automobiles were reflected, albeit with a good deal of damage, while the bus broke through. In no case was the ten-inch curb a large factor in the results.

The last set of curb-guardrail tests ocnducted in California were carried out in 1963 [30]. The objective of the tests was to determine the installation height for a retaining cable in a cable chain-link median barrier. The median barrier is often installed on top of a raised median, fronted by a six-inch mountable curb, and offset 36 inches from the road edge. In conjunction with the median barrier tests, a series of dynamic jump tests were conducted on the six-inch curb so as to formulate

preliminary recommendations on an effective height. Most tests were with sports cars, since accident data had suggested these were the kinds of vehicles that were wedging under barriers with cable heights of 30 inches. In some cases, larger vehicles were vaulting over, however.

Results of the jump tests indicated there was a wide variation among vehicles in terms of their response to crossing the six-inch curb. For 25° approach angles, the three different sports cars in the tests had risen about five inches by the time their c.g.'s had crossed the middle of the six-foot median. At a 7° angle, these vehicles had risen between seven and nine inches at the middle point. A standard sedan (a 1960 Ford) behaved somewhat differently, in that it rose only two inches for the 25° approach, and nine inches for the 7° approach. The total range in jump elevations was seven inches with the variation being a function of vehicle type and approach angle. Since all velocities were within ten mph, however, the effect of velocity was not determined.

The most extensive series of curb/guardrail tests to date has been conducted by New York State [8]. The test exercises extended over a period of six years, and involved over 21 tests of various curb/guardrail combinations. Of these tests, 17 involved a ten-inch barrier curb while four were with a similar six-inch curb. Rail offset from the ten-inch curb face varied between 18 and 60 inches. Offset in all cases involving the six-inch curb was six inches.

In the first test with the ten-inch curb, the backup rail was placed five feet behind the curb face. This was done for the express purpose of determining the jump producing properties of the curb. The test was conducted with a standard automobile at 60 mph and 25°, and the vehicle reportedly did not jump. The car body was evidently raised about ten inches above the curb, however, and the curb damaged the steering system. This latter effect was also noticed in subsequent tests where the rail offset had been reduced to 20 inches.

Tests with the six-inch curb were first performed without any railing. These tests were reported to show that this curb had almost no effect on the vehicle steering system. Little effect on vehicle motion was also reported for several shallow angle, low speed impacts. In subsequent tests of the six-inch curb with various backup railings, it was found that the curb had no noticeable effect on vehicle reactions.

A series of tests were conducted in Montreal on several curb/guardrail combinations during 1965 [14]. The various configurations are shown on Figure 5-9 (Items A through H). These designs resist vehicle impacts in three stages. Low angle impacts result in the vehicle being reflected by the ten-inch, undercut barrier curb without vehicle damage; higher angle, medium energy impacts are redirected by the protruding guardrail; and high energy, high angle impacts are contained by the backup rail, albeit with substantial vehicle damage. The designs were

evaluated as a guide rail system for an elevated expressway and were judged primarily on the basis of the magnitude of the reflection angle following initial impact. Using this criteria, the most efficient configuration was found to be Model H. This design incorporated a trapezoidal wall in place of the protruding guardrail. If the evaluation criteria had included vehicle damage and impact acceleration histories, the recommended design might very probably have been somewhat different.

As mentioned in Section 4.0, a single test was conducted on the ten-inch, undercut barrier curb without either guardrail being in place. With test conditions of 64 mph and 20°, the result was, as had been predicted, that the vehicle mounted the curb. Other research indicates less stringent impact conditions would have produced a redirection, however. A second test with the ten-inch curb backed up by a two-foot concrete wall did result in a redirection.

In Germany tests have been conducted on curb/guardrail combinations where the curb height is less than two inches above the pavement [25]. The vehicle easily mounted this curb in all test cases and was redirected by the guardrail. With the rail set back a distance of about 20 inches, the influence of the curb on redirection was not measurable.

5.2 EVALUATION EXERCISES

Curb/guardrail evaluations consisted of two separate activities. First, as in the case of curbs alone, test data

from test programs of other organizations was assembled and synthesized. Second, the results of the curb impact simulation exercises were extended so as to predict the consequences of a vehicle striking a guardrail following its initial impact with the curb. (In the present context, a guardrail will be considered to be a metal or concrete barrier.) The curb/guardrail combinations evaluated were those suggested for evaluation by the Michigan Department of State Highways [46].

5.3 CURB/GUARDRAIL TEST DATA

A summary of all tests made on guardrails fronted by curbs are shown on Figures 5-5 through 5-9. The data are for a large variety of curb/guardrail combinations, none of which are exactly like any of MDSH designs. In addition, most configurations have only been tested once, while a wide variety of test conditions have been used. These facts make generalizing on the accumulated data rather difficult. The following discussions detail areas where, despite the difficulties, specific generalizations could be made.

The primary question relative to using guardrail in combination with a curb is whether the curb contributes adversely to the redirective performance of the guardrail. In order to answer this question, an attempt was made to categorize existing test results in terms of the three parameters of curb height, rail height, and rail setback. It was hoped that this structuring would shed some light on the likelihood of vaulting over, or

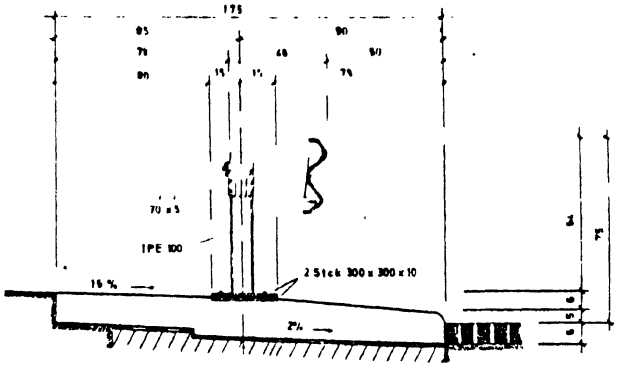

German Curb/Guardrail Combination [25]

(Dimensions in mm.)

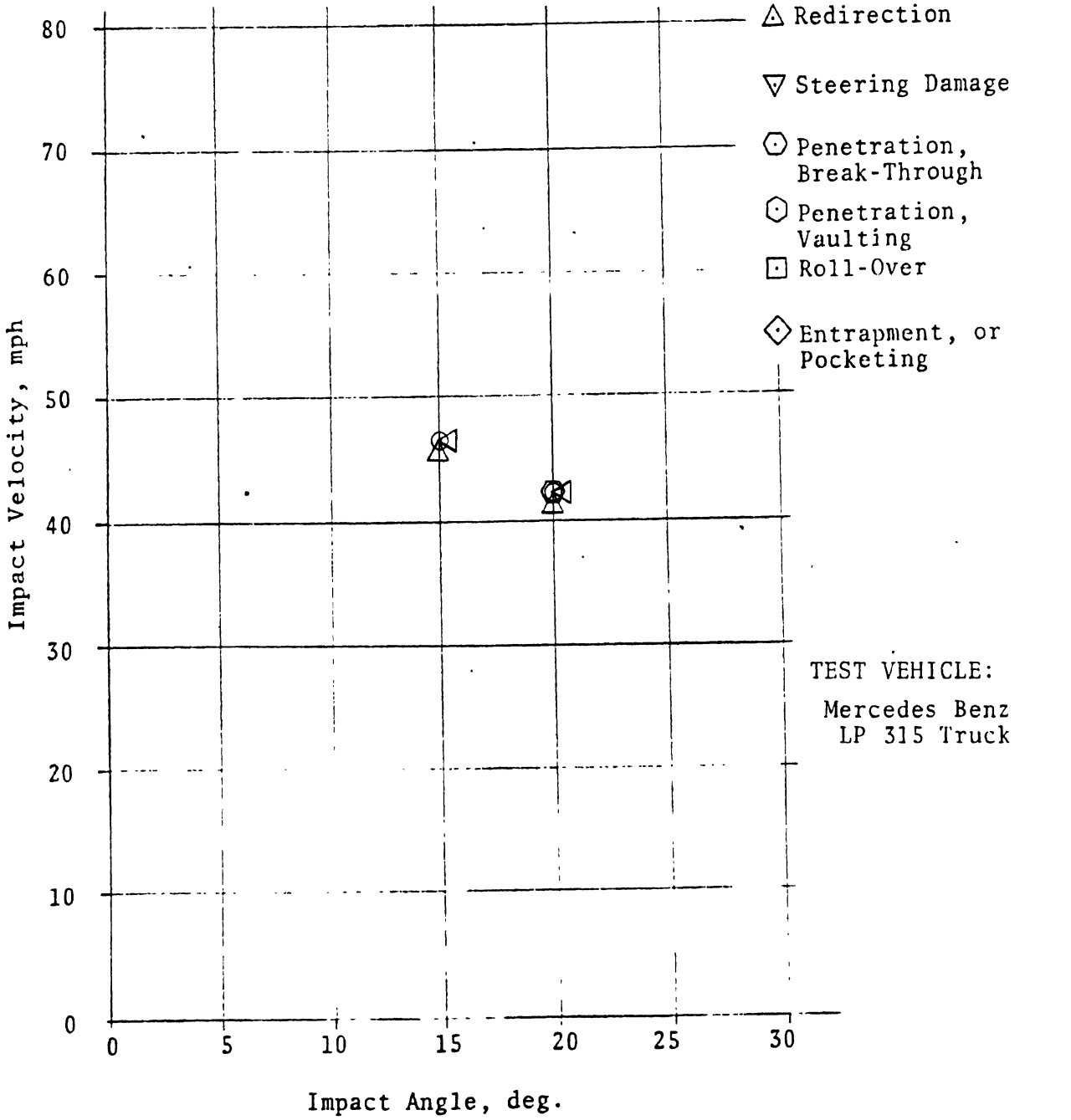

FIGURE 5-5. TWO INCH CURB FRONTING GUARDRAIL TEST RESULTS SUMMARY

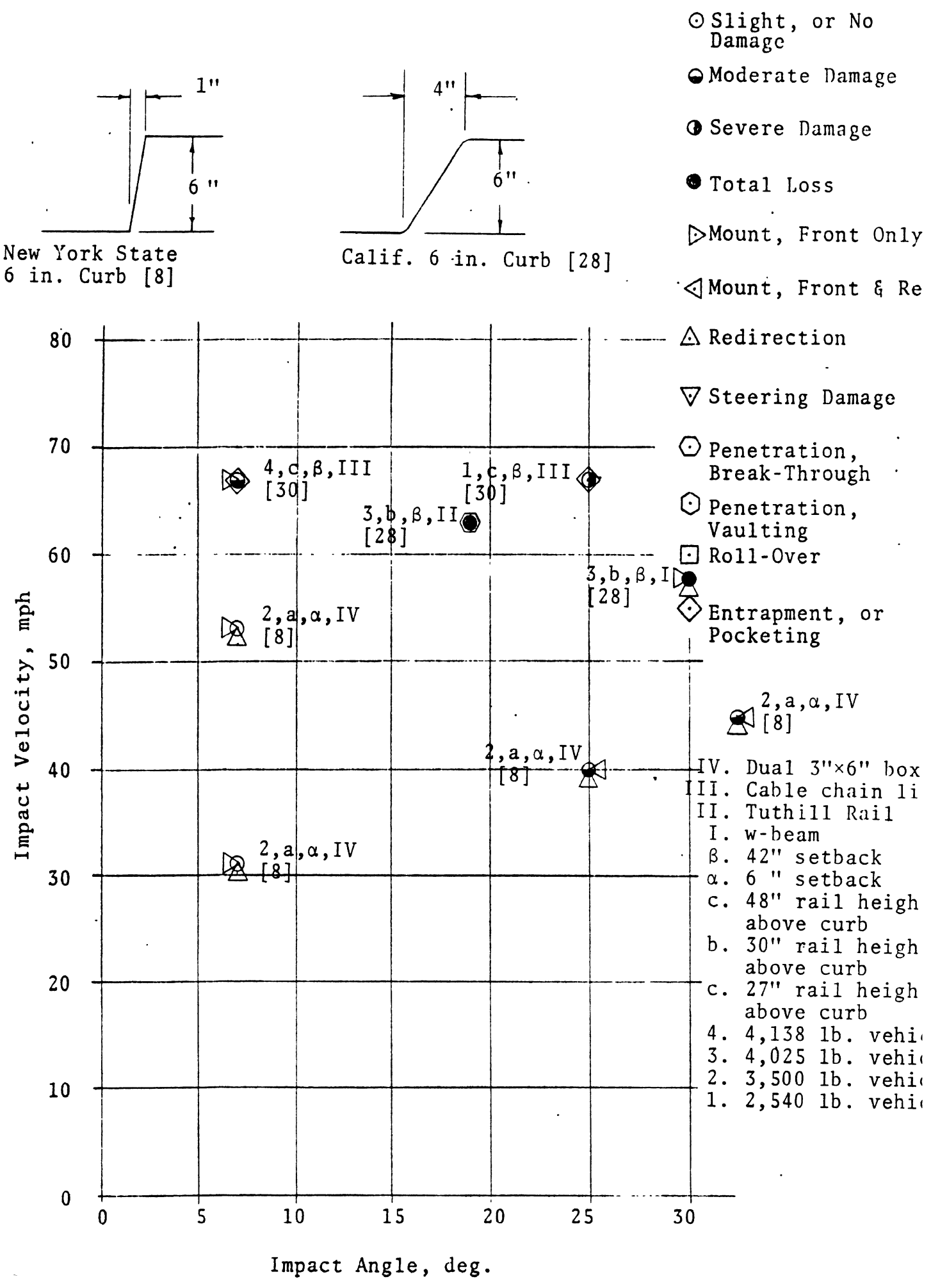

FIGURE 5-6. SIX INCH CURB FRONTING GUARDRAIL TEST RESULTS SUMMARY

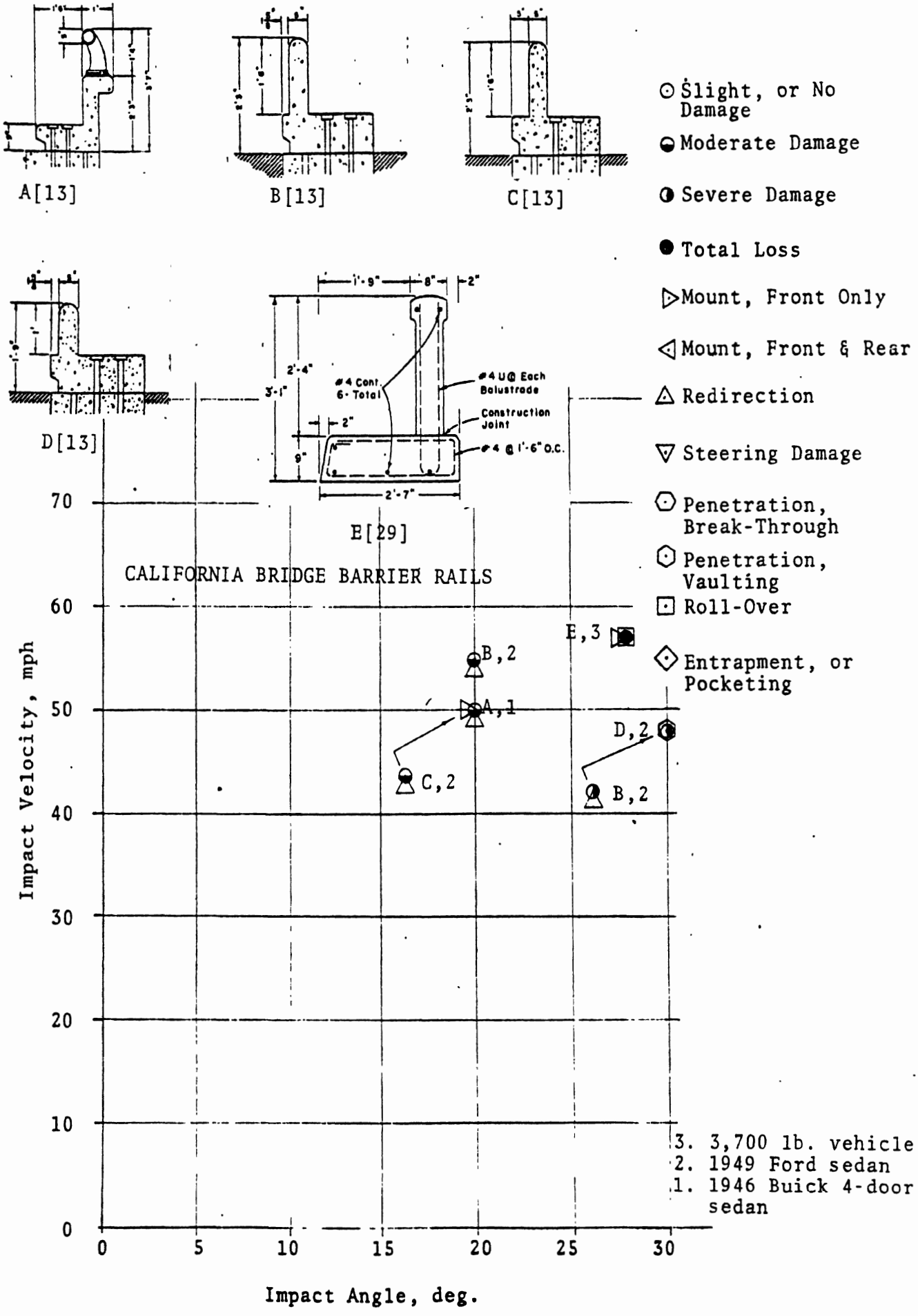

FIGURE 5-7. NINE INCH CURB FRONTING BRIDGE RAIL TEST RESULTS SUMMARY

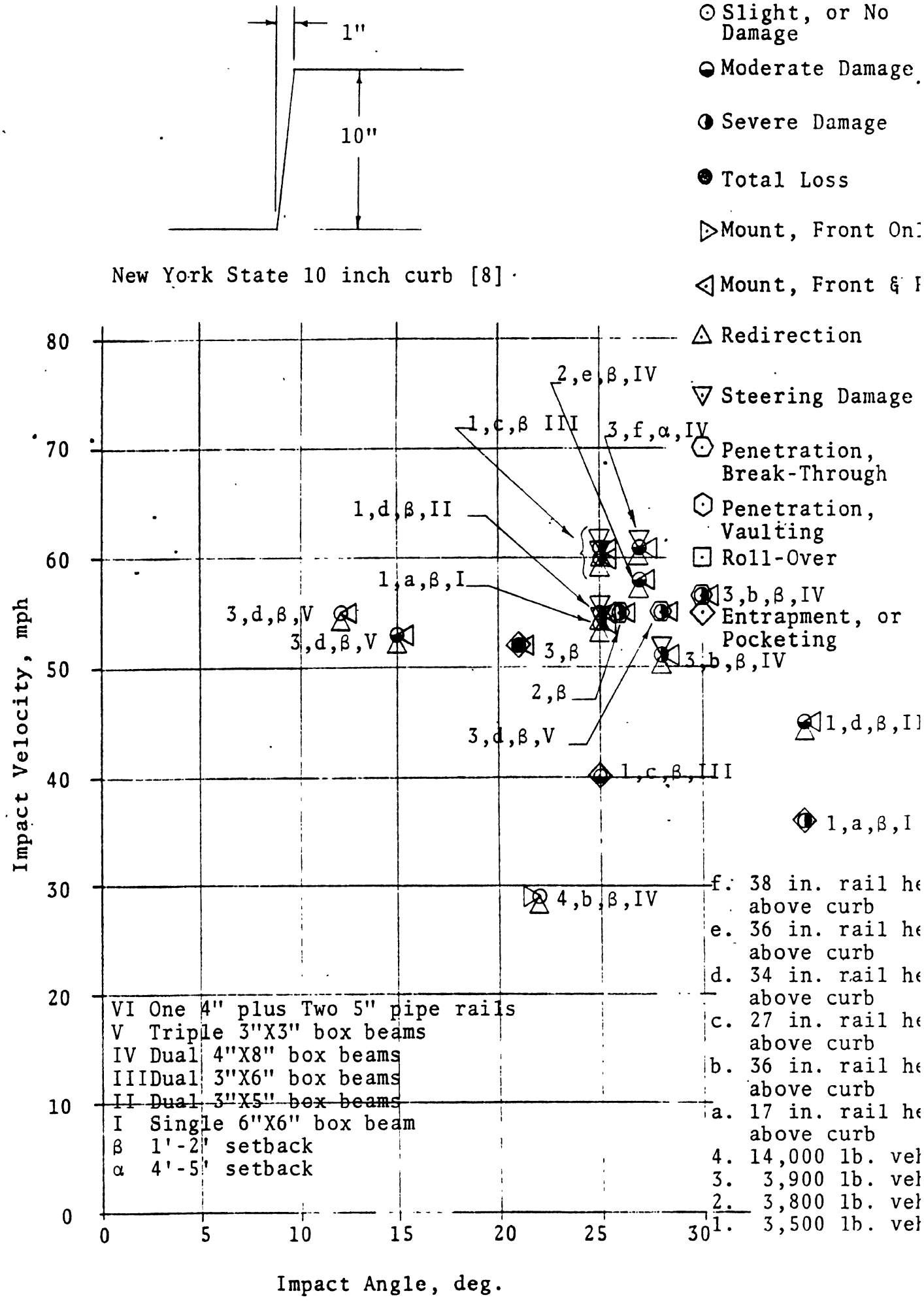

FIGURE 5-8 NEW YORK STATE TEN INCH CURB FRONTING GUARDRAIL TEST RESULTS SUMMARY

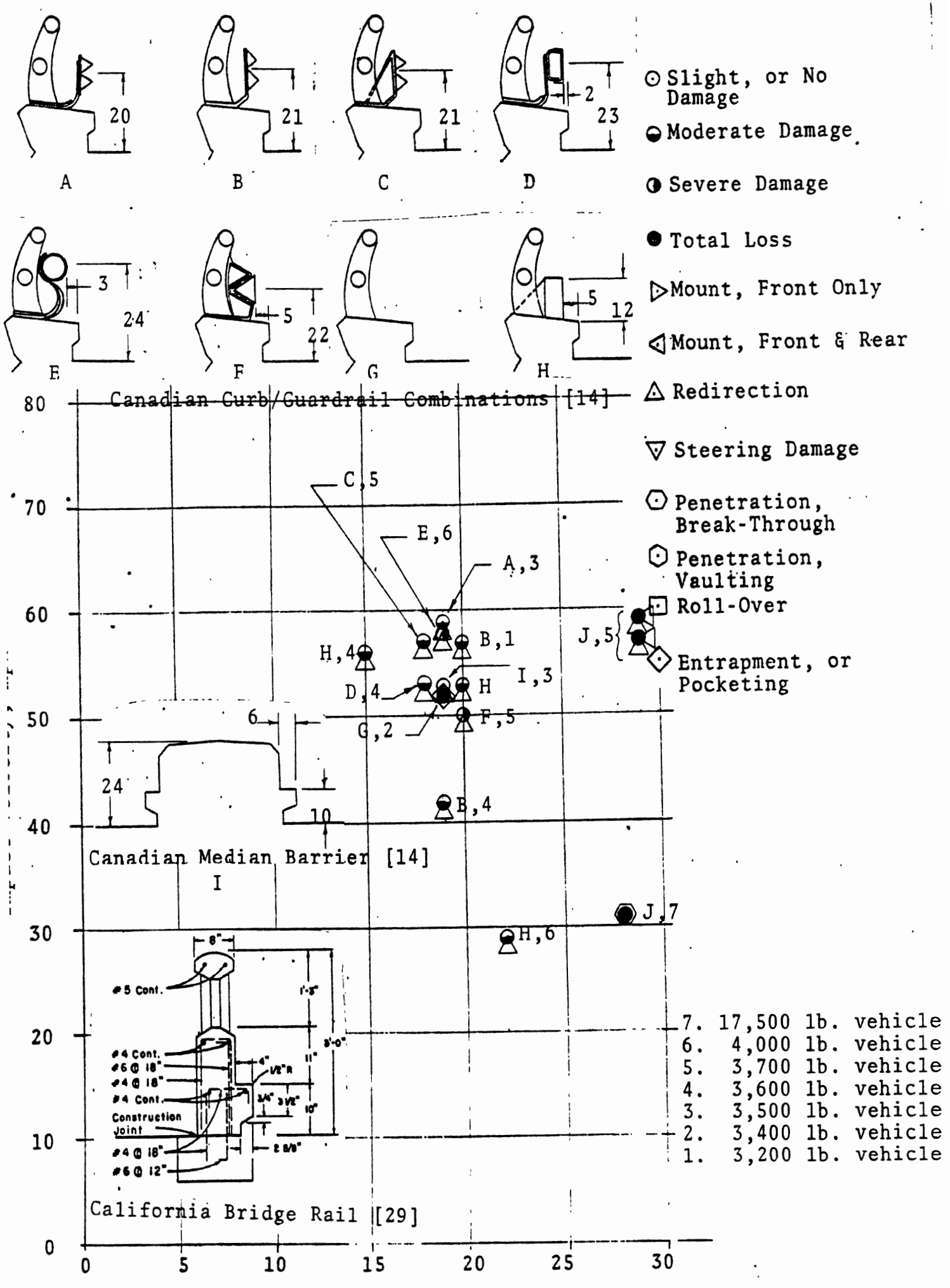

FIGURE 5-9 TEN INCH CURB FRONTING GUARDRAIL TEST RESULTS SUMMARY

tunneling under, a guardrail fronted by a curb. The exercise proved fruitless, however, in that of all tests examined, no cases of tunneling were discovered and only one questionable case of vaulting. Several cases of structural failure on the part of the guardrail were noted, but these were considered to be independent of curb/guardrail dynamics. In the single case of possible vaulting, a 17,500-pound city bus struck a concrete bridge rail (Figure 5-9, Item J), broke through the rail and came to rest straddling the rail [29]. It is uncertain, therefore, as to whether the structural failure of the rail contributed to the final position of the bus, or whether no "vaulting" would have occurred if the rail had remained intact. With the questionable result of this test, and the unusually large test vehicle which was employed, it is safe to say that vaulting, as a result of curb/guardrail dynamic interaction, has not been identified as a serious problem in any known test program.

Engineering intuition would suggest that vaulting is a problem, however, and attempts have been made to use vehicle/curb dynamic jump data as a means of specifying guardrail height and setback as a function of curb height. This technique is used in the next section to specify similar relationships for the various specified MDSH curb/guardrail combinations. The technique used is analytical due to the fact that simulation capability for impacting a curb and guardrail during the same run was not available in any existing program.

5.4 CURB/GUARDRAIL SIMULATION ANALYSIS

The conditions which will result in avehicle vaulting a guardrail through dynamic interaction with a curb can come about in two different ways. In one case, the vehicle can receive enough impulse from the curb to vault completely over the guardrail without making contact. In the second case, the vehicle does not clear the guardrail, but makes contact. With the rail top acting as a fulcrum, the vehicle then proceeds to roll over the rail. Knowing vehicle geometry and using the dynamic jump data from the curb simulation exercises (Section 4.5), cases of complete vaulting can be readily determined. Roll-over vaulting, however, requires some additional analysis.

The limiting conditions which will result in roll over vaulting can be determined by energy and momentum considerations. Suppose, as shown on Figure 5-10, that the vehicle has been redirected parallel to the guardrail and has just made initial contact. As indicated, the vehicle has a roll rate of $\dot{\bar{\phi}}_0$ and a velocity $\bar{V}_G$ in a plane normal to the rail line. It will be assumed that the line of contact is the axis O, the axis about which the vehicle would roll if roll-over vaulting occurs, and that this axis remains fixed. $\bar{V}_G$ can then be broken up into velocity components along and normal to the line between the vehicle C.G. and the axis of rotation, $\bar{V}_a$ and $\bar{V}_n$, respectively.

It will be assumed, now, that the velocity component $\bar{V}_a$ is lost through energy dissipated in the collision process

Geometry Equations:

$F = F_o + K + (C-L)S$

$G = -(z'+F)$

$h = \dfrac{G - d \sin\phi_o}{\cos\phi_o}$

$D = \sqrt{h^2+d^2}$

$\beta = \tan^{-1}\dfrac{h}{d}$

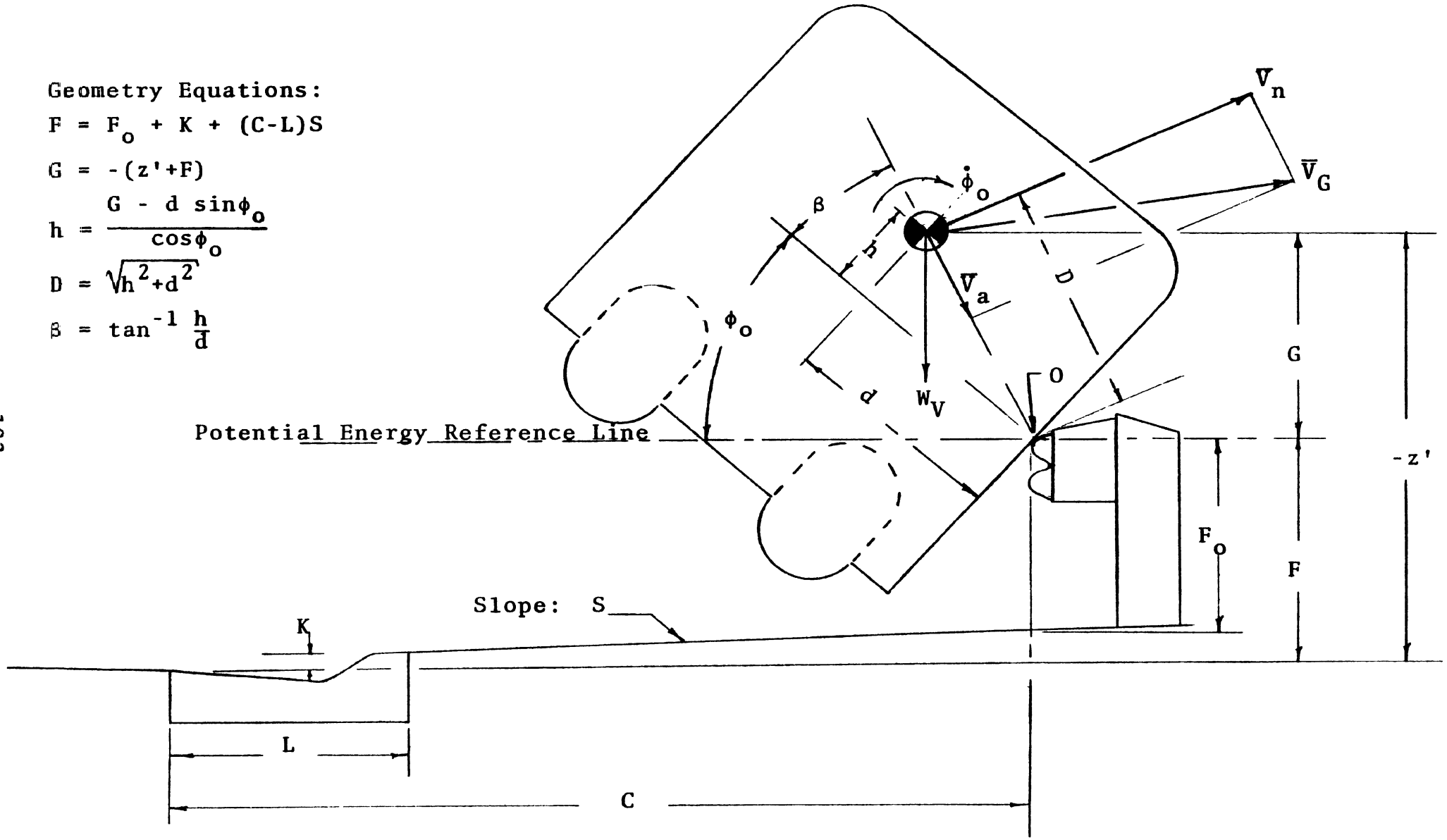

FIGURE 5-10 ROLL OVER VAULTING ANALYSIS GEOMETRY

(i.e., the impulsive forces acting along the line between the C.G. and axis of rotation are dissipated in a perfectly inelastic collision process. This velocity component contributes nothing to the resulting roll-over phenomenon, and merely allows the vehicle to remain in contact with the rail without rebound). The resulting vehicle motion then will be a pure rotation about the point O.

The only torque applied to the vehicle during the collision process is the result of forces applied at the point O. Therefore, if moments are summed about this point, the sum of moments will be zero. Similarly, the moment of momentum about the point will be constant during the collision since no moments act to change it. Thus, the moment of momentum about O is conserved and the following equation can be written.

$$\underbrace{I_{C.G.}\dot{\phi}_O + \frac{W_V}{g} DV_h}_{\text{Initial Moment of Momentum About O}} = \underbrace{(I_{C.G.} + \frac{W_V}{g} D^2)\dot{\phi}_f}_{\text{Final Moment of Momentum About O}} \qquad (5.1)$$

Therefore, just after impact, the vehicle angular rate about O, as the result of the collision, will be:

$$\dot{\phi}_f = \frac{I_{C.G.}\dot{\phi}_O + \frac{W_V}{g} DV_h}{I_{C.G.} + \frac{W_V}{g} D^2} \qquad (5.2)$$

where

$I_{C.G.}$ = Vehicle roll moment of inertia about a longitudinal axis through the c.g.

W_V = Total vehicle weight.

The remaining terms are defined on Figure 5-10.

The limiting conditions which will result in roll-over vaulting can now be determined by energy considerations. Suppose that at the time of initial guardrail contact, the vehicle is in such a position and has just the necessary angular and linear velocities to roll over the guardrail, and no more. As the vehicle rolls under these conditions, it will come to rest with its C.G. directly over the rail top as illustrated on Figure 5-10 when $\phi+\beta=90°$. The vehicle's potential energy at this roll position will just equal the kinetic energy associated with the angular velocity at the time of initial impact.

The kinetic energy just after impact is given by the expression:

$$K.E. = \frac{1}{2}\left[I_{C.G.} + \frac{W_V}{g} D^2\right]\dot{\phi}_f^2 \qquad (5.3)$$

The potential energy relative to a horizontal reference line through the pivot point is:

$$P.E. = W_V D \sin(\phi+\beta) \qquad (5.4)$$

At initial impact, the potential energy is:

$$P.E. = W_V D \sin(\phi_0+\beta) \ , \qquad (5.5)$$

and at the neutral point, where $\phi+\beta= 90°$,

$$P.E. = W_V\ D \tag{5.6}$$

The difference in the two quantities is the kinetic energy that is converted to potential energy as the vehicle rolls over.

Thus, if the roll motion results in the vehicle coming to rest at $\phi+\beta= 90°$, then:

$$\frac{1}{2}\left[I_{C.G.} + \frac{W_V}{g} D^2\right]\dot{\phi}_f^2 = W_V\ D[1 - \sin(\phi_O+\beta)]$$

or

$$\dot{\phi}_f = \sqrt{\frac{2W_V\ D[1 - \sin(\phi_O+\beta)]}{I_{C.G.} + \frac{W_V}{g} D^2}} = \Lambda \tag{5.7}$$

If the vehicle does not come to rest and the quantity on the left side exceeds the right side, roll-over vaulting will occur, and vice versa.

In using Equation (5.7), several assumptions were necessary regarding the choice of the time point for values of ϕ_O, $\dot{\phi}_O$, and V_n. As the vehicle crosses the curb, it does not strike the guardrail such that the vehicle is parallel to the rail as depicted in Figure 5-10. Rather, as shown on Figure 5-11, the left front of the vehicle first strikes the rail, with the vehicle rotating parallel to the rail as it is redirected.

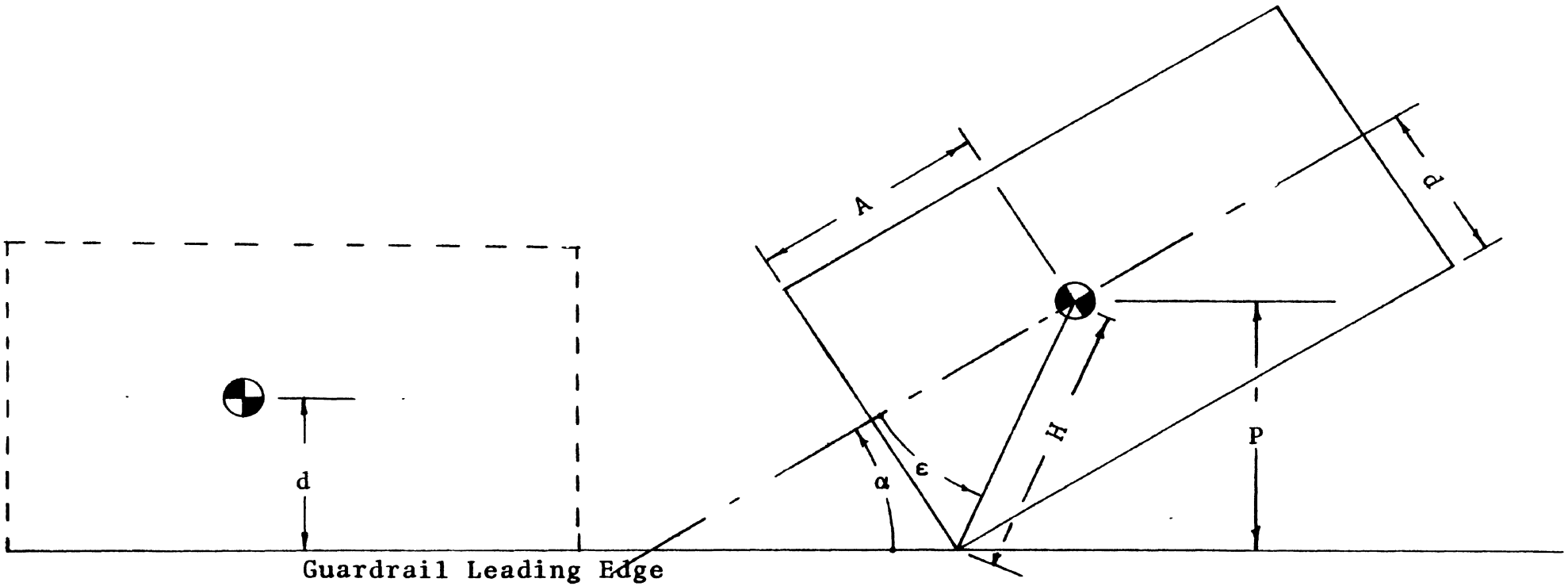

FIGURE 5-11 REDIRECTION GEOMETRY

During the process, the distance, P, varies from H $\sin(\alpha+\varepsilon)$ to d. Therefore, in order to determine whether roll-over vaulting will occur, Equation (5.7) was evaluated for the most adverse values of ϕ_0, $\dot{\phi}_0$, and V_n occurring during the interval of redirection. In addition, values of F_0 representing both the top and bottom of the W-beam guardrail were chosen as pivot points so as to bound the effects of barrier torsional deflection. Predictions of satisfactory curb/guardrail performance relative to roll-over vaulting are, therefore, expected to be conservative.

5.5 ANALYSIS RESULTS

In this subsection, each of the curb/guardrail combinations recommended by the MDSH [46] is evaluated through the use of Equation (5.7). Initial values for ϕ_0, $\dot{\phi}_0$, Z', and V_n were obtained from the simulated curb impact runs discussed in Section 4.5 . The sole exception involves the combination of curb B and the Concrete Safety Parapet. In this case, direct computer simulation runs were made to obtain the desired results.

5.5.1 CURBS, A, B, AND D AND DUAL BLOCKED-OUT MEDIAN BARRIER.

A typical cross-section for either a curb A, B, or D and the dual blocked-out median barrier is shown on Figure 5-12. The dimension C as defined on Figure 5-10 has a maximum value of 167 inches, or 13 feet, 11 inches. The minimum value was taken to be three feet or 35 inches (i.e., this means the minimum distance between the barrier face and the back of the curb and gutter section is four inches).

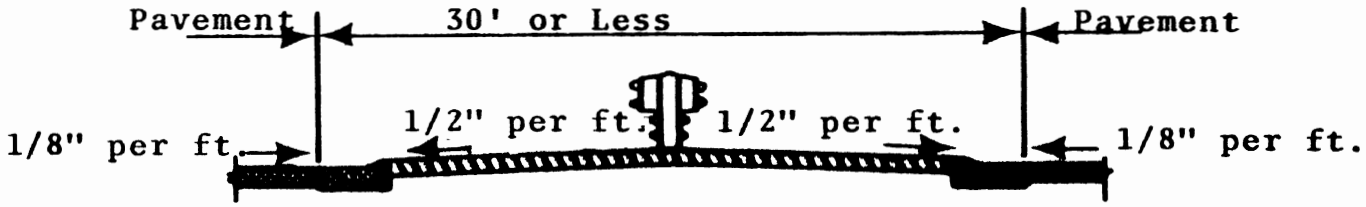

FIGURE 5-12 TYPICAL MEDIAN CROSS SECTION WITH CURBS A, B, OR D, AND THE DOUBLE BLOCKED OUT MEDIAN BARRIER

Results from the application of Equation (5.7) and the assumptions described thereafter are given on Table 5-1 for curb A. The ratio of Max $\dot{\phi}_f/\Lambda$ is never greater than one for any of the impact conditions. Therefore, neither vaulting (jumping the rail completely without contact), nor roll-over vaulting occurs. The closest approach to incipient roll-over vaulting occurs for the 60 mph, 25° case with the rail set back 12 ft. and with the pivot point assumed to be at the rail bottom. As can be noted, the ratio for these conditions is 0.79.

Some of the data for the 60 mph, 10° case is missing for values of setback between ten and fourteen feet. This is due to the fact that the vehicle was entrapped by the curb before reaching these set back distances. The situation is shown on Figure 4-32.

Results for curb B are tabulated in Table 5-2. The dimension C (Figure 5-10) has the same range of values as for curb A. Again, no vaulting or roll-over vaulting is predicted with the largest value of $\dot{\phi}_f/\Lambda$ being 0.47. As with curb A this occurs at 60 mph and 25° for a 12 ft. setback. Since curb B is lower than curb A, assessment of no vaulting in light of the curb A results is to be expected.

Curb D (4 in. height) is yet lower than both curb B (5 1/2 in. height) and curb A (9 in. height). Therefore, roll-over vaulting should be even less a factor with this curb and the data tabulated on Table 5-3 confirms this to be true. The largest value of $\dot{\phi}_f/\Lambda$ is but 0.31 and this again occurs in the 60 mph, 25° case near maximum set back.

TABLE 5-1

CURB A AND DOUBLE BLOCK OUT MEDIAN BARRIER

Initial Conditions		C	Max $\dot{\phi}_f/\Lambda$		Vaulting Assessment
V	α		Rail Top	Rail Bottom	
mph	deg	ft.	32.125"	20.125"	
40	25	14	-.03	.16	No Vaulting, or Roll-Over Vaulting
		12	-.05	.25	"
		10	-.06	.28	"
		8	-.03	.32	"
		6	-.03	.27	"
		4	-.15	.14	"
		3	-.20	.16	
60	10	14	----	---	"
		12	----	---	"
		10	----	---	"
		8	.24	.32	"
		6	.25	.33	"
		4	.25	.34	"
		3	-.05	.14	"
60	25	14	.15	.74	"
		12	.19	.79	"
		10	.09	.67	"
		8	-.01	.57	"
		6	-.28	.29	"
		4	-.37	.17	"
		3	-.42	.14	"
80	10	14	.18	.22	"
		12	.18	.23	"
		10	.18	.24	"
		8	.13	.36	"
		6	.14	.38	"
		4	.16	.39	"
		3	-.10	.17	"

TABLE 5-2

CURB B AND DOUBLE BLOCKED OUT MEDIAN BARRIER

Initial Conditions		C	Max $\dot{\phi}_f/\Lambda$		Vaulting Assessment
V	α		Rail Top	Rail Bottom	
mph	deg	ft.	32.125"	20.125"	
40	25	14	-.12	.30	No Vaulting, or Roll-Over Vaulting
		12	-.10	.30	"
		10	-.15	.24	"
		8	-.16	.25	"
		6	-.24	.12	"
		4	-.27	.13	"
		3	-.26	.13	"
60	10	14	-.06	.17	"
		12	-.05	.20	"
		10	-.05	.19	"
		8	-.11	.12	"
		6	-.13	.08	"
		4	-.14	.07	"
		3	-.15	.08	"
60	25	14	-.18	.46	"
		12	-.18	.47	"
		10	-.27	.35	"
		8	-.30	.31	"
		6	-.41	.11	"
		4	-.38	.16	"
		3	-.45	.13	"
80	10	14	-.06	.25	"
		12	-.05	.25	"
		10	-.07	.28	"
		8	-.15	.19	"
		6	-.17	.13	"
		4	-.20	.11	"
		3	-.21	.11	"

TABLE 5-3

CURB D AND DOUBLE BLOCKED OUT MEDIAN BARRIER

Initial Conditions		C	Max $\dot{\phi}_f/\Lambda$		Vaulting Assessment
V	α		Rail Top	Rail Bottom	
mph	deg	ft.	32.125"	20.125"	
40	25	14	-.14	.27	No Vaulting, or Roll-Over Vaulting
		12	-.18	.24	"
		10	-.21	.21	"
		8	-.21	.16	"
		6	-.26	.11	"
		4	-.25	.13	"
		3	-.26	.14	"
60	10	14	-.06	.17	"
		12	-.04	.20	"
		10	-.08	.16	"
		8	-.13	.09	"
		6	-.14	.07	"
		4	-.16	.08	"
		3	-.17	.08	"
60	25	14	-.26	.31	"
		12	-.28	.30	"
		10	-.32	.22	"
		8	-.35	.23	"
		6	-.40	.14	"
		4	-.36	.21	"
		3	-.39	.21	"
80	10	14	-.10	.25	"
		12	-.10	.25	"
		10	-.11	.18	"
		8	-.17	.12	"
		6	-.17	.10	"
		4	-.21	.12	"
		3	-.22	.11	

On the basis of the analysis presented here, it can be concluded that each of curbs A, B, and D will perform satisfactorily in combination with all standard set back configurations of the double blocked-out median barrier.

5.5.2 CURBS B AND D AND THE TYPE B GUARDRAIL. A typical installation for a type B guardrail in combination with either a B or D curb is shown on Figure 5-13. The set back dimension C is 25 in. for curb B and 23 in. for curb D. Data for curb B is given in Table 5-4 and that for curb D in Table 5-5. Maximum values for both cases occur for 60 mph, 25° impact conditions. In neither situation is there a likelihood of vaulting, however. It can be concluded, therefore, that curbs B and D can be expected to perform satisfactorily in combination with the type B guardrail.

5.5.3 CURB C AND TYPE B GUARDRAIL. A typical installation combination for curb C and type B guardrail is shown on Figure 5-14. Tabulated values of Max $\dot{\phi}_f/\Lambda$ are given in Table 5-6 for the various impact conditions. For the worst set of impact conditions (V = 50 mph, α = 25°) the ratio of $\dot{\phi}_f/\Lambda$ is, at most, 0.40. Therefore roll-over vaulting is not expected to occur and this curb/guardrail combination can be expected to perform satisfactorily.

5.5.4 CURB K AND TYPES B AND C GUARDRAIL. Typical cross-sections showing curb K in combination with type B and type C guardrails are shown on Figure 5-15. Tabulated data for predicting vaulting is given on Tables 5-7 and 5-8 for guardrail types B and C, respectively. Since there is only 1 1/2" difference in elevation in the two rails, the data are somewhat similar. The type B rail is the lower of the two, however, the values for it are slightly higher.

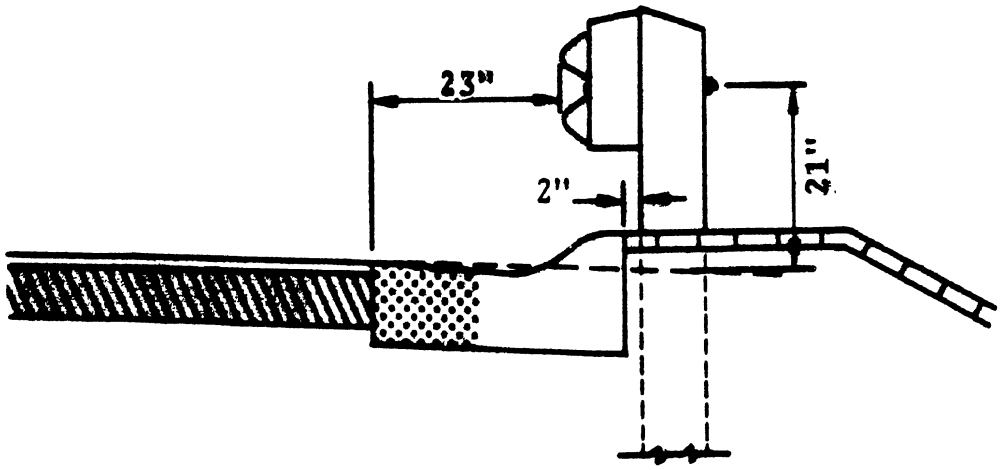

FIGURE 4-13 TYPE B GUARDRAIL WITH CURBS B, OR D

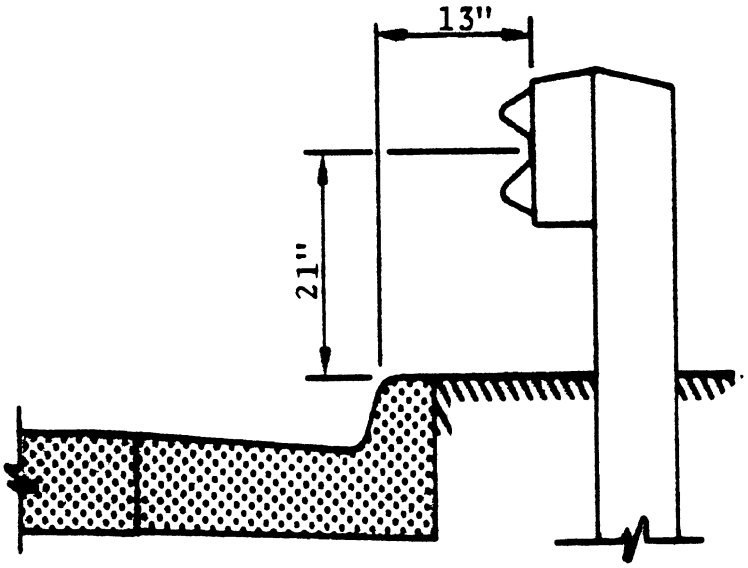

FIGURE 4-14 TYPE B GUARDRAIL WITH CURB C

TABLE 5-4

CURB B AND TYPE B GUARDRAIL

Initial Conditions		C	Max $\dot{\phi}_f/\Lambda$		Vaulting Assessment
V	α		Rail Top	Rail Bottom	
mph	deg	in	27"	15"	
40	25	25	-.15	.31	No Vaulting, or Roll-Over Vaulting
60	10	25	-.09	.19	"
60	25	25	-.19	.44	"
80	10	25	-.12	.27	"

TABLE 5-5

CURB D AND TYPE B GUARDRAIL

Initial Conditions		C	Max $\dot{\phi}_f/\Lambda$		Vaulting Assessment
V	α		Rail Top	Rail Bottom	
mph	deg	in	27"	15"	
40	25	23	-.11	.35	No Vaulting, or Roll-Over Vaulting
60	10	23	-.07	.23	"
60	25	23	-.15	.52	"
80	10	23	-.09	.32	"

TABLE 5-6

CURB C AND TYPE B GUARDRAIL

Initial Conditions		C	Max $\dot{\phi}_f/\Lambda$		Vaulting Assessment
V	α		Rail Top	Rail Bottom	
mph	deg	in	27"	15"	
30	25	30.5	-.07	.25	No Vaulting, or Roll-Over Vaulting
50	10	30.5	-.03	.17	"
50	25	30.5	-.14	.40	"

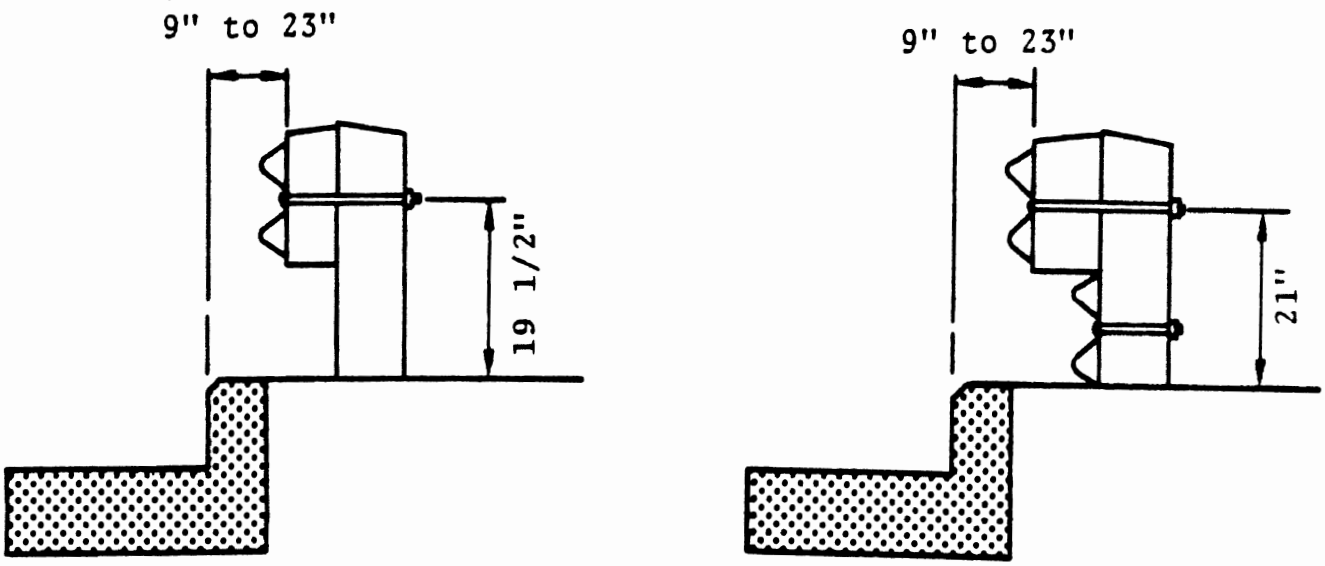

Type B Guardrail

Type C Guardrail

FIGURE 5-15 TYPES BAND C GUARDRAIL WITH CURB K

TABLE 5-7

CURB K AND TYPE B GUARDRAIL

Initial Conditions		C	Max $\dot{\phi}_f/\Lambda$		Vaulting Assessment
V	α		Rail Top	Rail Bottom	
mph	deg	in	25.5"	13.5"	
40	25	42	.01	.40	No Vaulting, or Roll-Over Vaulting
		36	-.03	.35	"
		30	-.03	.35	"
60	10	42	.32	.46	"
		36	.12	.30	"
		30	.06	.26	"
60	25	42	-.11	.53	"
		36	-.13	.48	"
		30	-.17	.42	"
80	10	42	.43	.70	"
		36	.08	.37	"
		30	.01	.29	"

TABLE 5-8

CURB K AND TYPE C RAIL

Initial Conditions		C	Max $\dot{\phi}_f/\Lambda$		Vaulting Assessment
V	α		Rail Top	Rail Bottom	
mph	deg	in	27"	15"	
40	25	42	-.03	.34	No Vaulting, or Roll-Over Vaulting
		36	-.07	.30	"
		30	-.07	.30	"
60	10	42	.30	.45	"
		36	.10	.28	"
		30	.04	.23	"
60	25	42	-.18	.45	"
		36	-.19	.40	"
		30	-.24	.34	"
80	10	42	.40	.67	"
		36	.04	.33	"
		30	-.02	.25	"

The maximum value of $\dot{\phi}_f/\Lambda$ is 0.70, and this occurs for a maximum set back of 42 in. with the impact speed and angle of 80 mph and 10°, respectively. This value indicates no vaulting will occur. There is an indicated trend, however, that suggests vaulting might occur if the set back were on the order of five feet. Therefore, it should be emphasized that a prediction of no vaulting is solely based on an assessment of the indicated design (Figure 5-15) with the specified set back limits. Within these ground rules, curb K in combination with guardrail types B and C can be expected to perform satisfactorily.

5.5.5 CURB B AND THE CONCRETE SAFETY PARAPET. A median cross section showing curb B and the concrete safety parapet is illustrated on Figure 5-16. As mentioned earlier, curb B in combination with the concrete safety parapet was not evaluated by using Equation (5.7). Rather, simulated runs were made with representations of both the curb and the safety parapet. (This was not possible in the case of curb and guardrail combinations.) Only two runs were made, however, since the interaction of the vehicle body with the parapet could not be simulated.

In the many tests that have been made on the New Jersey and General Motors versions of the safety parapet, it has been found that extensive vehicle damage occurs at impact angles larger than about 15°, or 20° (see Figures 4-24). Therefore, simulated impact conditions were limited to cases where only tire-parapet interactions could be expected. In test cases where vehicle damage is excessive (or in any other test case, for that matter) no vaulting has ever been recorded. It can be expected, then, that vehicle body/parapet interaction does not contribute to vaulting.

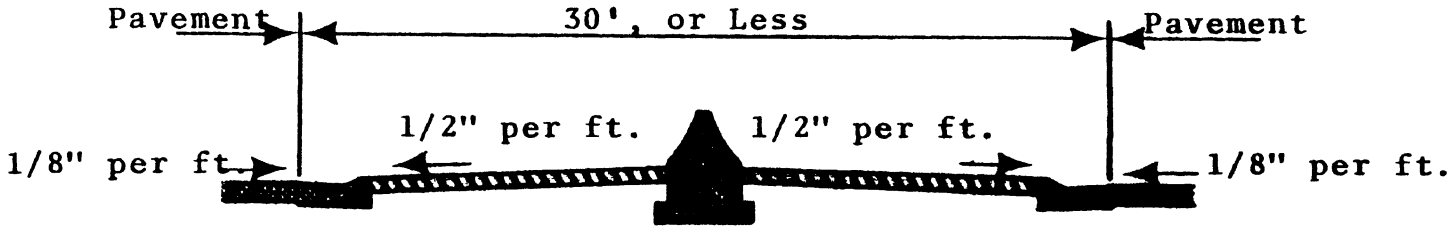

FIGURE 5-16 TYPICAL MEDIAN CROSS SECTION WITH CURB B AND THE CONCRETE SAFETY PARAPET

Finally, since the parapet has been tested extensively, it was further decided to limit the simulation exercises to conditions where testing had not been done. It was found, therefore, that only two sets of impact conditions need by examined—one at 60 mph and 20°, and a second at 80 mph and 10°. Because of program priorities, only one parapet set back distance was considered, however. This may dictate a need for further evaluations at a later time.

A plan view of the 60 mph, 20° case is shown on Figure 5-17. The total median width (pavement edge to pavement edge) is 19 ft. 8 in. (six feet from the back of the curb and gutter section to the front of the parapet face). As indicated, the vehicle is easily redirected. Histories of yaw and roll angle for the run are shown on Figure 5-18, while similar data for acceleration is shown on Figure 5-19. The yaw data confirms that the redirection is relatively smooth (vehicle body crushing forces being absent, however). Roll angle is still increasing at the end of the run with the roll angle at the final time point being about 25°. The roll angular rate is becoming smaller, however, which indicates roll over will not be a problem. Acceleration histories, on the other hand, show modest levels which are well within acceptable tolerance levels.

A similar plan view for the 80 mph, 10° case is shown on Figure 5-20. Again redirection is evident. Yaw and roll data on Figure 5-21 show a smooth redirection and very modest roll angles (<10°). Acceleration data on Figure 5-22 shows a few peaks of significant amplitude, but nothing of a level which is sustained long enough to cause injury. C.G. height data on the

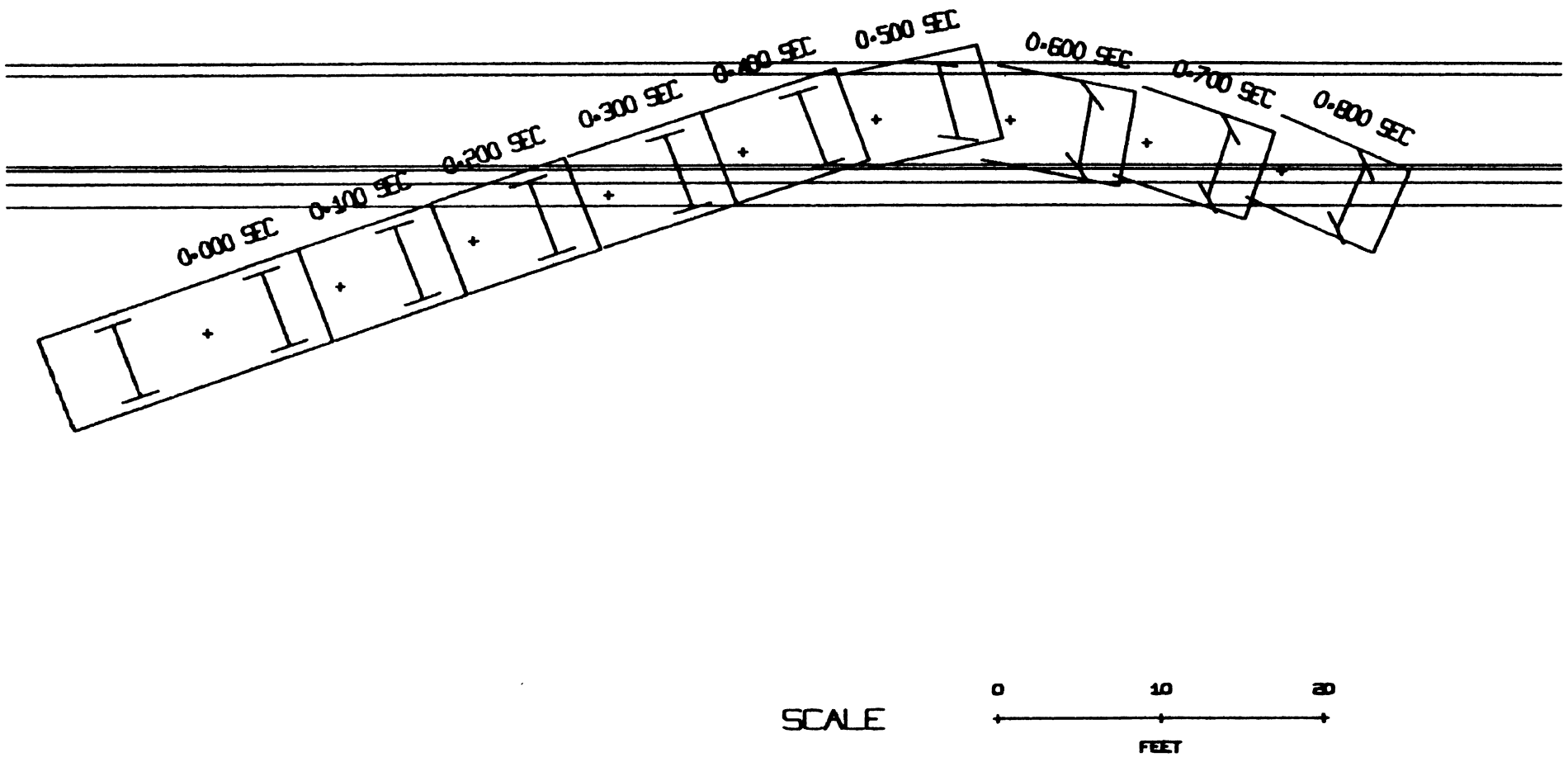

FIGURE 5-17 CONCRETE SAFETY PARAPET WITH CURB AND GUTTER

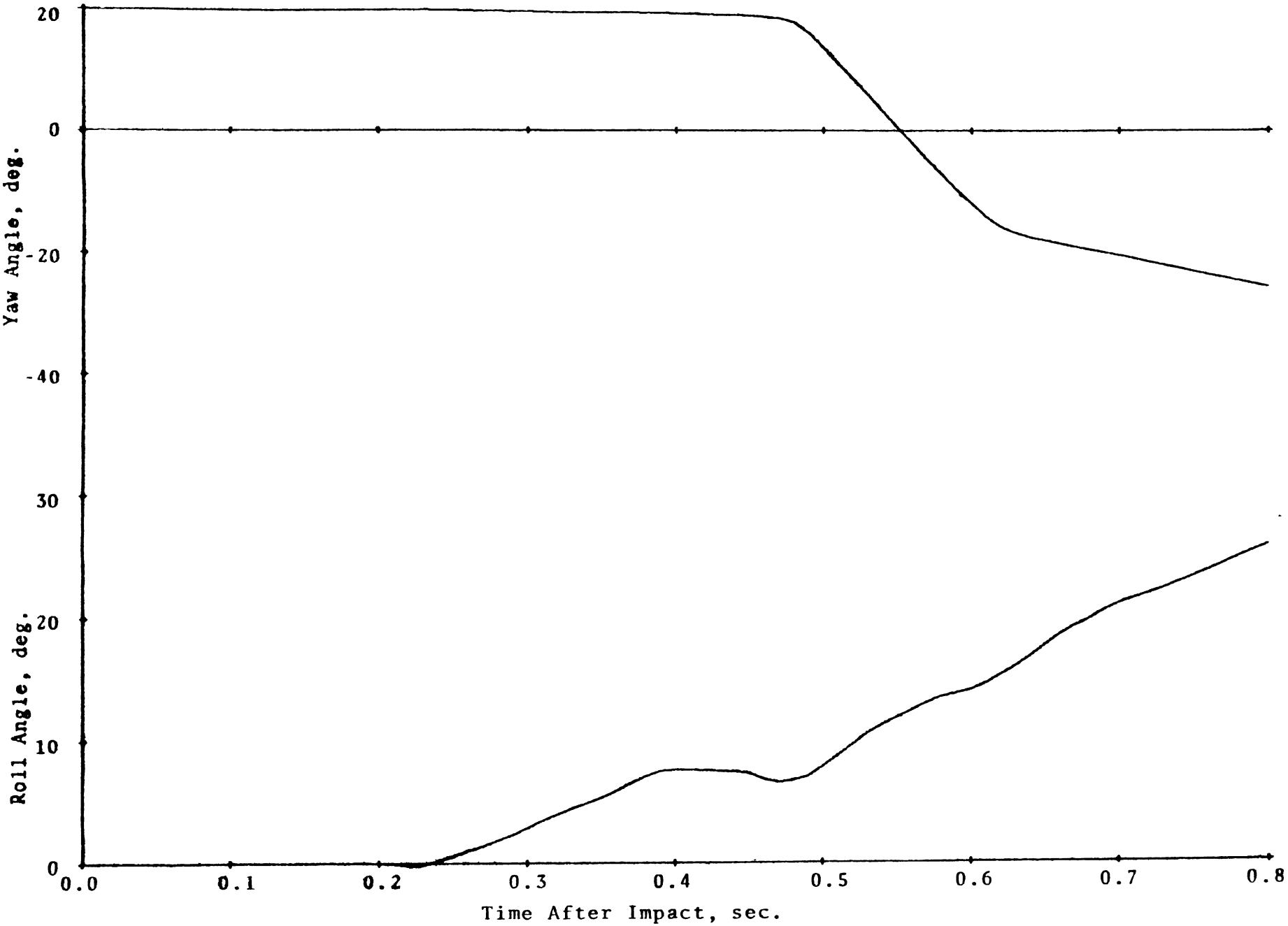

FIGURE 5-18 RUN III-1 - CURB B AND THE CONCRETE SAFETY PARAPET
60 MPH, 20 DEG. - YAW AND ROLL ANGLE HISTORIES

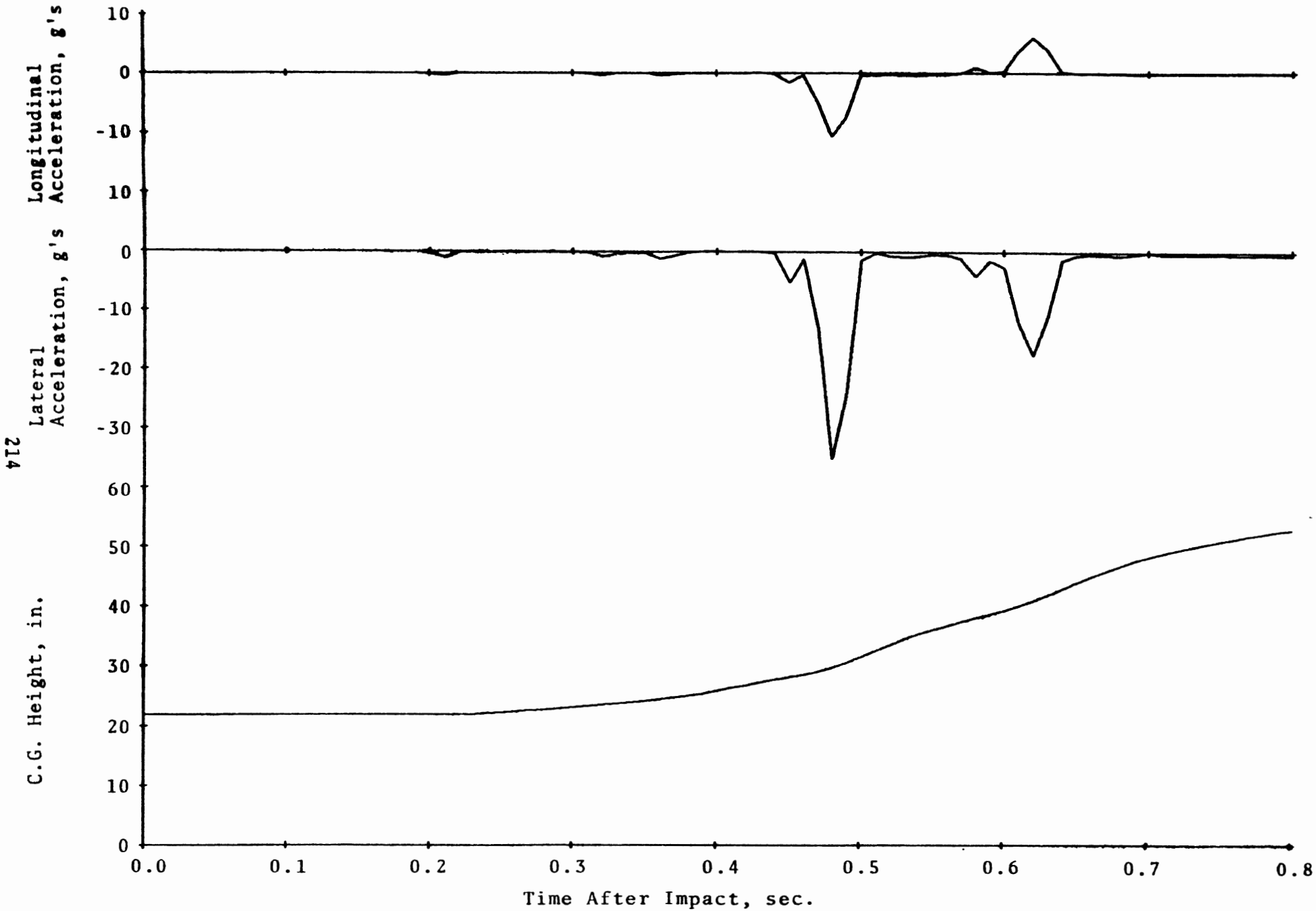

FIGURE 5-19 RUN III-2 - CURB BAAND THE CONCRETE SAFETY PARAPET. 60 MPH, 20 DEG. - ACCELERATION AND C.G. HEIGHT HISTORIES

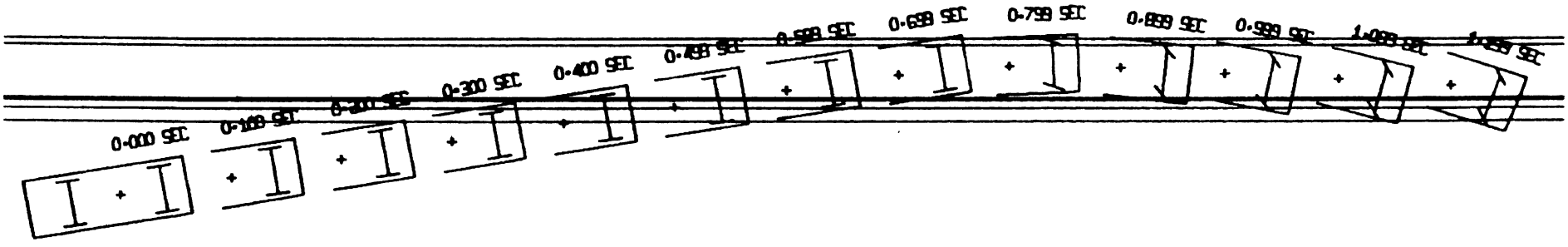

SCALE 0 10 20 FEET

FIGURE 5-20 CONCRETE SAFETY PARAPET WITH CURB AND GUTTER

TEST III-2 - 1963 GALAXIE - 80 MPH - 10 DEG IMPACT - 6 FOOT MEDIAN

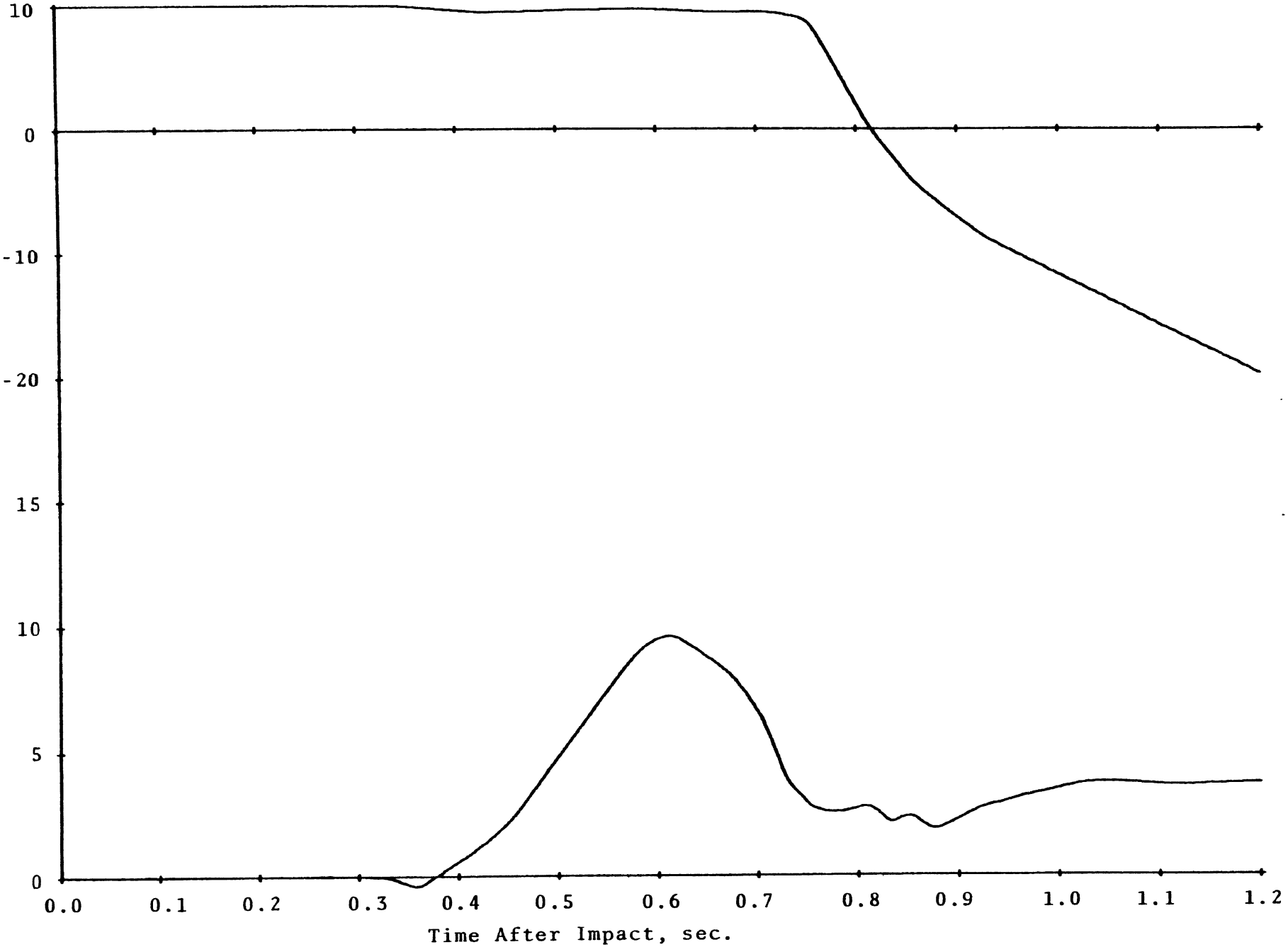

FIGURE 5-21 RUN III-2 - CURB B AND THE CONCRETE SAFETY PARAPET
80 MPH, 10 DEG. - YAW AND ROLL ANGLE HISTORIES

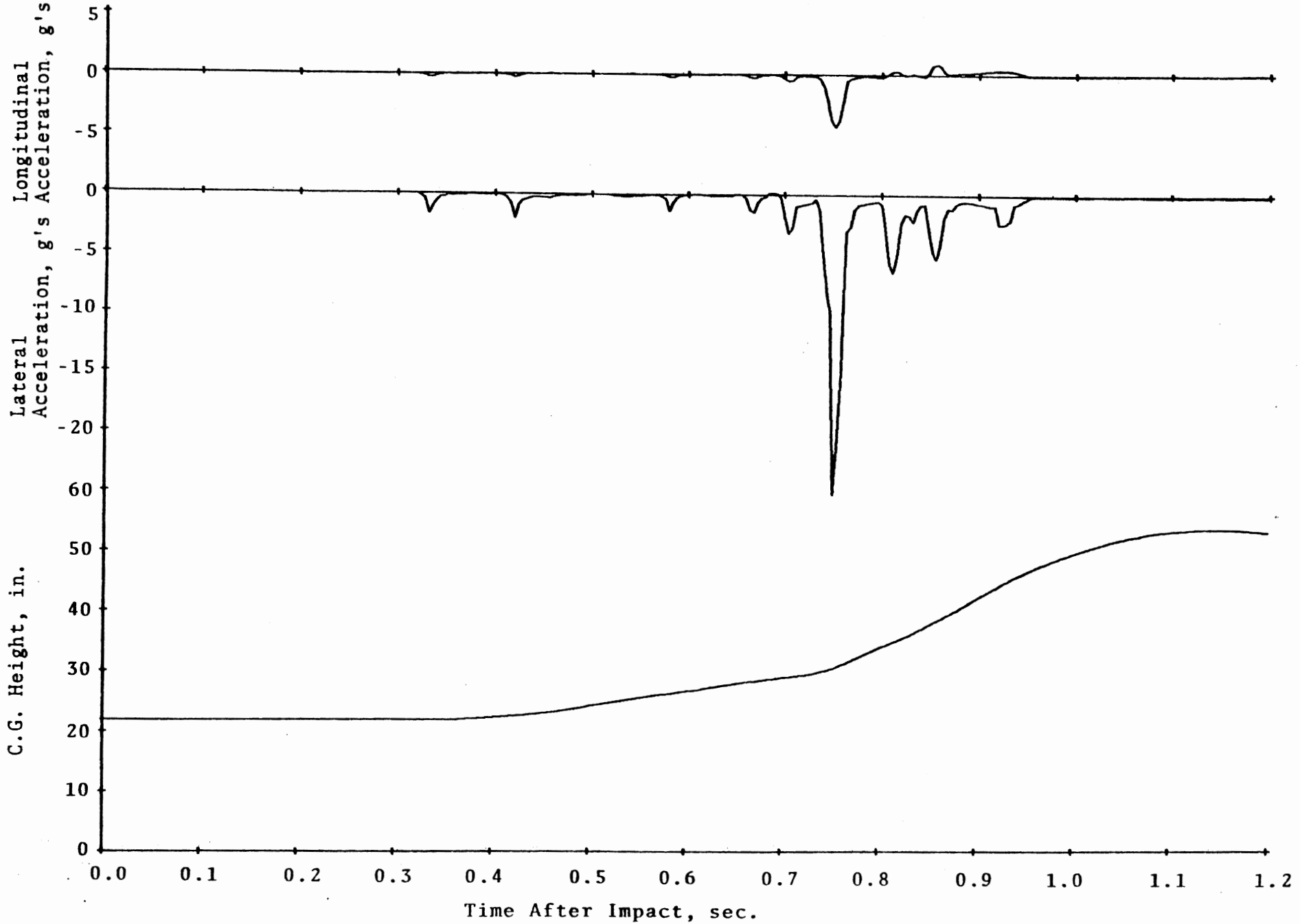

FIGURE 5-22 RUN III-2 - CURB B AND THE CONCRETE SAFETY PARAPET, 80 MPH, 10 DEG. - ACCELERATION AND C.G. HEIGHT HISTORIES

same figure is not as assuring, however, in that the vehicle is past its elevation peak and falling, but is still over two feet about the median deck. Experience with the median dike studies described in Section 6 indicate that the greatest passenger loadings occur when the vehicle strikes the ground after an airborne period. Elevations on the order of two feet do not produce overly adverse passenger loads, however, and therefore indicate satisfactory barrier performance.

5.6 VALIDATION OF RESULTS

The results presented in this section hinge upon the validity of the CALSVA model in simulating vehicle/curb impacts. In order to check simulation validity, a comparison was made between the simulation results and the dynamic jump data obtained from the California curb impact studies made in 1963 [30]. Unfortunately, the only vehicles used in those tests were small sports cars and a 1960 Ford four-door sedan. This latter vehicle weighed 4,318 lb. whereas the 1966 Ford Custom used in the simulation weighs 3,510 lb. The comparison is, therefore, not an exact one, but one which should be representative.

The test and simulation dynamic jump comparison is shown on Figure 5-23. These curves represent the trajectory of a point on the vehicle fender closest to the curb as it crosses a six-inch mountable curb (see Figure 4-5) at 64 mph and 25°. The maximum difference between the two trajectories is about four inches, with the lighter '66 vehicle jumping higher than the '60 model. It is evident, therefore, that the simulation results are within a reasonable tolerance of actual test data. Further, since the simulated vehicle jumps higher, it seems probable that if an

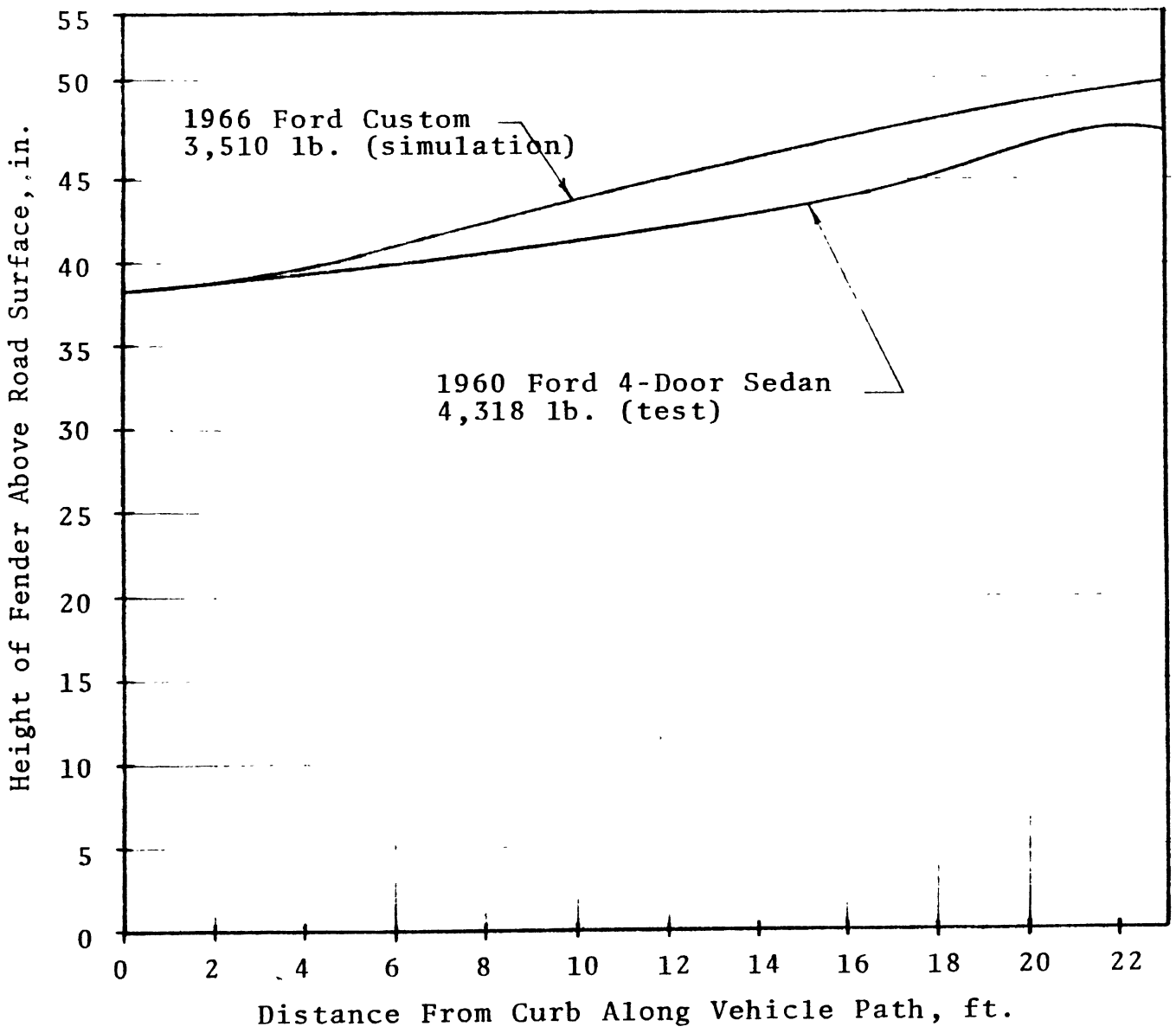

FIGURE 5-23 TEST AND SIMULATION DYNAMIC JUMP COMPARISON

error exists in predicting curb/guardrail vaulting performance, the er
lies in predicting vaulting when none occurs rather than vice versa. Thus, additional evidence is available which suggests the vaulting performance evaluations are conservative.

5.7 CURB/GUARDRAIL COMBINATION DESIGN CONSIDERATIONS

The primary objective in curb/guardrail design is to redirect errant vehicles at least as effectively as the guardrail by itself, but with less vehicle damage. With proper curb design and careful attention to rail set back distance, the test evidence presented in this section and in Section 4.0 suggests that a curb/guardrail combination can act effectively as a two-stage redirection barrier. It would be more efficient than either a curb, or guardrail installed separately.

Design guidelines for a curb/guardrail include considerations of both the curb and guardrail separately as well as their interaction. As before, these are broken down into categories of performance, climate, cost, esthetics, traffic control, and drainage control.

I. Performance

1.-5 Items 1-5 for barrier curbs

6. Guardrail service height shall be compatible with the selected range of the vehicle population which the guardrail is designed to retain. The guardrail shall maintain this height throughout its design deflection range.

7. Guardrail installation height shall be chosen as a function of service height, curb height, and

set back distance according to the following relationships:

a. For each one foot of set back, guardrail height shall be increased five inches to a maximum height of four feet above the pavement surface.

b. For each one inch of curb height over six inches, add one inch of guardrail height for each one foot of set back to the number determined in a., except that the maximum set back considered shall be six feet.

c. For guardrails set back beyond six feet, guardrail height may be reduced one inch for each one foot of set back, to a minimum height of the standard service height above the shoulder surface.

8. Guardrail longitudinal integrity (i.e., resistance to lateral break-through) shall be compatible with the range of impact conditions (i.e., weight, speed, and angle) which exists in the operational environment.

9. Guardrail resistance to deflection shall be compatible with the physical limits dictated by the site and by the resulting loads imparted to the vehicle as manifested in (a) occupant injury, (b) vehicle damage, (c) vehicle redirection into the traffic stream, and (d) driver orientation.

10. The guardrail surface shall be smooth and blocked out so as to prevent wheel snagging. A lower rub rail may, or may not, be required depending on the rail off-set distance.

II. Climate

1. The barrier curb face design shall be chosen such that it does not act as a snow, ice, or dirt accumulation repository.
2. The guardrail shall not act as a snow accumulation fence, nor shall it be easily damaged in snow removal operations.
3. The guardrail functional design shall be such as to minimize variations in performance resulting from seasonal and geographic variations in foundation properties.
4. Curb and guardrail materials shall be chosen such that corrosion, rot, sunlight deterioration and other age and deterioration factors are minimized.

III. Cost

1. Installation and materials costs for both the curb and guardrail shall be kept to a reasonable minimum.
2. The guardrail shall be capable of quick, safe, and easy repairs.
3. Maintenance costs shall be kept to a minimum.
4. Vehicle damage costs shall be kept to a compatible minimum in encounters with the guardrail, and shall be limited to minor body scrapes where the

barrier curb acts as a redirector.

IV. Esthetic

1. The curb/guardrail system shall permit adequate lateral visibility.

2. The curb/guardrail shall have a pleasing appearance.

V. Traffic Control

1. The curb/guardrail shall permit adequate site distance visibility.

2. The barrier curb shall delineate the road edge.

3. The curb/guardrail system shall not be so imposing as to cause the traffic to veer from the road edge and reduce the effective right of way.

VI. Drainage Control

1. The barrier curb shall act as one bank of a channel for surface water run-off.

5.8 CONCLUSIONS AND RECOMMENDATIONS

Curb/guardrail combinations of various varieties have been tested by several organizations. Dynamic jump data has shown the tendency for vehicles to bound into the air following a curb impact. The possibility therefore exists for a vehicle to receive a jump impulse from the curb and vault over the adjacent guardrail. No conclusive evidence of a vaulting problem has been identified as the result of any known test program, however. Further, the conservative analysis of vaulting potential carried out for each of the MDSH curb/guardrail combinations produced no predictions

of vaulting. Therefore, although intuition would suggest that vaulting is a potential problem, this has not proven to be the case. Care should be taken, however, to insure that the height and set back of guardrails installed behind curbs satisfy prescribed minimums. These are delineated as a part of design guidelines and are recommended for operational use.

Current practice is oriented toward not using curbs in front of guardrails [11]. It would seem worthwhile to examine this policy, however, in light of the current findings. The Elsholz curb discussed in Section 4.0 appears to be an efficient redirective device. Seventy percent of the vehicles striking the curb in urban traffic conditions can be expected to be redirected. Vehicle damage in these encounters can be expected to be modest--far less than can be expected if the vehicle were to strike a guardrail. For those vehicles climbing the curb, a secondary retainer is obviously required, however. Thus, the utility of the curb/guardrail combination is evident. It is recommended therefore that further research be initiated to clearly define the performace of the Elsholz curb and to optimize the total redirective performance of this curb in combination with standard guardrail configurations.

6. MEDIAN DIKE INVESTIGATIONS

The median dike investigations described here cover the simulation activities carried on at HSRI during 1970. The work is a preliminary evaluation of the standard dike cross section which is currently installed in the median of many of Michigan's interstate freeways [31]. The evaluation consists of a sensitivity analysis to determine the effect of six parameters on vehicle impact dynamics. The sensitivity analysis was performed as a forerunner to a test program. Design guidelines (preliminary at this stage pending the result of further research) are presented as an aid in developing a more effective dike cross section.

6.1 HISTORICAL REVIEW

Impact evaluation of earth-works has generally been involved with slopes [1, 32] and berms [33, 34]. These are structures which have been and are being considered as traffic control devices. Such devices are in limited use in place of guardrails in the states of Oregon, Ohio, Kentucky, West Virginia, Maryland and Illinois. Their function has been both in decelerating and deflecting vehicles which run off the road.

Dikes are somewhat different from slopes and berms in that their primary function is drainage control rather than vehicle control. As far as can be determined, no tests of specific structures of this type have ever been made. Related tests on various ditch cross-sections have been carried out at the General

Motors Proving Ground [1], but these are only applicable in a general sense.

Simulations of vehicle/dike impacts have recently been reported by the Texas Transportation Institute [35]. These were exercises which were conducted subsequent to the HSRI program and which produced very similar results. For a single impact speed of 60 mph, and for several impact angles and positions on a sloped concrete culvert grate, it was concluded that a maximum safe slope was 1:10. This slope was just at the limit of tolerance for an unrestrained passenger as determined by a "Severity Index" defined by the authors. As will be pointed out in the following, however, 60 mph is more of a median value for impact speed rather than an upper value which should be used for design purposes (see Appendix E). Therefore, it will be concluded here that dike slopes should be even flatter than 1:10.

6.2 DIKE EVALUATION EXERCISES

The dike evaluation exercises consisted of performing a simulation sensitivity analysis. The purpose of the analysis was to determine vehicle dynamic response to several selected vehicle/dike parameters. Ultimately, the objective of the work is to (1) evaluate the existing dike cross section standard [31], and (2) suggest a new standard if the existing one is found to be unsafe. The short term goals of the sensitivity analysis were to (1) determine the parameter sensitivities, (2) establish a base for the eventual correlation of test and simulation results, and (3) define future test and simulation activities.

The sensitivity analysis consisted of a series of simulation runs carried out with the FHWA-CAL Single Vehicle Accident (CALSVA) simulation program (see Appendix A). The sensitivity analysis runs were intended to identify those vehicle and dike parameters which have the greatest influence on vehicle kinematic variables which are related to occupant injury.

In general, the procedure for a sensitivity analysis consists of making variations on a single standard case. The sensitivity of the system to a particular parameter is then determined by varying only that parameter from the standard. This results in a series of straight line (two point) estimates of the true variation for each parameter. Such an analysis can be carried out with a minimum number of simulation runs and can be used for planning a test program and more in-depth simulation activities.

The parameters and their respective values which were used in the sensitivity analysis are listed as follows:

1. Approach velocity: 40 mph*, 80 mph
2. Approach angle: 0°*, 25°
3. Vehicle type: '63 Ford Galaxie four-door eight*, '63 Falcon two-door six
4. Dike approach slope: 1:6*, 1:10
5. Impact position along dike: center*, one wheel on flat - one wheel on dike

---

*Standard case value.

6. Approach profile: flat to dike*, full median profile

7. Soil type: hard-frozen*, soft-moist

Approach velocity and angle values were chosen as the maximum and minimum values from the respective operational distributions of these parameters as indicated in Appendix E. The vehicle types represent standard test vehicles for weight categories of 3,500 pounds and 2,500 pounds. A dike approach slope of 1:6 represents the present standard, while 1:10 is in line with recommendations that have been made in the past by personnel at the General Motors Proving Ground [37]. Impact positions along the dike were chosen to cover both the center and the one-wheel-on-one-end encounters. The flat dike approach was chosen so as to compare it with results from a full median approach profile. It was hoped that differences would be small enough so that the simpler flat approach could be used to reduce the complexity of the extended simulation exercises. The hard-frozen soil was chosen as representing the worst case in terms of vehicle loading whereas the solf-moist soil is typical of conditions in the spring and in low-lying areas.

The simulation exercise program for the specific cases which were examined are shown on Table 6-1. Parameters and variables which were held constant for these runs are:

1. A dike height equal to 18 inches.

2. A horizontal median floor parallel to the roadway.

---

*Standard case value.

TABLE 6-1

DIKE INTERACTION SENSITIVITY ANALYSIS

Simulation Run Program

	Approach Angle	Approach Velocity	Lateral Position	Dike Approach Slope	Soil Type	Approach Profile
(Baseline) 1	0°	40 mph	Center	1/6	Hard, Frozen	Flat to Dike
2	25°	40 mph	Center	1/6	Hard, Frozen	Flat to Dike
3	0°	80 mph	Center	1/6	Hard, Frozen	Flat to Dike
4	0°	40 mph	One wheel on flat, one on dike	1/6	Hard, Frozen	Flat to Dike
5	0°	40 mph	Center	1/10	Hard, Frozen	Flat to Dike
6	25°	40 mph	Center	1/6	Hard, Frozen	Full Median Profile
7	0°	40 mph	Center	1/6	Soft, Moist	Flat to Dike
8	25°	80 mph	Center	1/6	Hard, Frozen	Full Median Profile

3. A fixed steering wheel position.
4. An unpowered vehicle
5. Up to 75 parameters defining the vehicle's dynamic properties.

A set of drawings defining the full median profile are shown on Figure 6-1 [31, 38].

Criteria for evaluating the dike cross section were based on occupant safety, since as indicated earlier, the primary criteria for drainage control efficiency translates to a minimum dike height dimension. This was accomplished by correlating occupant safety with the time histories of injury-related kinematic variables as the vehicle contracts the dike. The specific criteria used are discussed in Appendix E.

Vehicle center of gravity (C.G.) height was also used as an evaluation criterion inasmuch as this is an indicator of the vehicle path.

6.3 RESULTS

The results of the study are presented in two ways. Kinematic data for several selected runs are shown in Figures 6-2 through 6-6. Comparative data for all cases is given in Tables 6-2 through 6-7.

6.3.1 KINEMATIC DATA. Kinematic data for five of the nine cases is shown on Figures 6-2 through 6-6. These were cases 1, 3, 6, 8 and 9. These cases were considered to be the most

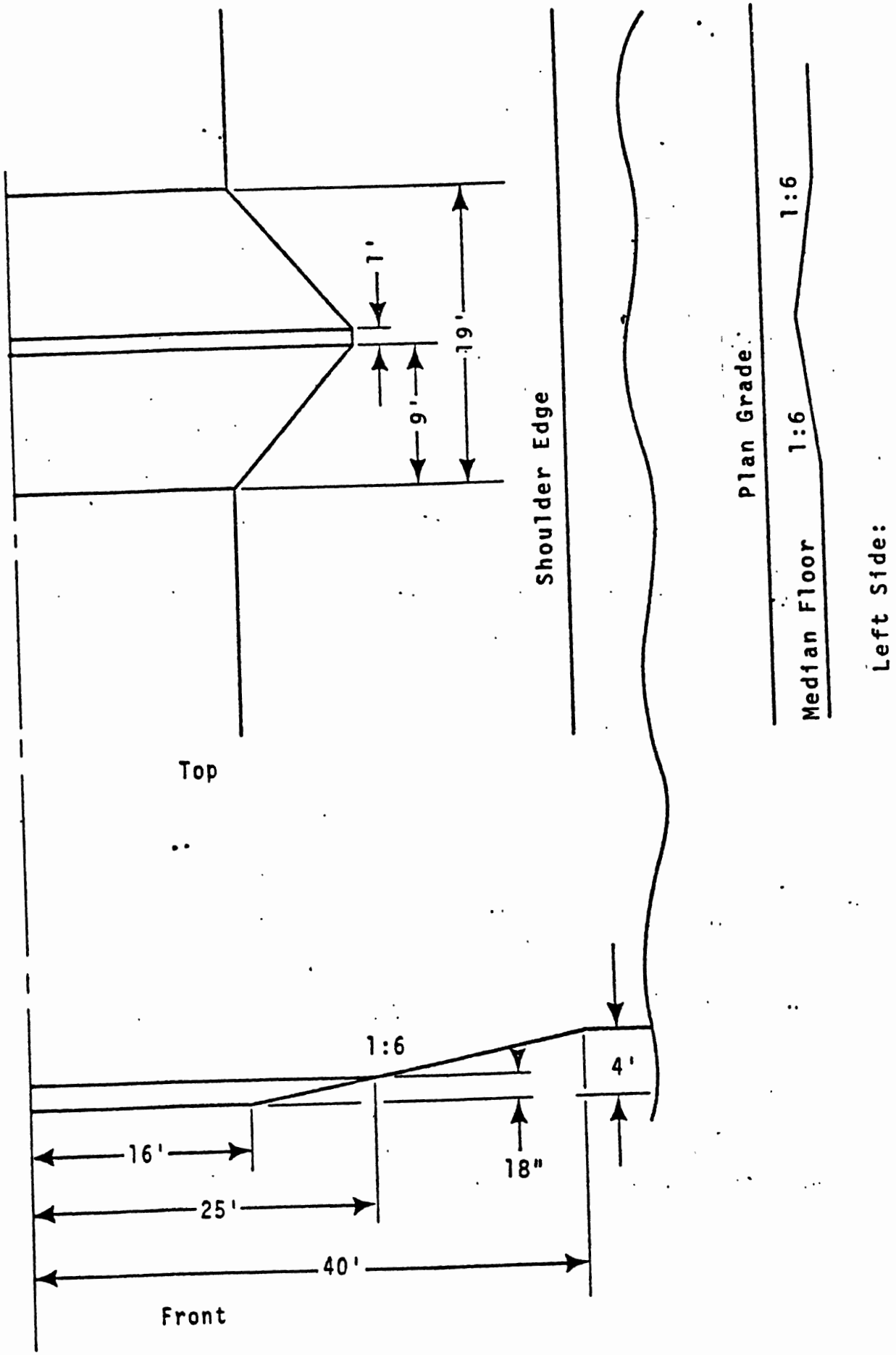

FIGURE 6-1. BASIC MEDIAN PROFILE WITH 1:6 DIKE

interesting and informative and in the interest of brevity were selected as representative of the entire group.

6.3.1.1 Case 1. Kinematic data for case 1, the baseline, is shown on Figure 6-2. The conditions for the run are listed in Table 6-1 and are shown on the figure. The variable histories shown are for vertical acceleration, vertical velocity, and C.G. height. C.G. height is measured with respect to the earth, with zero corresponding to the at rest C.G. position. The acceleration and velocity variables are measured with respect to a body fixed coordinate system. Therefore, the term "vertical" is not strictly correct but refers to a nominally vertical direction.

The arrows attached to the vehicle C.G. height time points represent the vehicle pitch attitude. For convenience, the dike profile was also shown on this trace. It is actually about 22 inches below the indicated height since the at rest C.G. position is taken as zero. Also, the dike profile is distorted since the vertical scale is in inches while the horizontal scale is in feet.

In examining the data, it can be noted that the vehicle flies into the air a maximum height of about five feet following initial contact with the dike. The vehicle pitch angle reaches an upper value of about 16° during this time.

The peak acceleration of about 17 g's occurs at the landing point following the initial airborne phase. This acceleration is the peak of a fairly narrow spike, however. Average acceleration during the 100 msec. interval between the time marks within

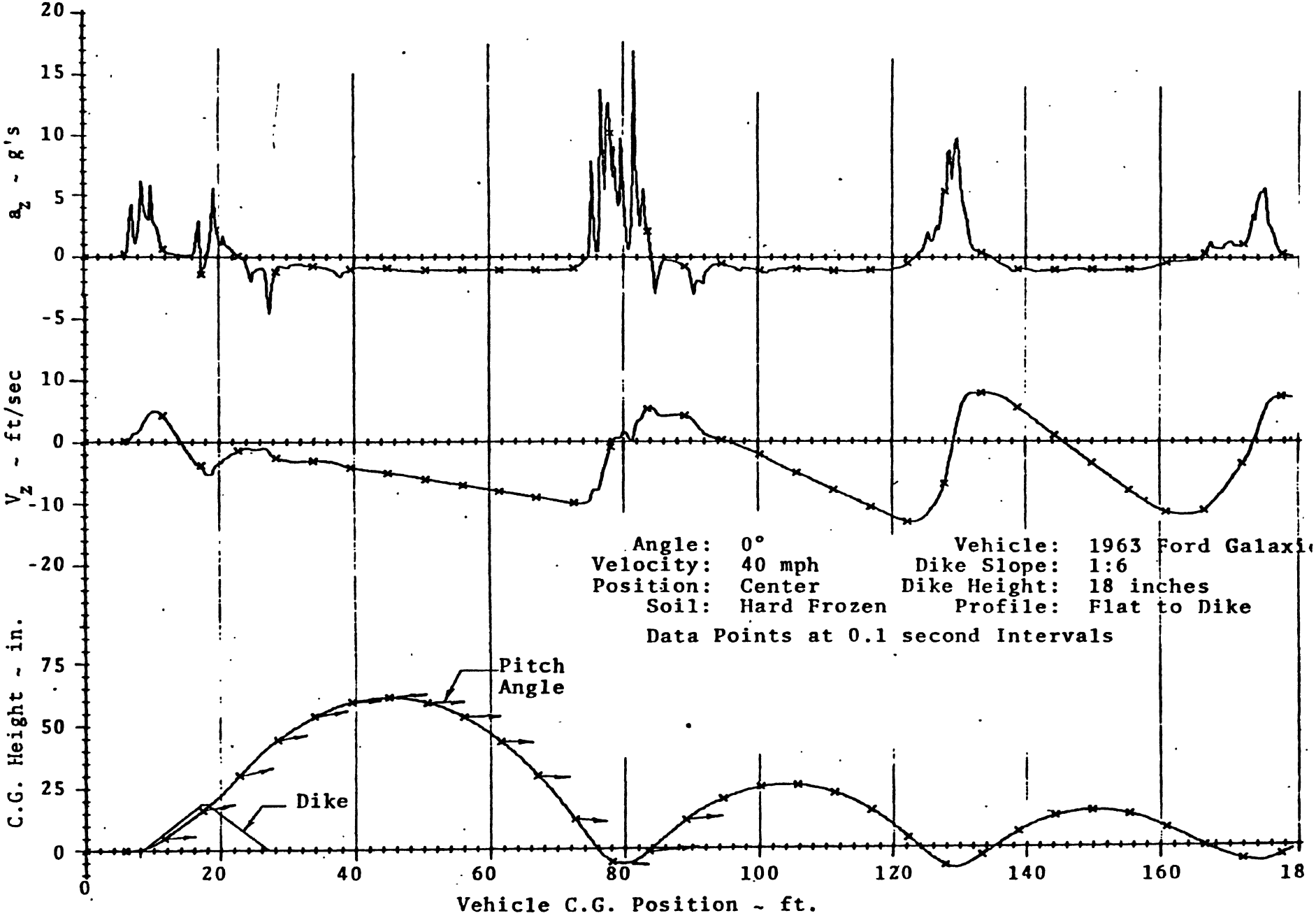

FIGURE 6-2. CASE #1 KINEMATIC DATA

120 msec interval. This change occurs at the initial landing when the vehicle strikes the ground and rebounds into the air. The veolcity is not entirely vertical during this time, since it is measured with respect to a coordinate system fixed in the car. Large pitch angles of the vehicle tend to complicate the situation, with the result that some of the velocity change is a component of forward velocity. The vehicle attached coordinate system is realistic relative to passenger attitude, however. Therefore, the passenger feels these velocity changes through a reorientation of his motion with respect to the vehicle interior. Needless to say, this magnitude of velocity change would very probably cause injury.

6.3.1.3 Case 6. Case 6 kinematic data is shown on Figure 6-4. Case 6 differs from case 1 in that the dike slope is 1:10, rather than 1:6.

In this case, the vehicle travels less than three feet into the air following initial dike contact. The maximum pitch angle is about10° downward at the first landing point.

Maximum acceleration occurs at the initial landing point, and this is about 9 g's. Average acceleration is about 6 g's for an interval of 70 msec surrounding the maximum peak. This should have little effect on vehicle occupants.

Maximum ΔV is about 10 ft/sec and this occurs at the initial landing. This also is not considered hazardous.

6.3.1.4 Case 8. Case 8 differs from the baseline in that

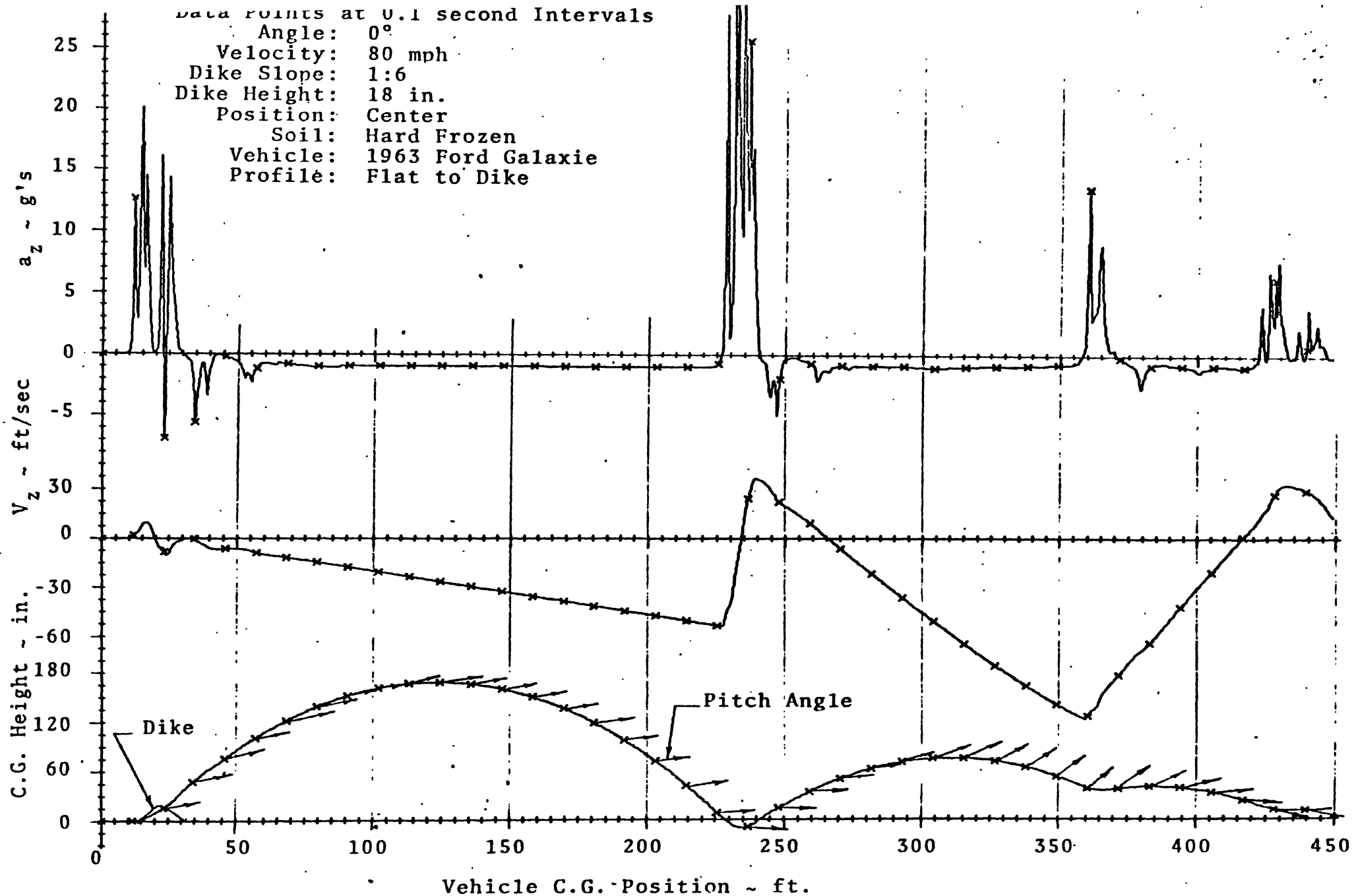

FIGURE 6-3. CASE #3 KINEMATIC DATA

120 msec interval. This change occurs at the initial landing when the vehicle strikes the ground and rebounds into the air. The veolcity is not entirely vertical during this time, since it is measured with respect to a coordinate system fixed in the car. Large pitch angles of the vehicle tend to complicate the situation, with the result that some of the velocity change is a component of forward velocity. The vehicle attached coordinate system is realistic relative to passenger attitude, however. Therefore, the passenger feels these velocity changes through a reorientation of his motion with respect to the vehicle interior. Needless to say, this magnitude of velocity change would very probably cause injury.

6.3.1.3 Case 6. Case 6 kinematic data is shown on Figure 6-4. Case 6 differs from case 1 in that the dike slope is 1:10, rather than 1:6.

In this case, the vehicle travels less than three feet into the air following initial dike contact. The maximum pitch angle is about10° downward at the first landing point.

Maximum acceleration occurs at the initial landing point, and this is about 9 g's. Average acceleration is about 6 g's for an interval of 70 msec surrounding the maximum peak. This should have little effect on vehicle occupants.

Maximum ΔV is about 10 ft/sec and this occurs at the initial landing. This also is not considered hazardous.

6.3.1.4 Case 8. Case 8 differs from the baseline in that

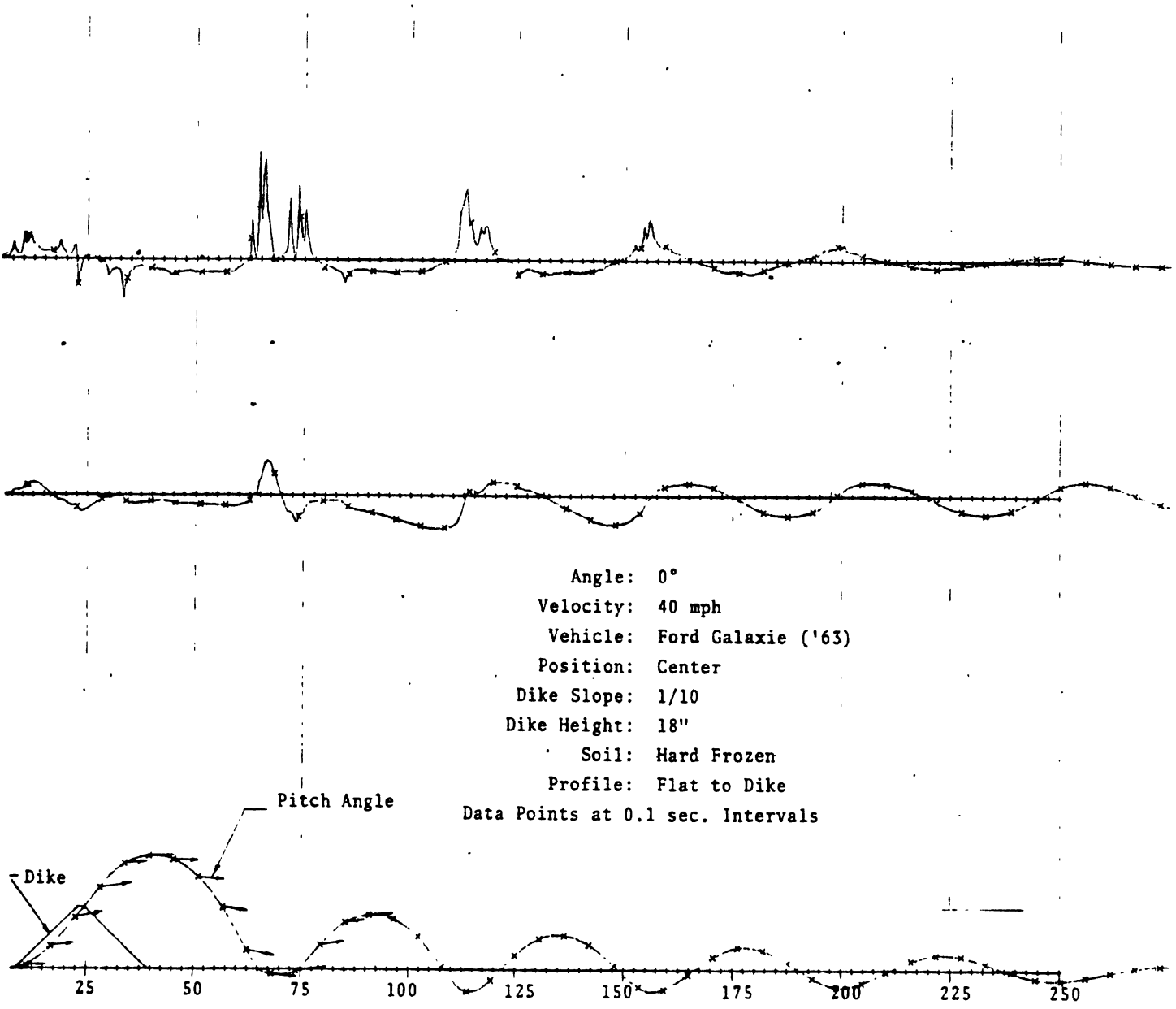

FIGURE 6-4. CASE #6 KINEMATIC DATA

the soil was made substantially softer. Under quasi-static conditions, the vehicle sinks in about eight inches. Kinematic data for case 8 is shown on Figure 6-5.

Following initial contact with the dike, the vehicle rises about three feet into the air. The vehicle never leaves the surface after this, however. Maximum pitch attitude is about 14° upward.

Maximum deceleration again occurs at the initial landing, but this is under 5 g's. The average deceleration during the 50 msec interval surrounding the peak is about 3 g's. These are modest values relative to passenger injury.

Maximum ΔV is 13 ft/sec over an interval of 360 msec. This also is quite modest and should produce no passenger injury.

6.3.1.5 Case 9. Case 9 differs from case 1 in that the vehicle approaches the dike at an angle of 25° over a full median profile (i.e., starting from the roadside, on over the median bank, and onto the dike). In addition, the vehicle is traveling at 80 mph. The results are shown on Figure 6-6.

As indicated, the vehicle is initially on the shoulder of the road, four feet about the central median surface. Since the vehicle is approaching the dike from an angle, the right front wheel hits first. This induces a rolling motion. As the vehicle mounts the dike and flies into the air, the rolling motion causes the vehicle to completely turn over. A logic decision in the simulation then terminates the run. At this time, the

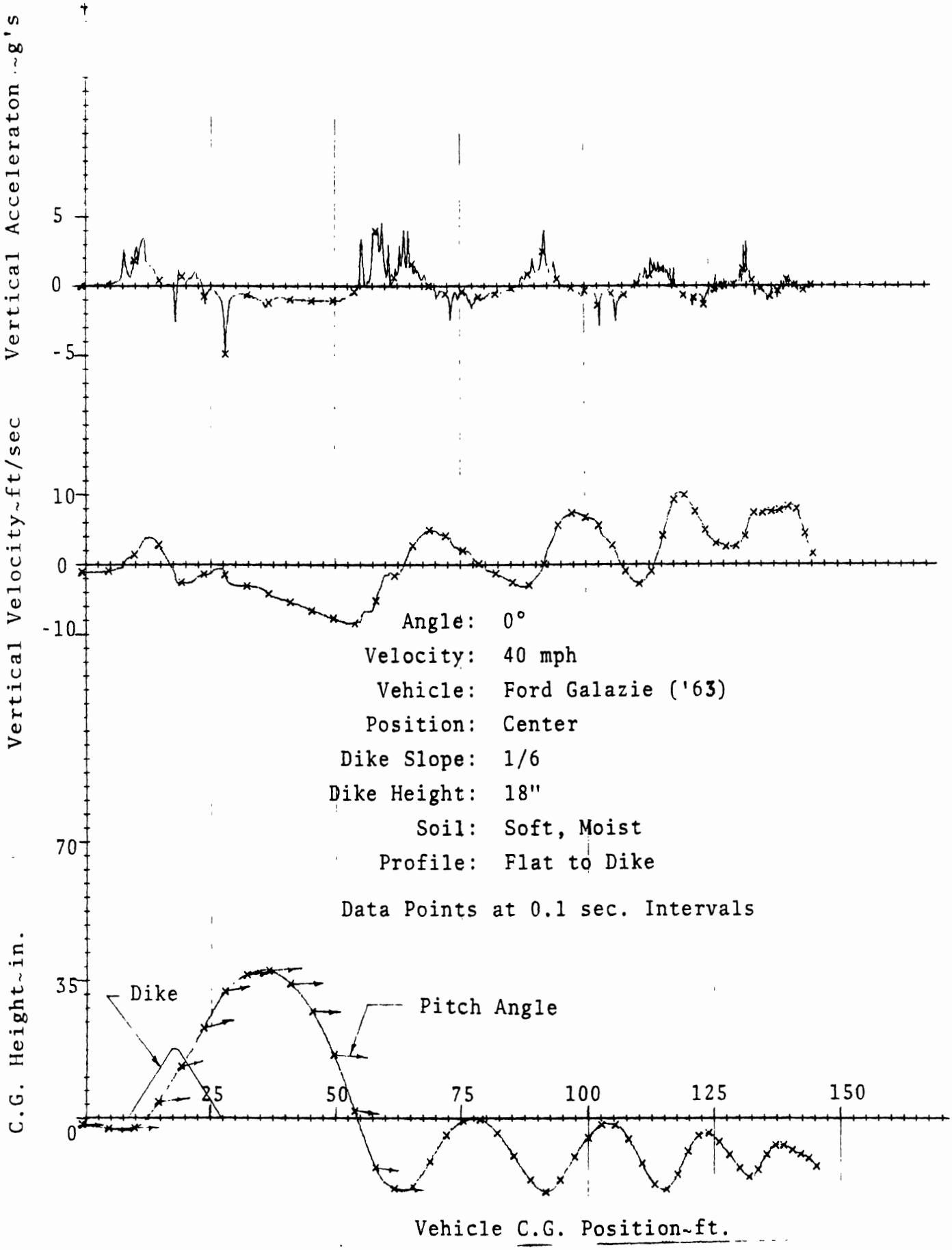

FIGURE 6-5. CASE #8 KINEMATIC DATA

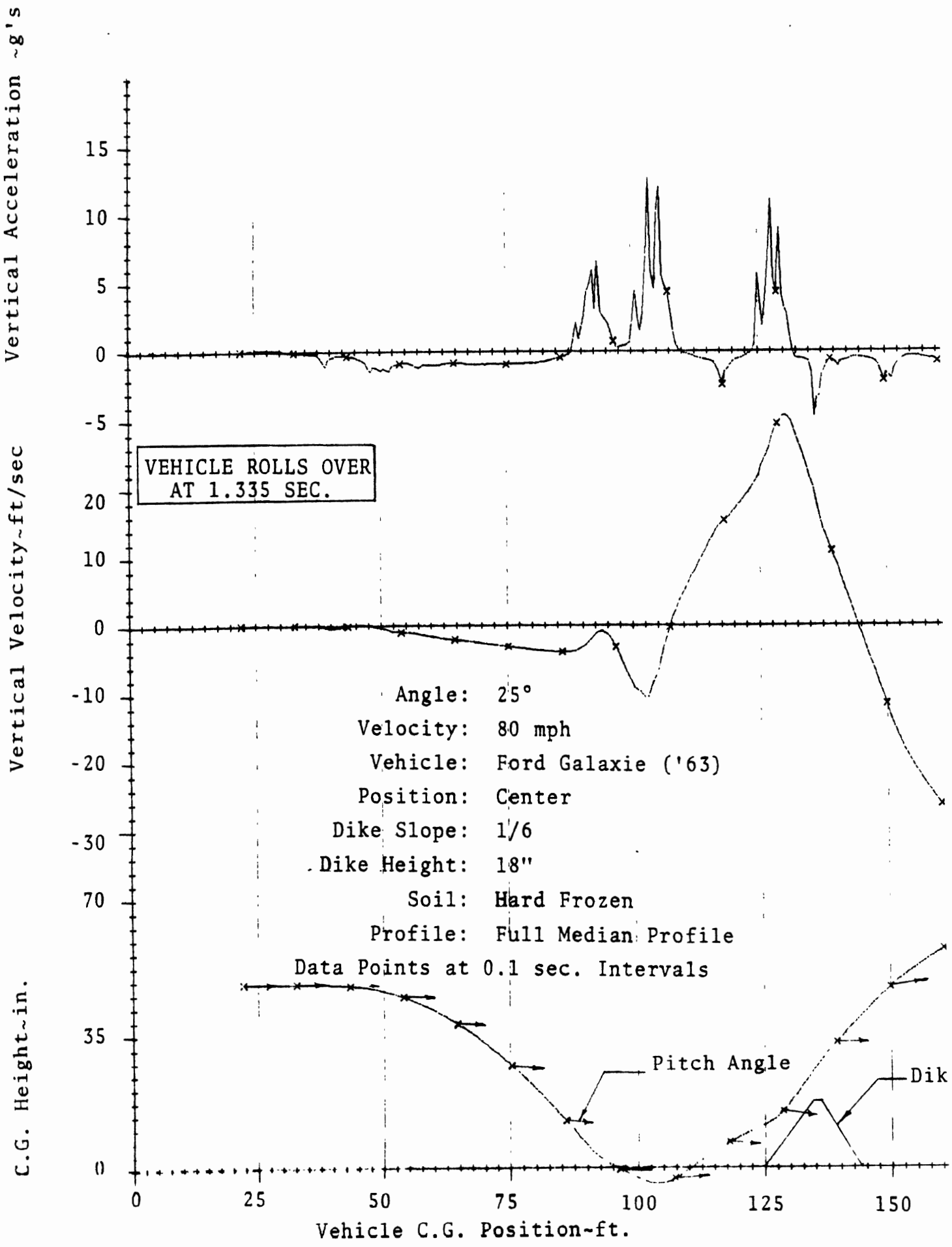

FIGURE 6-6. CASE #9 KINEMATIC DATA

vehicle is about five feet above the median surface and still rising. The maximum pitch angle is about 19°.

Since the simulation was stopped while the vehicle was airborne, maximum calculated accelerations occur at the take-off point. The peak is about 13 g's while the average during the 40 msec interval surrounding the peak is about 9 g's. These loads would probably not injure a vehicle occupant, but subsequent loads during landing undoubtedly would.

Maximum changes in velocity were calculated to be 59 ft/sec vertically over 330 msec, and 34 ft/sec laterally over 230 msec. Both of these are in the range of possible passenger injury in a secondary collision with the vehicle interior.

6.3.2 COMPARATIVE DATA. The sensitivity of the vehicle/dike system to a particular parameter was estimated by comparing the variation of selected evaluation measures as the parameter was varied. The measures were maximum vertical acceleration, maximum vertical velocity change and maximum C.G. height. The first two were compared with the threshold levels given in Table E-4 as a means of estimating occupant injury.

6.3.2.1 Angle Effect. The effect of varying the approach angle to the dike is given in Table 6-2. Cases 1 and 2 are compared, with approach angles of 0° and 25°, respectively. Interestingly, case 1 shows larger acceleration and greater C.G. movement whereas case 2 shows greater velocity change. The effects are due to the roll motion inherent in case 2, and tend to suggest that impact

angle has a sizeable effect on vehicle kinematics. Results in both cases are in the range of possible passenger injury.

TABLE 6-2

APPROACH ANGLE EFFECT ON VEHICLE DYNAMICS

Case	V	α	$a_{z_{max}}$	$\Delta V_{z_{max}}$	z_{max}
1	40 mph	0°	16.9 g's	21.2 ft/sec	60.9 in
2	40 mph	25°	9.9 g's	34.8 ft/sec	50.5 in

6.3.2.2 Approach Velocity Effect. The effect of approach velocity on the vehicle/dike system is shown on Table 6-3. Two sets of runs are compared with velocities of 40 mph and 80 mph. One set is for a 0° impact angle (cases 1 and 3), while the other is for a 25° angle with a full median approach profile (cases 6 and 8).

Examining the 0° approach angle first, one can observe that there are marked increases in all three measurements when the speed is increased from 40 mph to 80 mph. Passenger injury is virtually certain for the 80 mph case.

One could get a different impression from the 25° approach angle data, however, since the increases here are not nearly as great. Except for the C.G. height, this can be explained by the fact that the case 8 (V=80 mph, α=25°) run was terminated just after impact with the dike, when the vehicle had rolled over on its side. Therefore, the acceleration and ΔV_z values are

not strictly comparable. Each of these would undoubtedly have been higher had the run continued. C.G. height is fairly representative, however, since the vehicle appeared to be near maximum height at the termination point.

Approach velocity has a large effect on all measures, then, except perhaps for C.G. height at high approach angles. In the latter case, much of the energy which would normally cause the car to fly into the air is converted to roll motion.

TABLE 6-3

APPROACH VELOCITY EFFECT ON VEHICLE DYNAMICS

Case	V	α	Approach Profile	$a_{z_{max}}$	$\Delta V_{z_{max}}$	z_{max}
1	40 mph	0°	Flat	16.9 g's	21.2 ft/sec	60.9 in
3	80 mph	0°	Flat	30.3 g's	72.6 ft/sec	168.1 in
6	40 mph	25°	Full Median	8.2 g's	17.8 ft/sec	50.4 in
8	80 mph	25°	Full Median	12.7 g's	59.3 ft/sec	59.1 in

6.3.2.3 Lateral Position Effect. The effect of impact position along the dike is shown in Table 6-4. Cases 1 and 4 are compared. For case 1, the vehicle was directed toward the center of the dike, while in case 4 the vehicle was positioned along the median side slope such that one wheel went over the dike while the other just missed. The height of the dike under the traversing wheel was about ten inches.

From Table 6-4, it is quite clear that there is a dramatic decrease in vehicle loading for the off-center impact. Kinematic values are negligible by comparison. This indicates that position along the dike has a considerable effect on vehicle kinematics.

TABLE 6-4

LATERAL IMPACT POSITION EFFECT
ON VEHICLE DYNAMICS

Case	V	α	Lateral Position	$a_{z_{max}}$	$\Delta V_{z_{max}}$	z_{max}
1	40 mph	0°	Center	16.9 g's	21.2 ft/sec	60.9 in
4	40 mph	0°	One Wheel Flat, One On Dike	1.6 g's	2.8 ft/sec	4.8 in

6.3.2.4 Dike Approach Slope. The system sensitivity to dike approach slope is given in Table 6-5. Data for cases 1 and 5 are shown, while slopes of 1:6 and 1:10, respectively, are compared. In each case, values of acceleration, ΔV_z, and C.G. height for the 1:10 case are roughly half those for the 1:6 case. Whereas the 1:6 slope might cause injury, the 1:10 slope would probably not. Dike slope is an important factor, then, in vehicle/dike interaction.

TABLE 6-5

DIKE APPROACH SLOPE EFFECT
ON VEHICLE DYNAMICS

Case	V	α	Approach Slope	$a_{z_{max}}$	$\Delta V_{z_{max}}$	z_{max}
1	40 mph	0°	1:6	16.9 g's	21.2 ft/sec	60.9 in
5	40 mph	0°	1:10	9.0 g's	10.4 ft/sec	33.4 in

6.3.2.5 Soil Effect. The effect of soil variation on the system in indicated in Table 6-6. Cases 1 and 7 are compared. Evidently, soft soil causes a substantial reduction in vehicle acceleration and velocity change — in effect, altering the injury probability from likely to unlikely. The soil is quite soft, however, with the vehicle sinking in up to eight inches at highway speeds.

As indicated earlier, the soft soil model used in the simulation is strictly an intuitive one. Both theoretical and experimental work are required to develop a truly valid high speed soil model, and this has not been done. The model appears to be representative, however, and as a minimum, gives an indication of the attenuating benefits of softer soil.

Soil is therefore an important factor relative to vehicle kinematics.

TABLE 6-6

SOIL EFFECT ON VEHICLE DYNAMICS

Case	V	α	Soil Type	$a_{z_{max}}$	$\Delta V_{z_{max}}$	z_{max}
1	40 mph	0°	Rigid	16.9 g's	21.2 ft/sec	60.9 in
7	40 mph	0°	Soft, Moist	4.9 g's	13.0 ft/sec	47.6 in

6.3.2.6 Median Profile Effect. Cases 2 and 6 are for the same conditions, except that case 2 involves a flat approach to the dike while in case 6 the vehicle approaches over the full median profile. The approach angle in each case is 25°. Comparative data are given in Table 6-7.

Peak accelerations are slightly less for the full median case, while the maximum change in velocity is substantially less. Lower values for the full median case are due to the roll attitude of the vehicle as it travels down the median slope. Since the vehicle is approaching the dike at an angle, one front wheel strikes the dike before the other and this causes an initial rolling motion. The vehicle is already rolled by virtue of its traveling down the median slope, however, and the induced roll is less. Resulting impact loads on the front tire are also less. Although the difference in ΔV_z values is substantial, the general agreement is closer than any of the other cases.

TABLE 6-7

MEDIAN PROFILE EFFECT ON VEHICLE DYNAMICS

Case	V	α	Approach Profile	$a_{z_{max}}$	$\Delta V_{z_{max}}$	z_{max}
2	40 mph	25°	Flat	9.9 g's	34.8 ft/sec	50.5 in
6	40 mph	25°	Full Median	8.2 g's	17.8 ft/sec	50.4 in

6.4 DIKE DESIGN GUIDELINES

The two main considerations in median dike design are safety and drainage control. Unlike many other situations, optimizing a dike design for safety need not compromise its drainage control efficiency. This is because the primary drainage control requirement translates to a minimum dike height dimension. Therefore, given a minimum height constraint, the controlling factors in dike design are occupant safety oriented. The performance design guidelines which follow are therefore centered on safety. Considerations relating to climate, costs, esthetics, traffic control, and drainage control are also included.

I. Performance

1. Dike cross section slopes and those of the adjacent median banks shall be chosen such that vertical motions imparted to the vehicle are minimized. At this writing, slopes of about 1:12 are the steepest acceptable.
2. Slope changes in the dike cross section and adjacent median shall be gradual and shall not induce contact

with the vehicle undercarriage.

3. Dike material shall be chosen to promote wheel sinkage, but not to the point where the vehicle is immobilized or steering is obviated. This will enhance vehicle containment within the median and generally reduce passenger impact loads.

II. Climatic

1. Dike placement shall be chosen to enhance the possibility of moist soil occurring regularly.

III. Cost

1. Vehicle damage shall be limited to minor body scraping.

IV. Esthetics

1. The dike shall present a pleasing finished appearance.
2. The dike shall assist in the orderly development of the roadside.

V. Traffic Control

1. The dike shall not give the appearance of being a median cross-over so as to encourage vehicle use for this purpose.

VI. Drainage Control

1. Dike height shall be chosen consistent with site drainage control requirements.

6.5 CONCLUSIONS AND RECOMMENDATIONS

The sensitivity analysis has shown that most of the vehicle/dike parameters investigated have a marked influence on vehicle dynamics.

It also seems clear that, due to the general non-use of seat belts, the standard dike profile, with 1:6 approach slope, is unsafe. Indeed, a casual examination of several dike installations indicates that dikes in general are rather non-standard and that many have steeper slopes than 1:6. Thus, the problem is an acute one. Specific conclusions are listed as follows:

1. Possible injury to unrestrained passengers is indicated at all speeds above 40 mph when a vehicle strikes the middle of a dike similar to the current Michigan standard.
2. Approach velocity, angle, impact position, dike slope, and soil type have sizable effects on vehicle kinematics. Dike approach profile has a lesser effect.
3. An impact velocity of 80 mph produces about twice the passenger loading that is experienced at 40 mph.
4. Striking the dike in the middle is far more traumatic than hitting off to one side. This suggests that the hazardous portion of the dike may be limited to a relatively narrow region.
5. Striking a 1:10 slope reduces passenger loadings by a factor of about one-half when compared to a 1:6 slope.
6. Soft moist soil attenuates passenger loading on the order of 50%, when compared with rigid terrain.
7. Approaching the dike from the road shoulder appears to be less traumatic than approaching from a flat surface.

These conclusions are, of course, subject to verification by

full-scale test and by further simulation activities.

A recommended test program is given in Table 6-8. The purpose of the tests will be to insure that the simulation model adequately represents the actual dynamic interaction of a vehicle with a dike. An ancillary task in connection with the recommended test series includes the construction of a dike test site.

Following completion of the correlation test series, an expanded simulation exercise program is recommended. At this point, it is expected that the simulations will correlate adequately with the test results and that these simulation exercises will be the primary evaluation tool, thereafter. The objective of these exercises will be to define a dike cross-section which is optimum both from the standpoint of highway safety and for drainage control. Any testing that takes place during these exercises will be to insure continued validity of the simulation program. This promises to be a most economical and fruitful approach.

An output of the recommended study will include, but not be limited to, a set of curves giving the relationship between dike height and approach slope, for various levels of passenger loading (in this case, $\Delta V_{z_{max}}$). An example is shown on Figure 6-8. The curves on the figure show constant levels of $\Delta V_{z_{max}}$ which occur as a function of dike height and approach slope parameters. These represent selectable boundaries of safe design. The arbitrary boundary indicated signifies that dike parameter combinations to the left are unsafe whereas those to the right

TABLE 6-8

PROPOSED DIKE CORRELATION VALIDATION TEST SERIES

Test	Velocity	Angle	Position	a	b	c	d	e
1	40 mph	0°	Center	108"	12"	18"	18"	108"
2	80 mph	25°	Center	108"	12"	18"	18"	108"
3	40 mph	25°	One Wheel On, One Wheel Off	108"	12"	18"	18"	108"
4	40 mph	0°	Center	180"	12"	18"	18"	180"
5*	40 mph	0°	Center	108"	12"	18"	18"	108"

*Soft, moist soil

The letters a, b, c, d, and e are identified on Figure 6-7 below.

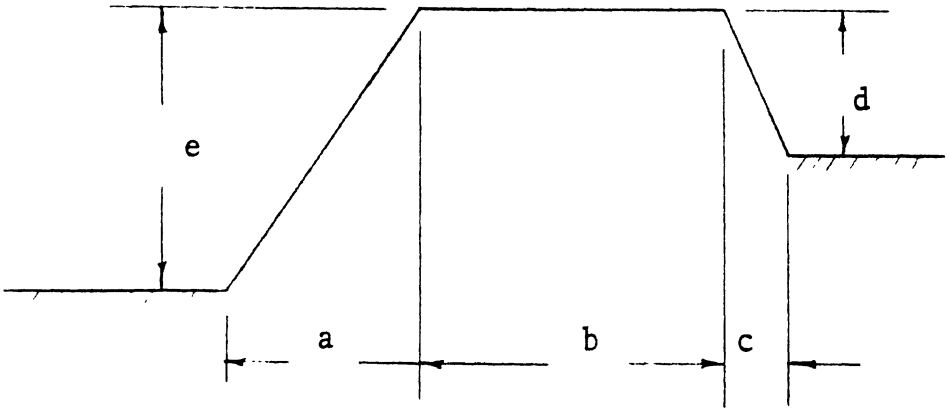

FIGURE 6-7. DIKE GEOMETRY PARAMETERS

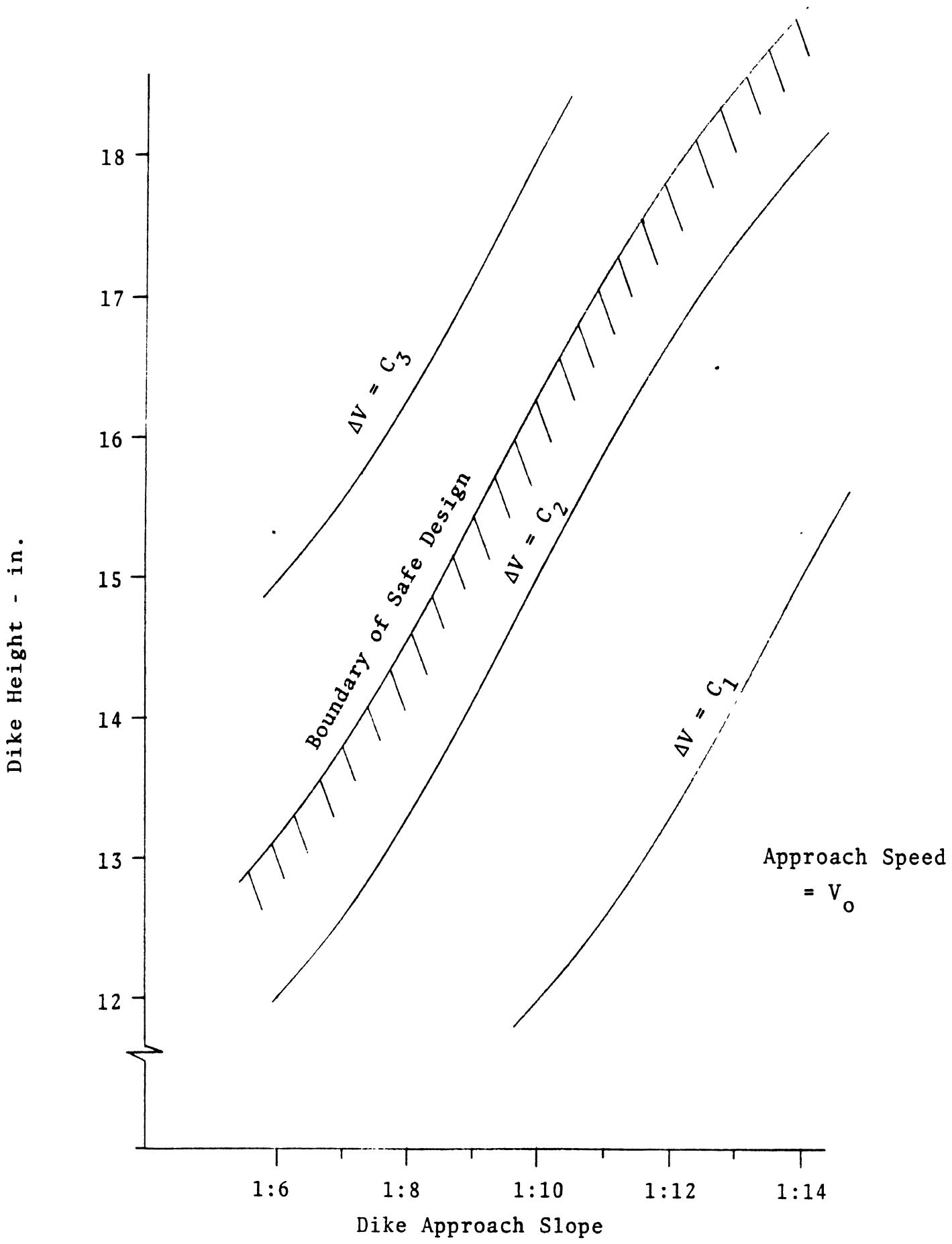

FIGURE 6-8. EXAMPLE DIKE DESIGN DATA

are acceptable. A series of plots of this type, for various approach speeds, will allow the designer to select a dike configuration for the existing traffic and drainage conditions and for whatever safety criteria he may choose.

7. REFERENCES

1. Stonex, K.A., "Roadside Design for Safety", Proc. of the 39th Annual Meeting of the HRB, Vol. 39, 1960.

2. Cichowski, W.G., Skeels, P.C., and Hawkins, W.R., "Guardrail Installations - Appraisal by Proving Ground Car Impact and Laboratory Tests", Presented at the 40th Annual Meeting of the HRB, 1961.

3. "Metal Beam Guard Fence, GF(TD) - 69B", Texas Highway Department.

4. "Guard Rail Anchorage, E-4-A-152E", Michigan Department of State Highways.

5. Nordlin, E.F., Field, R.N., and Folsom, J.J., "Dynamic Test of Short Sections of Corrugated Metal Beam Guardrail", Highway Research Record 259, 1969.

6. Armstrong, M.D., Smith, P., Wolkowicz, M., and Jasper, R.G., "Full-Scale Impact Tests on Low-Cost Barrier Systems, Lighting Poles and Sign Supports, 1967", D.H.O. Report No. IR22, Department of Highways, Ontario, June, 1968.

7. Michie, J.D., and Bronstad, M.E., "Guardrail Performance: End Treatments", Presented at the 2nd Western Summer Meeting of the HRB, August 1969.

8. Graham, M.D., Burnett, W.C., Gibson, J.L., and Freer, R.H., "New Highway Barriers: The Practical Application of Theoretical Design", Highway Research Record 174, 1967.

9. Bronstad, M.E., and Michie J.D., "Evaluation of a New Guardrail Terminal", Presented at the 51st Annual Meeting of the HRB, January 1972.

10. Lundstrom, L.C. and Skeels, P.C., "Full-Scale Appraisals of Guardrail Installations by Car Impact Tests", HRB Proc., 38th Annual Meeting, 1959.

11. A Policy on Geometric Design on Rural Highways, American Association of State Highway Officials, 1965.

12. Beaton, J.L., and Peterson, H., "A Report on Dynamic Testing of Various Designs of Highway Bridge Curbing - Roadway Barrier Curb Investigation", California Division of Highways December 31, 1953.

13. Field, R.N., and Beaton, J.L., "Final Report of Full Scale Dynamic Tests of Bridge Curbs and Rails", California Division of Highways, August 30, 1957.

14. Heneault, G.G., and Perron, H., "Research and Development of A Guide Rail System for a High-Speed Elevated Expressway", Highway Research Record No. 152, 1966.

15. Elsholz, J., "Versuche über die Ablenkwirkung von Bordschwellen (Tests Concerning the Turn Away Effect of Kerb Stones)", Strasse and Autobahn, Vol. 19, n. 4, April, 1968.

16. Jehu, V.J., "Safety Fences and Kerbs", Traffic Engineering and Control", Vol. 5, n. 9, January 1964.

17. Lundstrom, L.C., Skeels, P.C., Englund, B.R., and Rogers R.A., "A Bridge Parapet Designed for Safety", Highway Research Record No. 83, 1965.

18. Nordlin, E.F., and Field, R.N., "Dynamic Tests of Steel Box Beam and Concrete Median Barriers", Research Report No. No. M&R 636392-3, California Division of Highways, January 1968.

19. P. Smith, "Development of A Three Cable Guide Rail System and Other Guide Rail Tests, 1967-1968", D.H.O. Report No. RR157, Department of Highways, Ontario, March, 1970.

20. Nordlin, E.F., Woodstrom, J.H., Hackett, R.P., and Folsom, J.J., "Dynamic Tests of the California Type 20 Bridge Barrier Rail", Research Report No. M&R HRB 636459, California Division of Highways, January, 1971.

21. Jehu, V.J., and Prisk, C.W., "Research on Crash Barriers, Their Design, Warrants for Use, Safety Aspects, Testing and Research", A Report of the OECD Crash Barrier Research Group, Paris, 1967.

22. Hveem, F.N., and Beaton, J.L., "Full Scale Testing of Highway Bridge Rails and Median Barriers", SAE Preprint 211B, August 1960.

23. "Vägräckesförsök (Road Guard Experiments)", Spec. Rep. No. 4 (1955) with Supplement No. 1 (1956) and Supplement No. 2 (1957), Statens Vaginstitut (State Road Institute, Stockholm, Sweden.

24. Böhringer, A., Roschmann, R., and Domhan, M., "Durchfuhrung von Anfahrversuchen an Leitplanken zur Erzulung einer möglichst hohen Verkehrssicherheit an Bundesfernstraben (The Conduct of Impact Tests on Guard Rails to Attain the Highest Possible Degree of Safety on Federal Trunk Roads)", Report 42, Strassenbau und Strassenverkehrstechnik (The Federal Ministry of Transport and Road Research Society), Germany, 1965.

25. Böhringer, A., Roschmann, R., and Domhan, M., "Anfahrversuche an Leitplanken (Collision Tests on Guardrails)", Report 98, Stassenbau und Strassenverkehrstechnik (The Federal Ministry of Transport and Road Research Society), Germany, 1970.

26. Jehu, V.J., "The D.A.V. and Blocked-Out Beam Crash Barriers", RRL Report LR 104, Road Research Laboratory, 1967.

27. Takahashi, N., "Report on D.A.V. Auto-guard Strength Tests/ Field Tests by Automobiles", Transport Technical Research Institute and Ministry of Transportation, Tokyo, March, 1960.

28. Beaton, J.L., and Field, R.N., "Dynamic Full-Scale Tests of Median Barriers", Highway Research Board Bulletin 266, 1960.

29. Beaton, J.L., and Field, R.N., "Dynamic Full-Scale Tests of Bridge-Rails", California Division of Highways, December, 1960.

30. Field, R.N., and Johnson, M.H., "Dynamic Full-Scale Impact Tests of Cable Type Median Barriers - Test Series IX", California Division of Highways, June 1965.

31. "Dykes in Median Ditches", Road Design Letter No. 525, from P.E. Plambech to Design Supervisors, Squad Leaders, and Consultants, Michigan Department of State Highways, August 10, 1959, revised August 2, 1963.

32. Weaver, G.D., "The Relation of Side Slope Design to Highway Safety", NCHRP Project 20-7, Task Order No. 2., Texas Transportation Institute Research Report 626-2, May, 1970.

33. Garner, G.R., and Venable, J.B., "A Preliminary Evaluation of Mounds to Direct Wayward Vehicles Away from Rigid Obstructions", Kentucky Department of Highways, August, 1969.

34. Hirsch, T.J., and Kappel, R.A., "Earth Berm Vehicle Deflector", NCHRP Project 20-7, Task Order No. 3, Texas Transportation Institute Research Report No. 20-7-3-1, May, 1970.

35. Ross, H.E., Jr., and Post, E.R., "Tentative Criteria for the Design of Safe Sloping Culvert Grates", Presented at the Annual Meeting of the HRB, January, 1972.

36. McHenry, R.R., and Deleys, N.J., "Vehicle Dynamics in Single Vehicle Accidents - Validation and Extension of a Computer Simulation", CAL No. VJ-2251-V-3, Cornell Aeronautical Laboratory, December, 1968.

37. Lundstrom, L.C., "Safety Aspects of Vehicle-Road Relationships", General Motors Corp., SAE Preprint 66B, Presented at the SAE Summer Meeting, June 8-13, 1958.

38. "Standard Typical Cross-Sections, Dual Concrete Roadways", Michigan Department of State Highways, January, 1970.

39. Snyder, R.G., "State-of-the-Art Human Impact Tolerance", The Highway Safety Research Institute, University of Michigan, SAE. Reprint 700398, Revised August, 1970.

40. Patrick, L.M., Mertz, H.J., Jr., and Kroell, C.K., "Cadaver Knee, Chest, and Head Impact Loads", Wayne State University, 11th Stapp Car Crash Conference, October 10-11, 1967.

41. "1968 Truck Weight and Characteristics Study", Michigan Department of State Highways, Bureau of Engineering, MDSH Report No. 63.

42. "Speed Report", Michigan Department of State Highways, Report No. 66, October, 1969.

43. "Accident Master Tapes of the Michigan Department of State Highways", 1966 and 1967.

44. Hutchinson, J.W., "The Significance and Nature of Vehicle Encroachment on Medians of Divided Highways", Civil Engineering Studies, Highway Engineering Series No. 8, University of Illinois, Urbana, December, 1962.

45. Shoemaker, N.E., and Radt, H., "Summary Report of Highway Barrier Analysis and Test Program", Report No. VJ-1472-V-3, Cornell Aeronautical Laboratory, July, 1961.

46. Letter from D.E. Orne, Michigan Department of State Highways, to E.C. Zobel, Wayne State University, August 20, 1971.

47. "Concrete Curb, Curb and Gutter, Driveway Openings and Headers, E-4-A-29G", Michigan Department of State Highways, August 22, 1969.

48. Michie, J.D., and Calcote, L.R., "Location, Selection, and Maintenance of Highway Guardrails and Median Barriers", NCHRP Report 54, 1968.

49. Shoemaker, N.E., and Radt, H., "Summary Report of Highway Barrier Analysis and Test Program", Report No. VJ-1472-V-3, Cornell Aeronautical Laboratory, July, 1961.

50. "Speed Report", Michigan Department of State Highways, Report No. 66, October, 1971.

51. "Parking Dimensions, 1971 Model Cars", Engineering Notes No. 711, Automobile Manufacturers Association, Engineering and Technical Department, Detroit, Michigan.

52. Letter from D.E. Orne, Michigan Department of State Highways, to Dr. S.E. Davis, Wayne State University, March 2, 1970.

53. Powell, G.H., "Computer Evaluation of Automobile Barrier Systems", University of California, Berkeley, August, 1970.

54. Speer, T.L., and Gorman, J.W., "Laboratory Evaluation of Pavement Damage Caused by Studded Tires, Salt, and Abrasive Sand", Report M71-81, American Oil Company, May 25, 1971.

55. Deleys, N.J. and McHenry, "Highway Guardrails - A Review of Current Practice", NCHRP Report 36, 1967.

56. Michie, J.E., "Response of Guardrail Posts During Impact", Final Report IR Project No. 03-9051, Southwest Research Institute, October 15, 1970.

57. Michie, J.D., Gatchell, C.J., and Duke, T.J., "Dynamic Evaluation of Timber Posts for Highway Guardrail", Southwest Research Institute, August, 1970.

58. Zobel, E.C., et. al, "Investigation of the Dynamic Impact on Roadside Obstacles - Interim Report", Wayne State University, November 15, 1971.

59. Edholm, S., "Examples of Vehicle Speed and Distance to Edge Marking", Svenska Vagfor Tidskr, Sweden, Vol. 52, pp. 366-370, November, 1965.

60. McHenry, R.R., Segal, D.J., and De Leys, N.J., "Determination of Physical Criteria for Roadside Energy Conversion Systems," CAL No. VJ-2251-V-1, Cornell Aeronautical Laboratory, July, 1967.

61. Mc Henry, R.R., and De Leys, N.J., "Automobile Dynamics - A Computer Simulation of Three - Dimensional Motions for Use in Studies of Braking Systems and of the Driving Task", CAL No. VJ-2251-V-7, Cornell Aeronautical Laboratory, August, 1970.

62. Bekker, M.G., Introduction to Terrain Vehicle Systems, University of Michigan Press, 1969.

63. Bekker, M.G., "Analysis of Towed Pneumatic Tires Moving on Soft Ground", Land Locomotion Laboratory, AD256315, March, 1960.

64. Dugoff, H., "Tire Performance Characteristics Affecting Vehicle Response to Steering and Braking Control Inputs", HSRI, August, 1969.

65. Fancher, P., "Experimental Studies of Tire Shear Force Mechanics", HSRI, July, 1970.

66. Rothwell, G.J., "The Performance Concept: A Basis For Standards Development", ASTME Vectors, Vol. 2, 1969.

67. Memo from D.F. Dunlap and P. Grote to E.C. Zobel, "Dike Impact Sensitivity Analysis", (PF-70-188), November 24, 1970.

APPENDIX A
CALSVA SIMULATION MODEL

The basic simulation model used in the project was the Cornell Aeronautical Laboratory Single Vehicle Accident Program (CALSVA) developed and validated for the Federal Highway Administration by McHenry, Segel, and DeLeys. The essential features of this model are as follows (further details may be found in the several reports published by Cornell [36, 60, 61]):

A-1 BASIC MODEL

In the model, the vehicle is represented as an assemblage of four rigid masses, corresponding to a body ("sprung mass"), a solid rear axle, plus rear wheels ("rear unsprung mass"), and two independent front wheels with attendant suspension systems ("front unsprung masses") as depicted in Figure A-1. The sprung mass has six degrees of freedom (roll, pitch, and yaw rotations, and longitudinal, lateral, and vertical displacements), the rear unsprung mass has two (roll rotation and vertical displacement), and the front unsprung masses have one each (vertical displacement). In addition, a steer mode degree of freedom is available as a user option (it is also activated automatically whenever rigid obstacles, e.g., curbs, are encountered by the wheels).

Camber angles of the individual front wheels relative to the sprung mass are determined by interpolation from a tabular input of camber angle versus suspension deflection (δ_1 and δ_2 in Figure A-1). The steer angles of the two front wheels are assumed to be equal and front wheel roll steer is neglected. Rear axle roll steer is treated as a linear function of the rear axle angular coordinate, ϕ_R.

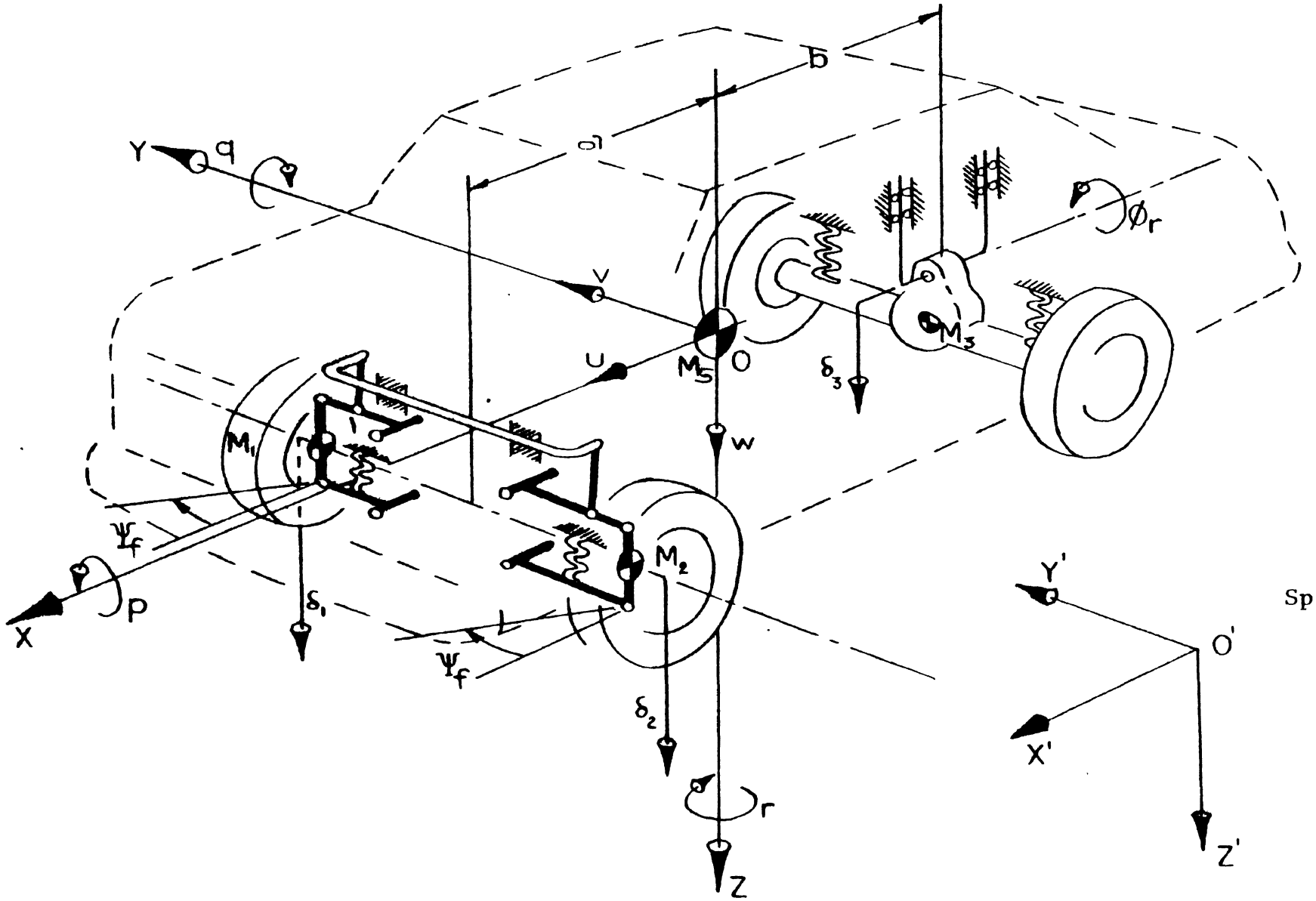

FIGURE A-1. ANALYTICAL REPRESENTATION OF VEHICLE

Anti-pitch effects in the suspension are approximated by means of coefficients that are entered separately for the front and for the rear as tabular functions of suspension deflections.

External forces are applied only at the tire/terrain contact surface. Aerodynamic forces and rolling resistance are neglected.

Radial loading of the tires is calculated in one of two modes, depending on the nature of the tire/terrain contact patch. When the contact patch may be considered essentially planar (e.g., riding over gently undulating terrain), a point-contact representation is used. However, when the contact patch is clearly non-planar (e.g., impacting with curbs), a more sophisticated radial spring model is adopted. Forces "within" the tire/terrain contact surface (lateral force, traction, braking) are computed by means of a "friction circle" concept. Whenever the steer mode degree of freedom is activated, a constant "pneumatic trail" dimension is employed to generate front wheel aligning torques.

The terrain over which the vehicle travels is entered into the program in tabular form. An x'-y' grid is established, and absolute elevations are specified for all the intersection points. Terrain elevations and terrain slopes are then calculated at intermediate points, as needed, through interpolation and numerical differentiation. Curb profiles are represented analytically in terms of the lateral positions and slopes of a number of curb faces.

The simulated load-deflection characteristics of the vehicle suspension include linear elastic spring rates; nonlinear energy-dissipating "bump" stops; elastic auxiliary roll stiffness; Coulomb friction; and viscous damping (shock absorbers).

A-2 HSRI MODIFICATIONS

The original CALSVA program, as supplied by Cornell, has been modified in several important ways in order to make it more representative of the various conditions of interest in the roadside structure impact program.

For the evaluation of earthen dikes, the primary program changes were the inclusion of a soft soil model and the addition of rotating wheel dynamics. Soft soil modeling was considered desirable since the primary function of dikes is runoff control and soft, moist soil is therefore likely to be encountered. Unfortunately, most of the available literature on tire/soil interaction is oriented toward military vehicles operating in swamp or sand environments. This emphasis usually implies track laying vehicles traveling at low velocities, under 5 mph. Wheeled off-road vehicles, on the other hand, are characterized by large diameter tires and low tire/soil contact pressures. Several investigators have claimed varying degrees of success in mathematically modeling these restricted situations, but few basic guidelines are generally agreed upon. The most widely accepted theory is based on the low speed, quasi-static analysis of Bekker [62, 63].

For stiff-tired passenger vehicles traveling over grassy medians at highway speeds, conditions are obviously different. Since the low speed quasi-static theory is all that is available, however, an attempt was made to apply it to the above conditions. The results, although strictly conjectural, are intuitively reasonable for representative soil characterizing parameters.

The two basic phenomena to be modeled are tire sinkage and forward motion resistance. According to Bekker, the basic pressure-sinkage relationship for a continuous, homogeneous, isotropic soil can be stated as:

$$p = \left(\frac{k_c}{b} + k_\phi\right) z^n \qquad \text{(A-1)}$$

where

p = pressure

z = sinkage

The constants k_c, k_ϕ, and n are determined by driving a flat plate of dimension b into the soil and measuring the necessary pressure to achieve a certain penetration. A graphical interpretation of test data for two sizes of plates yields the necessary constants.

If it is assumed that the wheel is rigid relative to the soil, the basic flat plate equation can be extended to a wheel of diameter D carrying a load W such that it will sink:

$$z = \left[\frac{3W}{(3-n)(k_c + bk_\phi)D^{1/2}}\right] \qquad \text{(A-2)}$$

Additional assumptions implicit in (A-1) and (A-2) imply that predicted values become more valid as the soil sinkage approaches zero and the wheel diameter approaches infinity. Practical limits indicate adequate agreement with test data at low speeds for a minimum diameter of 20 inches and a maximum sinkage of one-sixth of the diameter.

As the tire sinks while moving forward, it must displace the soil in its path. The soil is partly compacted beneath the rolling tire surface and partly bulldozed to the side. These two effects are generally lumped into one resistance force:

$$R = \frac{(3W)^{\varepsilon}}{(3-n)^{\varepsilon}(n+1)k^{\frac{1}{2n+1}}D^{\varepsilon/2}} \qquad \text{(A-3)}$$

where

$$\varepsilon = \frac{(2n+2)}{(2n+1)}$$

$$k = k_c + bk_\phi$$

This relationship is derived by considering the ground reaction over the surface of the tire/soil interface and integrating over that area to obtain the equivalent resistance force.

The mathematical relations embodied in Equations (A-1), (A-2), and (A-3) were programmed into the CALSVA simulation by means of a new subroutine called SOFSOL. The logic of this routine is depicted in the simplified flow diagram of Figure A-2. The basic procedure is to move the tire-soil interface up and down until the internal tire forces balance the ground reaction force. At subsequent time intervals, the imbalance of vertical forces on the wheel center (suspension forces reacting against the sprung mass, wheel inertial reaction, and radial tire force) will cause more or less rut penetration until an equilibrium condition is reached. The forward motion resistance is computed by substituting the net downward force for W in Equation (A-3).

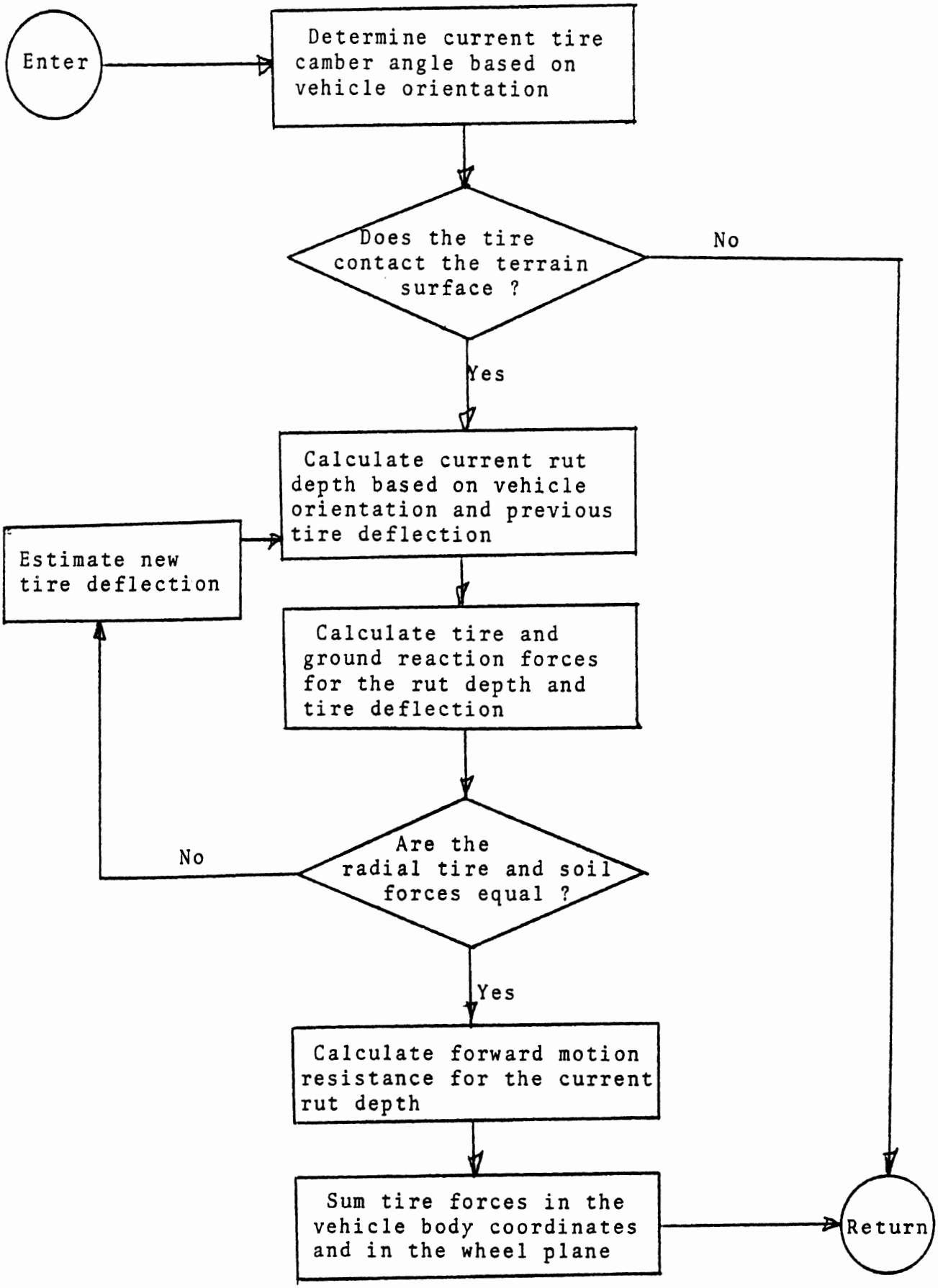

FIGURE A-2. SOFT SOIL TIRE MODEL - SIMPLIFIED FLOW DIAGRAM

Rotational wheel dynamics were introduced in order to more accurately represent vehicle slowdown through interaction with soft soil. The computational method adopted follows the recommendations of McHenry [36], while the theoretical tire force equations are based on work done at HSRI [64, 65].

Since wheel rotational dynamics generally extend to a higher frequency band than do other vehicle motions, it was necessary to include an adaptive integration increment into the new routine. The increment is determined through a criteria based on the ratio $\dot{\theta}/\ddot{\theta}$ and is patterned after McHenry suggestions. The solution flow is given in Figure A-3. Further information on both the soft soil modeling and the simulation of wheel rotation is available if needed [67].

For the evaluation of the earthen mound guardrail end, the main modification was the incorporation of a new subroutine capable of handling impacts of the wheels with a rigid rail emerging from the earthen mound. A listing of this new routine is given in Fig. A-4. Basically, the procedure is to send out radial springs from the center of the wheel and to intersect them, one by one, with the underlying surface, which may consist either of rail or of ground. No a priori assumptions are made concerning the relative height of the rail and the surrounding terrain. Rather, for each radial spring, an internal logical test is employed to decide whether rail or ground is higher, and then the spring is allowed to interact accordingly.

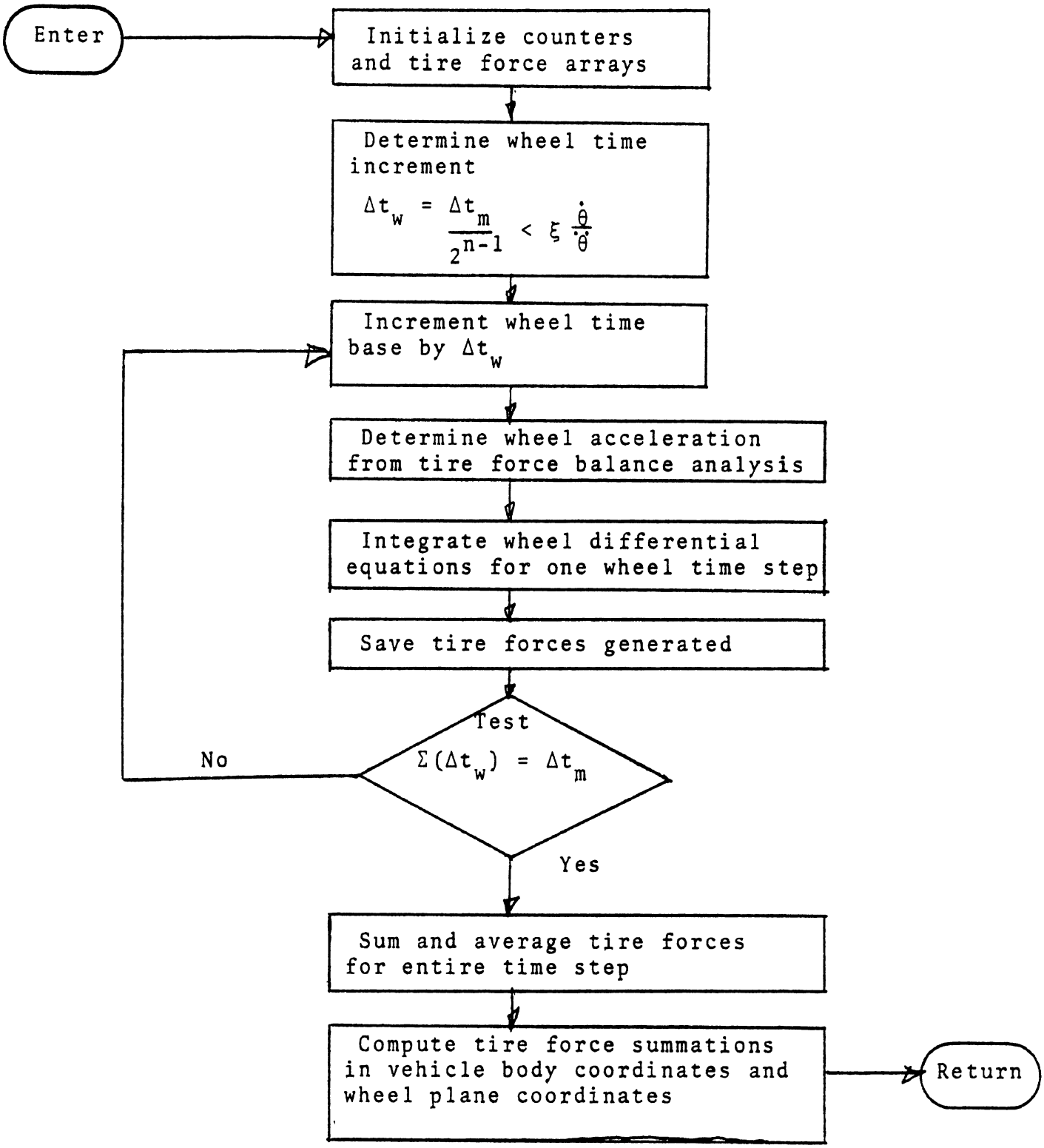

FIGURE A-3. ROTATING WHEEL DYNAMICS - SIMPLIFIED FLOW CHART

FIGURE A-4

BURIED GUARDRAIL END IMPACT SUBROUTINE

```
      SUBROUTINE BCIMP(I)
      SINGLE VEHICLE ACCIDENT SIMULATION WITH CURB IMPACT - BCIMP

      COMMON/INPT/PHI0,THETA0,PSI0,P0,Q0,R0,XC0P,YC0P,ZC0P,U0,V0,W0,A,B,
     1            DEL10,DEL20,DEL30,PHIR0,DEL10D,DEL20D,DEL30D,PHIR0D,
     2            TF,TR,ZF,ZR,RHO,RW,AKT,SIGT,XLAMT,A1,A2,A3,AKRS,AMU,
     3            XMUR,XMS,XMUF,XIX,XIY,XIZ,XIXZ,CF,AKF,XLAMF,OMEGF,
     4            CFP,EPSF,RF,CR,AKR,XLAMR,OMEGR,CRP,EPSR,RR,TS,
     5            THMAX,DTCOMP,T0,T1,DTPRNT,G,HED(36),DADE(3),XIR,
     6            X1,Y1,Z1,X2,Y2,Z2,PHIC(50),DELB,DELE,DDEL,
     7            PSIF(50),TQF(50),TQR(50),TB,TE,TINCR,A4,OMEGT,
     8            XBDRY(4,5),PSBDRY(4,5),YBDRY(2,5),ZGP(21,21,5)
      COMMON/INPT4/XB(5),XE(5),XINCR(5),YB(5),YE(5),YINCR(5),AMUG(5),
     1             UVWMIN,PQRMIN,XXZGP5(21),YYZGP5(21)
      COMMON/INPT1/YCRBP(10),ZCRBP(10),PHCRB(10),YPHIAV(10),PHIAV(10),
     1             DELTC,AMUC,FJP(35),XIPS,CPSP,OMGPS,AKPS,EPSPS,XPS,
     2             RWHJB,RWHJE,DRWHJ,PSIFI0,PSIFD0,YC1P,YC2P
      COMMON /DIMV/X1P,X2P,X3P,X4P,Y1P,Y2P,Y3P,Y4P,Z1P,Z2P,Z3P,Z4P,PHI1,
     1             PHI2,PHI3,PHI4,PSI1,PSI2,PSI3,PSI4,CAYW(4),CBYW(4),
     2             CGYW(4),ZPGI(4),THGI(4),PHGI(4),CPG(4),SPG(4),CTG(4),
     3             STG(4),CAGZ(4),CBGZ(4),CGGZ(4),D1(4),D2(4),D3(4),
     4             XLM1(4),XLM2(4),XLM3(4),AMTX(3,3),CMTX(3,4),XGPP(4),
     5             YGPP(4),ZGPP(4),DMATX(10,11),DELTA(4),CAR(4),CBR(4),
     6             CGR(4),FR(4),HI(4),FC(4),TI(4),AX(4),BX(4),CX(4),
     7             CTXG(4),UG(4),STXG(4),AY(4),BY(4),CY(4),CPYG(4),
     8             SPYG(4),VG(4),PSIIP(4),PHICI(4),CAC(4),CBC(4),CGC(4),
     9             FCXU(4),FCYU(4),FCZU(4),FS(4),CAXW(4),CBXW(4),CGXW(4)
      COMMON /DIMV/AS(4),BS(4),CS(4),CAS(4),CBS(4),CGS(4),BETP(4),
     1             BETBR(4),FSXU(4),FSYU(4),FSZU(4),FRXU(4),FRYU(4),
     2             FRZU(4),FXU(4),FYU(4),FZU(4),SI(4),F1FI(2),F1RI(2),
     3             F2FI(2),F2RI(2),CAH(4),CBH(4),CGH(4)
      COMMON /COMPN/ OMT2M1,FRSP(4),FRCP(4),DPSINT,
     1               TNPCRB(10),TNPAV(10),PHCRBR(10),PHIAVR(10),
     2               AMUCMP,PHI1D,PHI2D,AJMTX(3,3),BMTX(3,3),
     3               SFRX(4),SFRY(4),SFRZ(4),T1PSI,T2PSI,XMUGI(4)
      COMMON /COMP/SUMM,THETN,PHIN,PSIN,PI,RAD,GAM1,GAM2,GAM3,GAM4,GAM5,
     1             GAM6,GAM7,GAM8,GAM9,THETT,PHIT,PSIT,A12,A23,ZRO,TRO2,
     2             TFO2,TIZ,RHO2,RHOMUR,AMUF,BMUR,ZPR,TM4,RHMR2,AO2APB,
     3             BO2APB,RFTF,TSO2,RRTS,BROMUR,XMUFO2,AXMFO2,XMTFO4,
     4             XIZR,RTR,RHMR2I,XIXP,XIZP,XIXZP,XIYZP,D1PD2,D1MD2,
     5             ZRD3,ZRD3R,ZFD3R,ZFD12,TIZ2,TG61,DD1P2,DD1M2,RPR,PHRP
     6            ,TANTP,SPHTP,CPHTP,SECTP,SFXS,SFYS,SFZS,SNPS,SNTS,
     7             SNPSS,TPR,CAY,CBY,CGY,CAX,CBX,CGX,SFYU,SFXU,SFYUF,
     8             SFYUR,SFZU,COSTH,SINTH,COSPS,SINPS,COSPH,SINPH,ANG1,
     9             ANG2,CPHI,SPHI,CPSI,SPSI,P1,P7,P3,P4,P5,P6,TX,TY,TZ
      COMMON /COMP/TRH,DISTX,DISTY,DISTD,DISTS,D21,ZETA4,ZETA4D,ZETA3,
     1             ZETA3D,SFZ1,SNPU,SNTU,HCGH1,HCGH2,HCGH3,HCGH4,TERM1,
     2             TERM2,SNPSU,SNPR,HCBH1,HCBH2,HCBH3,HCBH4,HCAH1,HCAH2,
     3             HCAH3,HCAH4,UQ,WP,UR,QR,VP,PR,P2,Q2,R2,VR,WQ,PQ,PHIR2
     4            ,PHIRD2,RPHRD,GCTH,GSTH,GCTSP,GCTCP,XXX,YYY,XX1,
     5             XX2,YY1,YY2,THG1,THG2,PHG1,PHG2,ZZ1,ZZ2
      COMMON/ADTNL/U1,U2,U3,U4,V1,V2,V3,V4,W1,W2,W3,W4,XTRA(300)
      COMMON/INTGRS/NDEL,IWHLSW,INDCRB,INDB,IOUTC,IPRNT(16),NZTAB,NZ5,
```

Fig. A-4 (cont.)

```
     1               NBX(5),NBY(5),NX(5),NY(5),NBXRS(4,5),NEQ,IX,IY,LLL,
     2               IND,IHIT,ICBHIT,JCBHIT,IBHIT,JBHIT,IDPT(17),IPT,
     3               I1,I2,I3,I4,ININD,IPLN,ILOAD,NCRB,NCRBM1,NSCH,NSCHM1
C
      DIMENSION XP(4),YP(4),ZP(4),PHII(4),PSII(4),UI(4),VI(4),WI(4)
C
      EQUIVALENCE (XP,X1P),(YP,Y1P),(ZP,Z1P),(PHII,PHI1),(PSII,PSI1),
     1            (UI,U1),(VI,V1),(WI,W1)
      EQUIVALENCE (XIYP,XTRA(1)),(SPHIC,XTRA(2)),(CPHIC,XTRA(3))
C
C  INITIALIZE
      XLM2(I) = XP(I)*CAGZ(I)+YP(I)*CBGZ(I)+ZPGI(I)*CGGZ(I)
      SNPSI = SIN(PSII(I))
      CSPSI = COS(PSII(I))
      SNPHI = SIN(PHII(I))
      CSPHI = COS(PHII(I))
      SFRX(I) = 0.0
      SFRY(I) = 0.0
      SFRZ(I) = 0.0
      XJ = -26.0*RAD
C
C  CYCLE FOR ALL 53 RADIAL SPRINGS
      DO 99  J=1,53
      THTJ = 4.0*XJ
      STJ = SIN(THTJ)
      CTJ = COS(THTJ)
C  DEFINE A TRANSFORMATION MATRIX FOR EACH RADIAL SPRING
      AJMTX(1,1) = CTJ*CSPSI
      AJMTX(2,1) = CTJ*SNPSI
      AJMTX(3,1) = -STJ
      AJMTX(1,2) = -CSPHI*SNPSI+SNPHI*STJ*CSPSI
      AJMTX(2,2) = CSPHI*CSPSI+SNPHI*STJ*SNPSI
      AJMTX(3,2) = CTJ*SNPHI
      AJMTX(1,3) = SNPHI*SNPSI+CSPHI*STJ*CSPSI
      AJMTX(2,3) = -CSPSI*SNPHI+CSPHI*STJ*SNPSI
      AJMTX(3,3) = CTJ*CSPHI
C  DEFINE BMTX AS A MATRIX PRODUCT OF TRANSFORMATIONS
      DO 8  K=1,3
      DO 7  L=1,3
      BMTX(K,L) = 0.0
      DO 6  M=1,3
    6 BMTX(K,L) = BMTX(K,L)+AMTX(K,M)*AJMTX(M,L)
    7 CONTINUE
    8 CONTINUE
C  DETERMINE LENGTH OF EACH RADIAL SPRING
C  INTERSECT SUCCESSIVELY WITH EACH CURB FACE AND WITH GROUND PLANE
      HJ = RW
      DO 10 K=1,NCRBM1
      IF(YCRBP(K).NE.YCRBP(K+1)) GO TO 20
      HJT = (YCRBP(K)-YP(I))/BMTX(2,3)
      ZJPT = ZP(I)+BMTX(3,3)*HJT
      IF(((ZJPT.GE.ZCRBP(K).AND.ZJPT.LE.ZCRBP(K+1)).OR.
     1    (ZJPT.LE.ZCRBP(K).AND.ZJPT.GE.ZCRBP(K+1))).AND.
     2                  (HJT.LT.HJ)) HJ=HJT
      GO TO 10
   20 HJT = (ZCRBP(K)-ZP(I)+(YP(I)-YCRBP(K))*TNPCRB(K))
     1     /(BMTX(3,3)-BMTX(2,3)*TNPCRB(K))
```

Fig. A-4 (cont.)

```
      YJPT = YP(I)+BMTX(2,3)*HJT
      IF(((YJPT.GE.YCRBP(K).AND.YJPT.LE.YCRBP(K+1)).OR.
     1     (YJPT.LE.YCRBP(K).AND.YJPT.GE.YCRBP(K+1))).AND.
     2                    (HJT.LT.HJ)) HJ=HJT
   10 CONTINUE
      HJT = (XLM2(I)-CAGZ(I)*XP(I)-CBGZ(I)*YP(I)-CGGZ(I)*ZP(I))
     1      /(BMTX(1,3)*CAGZ(I)+BMTX(2,3)*CBGZ(I)+BMTX(3,3)*CGGZ(I))
      IF(HJT.LT.HJ) HJ=HJT
      IF(HJ.LT.0.0.OR.HJ.GE.RW) GO TO 70
      XJP = XP(I)+BMTX(1,3)*HJ
      YJP = YP(I)+BMTX(2,3)*HJ
      ZJP = ZP(I)+BMTX(3,3)*HJ
      CAJ = (XP(I)-XJP)/HJ
      CBJ = (YP(I)-YJP)/HJ
      CGJ = (ZP(I)-ZJP)/HJ
      CALL INTRPL(FJP,RWHJB,RWHJE,DRWHJ,RW-HJ,FJ)
   SUM CONTRIBUTION IN TRANSFORMED AXIS
      SFRX(I) = SFRX(I)+FJ*CAJ
      SFRY(I) = SFRY(I)+FJ*CBJ
      SFRZ(I) = SFRZ(I)+FJ*CGJ
   70 XJ = XJ+RAD
   99 CONTINUE

   CHECK FOR SPRING TOTAL EFFECT IN ACTION
   ZERO RESULTS AND RETURN IF NO ACTION
      FR(I) = SQRT(SFRX(I)**2+SFRY(I)**2+SFRZ(I)**2)
      IF(FR(I).NE.0.0)GO TO 110
      CAR(I) = 0.0
      CBR(I) = 0.0
      CGR(I) = 0.0
      HI(I) = RW
      RETURN

   DETERMINE EQUIVALENT GROUND CONTACT POINT
  110 CAR(I) = -SFRX(I)/FR(I)
      CBR(I) = -SFRY(I)/FR(I)
      CGR(I) = -SFRZ(I)/FR(I)
      HI(I) = RW-FR(I)/AKT
      IF(HI(I).GT.RW-SIGT) GO TO 115
      HI(I) = RW-(FR(I)/AKT+SIGT*(XLAMT-1.0))/XLAMT
  115 XGPP(I) = XP(I)+HI(I)*CAR(I)
      YGPP(I) = YP(I)+HI(I)*CBR(I)
      ZGPP(I) = ZP(I)+HI(I)*CGR(I)


   EVALUATE TERRAIN ELEVATION AT EQUIVALENT GCP
      ZTERR = (XLM2(I)-XGPP(I)*CAGZ(I)-YGPP(I)*CBGZ(I))/CGGZ(I)
   TEST TO SEE WHETHER CURB IS BURIED AT EQUIVALENT GCP
      DO 120 K=1,NCRBM1
      IF((YGPP(I).GT.YCRBP(K).AND.YGPP(I).GT.YCRBP(K+1)).OR.
     1   (YGPP(I).LT.YCRBP(K).AND.YGPP(I).LT.YCRBP(K+1)))  GO TO 120
      IF(YCRBP(K).EQ.YCRBP(K+1)) ZCURB=AMIN1(ZCRBP(K),ZCRBP(K+1))
      IF(YCRBP(K).NE.YCRBP(K+1)) ZCURB=ZCRBP(K)+(YGPP(I)-YCRBP(K))*
     1                                  TNPCRB(K)
      IF(ZCURB.LT.ZTERR) GO TO 130
  120 CONTINUE
      GO TO 200
```

Fig. A-4 (cont.)

```
C  CURB EXPOSED--RESET FRICTION COEFFICIENT AND SLOPES
C 130 XMUGI(I) = AMUC
C     DO 150 K=1,NSCHM1
C     KSAVE = K
C     IF(YGPP(I).GE.YPHIAV(K).AND.YGPP(I).LT.YPHIAV(K+1)) GO TO 160
C 150 CONTINUE
C     GO TO 200
C 160 THGI(I) = 0.0
C     PHGI(I) = PHIAVR(KSAVE)
C
C
C  DETERMINE SLOPES OF EQUIVALENT GROUND PLANE (NEW APPROACH)
C
      KSAVE=0
      HAUX=1.E25
      DO 310 K=1,NCRBM1
      IF(YCRBP(K).NE.YCRBP(K+1)) GO TO 320
      HAUXT = (YCRBP(K)-YP(I))/CBR(I)
      ZAUXT = ZP(I)+CGR(I)*HAUXT
      IF( (ZAUXT.GT.ZCRBP(K).AND.ZAUXT.GT.ZCRBP(K+1)) .OR.
     1    (ZAUXT.LT.ZCRBP(K).AND.ZAUXT.LT.ZCRBP(K+1)) .OR.
     2                    (HAUXT.GT.HAUX) ) GO TO 310
      HAUX=HAUXT
      KSAVE=K
      GO TO 310
  320 HAUXT = (ZCRBP(K)-ZP(I)+(YP(I)-YCRBP(K))*TNPCRB(K))
     1      /(CGR(I)-CBR(I)*TNPCRB(K))
      YAUXT = YP(I)+CBR(I)*HAUXT
      IF( (YAUXT.GT.YCRBP(K).AND.YAUXT.GT.YCRBP(K+1)) .OR.
     1    (YAUXT.LT.YCRBP(K).AND.YAUXT.LT.YCRBP(K+1)) .OR.
     2                    (HAUXT.GT.HAUX) ) GO TO 310
      HAUX=HAUXT
      KSAVE=K
  310 CONTINUE
      HAUXT = (XLM2(I)-CAGZ(I)*XP(I)-CBGZ(I)*YP(I)-CGGZ(I)*ZP(I))
     1      /(CAR(I)*CAGZ(I)+CBR(I)*CBGZ(I)+CGR(I)*CGGZ(I))
      IF(HAUXT.GT.HAUX) GO TO 350
      HAUX=HAUXT
      KSAVE=0
  350 IF(KSAVE.LE.0) GO TO 200
      XMUGI(I)=AMUC
      THGI(I)=0.0
      PHGI(I)=PHCRBR(KSAVE)
  200 TCI = CAR(I)*CBYW(I)-CBR(I)*CAYW(I)
      TAI = CBR(I)*CGYW(I)-CGR(I)*CBYW(I)
      TBI = CGR(I)*CAYW(I)-CAR(I)*CGYW(I)
      CPG(I) = COS(PHGI(I))
      SPG(I) = SIN(PHGI(I))
      CTG(I) = COS(THGI(I))
      STG(I) = SIN(THGI(I))
      TERM1 = (TAI**2+TCI**2)*SPG(I)
      TERM2 = (TBI**2+TCI**2)*CPG(I)*STG(I)
      TERM3 = (TAI**2+TBI**2)*CPG(I)*CTG(I)
      TERM4 = TBI*CPG(I)*(TAI*STG(I)+TCI*CTG(I))
      TERM5 = TAI*(TBI*SPG(I)-TCI*CPG(I)*CTG(I))
      TERM6 = TCI*(TBI*SPG(I)-TAI*CPG(I)*STG(I))
      DN1 = TERM5+TERM2
```

Fig. A-4 (cont.)

```
      DN2 =-TERM1-TERM4
      DN3 = TERM6+TERM3
      TERM7 = SQRT(DN1**2+DN2**2+DN3**2)
      PHGI(I) = ARSIN(-DN2/TERM7)
      THGI(I) = ATAN(DN1/DN3)
      CPG(I) = COS(PHGI(I))
      SPG(I) = SIN(PHGI(I))
      CTG(I) = COS(THGI(I))
      STG(I) = SIN(THGI(I))
      RETURN
      END
```

Finally, for the analysis of curb/guardrail combinations, several improvements and refinements were made to the curb-impact routine (CRBIMP) supplied with the original version of CALSVA. These improvements included:

1. increasing the number of possible curb faces from two to ten;
2. removing the zero elevation restriction on terrain level near the curb; and
3. providing for modeling undercut curbs

A program listing of the revised version of CRBIMP is given in Figure A-5.

FIGURE A-5

MODIFIED CURB IMPACT SUBROUTINE

```
      SUBROUTINE CRBIMP(I)
      SINGLE VEHICLE ACCIDENT SIMULATION WITH CURB IMPACT - CRBIMP

      COMMON/INPT/PHI0,THETA0,PSI0,P0,Q0,R0,XC0P,YC0P,ZC0P,U0,V0,W0,A,B,
     1            DEL10,DEL20,DEL30,PHIR0,DEL10D,DEL20D,DEL30D,PHIR0D,
     2            TF,TR,ZF,ZR,RHO,RW,AKT,SIGT,XLAMT,A1,A2,A3,AKRS,AMU,
     3            XMUR,XMS,XMUF,XIX,XIY,XIZ,XIXZ,CF,AKF,XLAMF,OMEGF,
     4            CFP,EPSF,RF,CR,AKR,XLAMR,OMEGR,CRP,EPSR,RR,TS,
     5            THMAX,DTCOMP,T0,T1,DTPRNT,G,HED(36),DADE(3),XIR,
     6            X1,Y1,Z1,X2,Y2,Z2,PHIC(50),DELB,DELE,DDEL,
     7            PSIF(50),TQF(50),TQR(50),TB,TE,TINCR,A4,OMEGT,
     8            XBDRY(4,5),PSBDRY(4,5),YBDRY(2,5),ZGP(21,21,5)
      COMMON/INPT4/XB(5),XE(5),XINCR(5),YB(5),YE(5),YINCR(5),AMUG(5),
     1             UVWMIN,PQRMIN,XXZGP5(21),YYZGP5(21)
      COMMON/INPT1/YCRBP(10),ZCRBP(10),PHCRB(10),YPHIAV(10),PHIAV(10),
     1             DELTC,AMUC,FJP(35),XIPS,CPSP,OMGPS,AKPS,EPSPS,XPS,
     2             RWHJB,RWHJE,DRWHJ,PSIFI0,PSIFD0,YC1P,YC2P
      COMMON /DIMV/X1P,X2P,X3P,X4P,Y1P,Y2P,Y3P,Y4P,Z1P,Z2P,Z3P,Z4P,PHI1,
     1             PHI2,PHI3,PHI4,PSI1,PSI2,PSI3,PSI4,CAYW(4),CBYW(4),
     2             CGYW(4),ZPGI(4),THGI(4),PHGI(4),CPG(4),SPG(4),CTG(4),
     3             STG(4),CAGZ(4),CBGZ(4),CGGZ(4),D1(4),D2(4),D3(4),
     4             XLM1(4),XLM2(4),XLM3(4),AMTX(3,3),CMTX(3,4),XGPP(4),
     5             YGPP(4),ZGPP(4),DMATX(10,11),DELTA(4),CAR(4),CBR(4),
     6             CGR(4),FR(4),HI(4),FC(4),TI(4),AX(4),BX(4),CX(4),
     7             CTXG(4),UG(4),STXG(4),AY(4),BY(4),CY(4),CPYG(4),
     8             SPYG(4),VG(4),PSIIP(4),PHICI(4),CAC(4),CBC(4),CGC(4),
     9             FCXU(4),FCYU(4),FCZU(4),FS(4),CAXW(4),CBXW(4),CGXW(4)
      COMMON /DIMV/AS(4),BS(4),CS(4),CAS(4),CBS(4),CGS(4),BETP(4),
     1             BETBR(4),FSXU(4),FSYU(4),FSZU(4),FRXU(4),FRYU(4),
     2             FRZU(4),FXU(4),FYU(4),FZU(4),SI(4),F1FI(2),F1RI(2),
     3             F2FI(2),F2RI(2),CAH(4),CBH(4),CGH(4)
      COMMON /COMPN/ OMT2M1,FRSP(4),FRCP(4),DPSINT,
     1               TNPCRB(10),TNPAV(10),PHCRBR(10),PHIAVR(10),
     2               AMUCMP,PHI1D,PHI2D,AJMTX(3,3),BMTX(3,3),
     3               SFRX(4),SFRY(4),SFRZ(4),T1PSI,T2PSI,XMUGI(4)
      COMMON /COMP/SUMM,THETN,PHIN,PSIN,PI,RAD,GAM1,GAM2,GAM3,GAM4,GAM5,
     1             GAM6,GAM7,GAM8,GAM9,THETT,PHIT,PSIT,A12,A23,ZRO,TRO2,
     2             TFO2,TIZ,RHO2,RHOMUR,AMUF,BMUR,ZPR,TM4,RHMR2,AO2APB,
     3             BO2APB,RFTF,TSO2,RRTS,BROMUR,XMUFO2,AXMFO2,XMTFO4,
     4             XIZR,RTR,RHMR2I,XIXP,XIZP,XIXZP,XIYZP,D1PD2,D1MD2,
     5             ZRD3,ZRD3R,ZFD3R,ZFD12,TIZ2,TG61,DD1P2,DD1M2,RPR,PHRP
     6            ,TANTP,SPHTP,CPHTP,SECTP,SFXS,SFYS,SFZS,SNPS,SNTS,
     7             SNPSS,TPR,CAY,CBY,CGY,CAX,CBX,CGX,SFYU,SFXU,SFYUF,
     8             SFYUR,SFZU,COSTH,SINTH,COSPS,SINPS,COSPH,SINPH,ANG1,
     9             ANG2,CPHI,SPHI,CPSI,SPSI,P1,P7,P3,P4,P5,P6,TX,TY,TZ
      COMMON /COMP/TRH,DISTX,DISTY,DISTD,DISTS,D21,ZETA4,ZETA4D,ZETA3,
     1             ZETA3D,SFZ1,SNPU,SNTU,HCGH1,HCGH2,HCGH3,HCGH4,TERM1,
     2             TERM2,SNPSU,SNPR,HCBH1,HCBH2,HCBH3,HCBH4,HCAH1,HCAH2,
     3             HCAH3,HCAH4,UQ,WP,UR,QR,VP,PR,P2,Q2,R2,VR,WQ,PQ,PHIR2
     4            ,PHIRD2,RPHRD,GCTH,GSTH,GCTSP,GCTCP,XXX,YYY,XX1,
     5             XX2,YY1,YY2,THG1,THG2,PHG1,PHG2,ZZ1,ZZ2
      COMMON/ADTNL/U1,U2,U3,U4,V1,V2,V3,V4,W1,W2,W3,W4,XTRA(300)
      COMMON/INTGRS/NDEL,IWHLSW,INDCRB,INDB,IOUTC,IPRNT(16),NZTAB,NZ5,
```

Fig. A-5 (cont.)

```
     1               NBX(5),NBY(5),NX(5),NY(5),NBXRS(4,5),NEQ,IX,IY,LLL,
     2               IND,IHIT,ICBHIT,JCBHIT,IBHIT,JBHIT,IDPT(17),IPT,
     3               I1,I2,I3,I4,ININD,IPLN,ILOAD,NCRB,NCRBM1,NSCH,NSCHM1
C
      DIMENSION XP(4),YP(4),ZP(4),PHII(4),PSII(4),UI(4),VI(4),WI(4) .
C
      EQUIVALENCE (XP,X1P),(YP,Y1P),(ZP,Z1P),(PHII,PHI1),(PSII,PSI1),
     1            (UI,U1),(VI,V1),(WI,W1)
      EQUIVALENCE (XIYP,XTRA(1)),(SPHIC,XTRA(2)),(CPHIC,XTRA(3))
C
C  INITIALIZE
      XLM2(I) = XP(I)*CAGZ(I)+YP(I)*CBGZ(I)+ZPGI(I)*CGGZ(I)
      SNPSI = SIN(PSII(I))
      CSPSI = COS(PSII(I))
      SNPHI = SIN(PHII(I))
      CSPHI = COS(PHII(I))
      SFRX(I) = 0.0
      SFRY(I) = 0.0
      SFRZ(I) = 0.0
      XJ = -26.0*RAD
C
C  CYCLE FOR ALL 53 RADIAL SPRINGS
      DO 99  J=1,53
      THTJ = 4.0*XJ
      STJ = SIN(THTJ)
      CTJ = COS(THTJ)
C  DEFINE A TRANSFORMATION MATRIX FOR EACH RADIAL SPRING
      AJMTX(1,1) = CTJ*CSPSI
      AJMTX(2,1) = CTJ*SNPSI
      AJMTX(3,1) = -STJ
      AJMTX(1,2) = -CSPHI*SNPSI+SNPHI*STJ*CSPSI
      AJMTX(2,2) = CSPHI*CSPSI+SNPHI*STJ*SNPSI
      AJMTX(3,2) = CTJ*SNPHI
      AJMTX(1,3) = SNPHI*SNPSI+CSPHI*STJ*CSPSI
      AJMTX(2,3) = -CSPSI*SNPHI+CSPHI*STJ*SNPSI
      AJMTX(3,3) = CTJ*CSPHI
C  DEFINE BMTX AS A MATRIX PRODUCT OF TRANSFORMATIONS
      DO 8  K=1,3
      DO 7  L=1,3
      BMTX(K,L) = 0.0
      DO 6  M=1,3
    6 BMTX(K,L) = BMTX(K,L)+AMTX(K,M)*AJMTX(M,L)
    7 CONTINUE
    8 CONTINUE
C  DETERMINE LENGTH OF EACH RADIAL SPRING
C  INTERSECT SUCCESSIVELY WITH EACH CURB FACE AND WITH GROUND PLANE
      HJ = RW
      DO 10 K=1,NCRBM1
      IF(YCRBP(K).NE.YCRBP(K+1)) GO TO 20
      HJT = (YCRBP(K)-YP(I))/BMTX(2,3)
      ZJPT = ZP(I)+BMTX(3,3)*HJT
      IF(((ZJPT.GE.ZCRBP(K).AND.ZJPT.LE.ZCRBP(K+1)).OR.
     1    (ZJPT.LE.ZCRBP(K).AND.ZJPT.GE.ZCRBP(K+1))).AND.
     2                   (HJT.LT.HJ)) HJ=HJT
      GO TO 10
   20 HJT = (ZCRBP(K)-ZP(I)+(YP(I)-YCRBP(K))*TNPCRB(K))
     1     /(BMTX(3,3)-BMTX(2,3)*TNPCRB(K))
```

Fig. A-5 (cont.)

```
      YJPT = YP(I)+BMTX(2,3)*HJT
      IF(((YJPT.GE.YCRBP(K).AND.YJPT.LE.YCRBP(K+1)).OR.
     1     (YJPT.LE.YCRBP(K).AND.YJPT.GE.YCRBP(K+1))).AND.
     2                    (HJT.LT.HJ)) HJ=HJT
   10 CONTINUE
C  INTERSECT WITH LAST FACE
      HJT = (ZCRBP(NCRB)-ZP(I)+(YP(I)-YCRBP(NCRB))*TNPCRB(NCRB))
     1      /(BMTX(3,3)-BMTX(2,3)*TNPCRB(NCRB))
      YJPT = YP(I)+BMTX(2,3)*HJT
      IF((YJPT.GE.YCRBP(NCRB)).AND.(HJT.LT.HJ)) HJ=HJT
C  INTERSECT WITH GROUND
C  YJP MUST BE LESS THAN OR EQUAL TO YCRBP(1)
      HJT = (XLM2(I)-CAGZ(I)*XP(I)-CBGZ(I)*YP(I)-CGGZ(I)*ZP(I))
     1      /(BMTX(1,3)*CAGZ(I)+BMTX(2,3)*CBGZ(I)+BMTX(3,3)*CGGZ(I))
      YJPT = YP(I)+BMTX(2,3)*HJT
      IF((YJPT.LE.YCRBP(1)).AND.(HJT.LT.HJ)) HJ=HJT
      IF(HJ.LT.0.0.OR.HJ.GE.RW) GO TO 70
      XJP = XP(I)+BMTX(1,3)*HJ
      YJP = YP(I)+BMTX(2,3)*HJ
      ZJP = ZP(I)+BMTX(3,3)*HJ
      CAJ = (XP(I)-XJP)/HJ
      CBJ = (YP(I)-YJP)/HJ
      CGJ = (ZP(I)-ZJP)/HJ
      CALL INTRPL(FJP,RWHJB,RWHJE,DRWHJ,RW-HJ,FJ)
C  SUM CONTRIBUTION IN TRANSFORMED AXIS
      SFRX(I) = SFRX(I)+FJ*CAJ
      SFRY(I) = SFRY(I)+FJ*CBJ
      SFRZ(I) = SFRZ(I)+FJ*CGJ
   70 XJ = XJ+RAD
   99 CONTINUE

C  CHECK FOR SPRING TOTAL EFFECT IN ACTION
C  ZERO RESULTS AND RETURN IF NO ACTION
      FR(I) = SQRT(SFRX(I)**2+SFRY(I)**2+SFRZ(I)**2)
      IF(FR(I).NE.0.0)GO TO 110
      CAR(I) = 0.0
      CBR(I) = 0.0
      CGR(I) = 0.0
      HI(I) = RW
      RETURN

C  DETERMINE EQUIVALENT GCP AND SLOPES
  110 CAR(I) = -SFRX(I)/FR(I)
      CBR(I) = -SFRY(I)/FR(I)
      CGR(I) = -SFRZ(I)/FR(I)
      HI(I) = RW-FR(I)/AKT
      IF(HI(I).GT.RW-SIGT) GO TO 115
      HI(I) = RW-(FR(I)/AKT+SIGT*(XLAMT-1.0))/XLAMT
  115 XGPP(I) = XP(I)+HI(I)*CAR(I)
      YGPP(I) = YP(I)+HI(I)*CBR(I)
      ZGPP(I) = ZP(I)+HI(I)*CGR(I)
      DO 150 K=1,NSCHM1
      KSAVE = K
      IF(YGPP(I).GE.YPHIAV(K).AND.YGPP(I).LT.YPHIAV(K+1)) GO TO 160
   50 CONTINUE
      IF(YGPP(I).LT.YPHIAV(NSCH)) GO TO 200
      KSAVE=NSCH
```

Fig. A-5 (cont.)

```
C 160 THGI(I) = 0.0
C     PHGI(I) = PHIAVR(KSAVE)
      KSAVE=0
      HAUX=1.E25
      DO 310 K=1,NCRBM1
      IF(YCRBP(K).NE.YCRBP(K+1)) GO TO 320
      HAUXT = (YCRBP(K)-YP(I))/CBR(I)
      ZAUXT = ZP(I)+CGR(I)*HAUXT
      IF( (ZAUXT.GT.ZCRBP(K).AND.ZAUXT.GT.ZCRBP(K+1)) .OR.
     1    (ZAUXT.LT.ZCRBP(K).AND.ZAUXT.LT.ZCRBP(K+1)) .OR.
     2                    (HAUXT.GT.HAUX) ) GO TO 310
      HAUX=HAUXT
      KSAVE=K
      GO TO 310
  320 HAUXT = (ZCRBP(K)-ZP(I)+(YP(I)-YCRBP(K))*TNPCRB(K))
     1      /(CGR(I)-CBR(I)*TNPCRB(K))
      YAUXT = YP(I)+CBR(I)*HAUXT
      IF( (YAUXT.GT.YCRBP(K).AND.YAUXT.GT.YCRBP(K+1)) .OR.
     1    (YAUXT.LT.YCRBP(K).AND.YAUXT.LT.YCRBP(K+1)) .OR.
     2                    (HAUXT.GT.HAUX) ) GO TO 310
      HAUX=HAUXT
      KSAVE=K
  310 CONTINUE
      HAUXT = (ZCRBP(NCRB)-ZP(I)+(YP(I)-YCRBP(NCRB))*TNPCRB(NCRB))
     1      /(CGR(I)-CBR(I)*TNPCRB(NCRB))
      YAUXT = YP(I)+CBR(I)*HAUXT
      IF((YAUXT.LT.YCRBP(NCRB)).OR.(HAUXT.GT.HAUX)) GO TO 350
      HAUX=HAUXT
      KSAVE=NCRB
  350 HAUXT = (XLM2(I)-CAGZ(I)*XP(I)-CBGZ(I)*YP(I)-CGGZ(I)*ZP(I))
     1      /(CAR(I)*CAGZ(I)+CBR(I)*CBGZ(I)+CGR(I)*CGGZ(I))
      YAUXT = YP(I)+CBR(I)*HAUXT
      IF((YAUXT.GT.YCRBP(1)).OR.(HAUXT.GT.HAUX)) GO TO 360
      HAUX=HAUXT
      KSAVE=0
  360 IF(KSAVE.LE.0) GO TO 200
      THGI(I)=0.0
      PHGI(I)=PHCRBR(KSAVE)
  200 TCI = CAR(I)*CBYW(I)-CBR(I)*CAYW(I)
      TAI = CBR(I)*CGYW(I)-CGR(I)*CBYW(I)
      TBI = CGR(I)*CAYW(I)-CAR(I)*CGYW(I)
      CPG(I) = COS(PHGI(I))
      SPG(I) = SIN(PHGI(I))
      CTG(I) = COS(THGI(I))
      STG(I) = SIN(THGI(I))
      TERM1 = (TAI**2+TCI**2)*SPG(I)
      TERM2 = (TBI**2+TCI**2)*CPG(I)*STG(I)
      TERM3 = (TAI**2+TBI**2)*CPG(I)*CTG(I)
      TERM4 = TBI*CPG(I)*(TAI*STG(I)+TCI*CTG(I))
      TERM5 = TAI*(TBI*SPG(I)-TCI*CPG(I)*CTG(I))
      TERM6 = TCI*(TBI*SPG(I)-TAI*CPG(I)*STG(I))
      DN1 = TERM5+TERM2
      DN2 =-TERM1-TERM4
      DN3 = TERM6+TERM3
      TERM7 = SQRT(DN1**2+DN2**2+DN3**2)
      PHGI(I) = ARSIN(-DN2/TERM7)
      THGI(I) = ATAN(DN1/DN3)
```

Fig. A-5 (cont.)

```
      CPG(I) = COS(PHGI(I))
      SPG(I) = SIN(PHGI(I))
      CTG(I) = COS(THGI(I))
      STG(I) = SIN(THGI(I))
      RETURN
      END
```

APPENDIX B
VEHICLE PARAMETER MEASUREMENTS

In using the CALSVA program to simulate a curb, dike, or earthen end treatment, a rather comprehensive set of data is required to describe the impact vehicle. The most important parameters are those relating to the vehicle's suspension and inertia properties.

Making the necessary measurements requires a good deal of time and effort. Because of this time requirement, it was decided early in the program year that test vehicles ought to be standardized. With standardized test vehicles, measurements on a single vehicle were used to represent all vehicles.

The standard vehicle data, available as part of the CALSVA package, are for a 1963 Ford Galaxie, V-8 four-door sedan (Police Special). At the time of the current test series, vehicles of this type were no longer common and were difficult to find. It was also determined that the model representation was more applicable to vehicle handling types of investigations rather than the severe suspension bottoming, airborne maneuvers which could be expected in impact testing. Parameter values for the latter kinds of tests in many cases had either not been made or were very roughly approximated. It was therefore concluded that a new standardized test vehicle was required. After considering cost and availability, the vehicle chosen was a 1966 Ford Custom, six cylinder, two-door sedan. Six of these vehicles were purchased for use in the test program.

Vehicle parameter data in the CALSVA notation as used in the simulation exercises are given in Tables B-1 and B-2. Specific measured values which were obtained for individual automobiles is shown on Table B-3.

1966 FORD CUSTOM, SIX CYLINDER, TWO-DOOR SEDAN CALSVA INPUT DATA

Parameter	Definition	Value
A_0	Constant term in tire cornering stiffness parabola fitted properties	1,830 lb/rad.
A_1	Linear term in tire cornering stiffness parabola fitted properties	11.8 lb/rad.
A_2	Second-order term in tire cornering stiffness parabola fitted properties	2,960 lb.
A_3	Linear term in tire camber stiffness parabola fitted properties	1.78 rad.$^{-1}$
A_4	Second-order term in tire camber stiffness parabola fitted properties	3,600 lb.
a	Distance from the sprung mass center of gravity to the center line of the front wheels	53.9 in.
b	Distance from the sprung mass center of gravity to the center line of the rear wheels	65.1 in.
C_F'	Coulomb damping for a single front wheel, effective at the wheel.	97.6 lb.
C_R'	Coulomb damping for a single rear wheel effective at the spring	38.0 lb.
C_{FC}	Viscous damping coefficient for a single front wheel in compression, effective at the wheel	1.27 lb. sec.
C_{FE}	Viscous damping coefficient for a single front wheel in extension, effective at the wheel	3.05 lb sec/i
C_{RC}	Viscous damping coefficient for a single rear wheel in compression, effective at the wheel	3.39 lb sec/i
C_{RE}	Viscous damping coefficient for a single rear wheel in extension, effective at the wheel	10.20 lb sec.i
C_ψ'	Coulomb resistance in steering system, effective at the wheels (both sides included)	1,360 in. lb.
I_R	Rear unsprung mass moment of inertia about a line through its center of gravity and parallel to the vehicle x axis.	426 in. lb. se

Parameter	Definition	Value
I_x	Moment of inertia about the vehicle X axis	6,090 in lb sec^2
I_y	Moment of inertia about the vehicle Y axis	22,090 in lb sec^2
I_z	Moment of inertia about the vehicle Z axis	27,480 in lb sec^2
I_{xz}	Product of inertia about the vehicle X and Z axis	-192 in lb sec^2
I_x	Moment of inertia of steering system, effective at front wheels (both sides included)	492 in lb sec^2
K_{FC}	Coefficient of complete suspension bumper term for compression at the front wheel, effective at the wheel	8,000 lb/in
K_{FC}'	Coefficient of the cubic term within the suspension bumper force expression for the front wheel in compression, effective at the wheel	0
K_{FE}	Coefficient of complete suspension bumper term for extension at the front wheel, effective at the wheel	1,091 lb/in
K_{FE}'	Coefficient of cubic term within the suspension bumper force expression for the front wheel in extension, effective at the wheel	0
K_{RC}	Coefficient of complete suspension bumper term for compression at the axle, effective at the spring	-17.8 lb/in
K_{RC}'	Coefficient of cubic term within the suspension bumper force expression for the rear axle, effective at the spring	1,470 lb/in
K_{RE}'	Coefficient of cubic term within the suspension bumper force expression for the rear axle in extension, effective at the spring	0
K_{RS}	Rear axle roll-steer coefficient (positive for roll understeer)	-.190 in/in

Parameter	Definition	Value
K_T	Radial tire spring rate in linear range for a single tire	1,225 lb/in
K_ψ	Load deflection spring rate of elastic stops in the steering system, effective at the wheels (both sides included)	3,000 in lb/rad
M_S	Sprung mass	7.769 lb sec^2/in
M_{UF}	Front unsprung mass (both sides)	.551 lb sec^2/in
M_{UR}	Rear unsprung mass	.750 lb sec^2/in
R_F	Auxiliary roll stiffness in excess of the front wheel spring rates in ride at the front suspension	129,200 in lb/r
R_R	Auxiliary roll stiffness in excess of the rear spring rates and spacing at the rear suspension	0
R_W	Undeflected wheel radius	13.94 in.
T_F	Tread at the front suspension	61.75 in.
T_R	Tread at the rear suspension	61.875 in.
T_S	Distance between spring connections for solid rear axle	37.5 in.
X_{VF}	Distance from center of gravity to front of vehicle	86.1 in
X_{VR}	Distance from center of gravity to rear of vehicle	120.9 in.
Y_V	Distance of center of gravity to side of vehicle	39.0 in.
Z_F	Static distance along the Z axis between the center of gravity of the sprung mass and the center of gravity of the front unsprung masses. (The centers of gravity of the individual front masses are assumed to coincide with the wheel centers)	13.1 in.

Parameter	Definition	Value
Z_R	Static distance along the Z axis between the center of gravity of the sprung mass and the roll center of the rear axle.	15.0 in.
Z_{VB}	Vertical clearance from ground to vehicle body	11.0 in.
Z_{VT}	Vertical height of vehicle center of gravity above Z_{VB} dimension	12.0 in.
λ_F	Multiple of K_F for computing front suspension stop spring rate	0.5
λ_R	Multiple of K_R for computing rear suspension stop spring rate	0.5
λ_T	Multiple of K_T for computing in nonlinear range of tire deflection	14.2
μ	Tire to ground friction coefficient	0.8
ρ	Distance between center of gravity of rear axle and rear roll center, positive for roll center above center of gravity	-2.0 in.
δ_T	Maximum radial tire deflection for linear deflection range	5.0 in.
Ω_{FC}	Maximum suspension deflection from static equilibrium for linear front spring deflection range in compression	-3.25 in.
Ω_{FE}	Maximum suspension deflection from static equilibrium for linear front spring deflection range in extension	2.7 in.
Ω_{RC}	Maximum suspension deflection from static equilibrium for linear rear spring deflection range in compression	-5.0 in.
Ω_{RE}	Maximum suspension deflection from static equilibrium for linear rear spring deflection range in extension	1.875 in.
Ω_T	Multiple of A_2 at which the assumed parabolic variations of small-angle cornering and camber stiffness with tire loading are abandoned to preclude reversal in the sign of the side force under conditions of excessive tire loading	0.8-1.0

Parameter	Definition	Value
Ω_{ψ}	Angular deflection of steering system at which elastic stops are encountered	0.54 rad.

TABLE B-2

FRONT WHEEL CAMBER ANGLE, ϕ_c VS. SUSPENSION DEFLECTION, δ_F

δ_F(in.)	ϕ_c(deg.)
-7	-4.575
-6	-3.545
-5	-2.58
-4	-1.63
-3	-0.875
-2	-0.166
-1	0.125
0	0.25
1	0.042
2	-0.46
3	-1.17
4	-2.42

TABLE B-3

MEASURED PARAMETERS FOR INDIVIDUAL VEHICLES

Parameter	Vehicle #1	#2	#3	#4	#5	#6
W	3,404	3,465	3,438	3,330	3,376	3,366
a	52.5	53.4	53.9	53.3	53.5	54.0
b	66.5	65.6	65.1	65.7	65.5	65.0
$h_{c.g.}$	22.84	22.67	22.84	22.89	22.69	22.53
Z_f	9.80	9.63	9.80	9.85	9.65	9.49
Z_r	11.50	11.33	11.50	11.55	11.35	11.19
X_{VF}	81.6	82.5	83.0	82.4	82.6	83.1
X_{VR}	125.4	124.5	124.0	124.6	124.4	123.9
Ω_{FE}	2.76	2.76	2.76	2.70	2.89	2.98
Ω_{FC}	-5.39	-3.34	-5.39	-3.40	-5.26	-5.17
Ω_{RE}	1.9	2.0	1.9	1.9	2.1	2.4
Ω_{RC}	-5.0	-4.9	-5.0	-5.0	-4.8	-4.5

APPENDIX C

BARREL ANGLE END TREATMENT MATHEMATICAL IDEALIZATION

In using the BARRIER V computer program [53], it is required that a mathematical idealization of the simulated structure be developed. The idealization consists of a two-dimensional assemblage of beams, cables, posts, springs, pinned links, and damping devices. The automobile is modeled as a body of shape prescribed by the user which is surrounded by inelastic springs. During impact, the dynamic interaction between the vehicle and barrier is solved by using step-by-step, inelastic, large displacement, structural analysis methods.

The barrel angle end treatment mathematical idealization is shown on Figure C-1. The numbered nodal points represent joints between structural elements. Coordinates of the points and properties of the member elements for a typical run are listed on Table C-1. Also listed are the position of each member between nodes, the designation of member type (i.e., a type designation of 112 signifies a type 12 beam element since beams are coded as the 100 series), and its prestress. In general, the information is self explanatory.

Features of the idealization include:

1. Barrel crush characteristics which are represented by eight connected beams. Crushing occurs through bending

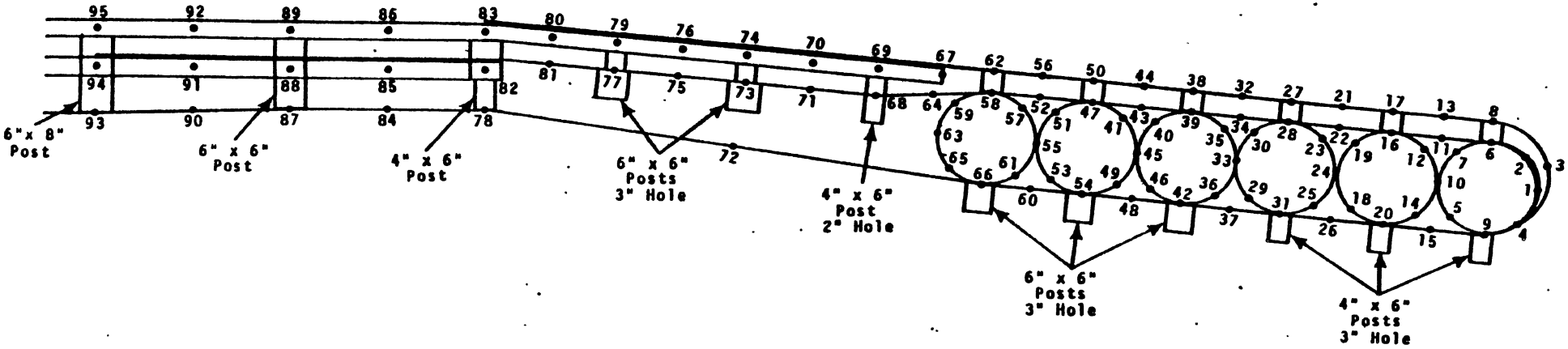

FIGURE C-1 BARREL ANGLE END TREATMENT MATHEMATICAL IDEALIZATION

at the nodal points.

2. Beam and pinned link representations of certian beam members so as to account for both bending and column mode failure.

The idealization has been found to duplicate test results very closely (see Section 3.4). Further, it has provided needed insight into the end treatment performance for impact conditions substantially different than those prevailing in the test. The result has been a substantial increase in understanding, but at far less cost than would have been required for corresponding test series.

The versatility of the idealization also promises to be an aid in evaluating end treatment modofications.

BARREL ANGLE END MOD#2 - END-ON IMPACT - ZERO DEGREES AT 60 MPH

TABLE C-1

STRUCTURE CONTROL DATA

NUMBER OF NODAL POINTS	=	95
NUMBER OF INTERFACES	=	2
NUMBER OF ELEMENTS	=	184
NUMBER OF ELEMENT SERIES	=	3
NUMBER OF EXTRA MASSES	=	12
BASIC TIME STEP (SEC)	=	0.00200
LARGEST ALLOWABLE TIME STEP (SEC)	=	0.00800
MAXIMUM TIME SPECIFIED (SEC)	=	0.20000
MAX. NO. OF STEPS WITH NO CONTACT	=	5
OVERSHOOT INDEX	=	1
ROTATIONAL DAMPING MULTIPLIER	=	2.00

OUTPUT FREQUENCIES

VEHICLE DATA	=	1
BARRIER DEFLECTIONS	=	5
BARRIER FORCES	=	5
PUNCHED JOINT DATA	=	5
PUNCHED TRAJECTORY	=	1

TABLE C-1 (cont.)

POINT	X-ORD	Y-ORD
1	99.17	150.36
2	101.22	143.36
3	97.50	146.85
4	102.72	156.87
5	116.23	156.53
6	107.73	140.08
7	114.73	143.02
8	107.70	136.82
9	109.72	159.92
10	118.29	149.53
11	117.29	139.97
12	120.84	142.53
13	117.26	135.99
14	121.84	156.04
15	119.28	159.09
16	126.85	139.13
17	126.82	135.15
18	135.35	154.86
19	133.85	141.35
20	128.84	158.25
21	136.38	134.32
22	136.41	138.30
23	139.45	140.86
24	137.41	147.86
25	140.95	154.37
26	138.40	157.42
27	145.93	133.48
28	145.96	137.46
29	154.46	153.18
30	152.96	139.67
31	147.95	156.58
32	155.49	132.64
33	156.52	146.18
34	155.52	136.62
35	158.57	139.18
36	160.07	152.69
37	157.51	155.75
38	165.05	131.81
39	165.08	135.79
40	172.08	138.00
41	177.68	137.51
42	167.07	154.91
43	174.63	134.95
44	174.60	130.97
45	175.63	144.51
46	173.58	151.51
47	184.19	134.12
48	176.63	154.08
49	179.18	151.02
50	184.16	130.14
51	191.19	136.33
52	193.75	133.28
53	192.69	149.84
54	186.18	153.24
55	194.75	142.84

TABLE C-1 (cont.)

56	193.72	129.30
57	196.80	135.84
58	203.31	132.44
59	210.31	134.66
60	195.74	152.40
61	198.30	149.35
62	203.28	129.46
63	213.93	141.17
64	214.64	133.07
65	211.81	148.17
66	205.30	151.56
67	212.83	127.63
68	225.98	133.70
69	225.29	126.54
70	237.74	125.45
71	238.43	132.61
72	252.65	142.46
73	250.88	131.52
74	250.19	124.36
75	263.33	130.43
76	262.64	123.27
77	275.79	129.34
78	300.00	134.19
79	275.10	122.18
80	287.55	121.09
81	288.24	128.67
82	300.00	128.00
83	300.00	120.00
84	318.75	134.19
85	318.75	128.00
86	318.75	120.00
87	337.50	134.19
88	337.50	128.00
89	337.50	120.00
90	356.25	134.69
91	356.25	128.00
92	356.25	120.00
93	375.00	135.19
94	375.00	128.00
95	375.00	120.00

TABLE C-1 (cont.)

INTERFACE 1

62,	56,	50,	44,	38,	32,	27,	21,	17,	13,
9,	3,	4,	9,	15,	20,	26,	31,	37,	42,
48,	54,	60,	66,						

INTERFACE 2

58,	52,	47,	43,	39,	34,	28,	22,	16,	11,
6,	2,	1,	4,	5,	14,	18,	25,	29,	36,
46,	49,	53,	61,	65,					

FRICTION COEFFICIENTS ALONG INTERFACES

INTERFACE	COEFF
1	0.0
2	0.0

BEAM ELEMENTS, 100 SERIES

TABLE C-1 (cont.)

TYPE NUMBER	=	1	2	3	4	5	6	7	8
M. OF I. (IN4)	=	2.265D 00	4.531D 00	4.531D 00	4.395D-03	4.395D-03	4.395D-03	4.395D-03	4.395D-03
AREA (IN2)	=	1.996D 00	3.496D 00	3.496D 00	1.000D-10	1.000D-10	1.000D-10	1.000D-10	1.000D-10
LENGTH (IN)	=	1.875D 01	1.875D 01	1.250D 01	1.875D 01	1.250D 01	4.807D 01	1.150D 01	9.594D 00
YOUNGS MODULUS (KSI)	=	3.000D 04	3.000D 04	3.000D 04	3.000D 04	3.000D 04	3.000D 04	3.000D 04	3.000D 04
WEIGHT (LB/FT)	=	7.200D 00	1.230D 01	1.230D 01	5.100D 00	5.100D 00	5.100D 00	5.100D 00	5.100D 00
YIELD FORCE (K)	=	1.250D 02	1.615D 02	1.615D 02	1.000D 02	1.000D 02	1.000D 02	1.000D 02	1.000D 02
YIELD MOMENT (K.IN)	=	8.560D 01	1.204D 02	1.204D 02	1.150D 00	1.150D 00	1.150D 00	1.150D 00	1.150D 00
YIELD ACCURACY LIMIT	=	1.000D-01	1.000D-01	1.000D-01	1.000D-01	1.000D-01	1.000D-01	1.000D-01	1.000D-01

TYPE NUMBER	=	9	10	11	12	13	14	15	16
M. OF I. (IN4)	=	4.395D-03	7.490D-03	7.490D-03	6.610D-03	7.490D-03	7.490D-03	7.490D-03	7.490D-03
AREA (IN2)	=	1.000D-10	3.070D-01	3.070D-01	7.800D-01	3.070D-01	3.070D-01	3.070D-01	3.070D-01
LENGTH (IN)	=	1.430D 01	8.000D 00	1.619D 01	7.340D 00	4.000D 00	1.012D 01	1.419D 01	6.000D 00
YOUNGS MODULUS (KSI)	=	3.000D 04	3.000D 04	3.000D 04	3.000D 04	3.000D 04	3.000D 04	3.000D 04	3.000D 04
WEIGHT (LB/FT)	=	5.100D 00	2.000D 00	4.000D 00	2.500D 00	1.000D 00	3.000D 00	4.000D 00	2.000D 00
YIELD FORCE (K)	=	1.000D 02	1.200D 01	1.200D 01	3.110D 01	1.200D 01	1.200D 01	1.200D 01	1.200D 01
YIELD MOMENT (K.IN)	=	1.150D 00	5.000D 00	5.000D 00	1.020D 01	5.000D 00	5.000D 00	5.000D 00	5.000D 00
YIELD ACCURACY LIMIT	=	1.000D-01	1.000D-01	1.000D-01	1.000D-01	1.000D-01	1.000D-01	1.000D-01	1.000D-01

TABLE C-1 (cont.)

TYPE NUMBER	=	1	2	3	4	5	6
STIFFNESS ON A AXIS (K/IN)	=	3.5000-01	3.0000-01	8.0000 00	4.5000 00	1.0000 03	3.8000-01
STIFFNESS ON B AXIS (K/IN)	=	7.5000-01	6.5000-01	8.0000 00	6.0000 00	1.0000 03	8.0000-01
EFFECTIVE WEIGHT (LB)	=	3.6000 01	3.6000 01	5.5000 01	5.4000 01	1.0000 03	3.6000 01
YIELD FORCE ON A AXIS (K)	=	8.9000-01	6.7000-01	9.3000 00	4.6500 00	1.0000 03	1.3300 00
YIELD FORCE ON B AXIS (K)	=	2.8900 00	2.6200 00	9.3000 00	8.1400 00	1.0000 03	3.0000 00
YIELD ACCURACY LIMIT	=	1.0000-01	1.0000-01	1.0000-01	1.0000-01	1.0000-01	1.0000-01
A DEFLN AT FAILURE (IN)	=	3.5000 00	3.0000 00	3.0000 00	2.0000 00	1.0000 02	4.5000 00
B DEFLN AT FAILURE (IN)	=	5.5000 00	5.0000 00	3.0000 00	2.2500 00	1.0000 02	6.0000 00

PINNED LINKS, 700 SERIES

TABLE C-1 (cont.)

TYPE NUMBER	=	1	2	3	4	5	6
AREA (IN2)	=	1.5000 00	1.5000 00	1.5000 00	1.5000 00	1.5000 00	1.5000 00
LENGTH (IN)	=	1.8750 01	1.2500 01	4.8070 01	1.1500 01	9.5940 00	1.4300 01
YOUNGS MODULUS (KSI)	=	3.0000 04	3.0000 04	3.0000 04	3.0000 04	3.0000 04	3.0000 04
WEIGHT (LB/FT)	=	0.0	0.0	0.0	0.0	0.0	0.0
YIELD FORCE (K)	=	4.5000 01	4.5000 01	4.5000 01	4.5000 01	4.5000 01	4.5000 01
BUCKLING FORCE	=	9.2500-01	1.8120 00	1.4070-01	2.5250 00	3.5420 00	1.5900 00
YIELD ACCURACY LIMIT	=	2.0000-01	2.0000-01	2.0000-01	2.0000-01	2.0000-01	2.0000-01

TABLE C-1 (cont.)

MEMBER	I-NODE	J-NODE	TYPE	F OR F(A) M(I),	F(B) OR SLACK	M(J) OR ANGLE
1	1	2	112	0.0	0.0	0.0
2	2	6	112	0.0	0.0	0.0
3	6	7	112	0.0	0.0	0.0
4	7	10	112	0.0	0.0	0.0
5	5	10	112	0.0	0.0	0.0
6	5	9	112	0.0	0.0	0.0
7	4	9	112	0.0	0.0	0.0
8	1	4	112	0.0	0.0	0.0
9	10	12	112	0.0	0.0	0.0
10	12	16	112	0.0	0.0	0.0
11	16	19	112	0.0	0.0	0.0
12	19	24	112	0.0	0.0	0.0
13	18	24	112	0.0	0.0	0.0
14	18	20	112	0.0	0.0	0.0
15	14	20	112	0.0	0.0	0.0
16	10	14	112	0.0	0.0	0.0
17	23	24	112	0.0	0.0	0.0
18	23	28	112	0.0	0.0	0.0
19	28	30	112	0.0	0.0	0.0
20	30	33	112	0.0	0.0	0.0
21	29	33	112	0.0	0.0	0.0
22	29	31	112	0.0	0.0	0.0
23	25	31	112	0.0	0.0	0.0
24	24	25	112	0.0	0.0	0.0
25	33	35	112	0.0	0.0	0.0
26	35	39	112	0.0	0.0	0.0
27	39	40	112	0.0	0.0	0.0
28	40	45	112	0.0	0.0	0.0
29	45	46	112	0.0	0.0	0.0
30	42	46	112	0.0	0.0	0.0
31	36	42	112	0.0	0.0	0.0
32	33	36	112	0.0	0.0	0.0
33	41	45	112	0.0	0.0	0.0
34	41	47	112	0.0	0.0	0.0
35	47	51	112	0.0	0.0	0.0
36	51	55	112	0.0	0.0	0.0
37	53	55	112	0.0	0.0	0.0
38	53	54	112	0.0	0.0	0.0
39	49	54	112	0.0	0.0	0.0
40	45	49	112	0.0	0.0	0.0
41	55	57	112	0.0	0.0	0.0
42	57	58	112	0.0	0.0	0.0
43	58	59	112	0.0	0.0	0.0
44	59	63	112	0.0	0.0	0.0
45	63	65	112	0.0	0.0	0.0
46	65	66	112	0.0	0.0	0.0
47	61	66	112	0.0	0.0	0.0
48	55	61	112	0.0	0.0	0.0
49	60	66	108	0.0	0.0	0.0
50	54	60	108	0.0	0.0	0.0
51	48	54	108	0.0	0.0	0.0
52	42	48	108	0.0	0.0	0.0
53	37	42	108	0.0	0.0	0.0
54	31	37	108	0.0	0.0	0.0
55	26	31	108	0.0	0.0	0.0
56	20	26	108	0.0	0.0	0.0

TABLE C-1 (cont.)

57	15	20	108	0.0	0.0	0.0
58	9	15	108	0.0	0.0	0.0
59	6	11	108	0.0	0.0	0.0
60	8	13	108	0.0	0.0	0.0
61	11	16	108	0.0	0.0	0.0
62	13	17	108	0.0	0.0	0.0
63	16	22	108	0.0	0.0	0.0
64	17	21	108	0.0	0.0	0.0
65	22	28	108	0.0	0.0	0.0
66	21	27	108	0.0	0.0	0.0
67	28	34	108	0.0	0.0	0.0
68	27	32	108	0.0	0.0	0.0
69	34	39	108	0.0	0.0	0.0
70	32	38	108	0.0	0.0	0.0
71	39	43	108	0.0	0.0	0.0
72	38	44	108	0.0	0.0	0.0
73	43	47	108	0.0	0.0	0.0
74	44	50	108	0.0	0.0	0.0
75	47	52	108	0.0	0.0	0.0
76	50	56	108	0.0	0.0	0.0
77	52	58	108	0.0	0.0	0.0
78	56	62	108	0.0	0.0	0.0
79	62	67	108	0.0	0.0	0.0
80	58	64	107	0.0	0.0	0.0
81	64	68	107	0.0	0.0	0.0
82	68	71	105	0.0	0.0	0.0
83	71	73	105	0.0	0.0	0.0
84	73	75	105	0.0	0.0	0.0
85	75	77	105	0.0	0.0	0.0
86	77	81	105	0.0	0.0	0.0
87	81	82	107	0.0	0.0	0.0
88	66	72	106	0.0	0.0	0.0
89	72	78	106	0.0	0.0	0.0
90	78	84	104	0.0	0.0	0.0
91	84	87	104	0.0	0.0	0.0
92	87	90	104	0.0	0.0	0.0
93	90	93	104	0.0	0.0	0.0
94	67	69	103	0.0	0.0	0.0
95	69	70	103	0.0	0.0	0.0
96	70	74	103	0.0	0.0	0.0
97	74	76	103	0.0	0.0	0.0
98	76	79	103	0.0	0.0	0.0
99	79	80	103	0.0	0.0	0.0
100	80	83	103	0.0	0.0	0.0
101	83	86	101	0.0	0.0	0.0
102	86	89	101	0.0	0.0	0.0
103	89	92	101	0.0	0.0	0.0
104	92	95	101	0.0	0.0	0.0
105	82	85	102	0.0	0.0	0.0
106	85	88	102	0.0	0.0	0.0
107	88	91	102	0.0	0.0	0.0
108	91	94	102	0.0	0.0	0.0
109	93	0	305	0.0	0.0	0.0
110	87	0	303	0.0	0.0	0.0
111	78	0	306	0.0	0.0	0.0
112	77	0	304	0.0	0.0	5.0000 00
113	73	0	304	0.0	0.0	5.0000 00
114	68	0	301	0.0	0.0	5.0000 00

TABLE C-1 (cont.)

119	20	0	302	0.0	0.0	5.0000 00
120	9	0	302	0.0	0.0	5.0000 00
121	3	8	109	0.0	0.0	0.0
122	3	4	107	0.0	0.0	0.0
123	93	94	110	0.0	0.0	0.0
124	93	95	111	0.0	0.0	0.0
125	87	88	116	0.0	0.0	0.0
126	87	89	115	0.0	0.0	0.0
127	78	82	116	0.0	0.0	0.0
128	78	83	115	0.0	0.0	0.0
129	77	79	114	0.0	0.0	0.0
130	73	74	114	0.0	0.0	0.0
131	68	69	114	0.0	0.0	0.0
132	58	62	113	0.0	0.0	0.0
133	47	50	113	0.0	0.0	0.0
134	38	39	113	0.0	0.0	0.0
135	27	28	113	0.0	0.0	0.0
136	16	17	113	0.0	0.0	0.0
137	6	8	113	0.0	0.0	0.0
138	60	66	705	0.0	0.0	0.0
139	54	60	705	0.0	0.0	0.0
140	48	54	705	0.0	0.0	0.0
141	42	48	705	0.0	0.0	0.0
142	37	42	705	0.0	0.0	0.0
143	31	37	705	0.0	0.0	0.0
144	26	31	705	0.0	0.0	0.0
145	20	26	705	0.0	0.0	0.0
146	15	20	705	0.0	0.0	0.0
147	9	15	705	0.0	0.0	0.0
148	6	11	705	0.0	0.0	0.0
149	8	13	705	0.0	0.0	0.0
150	11	16	705	0.0	0.0	0.0
151	13	17	705	0.0	0.0	0.0
152	16	22	705	0.0	0.0	0.0
153	17	21	705	0.0	0.0	0.0
154	22	28	705	0.0	0.0	0.0
155	21	27	705	0.0	0.0	0.0
156	28	34	705	0.0	0.0	0.0
157	27	32	705	0.0	0.0	0.0
158	34	39	705	0.0	0.0	0.0
159	32	38	705	0.0	0.0	0.0
160	39	43	705	0.0	0.0	0.0
161	38	44	705	0.0	0.0	0.0
162	43	47	705	0.0	0.0	0.0
163	44	50	705	0.0	0.0	0.0
164	47	52	705	0.0	0.0	0.0
165	50	56	705	0.0	0.0	0.0
166	52	58	705	0.0	0.0	0.0
167	56	62	705	0.0	0.0	0.0
168	62	67	705	0.0	0.0	0.0
169	58	64	704	0.0	0.0	0.0
170	64	68	704	0.0	0.0	0.0
171	68	71	702	0.0	0.0	0.0
172	71	73	702	0.0	0.0	0.0
173	73	75	702	0.0	0.0	0.0
174	75	77	702	0.0	0.0	0.0
175	77	81	702	0.0	0.0	0.0
176	81	82	704	0.0	0.0	0.0

177	66	72	703	0.0	0.0	0.0
178	72	78	703	0.0	0.0	0.0
179	78	84	701	0.0	0.0	0.0
180	84	87	701	0.0	0.0	0.0
181	87	90	701	0.0	0.0	0.0
182	90	93	701	0.0	0.0	0.0
183	3	8	706	0.0	0.0	0.0
184	3	4	704	0.0	0.0	0.0

TABLE C-1 (cont.)

JOINT	WEIGHT(LB)
6	3.5000 00
16	3.5000 00
28	3.5000 00
39	3.5000 00
47	3.5000 00
58	3.5000 00
68	3.5000 00
73	3.5000 00
77	3.5000 00
78	1.0400 01
87	1.0400 01
93	1.0400 01

TABLE C-1 (cont.)

TABLE C-1 (cont.)

VEHICLE PROPERTIES

WEIGHT (LB)	=	3.5000 03
MOMENT OF INERTIA (LB.IN.SEC2)	=	3.3000 04
NO. OF CONTACT POINTS	=	20
NO. OF WHEELS	=	4
BRAKE CODE (1=ON, 0=OFF)	=	0
NO. OF OUTPUT POINTS	=	1

CONTACT POINT COORDINATES (IN), AND SPRING STIFFNESSES (K/IN)

POINT	R-ORD	S-ORD	K1	K2	K3	ROT DIST
1	-122.00	-39.00	3.0000 01	1.8000 02	2.4000 02	1.5000 01
2	88.00	-39.00	3.0000 01	1.8000 02	2.4000 02	1.5000 01
3	88.00	-24.00	8.7500 00	5.2500 01	7.0000 01	1.5000 01
4	88.00	-19.00	3.7500 00	2.2500 01	3.0000 01	1.5000 01
5	88.00	-15.00	2.5000 00	1.5000 01	2.0000 01	1.5000 01
6	88.00	-12.00	2.0800 00	1.2500 01	1.6670 01	1.5000 01
7	88.00	-10.00	1.6700 00	1.0000 01	1.3330 01	1.5000 01
8	88.00	-8.00	2.9200 00	1.7500 01	2.3330 01	1.5000 01
9	88.00	-3.00	4.5800 00	2.7500 01	3.6670 01	1.5000 01
10	88.00	3.00	3.7500 00	2.2500 01	3.0000 01	1.5000 01
11	88.00	6.00	1.6700 00	1.0000 01	1.3330 01	1.5000 01
12	88.00	7.00	8.3000-01	5.0000 00	6.6700 00	1.5000 01
13	88.00	8.00	8.3000-01	5.0000 00	6.6700 00	1.5000 01
14	88.00	9.00	1.6700 00	1.0000 01	1.3330 01	1.5000 01
15	88.00	12.00	2.5000 00	1.5000 01	2.0000 01	1.5000 01
16	88.00	15.00	2.5000 00	1.5000 01	2.0000 01	1.5000 01
17	88.00	18.00	3.7500 00	2.2500 01	3.0000 01	1.5000 01
18	88.00	24.00	8.7500 00	5.2500 01	7.0000 01	1.5000 01
19	88.00	39.00	3.0000 01	1.8000 02	2.4000 02	1.5000 01
20	-122.00	39.00	3.0000 01	1.8000 02	2.4000 02	1.5000 01

WHEEL COORDINATES (IN), STEER ANGLES (DEG), AND DRAG FORCES (LB)

POINT	R-ORD	S-ORD	STEER ANGLE	DRAG FORCE
1	53.00	29.00	0.0	460.00
2	53.00	-29.00	0.0	460.00
3	-66.00	-29.00	0.0	372.00
4	-68.00	29.00	0.0	372.00

OUTPUT POINT COORDINATES (IN)

POINT	R-ORD	S-ORD
1	0.0	0.0

APPENDIX D

IMPACT ACCELERATION MEASUREMENTS

Impact accelerations were recorded by means of accelerometers for tests 22 through 26. Test 22 involved an angle impact on a sodium silicate foam impact attenuator while tests 23 through 26 were of various varieties of guardrail end treatments.

Accelerations were recorded along each of three orthogonal directions fixed to the vehicle body. The accelerometers were mounted on a rigid plate. The plate in turn, was rigidly attached to the vehicle body at the longitudinal C.G. position, roughly in the position of the left front seat. The two cross-members used to support the seat were used as plate attachment points.

Accelerometers used in the measurements were of the quartz crystal type manufactured by the Kistler Instrument Corporation. These are devices which are sold under the trade name of "Piezotron" —the specific units being classified as Model 818. Selected specifications are listed in Table D-1. A typical low frequency response characteristic is shown on Figure D-1. Response is flat out to about 4,000 Hz.

Since the devices do not respond to a DC signal, there is a "drooping" of the output signal if it remains of one sign for an extended period of time. The drooping effect occurs according to an equivalent "storage time constant" of 0.25 sec. This means that if a step acceleration were impressed upon a Piezotron, the input/output relationship would be as indicated on Figure D-2.

TABLE D-1

PIEZOTRON MODEL 818 SPECIFICATIONS

Range	±250g
Electronic Noise	$\leq$0.01g rms
Sensitivity	10 mv/g
Resonant Frequency	30kHz
Amplitude Linearity	±1%
Temperature Sensitivity	0.03%/$^{o}_{F}$
Output Voltage	±2.5V

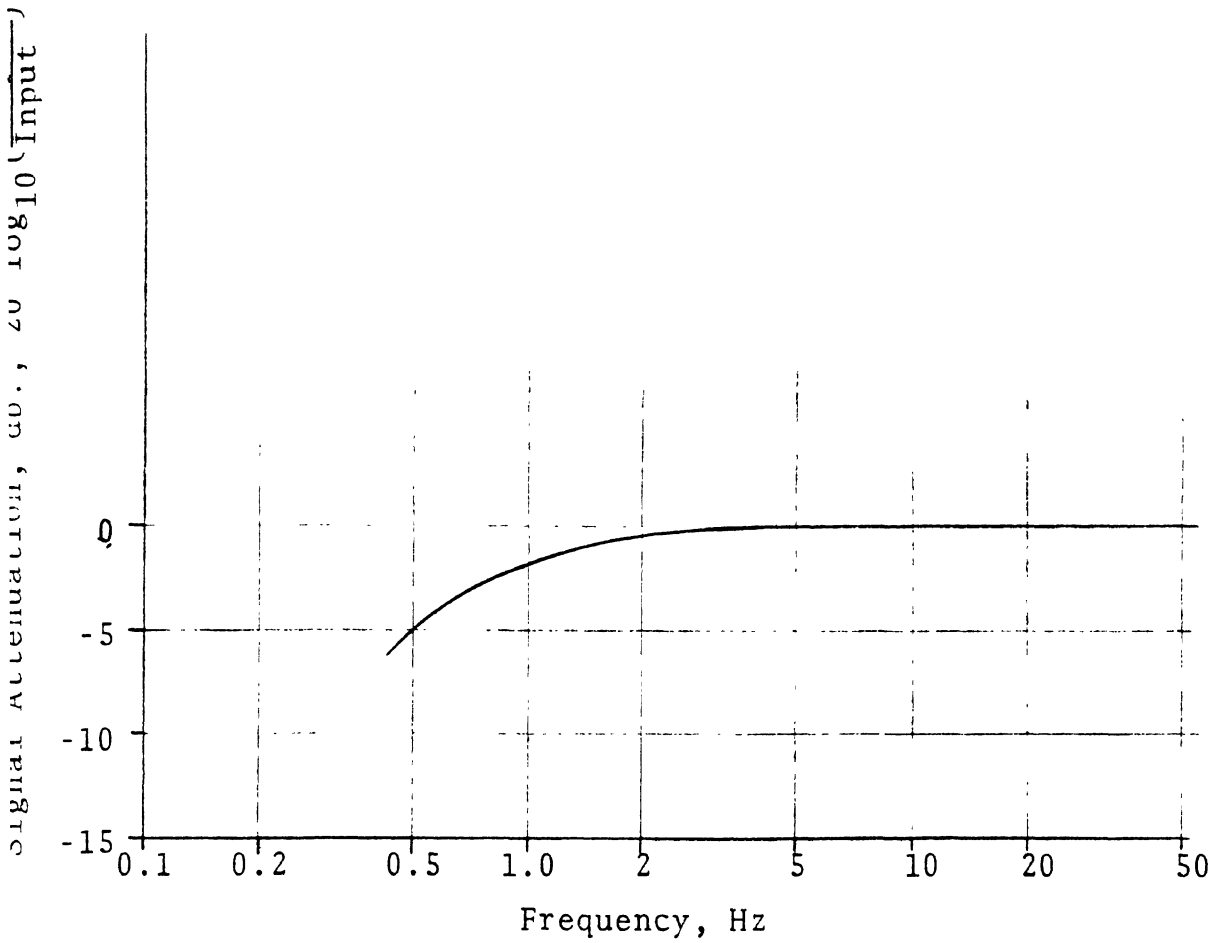

FIGURE D-1 TYPICAL PIEZOTRON LOW FREQUENCY CHARACTERISTIC

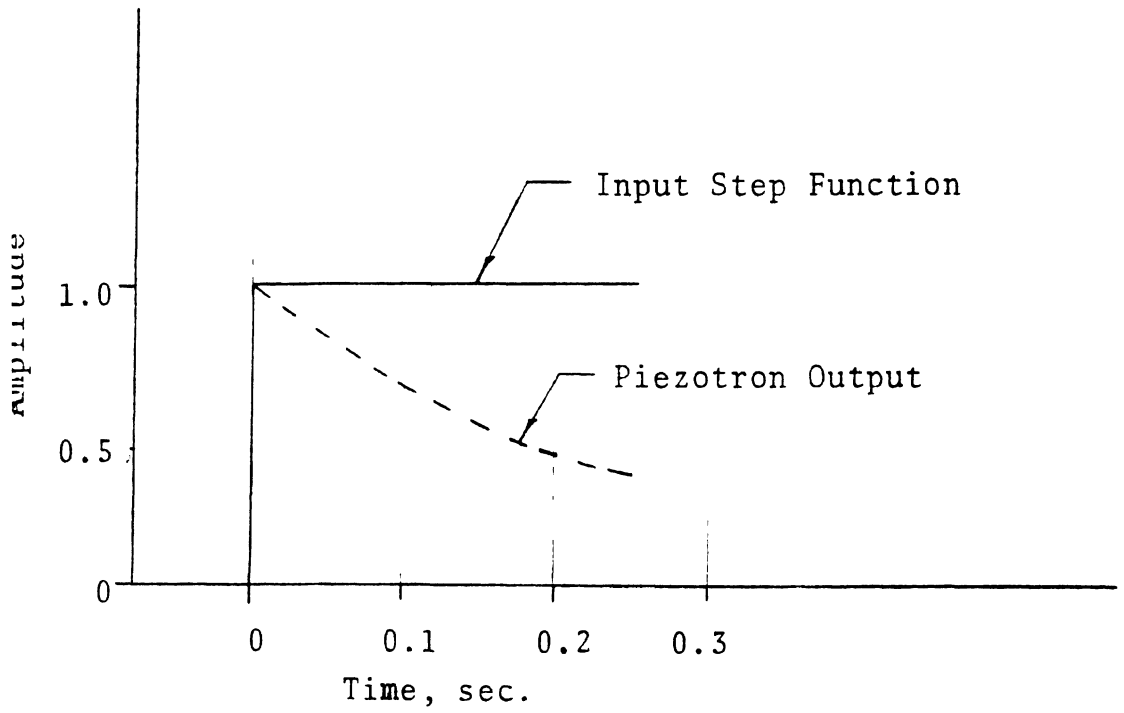

FIGURE D-2 PIEZOTRON STORAGE TIME CONSTANT CHARACTERISTIC

The output would follow the input very closely as the step is applied, but would trail off from the DC input level as shown. In most of the tests, the acceleration changes sign rapidly enough so that the drooping effect is of little consequence. On some occasions, however, drooping undoubtedly colors the results. These cases are discussed appropriately.

Data for each of the tests is shown on the remaining figures and is discussed as follows:

D.1 TEST 22 SODIUM SILICATE IMPACT ABSORBING BARRIER

This test involved a vehicle striking a sodium silicate impact absorbing barrier configuration [58]. The test speed was about 61 mph and the impact angle relative to traffic flow was about 19°.

As indicated on Figure D-3, acceleration values appear to be relatively modest until about 340 msec into the impact. At this point, the longitudinal acceleration begins to increase markedly. This increase corresponds to the point where the vehicle begins to pocket in the barrier. Decelerations exceeding 5 g's (see Table E-4) last for about 96 msec as shown by the indicated interval. The average acceleration during this period is about 12 g's, however, with a peak of about 28 g's. Although the entire interval is less than 100 msec, the drooping effect mentioned earlier probably causes as much as a 30% drop in amplitude near the end of the interval. Thus, the actual decelerations were undoubtedly somewhat higher than shown.

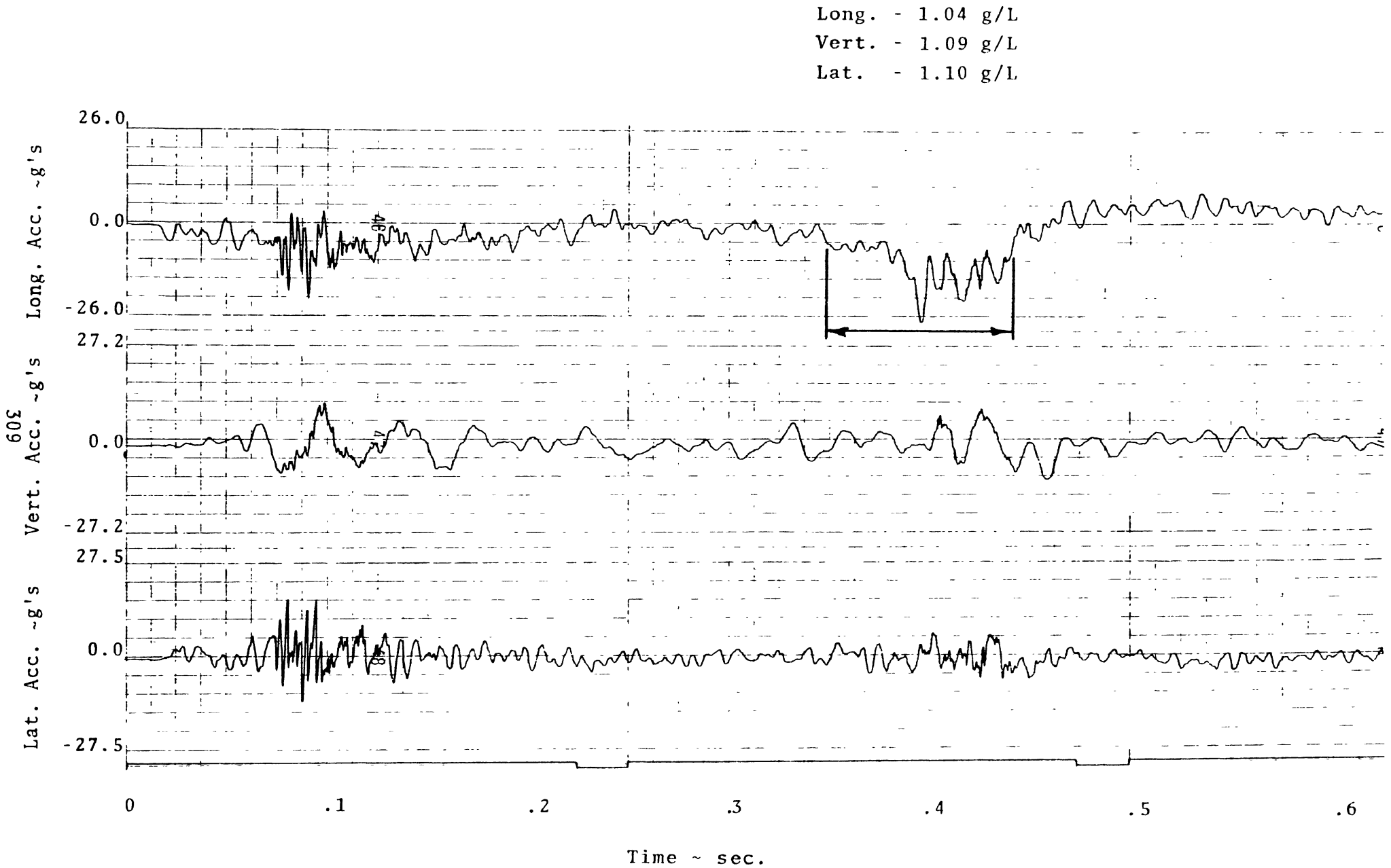

FIGURE D-3. TEST 22 ACCELERATION HISTORIES (IMPACT ABSORBING BARRIER, VELOCITY≈61 MPH, ANGLE≈19°)

Vertical and lateral accelerations did not appear to be excessive, or to be affected by drooping.

D.2 TEST 23 BARREL SWEEP GUARDRAIL END

This test involved a vehicle striking a guardrail end configuration. The test speed and angle were about 56 mph and 24°, respectively.

As shown on Figure D-4, longitudinal acceleration remains below 5 g's until about 75 msec following initial impact. At this point, it begins to increase, eventually reaching a peak of about 20 g's. The interval of acceleration over 5 g's lasts for about 160 msec and corresponds to the vehicle pocketing in the end section. The average longitudinal acceleration over this period is about 9 g's. Drooping of the signal is again a factor, and errors near the end of the interval on the order of 30 to 40% are probable.

A second major impact event occurs at about 500 msec. Although peaks in longitudinal acceleration up to 14 g's occur, the average acceleration over the next 100 msec is modest. This event probably corresponds to a secondary collision of the vehicle with the guardrail end anchor.

Vertical and lateral acceleration measurements were never excessive, although each peaked at about 13 g's during the second impact event. Drooping was not a factor in either of these acceleration histories.

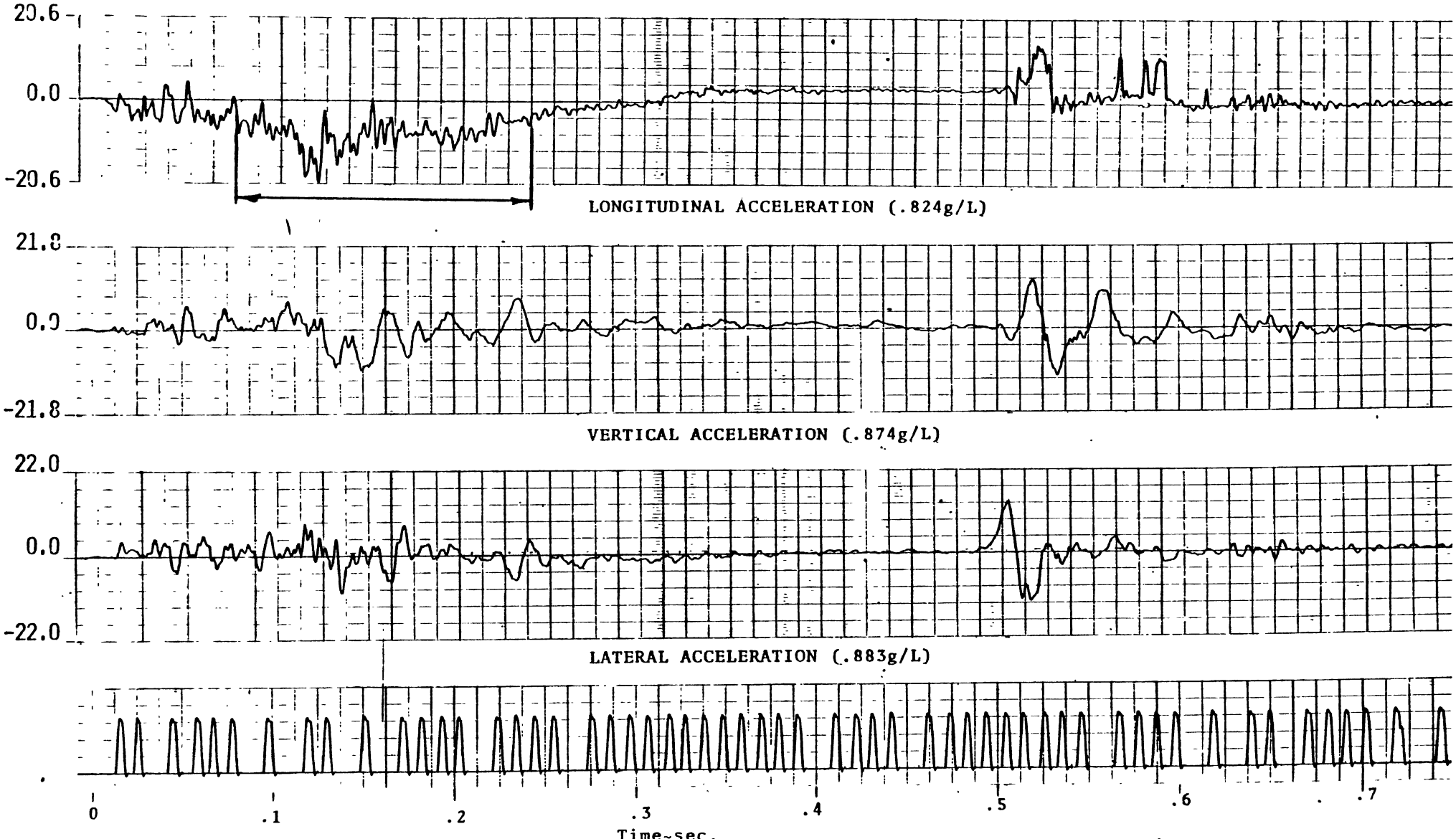

FIGURE D-4. TEST 23 ACCELERATION HISTORIES (BARREL SWEEP GUARDRAIL END, VELOCITY=56 MPH, ANGLE=24°)

D.3 TEST 24 BARREL ANGLED GUARDRAIL END

The guardrail end which was evaluated in this test is shown on Figure 3-5. The vehicle was directed into the structure at a point near the fifth barrel from the end. Speed and angle were 56 mph and 25°, respectively.

The acceleration traces shown on Figure D-5 were rather oscillatory in all three directions. Short interval peaks of up to 17 g's were recorded but these were not sustained long enough to be of serious consequence. No interval of sustained acceleration over 5 g's lasted more than about 20 msec. Drooping was never a factor.

D.4 TEST 25 CURVED RADIUS GUARDRAIL END

In this test, the impact speed was about 62 mph and the angle was 25°.

The acceleration traces (Figure D-6) as for test 24, again appear to be largely oscillatory. A period of about 195 msec. occurs in the longitudinal acceleration history, however, wherein the average acceleration is aobut 6 g's. The interval begins at about 360 msec. into the test. Although the interval is long, the average acceleration of 6 g's is not much over the injury threshold as indicated in Table E-4.

It is interesting to note that in both tests 24 and 25, a pattern of positive acceleration spikes was recorded in the longitudinal acceleration trace. The interval between spike varies

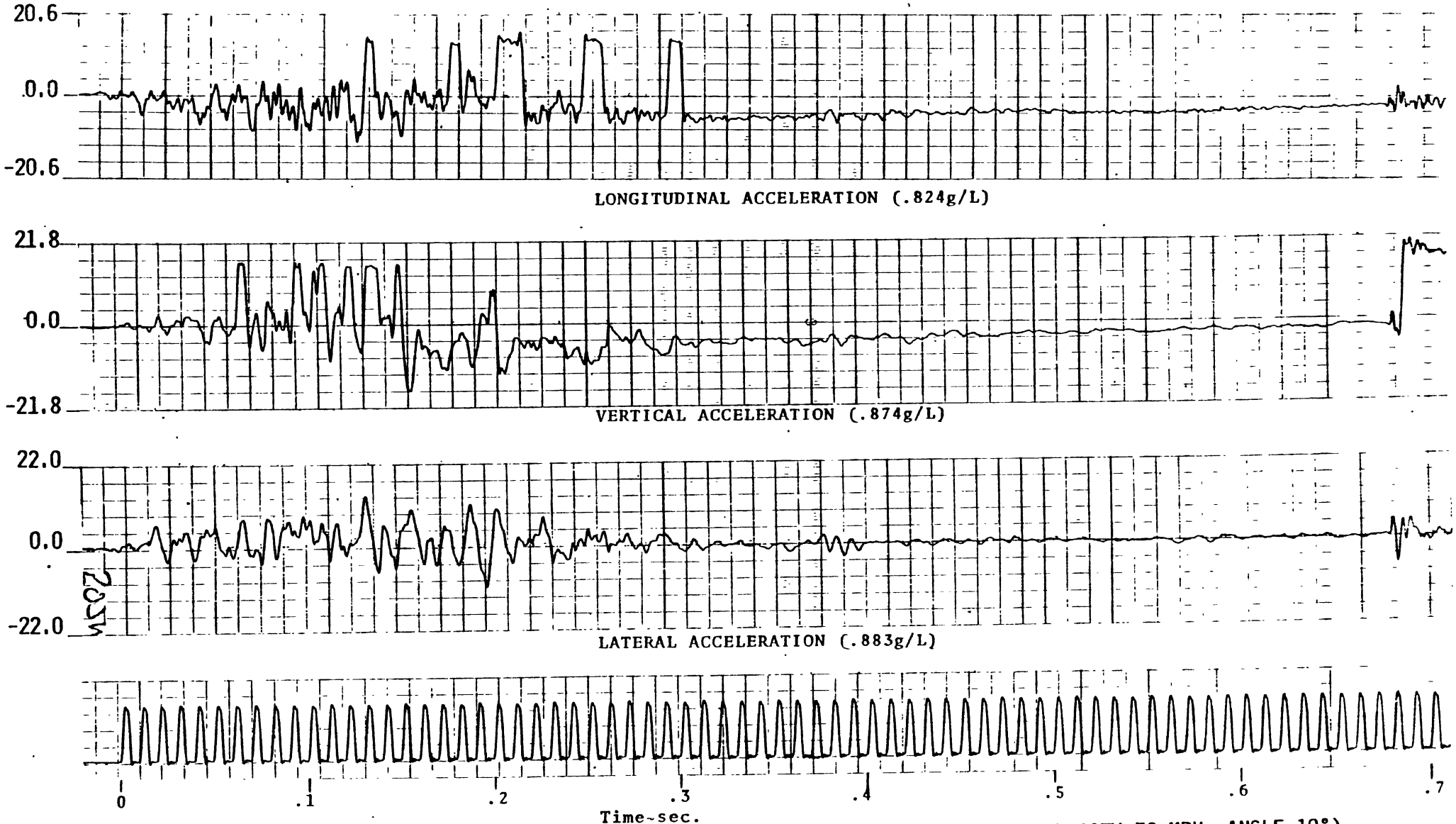

FIGURE D-5. TEST 24 ACCELERATION HISTORIES (BARREL ANGLED GUARDRAIL END, VELOCITY=56 MPH, ANGLE=10°)

FIGURE D-6. TEST 25 ACCELERATION HISTORIES (CURVED RADIUS GUARDRAIL END, VELOCITY=62 MPH, ANGLE=25°)

between 30 and 60 msec, which corresponds to a car movement of about two to six feet per interval. Two possible explanations are given for the presence of the spikes.

First of all, it must be concluded that the vehicle is storing energy in some way as it strikes the barrier, so that it springs back to produce the positive accelerations. Next, it seems likely that the spikes are in some way connected with the redirection process since both vehicles were redirected. One explanation would then seem to involve the guardrail alternately being compressed and then springing back as the car is turned. The actions in the guardrail would then show up as oscillating accelerations of the vehicle.

A second explanation involves a possible interaction of the vehicle and the guardrail posts. Posts were spaced at two and three feet for the structure tested in test 24, and this corresponds to an interval of 30 to 40 msec (roughly the same as that noted for the spikes), at the probable vehicle speed during impact. Posts were spaced at about six feet apart for test 25 and the acceleration spike interval (at least for the first four spikes) was about 60 msec. A six-foot spacing would correspond to about an 80 msec interval, however. Therefore, the correlation is not clear cut.

At any rate, the spike phenomena seems to be characteristic of redirection and is probably related to the vehicle/guardrail elastic interaction.

D.5 TEST 26 CORRUGATED CONDUIT GUARDRAIL END

Speed and angle for this test were 26 mph and 25°, respectively.

The acceleration traces for the test are shown on Figure D-7. Due to the low impact velocity, acceleration levels along all three axes were relatively modest. A 17 g peak acceleration of very short duration was recorded in the longitudinal direction, with similar values of 11 g's and 10 g's in the vertical and lateral directions, respectively. Average acceleration values are below 3 g's for all intervals exceeding 100 msec, however.

Positive spikes were again present in the longitudinal acceleration trace. Only two were found, however, and these were spaced 164 msec apart. The wider spacing suggests again that vehicle speed is a factor in the phenomena.

D.6 IMPACT ACCELERATION FREQUENCY CONTENT

In order to gain a partial understanding of the frequency spectrum associated with the measured acceleration data, the data for one of the tests was run through a series of low-pass filters. The filters ranged in cut-off frequency from 1 Hz to 200 Hz. The resulting acceleration traces are shown on Figure D-8.

The filter type used in the exercises was a third order maximally flat, or Butterworth type which can be represented by the equation:

$$T_3(s) = \frac{1}{\left(\frac{s}{\omega_e} + 1\right)\left(\frac{s^2}{\omega_c^2} + \frac{s}{\omega_c} + 1\right)} \qquad \text{(D-1)}$$

FIGURE D-7. TEST 26 ACCELERATION HISTORIES (CORRUGATED CONDUIT GUARDRAIL END, VELOCITY=26 MPH, ANGLE=25°

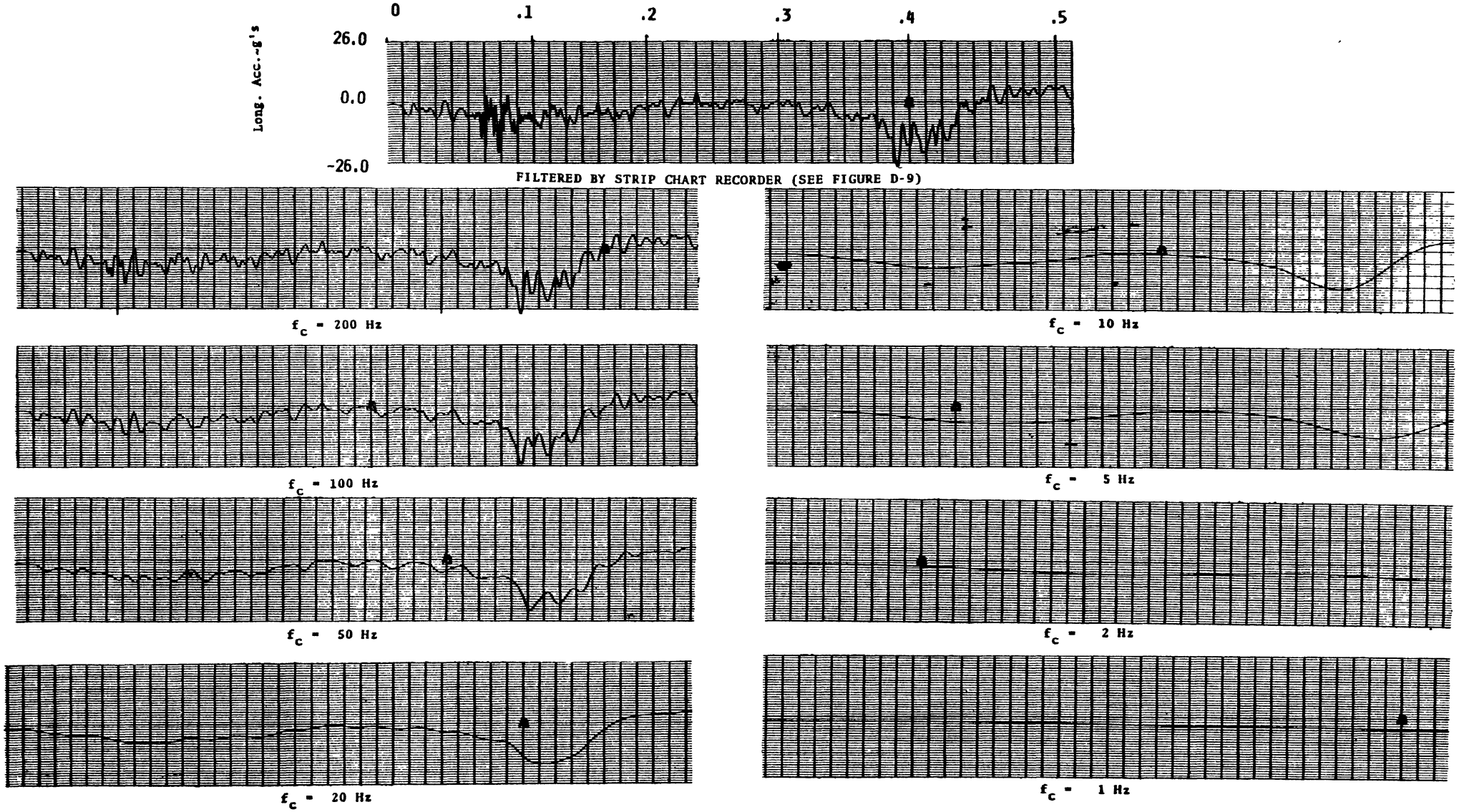

FIGURE D-8. TEST 22 LONGITUDINAL ACCELERATION AS AFFECTED BY VARIOUS OUTPUT FILTERS

where ω_c is the cut-off frequency equal to $2\pi f_c$, where f_c is in Hz.

Referring back to Figure D-8 now, the signal trace shown is the longitudinal acceleration history for test 22. The curve at the top is the raw data signal as it is filtered by the strip chart recorder (see Figure D-9). On the left and downward in sequence are signals with cut-off frequencies starting at 200 Hz and going down to 1 Hz on the lower right.

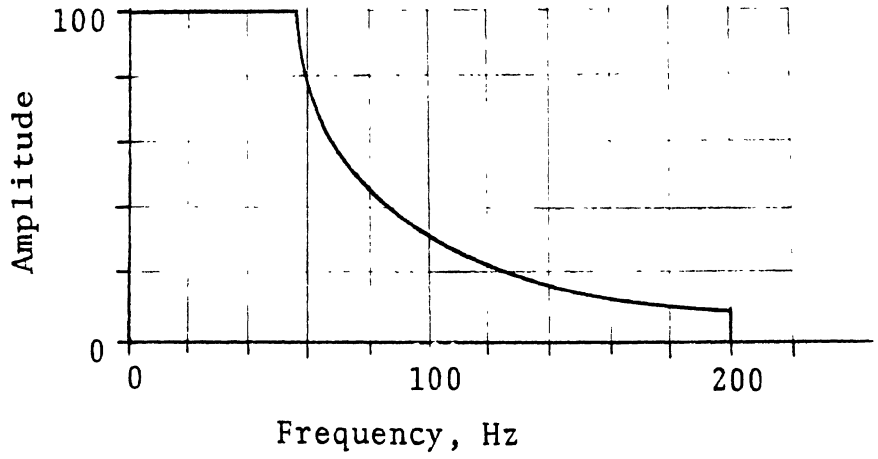

FIGURE D-9 STRIP CHART RECORDER FREQUENCY RESPONSE

It is obvious that as the cut-off frequency is reduced, the peak acceleration becomes lower and is moved to the right in time. This points up the fact that one should be careful in specifying peak acceleration without referring to the level of signal filtering.

For a 1 Hz cut-off frequency, the signal has become almost flat. There is a discernable signal movement, however, which confirms the fact that the accelerometer is functioning even at this low frequency level (The accelerometer frequency response characteristic shown on Figure D-1 would, of course, suggest this.)

APPENDIX E

BARRIER DEVELOPMENT PROCEDURES

Systematic barrier development procedures are described in detail in this appendix. The development process is outlined in Figure E-1. A discussion of the entire process would be lengthy, therefore, only the following topics indicated on the figure are considered:

1. The Operational Environment
2. Operational Requirements
3. Functional Requirements
4. Performance Measures

These are areas which are of specific importance in the current program and each will be discussed where appropriate in terms of the specific barrier systems which are treated in this report.

Design guidelines, an additional topic, have been included in the main discussion sections since these are more pertinent to operational applications.

E.1 THE OPERATIONAL ENVIRONMENT

The operational environment, in the case of barrier development, consists of the following factors:

1. The full range of impact conditions to which the barrier may be expected to be exposed;
2. The limits of load tolerance of a vehicle occupant reacting to the impact forces;
3. The entire range of additional factors (i.e., soil

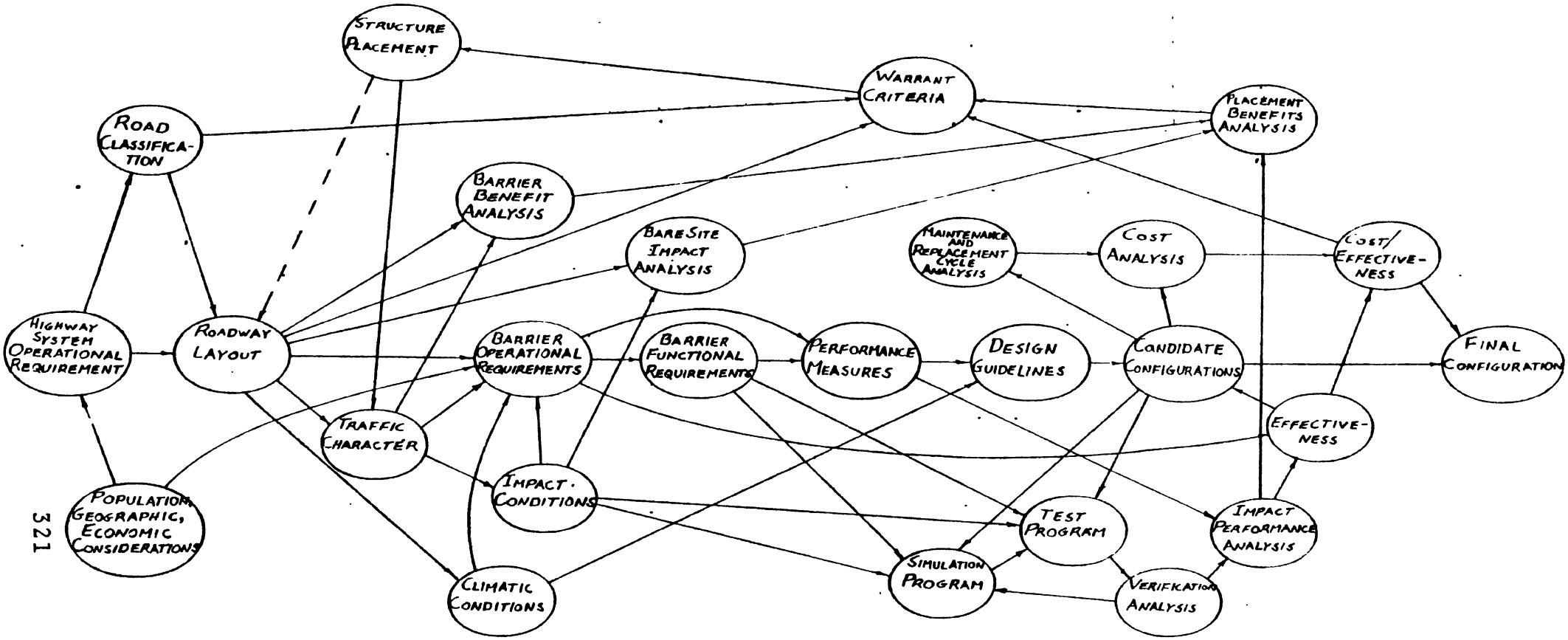

FIGURE E-1 BARRIER DEVELOPMENT PROCEDURE OUTLINE

properties, freezing conditions, snow accumulation, etc.) which tend to produce geographical and seasonal variations in barrier performance.

Significant impact conditions include vehicle weight, velocity, and collision angle. Distributions of these, from operational survey data, are given in tabular form, in Tables E-1 through E-3.

TABLE E-1 VEHICLE WEIGHT DISTRIBUTION

Weight, (1000 lb):	1-2	2.0-2.5	2.5-3.0	3.0-3.5	3.5-4.0	4.0-4.5	>4.5
%	2.2	1.2	5.9	19.4	33.8	23.3	14.2

TABLE E-2 SPEED DISTRIBUTIONS

Speed (mph):	<30	30-40	40-50	50-60	60-70	70-80	>80
Passenger: Survey %	---	0.2	3.4	21.1	45.0	28.0	2.3
Passenger: Estimate %	4.6	5.7	8.9	22.0	34.3	20.9	2.6
Commercial: Survey %	---	0.7	12.0	57.4	29.6	0.3	---
Commercial: Estimate %	16.8	12.4	20.5	38.1	9.9	2.2	0.2

TABLE E-3 ANGLE DISTRIBUTION

Angle (deg):	0-5	5-10	10-15	15-20	20-25	>25
%	37	24	19	8	2	10

The weight data [41], clearly indicates that a preponderance of vehicles weigh between 1,500 and 4,500 pounds (more than 85%).

There is a significant percentage in categories larger than 4,500 pounds, however, with the maximum weight measured being 190,000 pounds.

Impact velocity data is difficult to arrive at because of probable differences between highway speeds and actual impact speeds after some braking has occurred. Velocity data was therefore taken from two sources: actual highway speed survey data [42], and impact speed data as estimated by investigating police officers [43]. From these data, it is evident that the range of applicable impact speeds for passenger vehicles is between 40 and 80 mph and for commercial vehicles between 30 and 70 mph. This covers between 88 and 98% of the speeds listed for passenger vehicles and between 83 and 99% of those listed for trucks and buses.

The approach angle data [44] indicates that the operational range here, varies between 0° and 25°. Approach angle cannot be considered a separate parameter, independent of velocity, however. The maximum impact angle cannot exceed an angle which is determined by the minimum turning radius of the vehicle and the lateral distance of its path from the barrier. The factors controlling the relationship [45] include velocity, road/tire friction coefficient, road surface camber (super-elevation), and road curvature. Care should be taken, therefore, in selecting angle and velocity conditions which are compatible.

Human tolerance to injury can be correlated with the time histories of injury related kinematic variables as a vehicle

strikes a barrier. As presently understood [39], the variables that influence occupant injury are: incremental change in velocity, acceleration, and acceleration onset. Velocity change manifests itself in the relative velocity achieved by a passenger in a secondary collision with the vehicle interior; acceleration and acceleration onset through the internal loading and deformation of body parts. Of the three, least is known about the effects of acceleration onset.

The level, direction, and duration of action of these variables are generally considered in assigning tolerance levels. The situation is influenced by several factors, however, some of which include passenger restraint, age, vital condition, and body orientation. Therefore, a sharp cut-off between injury and no injury in terms of kinematic variables does not exist and injury assessment on this basis can only be made in a general sense. Working range thresholds in terms of the current state of the art are listed in Table E-4 [39, 40, 45]:

TABLE E-4

KINEMATIC INJURY THRESHOLD LEVELS

Variable	Restraint					
	Unrestrained		Lap Belt Restrained		Lap Belt and Shoulder Harness Restrained	
	Level	Duration	Level	Duration	Level	Duration
a_x(longitudinal)	5 g's	100-200 msec	10 g's	100-200 msec	25 g's	100-200 msec
a_y(lateral	3 g's	100-200 msec	5 g's	100-200 msec	15 g's	100-200 msec
a_z(vertical)	10 g's	100-200 msec	20 g's	100-200 msec	20 g's	100-200 msec
ΔV_x	12 ft/sec	N/A	15 ft/sec	N/A	30 ft/sec	N/A
ΔV_y	12 ft/sec	N/A	15 ft/sec	N/A	25 ft/sec	N/A
ΔV_z	12 ft/sec	N/A	25 ft/sec	N/A	40 ft/sec	N/A

No threshbld is indicated for $\frac{da}{dt}$ (acceleration onset) because of the general lack of reliable experimental data.

The remaining factors which go to make up the operational environment are indicated in the detailed design considerations shown on Figure E-2.

E.2 OPERATIONAL REQUIREMENTS

A systematic barrier development procedure requires that barrier operational requirements be established in the initial stages. These can then be used as a base for measuring the system effectiveness for the remainder of the program.

The foremost objective in traffic barrier design is to minimize personal injury in ran-off-the-road accidents. The second objective, must be concerned with minimizing the total sum of economic costs, with the third and least important consideration being the esthetic appearances of the design.

In considering personal injury, the first priority must be to potential victims who are not directly involved in the initial accident. This suggests that the first operational requirement should be concerned with containing the accident so as not to involve innocent vehicles. The next consideration is then to occupants in the errant vehicle, itself.

Ideally, operational requirements, so derived, would be based on coverage of the entire range of operational impact conditions as described previously. More practically, however, economic

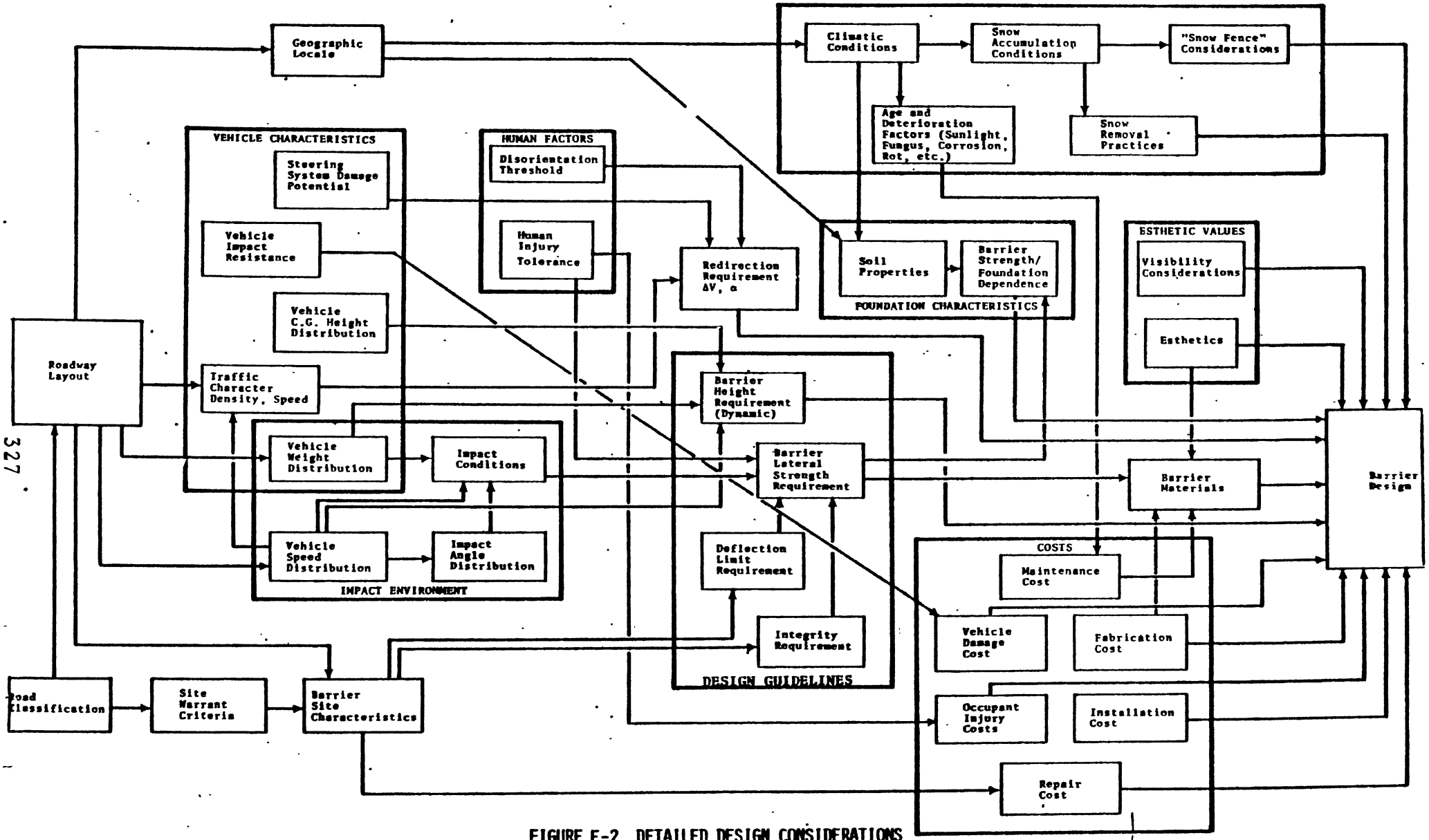

FIGURE E-2 DETAILED DESIGN CONSIDERATIONS

considerations dictate requirements that satisfy a more limited set of conditions. For example, as shown in Appendix A, 85% of the vehicle population weighs less than 4,500 pounds, but the heaviest vehicles weigh upwards of 190,000 pounds. A barrier designed to cover 100% of the range of vehicle weights would be at least an order of magnitude more expensive than one which covered 85%. A compromise on complete effectiveness is therefore necessary.

Before going to the next section, it should be remarked that a set of operational requirements should be established as a goal which deals with solving a particular problem in the most comprehensive and ideal way. A second set of requirements should also be established, however, which are within the practical limits of current technology and economics [66]. One purpose of operational requirements is to stimulate innovation. Therefore, the performance expected by eventual users must be stressed. Too much reliance on a slowly changing set of "practical requirements" often inhibits technological growth and serves to close the way to the development and introduction of new ideas. Therefore, a set of ideal requirements must be available as a carrot for stimulating improvement.

E.3 FUNCTIONAL REQUIREMENTS AND PERFORMANCE MEASURES

Functional requirements take the form of specific statements about what a barrier should or should not do in carrying out the general functions outlined under operational requirements.

Performance measures consist of those quantities, variables,

or phenomenological events which can be used in determining the barrier effectiveness.

E.4 SPECIFIC REQUIREMENTS AND MEASURES

In the remaining part of this appendix, specific operational requirements, functional requirements, and performance measures are listed for each of the four roadside traffic structures discussed in this report.

E.4.1 GUARDRAIL END TREATMENTS

E.4.1.1 Operational Requirements.

1. An errant vehicle must either be brought to rest by the end treatment, or be redirected in front of, or behind the parent guardrail.
2. In protecting the occupants of the errant vehicle, the end treatment must not allow penetration to the hazardous area which the guardrail separates from the roadway. In so doing, the end treatment must be capable of functioning over as broad a range of impact conditions as is economically practical.
3. In interacting with the vehicle, the end treatment shall not impart forces which will result in injury to unrestrained occupants over the range of impact conditions stipulated in 2.

E.4.1.2 Functional Requirements.

1. The end treatment structure shall not penetrate the vehicle passenger compartment.

2. The end treatment structure shall not entrap the vehicle either through pocketing or wheel snagging such that high decelerations result.
3. The end treatment structure shall not induce the vehicle to overturn about either its pitch or roll axis.
4. The end treatment structure shall not cause the vehicle to be vaulted into the air as the result of the structure acting as a ramp.
5. If the vehicle is redirected back into the traffic stream, the end treatment structure shall not:
   a. cause the vehicle to be redirected at an angle which will create a traffic hazard,
   b. cause the steering system to be damaged,
   c. cause the driver to be jostled to the extent he is unable to carry out the steering function.

E.4.1.3 Performance Measures. Guardrail end treatment performance measures are listed in Table E-5.

E.4.2 BARRIER CURBS.

E.4.2.1 Operational Requirements. The order of objectives in barrier curb design is very similar to that for a guardrail end, i.e.:

1. Personal injury
2. Costs
3. Esthetics

TABLE E-5

GUARDRAIL END TREATMENT PERFORMANCE MEASURES

Guardrail	Vehicle	Vehicle/Guardrail
1. Lateral Resistance History	1. Injury Related Kinematic Variables	1. Spearing
2. Longitudinal Resistance History	2. Pitch Over	2. Ramping
3. Vertical Resistance History	3. Roll Over	3. Redirection Character
4. Warranted Section Integrity	4. Stopping Distance	4. Contact Interval
5. End Anchorage Integrity	5. Airborne Distance	5. Undercarriage Snagging
6. Repair Cost	6. Exit Trajectory	
	7. Exit Attitude History	
	8. Deformation	
	9. Steering Damage	
	10. Damage Cost	

As before, the first priority is to potential victims not directly involved in the initial vehicle/curb encounter. Next in order would follow the passengers of the errant vehicle itself. Loads imparted to vehicle occupants in a curb impact are generally somewhat below those which would cause injury, however, and occupant injury is therefore of less concern. In addition, it would appear that one primary purpose in installing a barrier curb rather than a guardrail is to reduce vehicle damage. If this purpose is to be accomplished, the curb must be relatively low, or have a specially designed reflective cross section. A low curb will almost always be below the vehicle c.g., however, and will therefore reflect a smaller percentage of the errant vehicle population than would a guardrail. Therefore, in achieving lower vehicle damage costs, a lower redirective efficiency must be accepted. (As was pointed out in Section 5, however, a barrier curb backed up by a guardrail can be used to realize the best advantages of both the curb and the guardrail.) With these ideas established, barrier curb operational requirements are listed as follows:

1. An errant vehicle must either be brought to rest by the barrier curb or be safety redirected back into the traffic st
2. In protecting the occupants of the errant vehicle, the barrier curb shall resist vehicle penetration to the hazardous area which the curb separates from the roadway. In so doing, the barrier curb must be capable of redirecting vehicles over as broad a range of impact conditions as is practica consistent with minimum vehicle damage.

E.4.2.2 Functional Requirements.

1. The barrier curb shall not induce the vehicle to overturn about its pitch or roll axis.
2. The barrier curb shall not entrap a vehicle tire in the curb face so as to cause the vehicle to spin-out.
3. In redirecting a vehicle, the barrier curb shall not:
   a. cause the vehicle to be redirected at an angle which will create a traffic hazard
   b. cause the steering system to be damaged
   c. cause the driver to be jostled to the extent that he is unable to carry out the steering function
   d. cause anything other than minor vehicle body damage.

E.4.2.3 Performance Measures. Barrier curb performance measures are listed in Table E-6.

E.4.3 CURB/GUARDRAIL COMBINATIONS

E.4.3.1 Operational Requirements. Operational requirements for a curb/guardrail combination follow along lines very similar to those for a guardrail end. The main difference is that redirection behind the guardrail is not an acceptable performance mode. Priorities pertaining to injury, cost, and esthetics remain the same, however. Curb/guardrail operational requirements are therefore listed as follows:

TABLE E-6

CURB PERFORMANCE MEASURES

Curb	Vehicle	Vehicle/Curb
1. Critical Speed	1. Loss of Control Related Kinematic Variables	1. Redirection Character
2. Lateral Resistance History	2. Exit Trajectory	2. Dynamic Jump Phenomenon
	3. Exit Attitude History	3. Contact Interval
	4. Pitch Over	
	5. Roll Over	
	6. Steering Damage	

1. An errant vehicle must either be brought to rest by the curb/guardrail, or be safely redirected back into the traffic stream.
2. In protecting the occupants of the errant vehicle, the curb/guardrail must not allow penetration to the hazardous area which the curb/guardrail separates from the roadway. In so doing, the curb/guardrail must be capable of functioning over as broad a range of impact conditions as is economically practical.
3. The curb/guardrail shall not impart forces to the impacting vehicle which will result in injury to unrestrained occupants over the range of impact conditions stipulated in 2.

E.4.3.2 Functional Requirements.

1. The curb/guardrail shall not entrap the vehicle either through pocketing or wheel snagging such that high decelerations result.
2. The curb/guardrail shall not induce the vehicle to over-turn about either its pitch or roll axis.
3. In redirecting the vehicle back in to the traffic stream, the curb/guardrail shall not:
   a. cause the vehicle to be redirected at an angle which will create a traffic hazard,
   b. cause the steering system to be damaged,
   c. cause the driver to be jostled to the extent he is unable to carry out the steering function.

4. An impacting vehicle shall neither break through, vault over, nor wedge under the guardrail.

5. Dynamic interaction between the curb and guardrail during an impact shall be negligible.

E.4.3.3 Performance Measures. Performance measures used in determining curb/guardrail effectiveness are given in Table E-7.

E.4.4 MEDIAN DIKES.

E.4.4.1 Operational Requirements. The order of objectives in dike design are:

1. Personal injury
2. Costs

Unlike the previous structures, esthetics plays a small role since dikes very often go unnoticed by the general traveling public. As in the other cases, however, the first priority is to potential victims not directly involved in the vehicle/dike encounter. The second priority would go to occupants of the errant vehicle, with vehicle damage being the third order of priority.

Operational requirements are listed as follows:

1. The errant vehicle must be deflected and/or brought to rest by the dike prior to its entering the opposing traffic lane.
2. In interacting with the vehicle, the dike shall not impart forces which will result in injury to an unrestrained passenger. The dike shall be designed to function in this manner over as broad a range of impact conditions as is practical.

TABLE E-7

CURB/GUARDRAIL COMBINATION PERFORMANCE MEASURES

Curb/Guardrail	Vehicle	Vehicle/Curb&Guardrail
1. Critical Speed	1. Loss of Control Related Kinematic Variables	1. Redirection Character
2. Lateral Resistance History	2. Exit Trajectory	2. Rail Contact Height
3. Rail Integrity	3. Exit Attitude History	3. Dynamic Jump Phenomenon
	4. Pitch Over	4. Contact Interval
	5. Roll Over	
	6. Steering Damage	
	7. Deformation	
	8. Damage Cost	

E.4.4.2 Functional Requirements.

1. The dike shall not induce the vehicle to over-turn about its pitch or roll axis.
2. The vehicle shall not become mired in the dike to the extent that removal by a service vehicle is necessary.
3. The dike shall not cause the vehicle to be vaulted into the air as the result of the dike acting as a ramp.
4. In interacting with the vehicle, the dike shall not:
   a. cause the steering system to be damaged,
   b. cause the driver to be jostled to the extent he is unable to carry out the steering function,
   c. cause anything other than minor vehicle body damage.

E.4.4.3 Performance Measures. The performance measures recommended for use in dike evaluation are listed in Table E-8.

TABLE E-8

MEDIAN DIKE PERFORMANCE MEASURES

Dike	Vehicle	Vehicle/Dike
1. Soil Sinkage Resistance	1. Injury Related Kinematic Variables	1. Undercarriage Contact
	2. Median Cross Over	
	3. Attitude History	
	4. C.G. Height History	
	5. Airborne Distance	
	6. Pitch Over	
	7. Roll Over	